Preface

This special issue has two parts:

A) TP Model Transfromation-based Control Theories and Applications

B) Cognitive Infocommunications: Virtual Reality in Education

Part A)

The topic of Part A) belongs to multi-objective control design based on quasi Linear Parameter Varying (qLPV) models and Linear Matrix Inequality (LMI) based optimization. The special issue focuses on advanced theories and design solutions based on Tensor Product (TP) model transformation. The TP model transformation is capable of constructing and manipulating polytopic representations of given qLPV models, and can be applied generally without analytical intervention, regardless of whether the model is in the form of dynamics equations derived from basic principles, or the outcome of soft computing based identification techniques such as neural networks or fuzzy logic, or the combination of these. The LMI design is very sensitive for the features of the polytopic model, therefore the TP model based manipulation of the polytopic models play a crucial role in control performance optimization. This Part A) includes six papers such as:

1) Tensor Product Model Transformation Simplification of Takagi-Sugeno Control and Estimation Laws – An Application to a Thermoelectric Controlled Chamber

This paper presents a novel application of the Tensor Product Model Transformation: the approximation of fuzzy control and estimation laws. A thermoelectric controlled chamber is built using peltier coolers and an H Bridge. A Takagi-Sugeno discrete time fuzzy model and LMI-based design is used to derive a controller.

2) A Tensor Product Model Transformation Approach to the Discretization of Uncertain Linear Systems

This work proposes a novel approach based on a grid of the possible values for the matrix exponential function and an application of the tensor product model transformation technique to find a suitable polytopic model. Numerical examples are presented to illustrate the advantages and the applicability of the proposed technique.

3) Tensor Product Model-based Control Design with Relaxed Stability Conditions for Perching Maneuvers

This paper proposed a control design approach based on tensor product models for perching maneuvers of fixed-wing aircraft. The highly nonlinear longitudinal dynamics of perching maneuvers is transformed into a tensor product model. The properties of the time derivatives of premise membership functions are utilized in the control design process to further reduce the control conservatism.

4) Tensor Product Model-based Control for Space-Craft with Fuel Slosh Dynamics

TP model transformation based solution is developed in this paper to the problem of Large spacecrafts undertaking long-life mission. Such missions greatly suffer from the nonlinear fuel slosh when altering the orbit or maneuvering, which leads to the downgrade on the per-formance and even stability of the body attitude control by unintentionally generating the huge disturbance thrust.

5) A State and Input Constrained Control Method for Air-Breathing Hypersonic Vehicles

This paper presents a systematic constrained control framework for the longitudinal motion of an air-breathing hypersonic vehicle via a combination of tensor product (TP) transformation and command governor approach. The significance of this proposed method mainly lies in its capability to avoid the flight exceeding constraints with varying flight conditions.

6) Tensor Product Model Transformation-based Parallel Distributed Control of Tumor Growth

The current work investigates tumor growth control under antiangiogenic targeted molecular therapy by use of TP model transformation. During the dynamics of the tumor growth we have considered that the tumor volume is measurable, while due to the lack of information about the inhibitor level in the serum an appropriate Extended Kalman Filter is applied as an observer. The paper also deals with the sensor noise of the system. The paper show that using the proposed solution: (i) the tumor volume was lower than 1 mm^3 at the end of the therapy; (ii) the developed models have approached each other with good accuracy; (iii) the totally injected inhibitor level was physiologically acceptable.

Part B)

Cognitive infocommunications (CogInfoCom, CogInfoCom.hu) investigates the link between the research areas of infocommunications and cognitive sciences, as well as the various engineering applications which have emerged as the synergic combination of these sciences. The primary goal of CogInfoCom is to provide a systematic view of how cognitive processes can co-evolve with infocommunications devices so that the capabilities of the human brain may not only be extended through these devices, irrespective of geographical distance but may also be blended with the capabilities of any artificially cognitive system. This merging and extension of cognitive capabilities are targeted towards engineering applications in which artificial and/or natural cognitive systems are enabled to work together more effectively. This Part B) of the special issue is focusing on Virtual Reality (VR) based solution in education. It includes the following papers:

1) MaxWhere VR-Learning Improves Effectiveness over clasiccal Tools of e-learning

The paper focus primarily on the content and digital tools of e-learning and VR learning in general. It compares the effectiveness of three techniques, ranging from well-known to radically new: classical e-mail / attachment based sharing, sharing through web interfaces (through a Moodle frontend), and sharing through a VR interface provided by a recently developed VR engine called MaxWhere. The paper shows that the users were able to complete the required workflow at least 50% faster in the MaxWhere 3D environment than in all other competing cases.

2) Factors Contributing to the Enhanced Performance of the MaxWhere 3D VR Platform in the Distribution of Digital Information

This paper presents an experiment contrasting traditional 2D interfaces and the MaxWhere 3D VR educational platform in order to shed light on how the effectiveness of various operations and workflows constituting the core of digital literacy has evolved in recent times. In order to draw specific conclusions, a new framework of concepts, qualitative and quantitative metrics and experimental procedures is proposed in the paper. The paper concludes that MaxWhere VR platform offers users a number of ways to accomplish tasks that would otherwise require extremely complicated digital workflows in more traditional 2D environments.

3)   2D Advertising in 3D Virtual Spaces

In this paper, a comparison of the classic banner ads, and 2D ads placed in a 3D virtual world is desicussed. The effectiveness of the VR advertisement is higher than the classic web-based ads. As virtual space, we used the MaxWhere virtual platform. The paper concludes that the memory recall of users was considerable more effective in 3D VR environment.

4)   Towards a Modern, Integrated Virtual Laboratory System

The aim of this paper is to give an overview on virtual and remote laboratory systems and to evaluate current solutions focusing on feasibility and applicability in higher education. The paper proposes new set of requirements against a modern virtual laboratory system. Finally, an overview of state of the art cognitive infocommunication technologies are presented, which can help to create high user experience in the new virtual laboratory environment.

5)   Cooperative Learning in VR Environment

The paper aims to introduce how a lesson built on the improvement of different intelligence levels through cooperative techniques can be implemented with the help of virtual space, what opportunities are provided by the MaxWhere program for planning and organizing teamwork and for supporting learning.

6)   The Evaluation of BCI and PEBL-based Attention Tests

In this paper, an EEG-based engineering research work is demonstrated, which supports the acquirement of practical knowledge and can measure cognitive ability with a device capable of brain activity observation. In the engineering research task, a brain-computer interface (BCI) had to be developed for the measurement of the average level of attention. The results of the BCI have been compared and contrasted to the results of two tests applied in cognitive psychology, the PEBL Continuous Performance Test (pCPT) and the PEBL Test of Attentional Vigilance (pTOAV).

7)   Examining the Learning Efficiency by a Brain-Computer Interface System

The main goal of this paper is to develop a Brain-Computer Interface (BCI) system to observe the level of vigilance calculated by Think Gear-ASIC Module (TGAM1) technology and to evaluate the output with learning efficiency tests applied in cognitive neuroscience. The developed BCI system has a significant correlation with P CORSI and P EBBINGHAUS cognitive neuroscience tests. The BCI system is capable of observing attentional vigilance continuously.

Péter Baranyi

Tensor Product Model Transformation Simplification of Takagi-Sugeno Control and Estimation Laws – An Application to a Thermoelectric Controlled Chamber

Alisson Marden Fonseca Pereira, Letícia Maria Sathler Vianna, Natália Augusto Keles, Víctor Costa da Silva Campos

Departamento de Engenharia Elétrica, Instituto de Ciências Exatas e Aplicadas (ICEA), Universidade Federal de Ouro Preto (UFOP), Rua Trinta e Seis, 115, CEP 35931-008, João Monlevade/MG, Brazil, victor.campos@deelt.ufop.br

Abstract: This paper presents a novel application of the Tensor Product Model Transformation: the approximation of fuzzy control and estimation laws. In order to illustrate this application, a thermoelectric controlled chamber was built using peltier coolers and an H Bridge. Using 5 digital temperature sensors, a Takagi-Sugeno discrete time fuzzy model of the system was found with system identification techniques. A control and an estimation law were designed using state of the art LMI conditions for fuzzy systems. Making use of the Tensor Product Model Transformation, these control and estimation laws were approximated/simplified and implemented on a microcontroller. The results obtained from these simplified laws show that this is a viable option and allows the use of cheap microcontrollers in cases where it would not be able to implement the control and estimation laws.

Keywords: Tensor Product Model Transformation; Hinf model reference control; Takagi-Sugeno observer; LMI

1 Introduction

Takagi-Sugeno (TS) fuzzy systems [1] are widely studied due to their universal approximation capabilities. In addition, given the fact that they are capable of representing nonlinear systems by a convex combination of linear models, many control, estimation and analysis problems can be recast as Linear Matrix Inequality (LMI) problems [2-6].

The Tensor Product (TP) Model Transformation [7-11] is a numerical procedure that extracts a polytopic representation from a Linear Parameter Varying (LPV) one. This representation is equivalent to a TS fuzzy representation [8] and allows

the use of many TS analysis and synthesis conditions for these systems [9]. By doing so, it presents an alternative to the use of the sector nonlinearity approach [2] and automates the process by means of sampling, the Higher Order Singular Value Decomposition (HOSVD) and convex hull manipulations. In addition, it can also be used to reduce the number of rules in a TS model [11].

In this paper, we present a novel application of the TP model transformation under the TS LMI framework: the simplification of the control and estimation laws. In order to illustrate its effectiveness, a thermoelectric heating/cooling system is designed and implemented using Peltier effect. Two Thermoelectric coolers (TECs) modules are used to change the temperature inside of a chamber made out of wood and styrofoam. In order to ensure that the system could be controlled, a power circuit is built in such a way that the polarity and the level of the voltage applied to the TEC modules could be easily changed.

In order to find suitable control and estimation laws for the system, system identification techniques are employed to retrieve a discrete-time TS model of the system. In possession of this model, the control and estimation laws are found from suitable LMI conditions and the TP model transformation is used to simplify these laws in a way that they can be implemented in real-time.

The structure of this paper is as follows. Section 2 presents the system used to illustrate the paper's main idea. Section 3 presents the system's model identification. Section 4 shows the conditions required to design the control law. Section 5 presents the conditions required to synthesize the fuzzy observer. Section 6 presents the idea of approximating control and estimation laws through tensor product model transformation. Section 7 presents this works conclusions.

Notation Throughout this paper, scalars are represented by lowercase variables, column vectors by lowercase boldface variables, matrices by uppercase variables and tensors by calligraphic uppercase variables. A^T denotes the transpose of A, $P > 0$ ($P \geq 0$) indicates that matrix P is positive definite (semi-definite), and $*$ represents symmetric terms inside of a symmetric matrix. $\mathcal{S} \times_n U$ represents the *n-mode* product between tensor $\mathcal{S}$ and matrix U. $\mathcal{S} \boxtimes_{i=1}^n U_i$ is a shorthand notation for $\mathcal{S} \times_1 U_1 \ldots \times_n U_n$. $A \otimes B$ denotes the Kronecker product between A and B. A_h is a shorthand notation for $\sum_{i=1}^r h_i(x_k) A_i$, and A_{h^-} is a shorthand notation for $\sum_{i=1}^r h_i(x_{k-1}) A_i$.

2   Thermoelectric Cooler-based Chamber

Cooling systems based on Peltier modules have the advantage of being much more environmentally friendly compared to conventional refrigerators which, despite superior performance, release gas into the environment. The operating temperature range inside the built chamber can be varied from 16 to 40 degrees Celsius.

The chamber is 40 centimeters of length and 30 centimeters of width and height. Two 100 cm^2 square holes were opened to accommodate two structures, each containing one Peltier module TEC 12715, two heat sinks and two fans. The Peltier module is placed between the two heat sinks, which are responsible for increasing the superficial area of the Peltier module and thus increase the heat transfer. The remaining air gap is filled with pieces of Styrofoam. The fans spread the heat uniformly. Figure 1 shows the final version of the chamber.
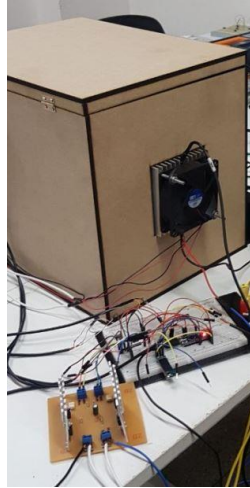

Figure 1
Thermoelectric chamber

We simplify the system's representation (to a lumped parameter one) and consider that its dynamics can be represented by five different temperatures: two on the external heat sinks, two on the internal heat sinks and one in the middle of the chamber. In order to measure these temperatures, five digital sensors were used, specifically DS18B20 sensors, which were configured to have an accuracy of 0.0625 °C.

The two TECs were connected in series and powered by a MOSFET H-Bridge so that they could be used to either cool or heat the chamber. A microcontroller was used to sample the sensor measurements and generate the PWM signals for the H-Bridge.

3 Takagi-Sugeno System Identification

Throughout this paper, we consider that the system is described by a discrete-time TS model given by

$$\boldsymbol{x}_{k+1} = \sum_{i=1}^{r} h_i(\boldsymbol{x}_k)(A_i \boldsymbol{x}_k + B_i \boldsymbol{u}_k) = A_h \boldsymbol{x}_k + B_h \boldsymbol{u}_k, \tag{1}$$

$$y_k = C\boldsymbol{x}_k. \tag{2}$$

Note that, if the membership functions are fixed and all states are measured (as we consider in this paper) this model is linear in the parameters and can be rewritten as

$$\boldsymbol{x}_{k+1} = [A_1 \quad B_1 \quad \cdots \quad A_r \quad B_r]\left(\boldsymbol{h}(\boldsymbol{x}_k) \otimes \begin{bmatrix} \boldsymbol{x}_k \\ \boldsymbol{u}_k \end{bmatrix}\right) \tag{3}$$

$$\boldsymbol{x}_{k+1} = (\boldsymbol{h}^T(\boldsymbol{x}_k) \otimes [\boldsymbol{x}_k^T \quad \boldsymbol{u}_k^T]) \begin{bmatrix} A_1^T \\ B_1^T \\ \vdots \\ A_r^T \\ B_r^T \end{bmatrix} \tag{4}$$

In this case, by making use of input and output data, we can make use of the Least Squares Method [1] and find a TS model as in (1).

For the Thermoelectric chamber, we consider that the left external temperature is the first state, the left internal temperature is the second state, the right internal temperature is the third state, the right external temperature is the fourth state and that the temperature in the middle of the chamber is the fifth state. We made use of a random input signal ranging from 0 to 12 V, shown in Figure 2, and measured the five states using the available sensors, shown in Figures 3 to 5.
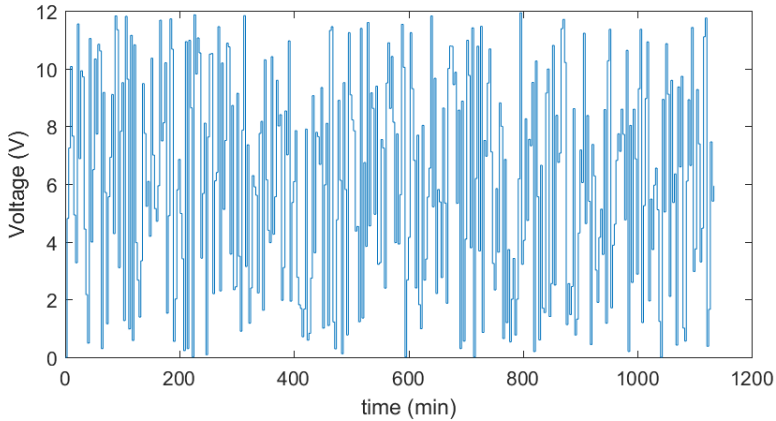

Figure 2
Input data used for the system identification

In this application case, we considered that the only premise/scheduling variable is the temperature in the middle of the chamber and we made use of a Takagi-Sugeno model with 13 rules and gaussian membership functions. We considered 16.6, 18.73, 20.87, 23, 25.13, 27.27, 29.4, 31.53, 33.67, 35.8, 37.93, 40.07 and

42.2 as the mean and 0.71 as the standard deviation for the gaussian membership functions. The resulting normalized membership functions are shown in Figure 6.

For the sake of comparison, Figure 7 shows, for a different set of input and output data, the measured temperatures in the middle of the chamber together with a free run simulation of the TS model found.
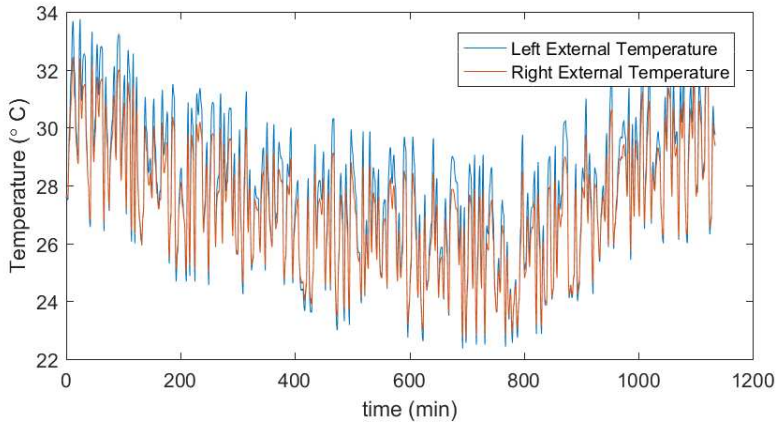

Figure 3
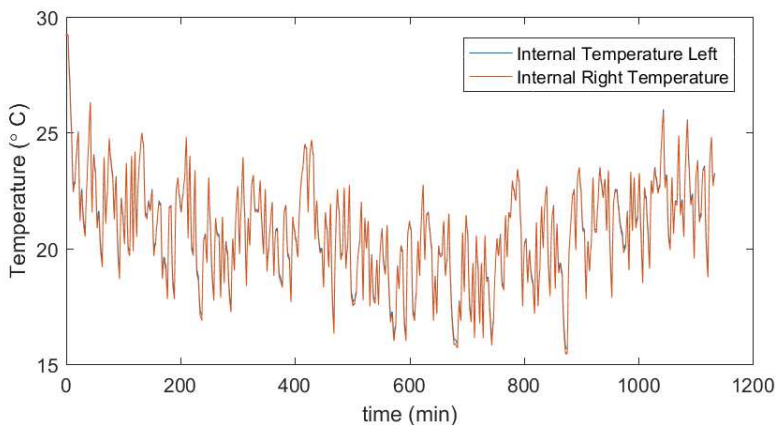Temperature on the chamber's external heat sinks

Figure 4
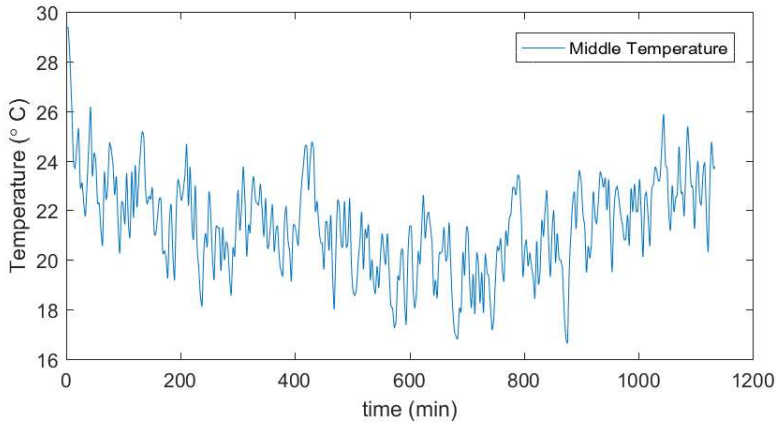Temperature on the chamber's internal heat sinks

Figure 5
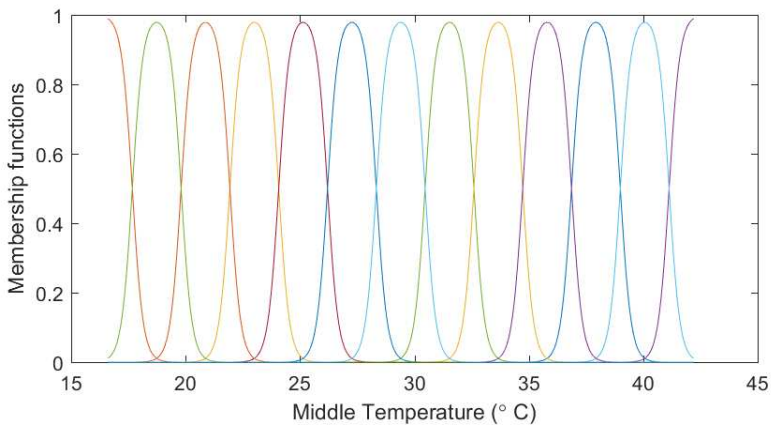Temperature in the middle of the chamber

Figure 6
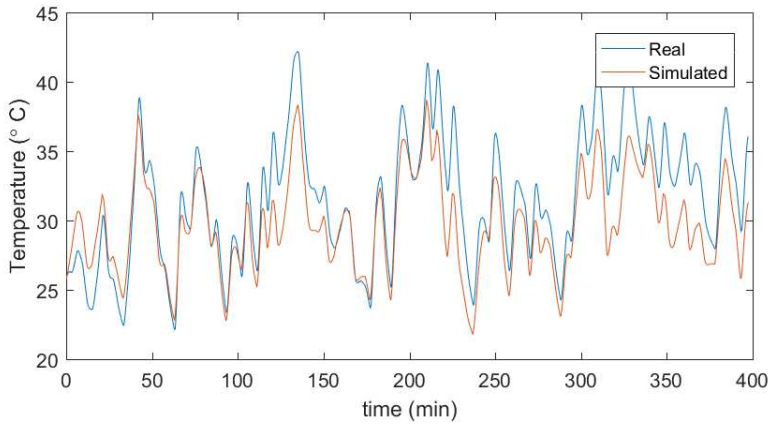Membership functions used in the example

Figure 7
Temperature on the middle of the chamber – real vs. simulated

4 $\mathcal{H}_\infty$ Model Reference PDC Control Law

In order to design a controller capable of reference tracking with a behavior close to a desired one, we make use of a $\mathcal{H}_\infty$ model reference approach.

With a small notational abuse, Figure 8 presents a block diagram of this approach. In this Figure, $H(z)$ represents a discrete-time TS fuzzy model (as in (1)), $H_m(z)$ represents a desired model for the system, and $\frac{z}{z-1}$ represents a discrete-time integrator (used to ensure that there will not be any steady state errors between the system and the reference model). In this setting, we aim to find an $\mathcal{H}_\infty$ controller that minimizes the gain from the reference of the desired model to the integral of the error between the two models.
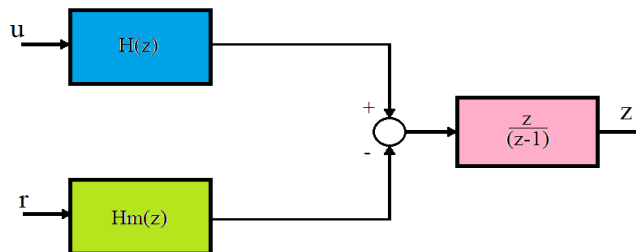

Figure 8
Open Loop Block Diagram for the $\mathcal{H}_\infty$ model reference control approach

If we consider a linear reference model given by

$$x_{m_{k+1}} = A_m x_k + B_m r_k, \tag{5}$$

$$y_{m_k} = C_m x_k,\tag{6}$$

We can represent the desired block diagram as the augmented system

$$\begin{bmatrix} x_{k+1} \\ x_{m_{k+1}} \\ l_{k+1} \end{bmatrix} = \begin{bmatrix} A_h & 0 & 0 \\ 0 & A_m & 0 \\ C & -C_m & I \end{bmatrix} \begin{bmatrix} x_k \\ x_{m_k} \\ l_k \end{bmatrix} + \begin{bmatrix} B_h \\ 0 \\ 0 \end{bmatrix} u_k + \begin{bmatrix} 0 \\ B_m \\ 0 \end{bmatrix} r_k,\tag{7}$$

$$z_k = \begin{bmatrix} 0 & 0 & I \end{bmatrix} \begin{bmatrix} x_k \\ x_{m_k} \\ l_k \end{bmatrix}.\tag{8}$$

A shorter representation for the augmented system is given by

$$\bar{x}_{k+1} = \bar{A}_h \bar{x}_k + \bar{B}_h u_k + \bar{B}_r r_k,\tag{9}$$

$$z_k = \bar{C} \bar{x}_k,\tag{10}$$

with $\bar{x}_k = \begin{bmatrix} x_k^T & x_{m_k}^T & l_k^T \end{bmatrix}^T$, $\bar{A}_h = \begin{bmatrix} A_h & 0 & 0 \\ 0 & A_m & 0 \\ C & -C_m & I \end{bmatrix}$, $\bar{B}_h = \begin{bmatrix} B_h \\ 0 \\ 0 \end{bmatrix}$, $\bar{B}_r = \begin{bmatrix} 0 \\ B_m \\ 0 \end{bmatrix}$, and

$\bar{C} = \begin{bmatrix} 0 & 0 & I \end{bmatrix}$.

From the literature [6], we know that, considering a control law, with delayed membership functions, of the form

$$u_k = K_{hh^-} G_{hh^-}^{-1} \bar{x_k},\tag{11}$$

a sufficient condition for

$$\frac{\|z\|_2}{\|w\|_2} \le \gamma,\tag{12}$$

is that there exist matrices P_i, with $i \in \{1,2,\dots,r\}$, and K_{ij} and G_{ij}, with $i,j \in \{1,2,\dots,r\}$, such that

$$\sum_{i=1}^{r} \sum_{j=1}^{r} \sum_{l=1}^{r} h_i(x_k) h_j(x_k) h_l(x_{k-1}) Q_{ijl} < 0,\tag{13}$$

with

$$Q_{ijl} = \begin{bmatrix} -G_{jl}^T - G_{jl} + P_l & 0 & G_{jl}^T \bar{A}_i^T + K_{jl}^T \bar{B}_i^T & G_{jl}^T \bar{C}^T \\ * & -\gamma I & \bar{B}_m^T & 0 \\ * & * & -P_i & 0 \\ * & * & * & -\gamma I \end{bmatrix}.\tag{14}$$

In order to implement this set of parameter-dependent LMIs, we make use of the following sufficient conditions

$$Q_{iil} < 0 \qquad \forall\, i, l,\tag{15}$$

$$Q_{ijl} + Q_{jil} < 0 \qquad \forall i, j > i, l.\tag{16}$$

Since we are dealing with a real physical system, and $\mathcal{H}_\infty$ controllers tend to have very large gains, we also make use of a set of limiting conditions for the controller gains. By making use of the S-procedure, it is easy to see that if there exists $\tau \in \mathbb{R}$ such that

$$\begin{bmatrix} -G_{ij}^T - G_{ij} & 0 & K_{ij}^T & I \\ * & -\delta_u^2 + \delta_x^2 \tau & 0 & 0 \\ * & * & -1 & 0 \\ * & * & * & -\tau I \end{bmatrix} < 0, \quad \forall i,j, \tag{17}$$

then, the control law found is such that

$$u^T u \leq \delta_u^2, \quad \forall x^T x \leq \delta_x^2. \tag{18}$$

5 Fuzzy State Observer with Measurable Premisse Variables

In many practical applications, the states of a given system are not always readily available. Therefore, given the output measurements and the system's input, a state observer can be used to estimate the system's state. In this work, we consider the particular case in which all of the premise variables are measured, and search for the TS observer with the highest decay rate possible.

Considering a TS model described by (1) and (2), we consider a fuzzy observer *with measurable premise variables* given by

$$\hat{x}_{k+1} = A_h \hat{x}_k + B_h u_k + M_h^{-1} N_{hh^-}(y_k - \hat{y}_k). \tag{19}$$

$$\hat{y}_{k+1} = C \hat{x}_k. \tag{20}$$

with M_{h^-} and N_{hh^-} the observer gains. With this observer, the estimation error, $e_k = x_k - \hat{x}_k$, dynamics is given by

$$e_{k+1} = (A_h - M_h^{-1} N_{hh^-} C) e_k. \tag{21}$$

As shown in [12], by making use of a Lyapunov function with delayed membership function,

$$V_k = e_k P_{h^-} e_k, \tag{22}$$

the system is asymptotically stable if there exist matrices P_i and M_i with $i \in \{1,2,\ldots,r\}$, and N_{ij} with $i,j \in \{1,2,\ldots,r\}$ such that

$$\begin{bmatrix} -P_i & A_i^T M_j^T + C^T N_{ij}^T \\ * & -G_j^T - G_j + P_j \end{bmatrix} < 0. \tag{23}$$

In addition to this, if the Lyapunov function is such that

$$V_{k+1} < \alpha^2 V_k, \tag{24}$$

then the system will be exponentially stable with a decay rate of α. It is easy to show that, in the case of the LMI conditions presented above, this amounts to

$$\begin{bmatrix} -\alpha^2 P_i & A_i^T M_j^T + C^T N_{ij}^T \\ * & -G_j^T - G_j + P_j \end{bmatrix} < 0. \tag{25}$$

6   Control and Estimation Laws Simplification

Having found the control and estimation gains, and remembering the fact that the separation principle is still valid when we use a fuzzy observer with measurable premise variables [2], we can use them together to form an output feedback control law for the system. In this case, the controller dynamics can be written as

$$\boldsymbol{u}_k = K_{hh^-} G_{hh^-}^{-1} \begin{bmatrix} \widehat{\boldsymbol{x}}_k^T & \boldsymbol{x}_{m_k}^T & \boldsymbol{l}_k^T \end{bmatrix}^T, \tag{26}$$

$$\widehat{\boldsymbol{x}}_{k+1} = (A_h - M_h^{-1} N_{hh^-} C) \widehat{\boldsymbol{x}}_k + B_h \boldsymbol{u}_k + M_h^{-1} N_{hh^-} \boldsymbol{y}_k, \tag{27}$$

$$\boldsymbol{x}_{m_{k+1}} = A_m \boldsymbol{x}_k + B_m \boldsymbol{r}_k, \tag{28}$$

$$\boldsymbol{l}_{k+1} = -C_m \boldsymbol{x}_{m_k} + \boldsymbol{l}_k + \boldsymbol{y}_k. \tag{29}$$

Notice that these equations are rather complicated to implement in real time on a microcontroller since the inverses $G_{hh^-}^{-1}$ and M_h^{-1} need to be calculated in real time.

A possible approach to circumvent this issue is to make use of the TP model transformation to approximate the control and estimation gains.

In that regard, consider a parameter varying matrix defined by

$$S_{hh^-} = \begin{bmatrix} A_h & B_h & M_h^{-1} N_{hh^-} \\ K_{hh^-} G_{hh^-}^{-1} & 0 \end{bmatrix}. \tag{30}$$

we may define a sampling grid over the current and past fuzzy premise variables and apply the Tensor Product Model Transformation to this parameter varying matrix.

One could argue that, in this case, we could just use the HOSVD step to reduce the control and estimation gains complexity since this particular TP model will not be used on a further LMI design step. Note, however, that the weights found from the HOSVD step may have any value, and as such make it hard to interpret the gains found. In that regard, it is advisable to make use of the convex hull manipulation step, preferably with a tighter transformation (like the Close to Normalized – CNO [13]), so that we can make sense of the control and estimation gains found.

It is important to note that, even though the choice of the convex hull transformation can be a decisive factor on whether or not an LMI synthesis

procedure is successful [14-16], they do not affect the feasibility of the LMIs in the strategy proposed in this paper (as they are used simply with the control and estimation laws as opposed to finding a convex representation used in the LMIs). Nevertheless, it is recommended to use the CNO transformation, as it will lead to control and estimation gains that can be more easily interpreted.

For the thermoelectric controlled chamber, since we are only using the middle temperature as a premise variable, the parameter varying matrix S_{hh^-} depends only on the current and one step past values of this premise variable. In that regard, we consider a 2-dimensional grid for these values, with 40 points in each direction.

In addition to this, we consider that there is a single control input; the desired controlled temperature is the one on the middle of the chamber, only the middle temperature and one of the external heat sinks' temperatures are measured, and we consider a stable linear reference model with a single state. With all of these considerations, we have that $S_{hh^-} \in \mathbb{R}^{6 \times 8}$ and we store the sampled matrices on a $\mathcal{S} \in \mathbb{R}^{40 \times 40 \times 6 \times 8}$ tensor.

Due to the microcontroller memory limitations, in the HOSVD step we keep only 3 columns, corresponding to the 3 highest singular values, in each of the 2 first directions. However, when making use of the convex hull manipulations, a fourth column was added in each direction, resulting in an equivalent fuzzy TP model with 16 rules (4×4).

By making use of triangular membership functions and a uniform grid distribution, it is easy to show that there exists an efficient ($O(1)$) linear interpolation scheme to implement the control and estimation membership functions, which justifies the use of the Tensor Product Model Transformation as an efficient way to implement the control and estimation laws.

For comparison purposes, Figures 9 and 10 present the membership functions found for the current and past middle temperature in the control and estimation laws. Note their difference from the original membership functions presented in Figure 6.
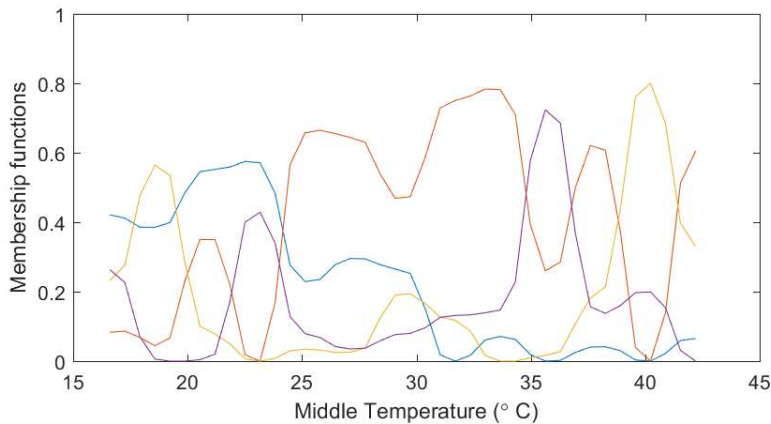
Figure 9

Control and Estimation membership functions found after the TP model transformation for the current
value of the middle temperature
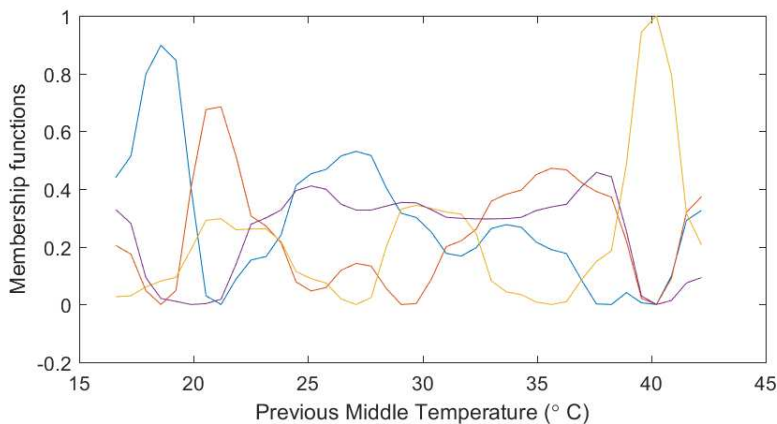
Figure 10

Control and Estimation membership functions found after the TP model transformation for the
previous value of the middle temperature

The system's behavior in closed loop with the approximate control and estimation
laws can be seen on Figures 11 to 17. Figure 11 presents the controlled
temperature against its desired values, Figure 12 presents the calculated control
input and the actual control input applied to the systems, whereas Figures 13 to 17
present the estimates found for the five temperatures against their measured
values.
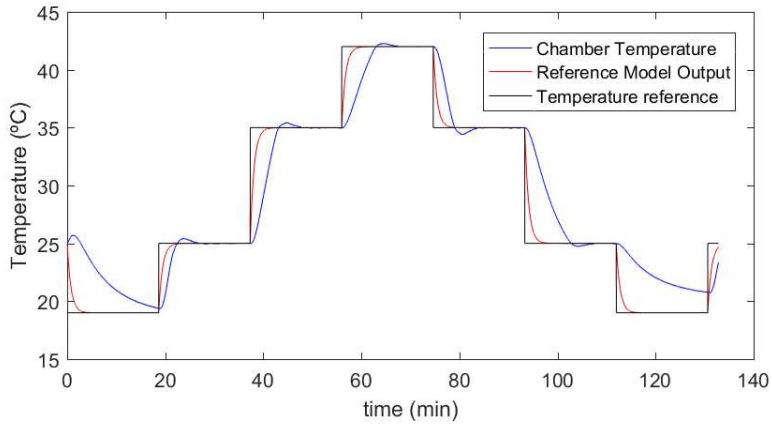
Figure 11
Controlled temperature inside of the chamber together with the desired reference model output and the desired temperature reference
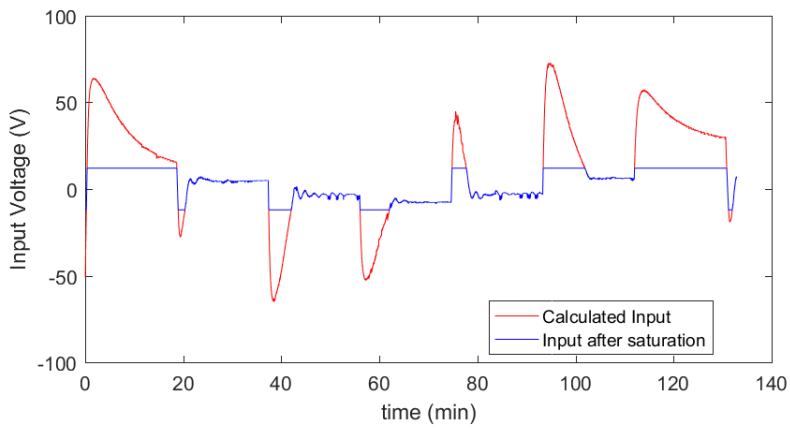
Figure 12
Calculated control input over time with the control input that was actually applied to the sysstem
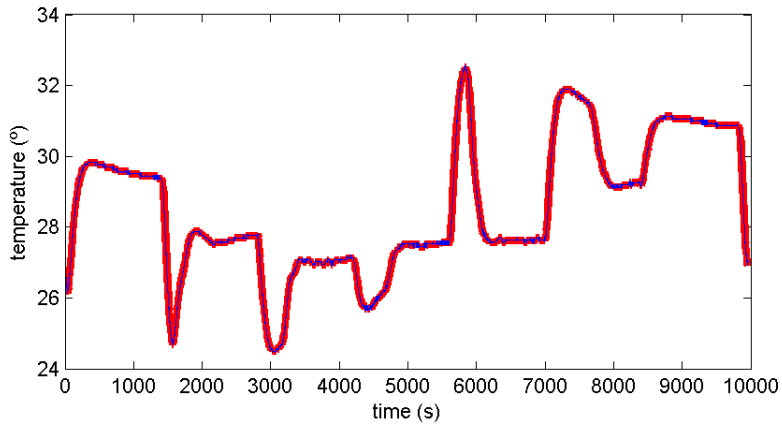
Figure 13
Estimated and measured temperatures on the left external heat sink. The red line represents the
measured values, whereas the blue one represents the estimated one
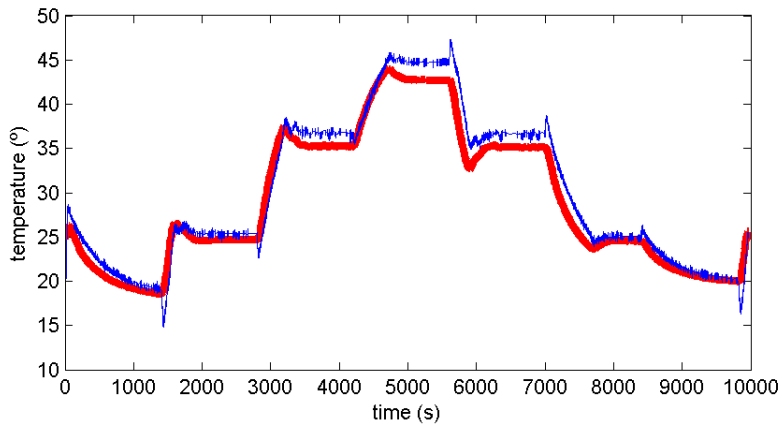
Figure 14
Estimated and measured temperatures on the left internal heat sink. The red line represents the
measured values, whereas the blue one represents the estimated one
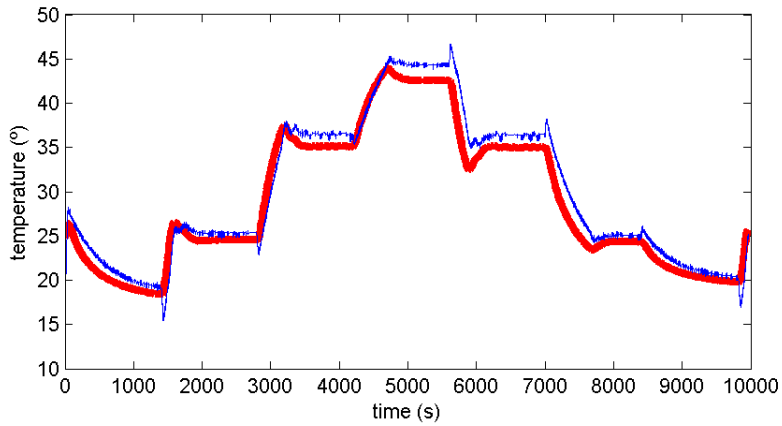
Figure 15

Estimated and measured temperatures on the right internal heat sink. The red line represents the measured values, whereas the blue one represents the estimated one
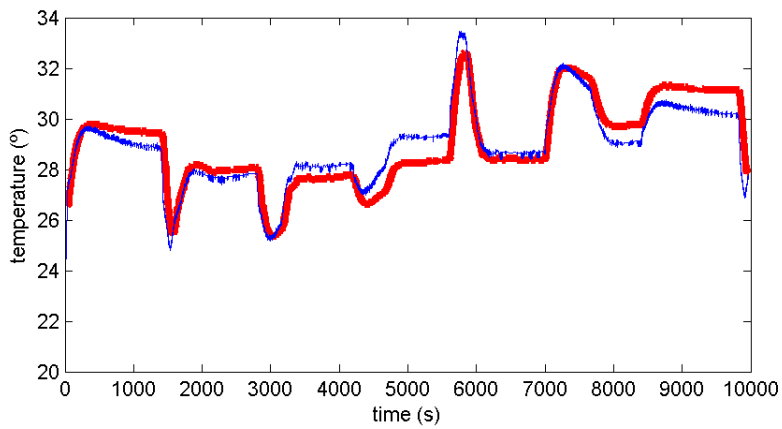
Figure 16

Estimated and measured temperatures on the right external heat sink. The red line represents the measured values, whereas the blue one represents the estimated one
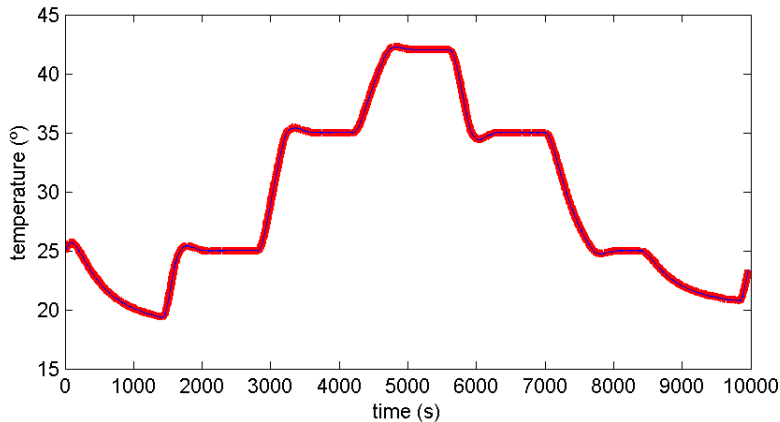
Figure 17

Estimated and measured temperatures on the middle of the chamber. The red line represents the
measured values, whereas the blue one represents the estimated one

Conclusions

This paper presented a novel application to the tensor product model transformation, specifically its use on the approximation and simplification of fuzzy control and estimation laws. The proposed methodology was applied to a thermoelectric controlled chamber and yielded satisfactory results.

Future works on this line will focus on the development of non-fragile controller and estimation conditions that are guaranteed to work even when there's a mismatch between the designed and the implemented control and estimation gains.

References

[1]   Takagi, T., & Sugeno, M. (1985) Fuzzy identification of systems and its applications to modeling and control. IEEE transactions on systems, man, and cybernetics (1) 116-132

[2]   Tanaka, Kazuo; Wang, Hua O. Fuzzy control systems design and analysis: a linear matrix inequality approach. John Wiley & Sons, 2004

[3]   Guerra, Thierry-Marie et al. An efficient Lyapunov function for discrete T–S models: observer design. IEEE Transactions on Fuzzy Systems, v. 20, n. 1, pp. 187-192, 2012

[4]   Tanaka, Kazuo; Ikeda, Takayuki; Wang, Hua O. Fuzzy regulators and fuzzy observers: relaxed stability conditions and LMI-based designs. IEEE Transactions on fuzzy systems, v. 6, n. 2, pp. 250-265, 1998

[5] Estrada-Manzo, Victor; Lendek, Zsófia; Guerra, Thierry Marie. Generalized LMI observer design for discrete-time nonlinear descriptor models. Neurocomputing, v. 182, pp. 210-220, 2016

[6] Lendek, Z., Guerra, T. M., & Lauber, J. (2015) Controller design for TS models using delayed nonquadratic Lyapunov functions. IEEE Transactions on Cybernetics, 45(3) 439-450

[7] Yam, Y., Baranyi, P., & Yang, C. T. (1999) Reduction of fuzzy rule base via singular value decomposition. IEEE Transactions on fuzzy Systems, 7(2) 120-132

[8] Baranyi, P., Tikk, D., Yam, Y., & Patton, R. J. (2003) From differential equations to PDC controller design via numerical transformation. Computers in Industry, 51(3) 281-297

[9] Baranyi, P. (2004) TP model transformation as a way to LMI-based controller design. IEEE Transactions on Industrial Electronics, 51(2) 387-400

[10] Baranyi, P., Yam, Y., &Várlaki, P. (2013) Tensor product model transformation in polytopic model-based control. CRC Press

[11] Campos, V. C. S., Tôrres, L. A. B., & Palhares, R. M. (2015) Revisiting the TP model transformation: Interpolation and rule reduction. Asian Journal of Control, 17(2) 392-401

[12] Guerra, T. M., Kerkeni, H., Lauber, J., & Vermeiren, L. (2012) An efficient Lyapunov function for discrete T−S models: observer design. IEEE Transactions on Fuzzy Systems, 20(1) 187-192

[13] Campos, V. C., Souza, F. O., Tôrres, L. A., & Palhares, R. M. (2013) New stability conditions based on piecewise fuzzy Lyapunov functions and tensor product transformations. IEEE Transactions on Fuzzy Systems, 21(4) 748-760

[14] Szollosi, A., & Baranyi, P. (2016) Influence of the Tensor Product model representation of qLPV models on the feasibility of Linear Matrix Inequality. Asian Journal of Control, 18(4) 1328-1342

[15] Baranyi, P. (2014) The generalized TP model transformation for T−S fuzzy model manipulation and generalized stability verification. IEEE Transactions on Fuzzy Systems, 22(4) 934-948

[16] Gróf, P., Baranyi, P., &Korondi, P. (2010) Convex hull manipulation does matter in LMI based observer design, a TP model transformation based optimisation. strategies, 11, 12

A Tensor Product Model Transformation Approach to the Discretization of Uncertain Linear Systems

Víctor Costa da Silva Campos, Letícia Maria Sathler Vianna, Márcio Feliciano Braga

Department of Electrical Engineering, Institute of Exact and Applied Sciences (ICEA), University of Ouro Preto – UFOP, 35931-008, João Monlevade, MG, Brazil, {victor.campos, mfbraga}@ufop.edu.br

Abstract: Most of the discretization approaches for uncertain linear systems make use of the series representation of the matrix exponential function and truncate the summation after a certain order. This usually leads to discrete-time uncertain polytopic models described by polynomial matrices with multiple indexes, which usually means that the higher the order used in the approximation, the higher the number of linear matrix inequalities (LMI) needed. This work, instead, proposes an approach based on a grid of the possible values for the matrix exponential function and an application of the tensor product model transformation technique to find a suitable polytopic model. Numerical examples are presented to illustrate the advantages and the applicability of the proposed technique.

Keywords: Discretization; LMIs; Uncertain Systems; Tensor Product Model Transformation

1 Introduction

Ever since efficient interior-point methods for semi-definite programming [1] made the use of Linear Matrix Inequalities (LMIs) computationally tractable, it has been extensively used for the robust control of linear systems [2], [3].

Despite the fact that many systems are described as continuous-time systems by differential equations, most controllers are implemented in a digital form.

The importance of digitally implemented controllers is corroborated by its extensive use in industrial applications, with various advantages, such as flexibility, ease of implementation of complex digital control laws, possibility of existence of interfaces with the users (including web interfaces), lower power consumption, greater reliability [4], [5].

Therefore, it is interesting to find an appropriate discrete-time representation of these systems that can be used in their analysis and synthesis of digital controllers.

The main hurdle in this direction is that, while there are exact discretization formulas for linear systems (see, for instance, [4], [6], [7] and references therein), the same is not true for uncertain linear systems, and approximations are used instead to deal with the exponential of an uncertain matrix.

For instance, one can cite the work in [8] where the state space matrices of the continuous-time systems are supposed to be interval matrices and, by employing the Chebyshev quadrature formula and interval arithmetic, a discrete-time representation of the system is acquired.

As main drawback of this approach, is the fact that it cannot treat systems described by uncertainties lying in a polytope with an arbitrary number of vertices.

To deal with uncertain network-induced delay, the authors in [9] performed a discretization of a switched system.

Others [10]-[13], as a primary approximation of the uncertain continuous-time systems, employ a first-order Taylor series expansion technique to represent the discrete-time systems.

However, such choice implies that the model becomes increasingly inaccurate with the augmentation of the sampling time.

Finally, in [14], the authors proposed a technique to discretize the uncertain system by applying a Taylor series expansion of a fixed order, resulting in a discrete-time model composed of homogeneous polynomial matrices plus an additive norm-bounded term that represents the discretization residual error.

Such representation produces polynomial matrix systems with multiple indexes, which usually means that the number of LMIs to be solved increases with the chosen order by the designer.

In order to avoid the aforementioned difficulties, this work proposes an approach based on a grid of the possible values for the matrix exponential function and an application of the tensor product model transformation technique to acquire a suitable polytopic model.

In this paper, we consider continuous-time uncertain linear systems described by polytopic models (which can also be regarded as linear differential inclusions [2]). These models represent the uncertain system as the convex sum of known linear models, whose weights are unknown. With that in mind, we consider that the models are written as

$$\dot{\boldsymbol{x}}(t) = A(\boldsymbol{\alpha})\boldsymbol{x}(t) + B(\boldsymbol{\alpha})\boldsymbol{u}(t),$$

$$\dot{\boldsymbol{x}}(t) = \sum_{i=1}^{r} \alpha_i \big(A_i \boldsymbol{x}(t) + B_i \boldsymbol{u}(t) \big)$$

in which $x(t) \in \mathbb{R}^n$ is the state vector, $u(t) \in \mathbb{R}^m$ is the control input, r is the number of vertex linear models, and α_i are the convex weights, such that

$$\alpha_i \in [0,1], \quad \sum_{i=1}^{r} \alpha_i = 1.$$

The main goal of this paper is to find an approximate discrete-time polytopic model, such as

$$x[k+1] = \hat{A}(\boldsymbol{\beta})x[k] + \hat{B}(\boldsymbol{\beta})u[k],$$

$$x[k+1] = \sum_{i=1}^{\hat{r}} \beta_i \left(\hat{A}_i x[k] + \hat{B}_i u[k] \right) \tag{1}$$

in which $\hat{r}$ is the number of vertex linear models and β_i are the convex weights such that

$$\beta_i \in [0,1], \quad \sum_{i=1}^{\hat{r}} \beta_i = 1$$

This representation allows us to derive robust analysis and synthesis conditions for this type of discrete-time polytopic systems as optimization problems involving LMIs [15]-[19]

If we consider that the uncertain weights α_i, as well as the control inputs, are constant over the sampling intervals, we know that the uncertain linear system can be discretized by [14], [20]

$$x[k+1] = e^{A(\boldsymbol{\alpha})T_s} x[k] + \int_0^{T_s} \left(e^{A(\boldsymbol{\alpha})\tau} d\tau \right) B(\boldsymbol{\alpha}) u[k] \tag{2}$$

in which T_s represents the constant sampling time. We can see that, under these assumptions, the discretization can be regarded as finding a polytopic representation for

$$\hat{A}(\boldsymbol{\alpha}) = e^{A(\boldsymbol{\alpha})T_s}, \quad \hat{B}(\boldsymbol{\alpha}) = \int_0^{T_s} \left(e^{A(\boldsymbol{\alpha})\tau} d\tau \right) B(\boldsymbol{\alpha}). \tag{3}$$

Whereas some works consider a simple forward Euler approximation to find the discrete-time uncertain model [10]-[13] and others consider a truncation of the power series for the matrix exponential [14], we instead propose to find an approximation for the discrete-time model by a grid approximation (over the possible values of α_i).

Given the values taken over the grid, one could simply consider that every grid point is a vertex of the discrete-time polytopic model. However, in order to find a reasonably good approximation, a high number of grid points is necessary and that would lead to a computationally untractable model for LMI approaches. Fortunately, the Tensor Product Model Transformation (TPMT) [21]-[23] is a technique that was proposed to find polytopic representations from grid values for a Linear Parameter Varying (LPV) model. In that regard, in this paper, we propose its use to find a suitable polytopic approximation for the discrete-time uncertain system in (2).

This paper is organized as follows: Section 2 presents some definitions and results used in this work. Section 3 presents the discretization methodology proposed in this paper. In Section 4, a numerical example is used to illustrate the proposed discretization strategy.} Section 5 draws some conclusions and proposes future works.

Notation Throughout this paper, scalars are represented by lowercase variables, column vectors by lowercase boldface variables, matrices by uppercase variables and tensors by calligraphic uppercase variables. A^T denotes the transpose of A, $P > 0$ ($P \geq 0$) indicates that matrix P is positive definite (semi-definite), and $*$ represents symmetric terms inside of a symmetric matrix. $\mathcal{S} \times_n U$ represents the n-mode product between tensor $\mathcal{S}$ and matrix $U.\mathcal{S} = 1 \boxtimes_{i=1}^{n} U_i$ is a shorthand notation for $\mathcal{S} \times_1 U_1 ... \times_n U_n$. For a detailed definition of the multilinear algebra operations used in this paper, we refer the reader to [24].

2   Background

Throughout this paper, some results will be of fundamental importance to develop the discretization strategy proposed. One of these results, presented in Theorem 1, is the Higher Order Singular Value Decomposition, which allows the decomposition of a tensor into a product of a core tensor and a set of matrices.

Theorem 1: *Higher Order Singular Value Decomposition (HOSVD)* [24, Theorem 2]

Every complex tensor $\mathcal{A} \in \mathbb{R}^{i_1 \times ... \times i_l}$ can be decomposed as the k-mode product of tensor $\mathcal{S}$ and matrices U_k, as $\mathcal{A} = \mathcal{S} \times_1 U_1 ... \times_l U_l = \mathcal{S} \boxtimes_{k=1}^{l} U_k$.

In order to illustrate the proposed strategy, a discrete-time LMI synthesis condition will be used to find a stabilizing digital controller for the continuous-time system. Since it is not the focus of this paper, a simple robust condition, presented in Theorem 2, is used. Note that any other set of robust stabilizing synthesis condition could be used.

Theorem 2: Discrete-Time LMI Synthesis Conditions [17]

Given a system described by (1), a control law of the form

$$\boldsymbol{u} = K\boldsymbol{x}$$

asymptotically stabilizes the system if there exists a symmetric matrix $X \in \mathbb{R}^{n \times n}$, and a matrix $Y \in \mathbb{R}^{m \times n}$ such that

$$\begin{bmatrix} -X & AX + X^T A^T + BY + Y^T B^T \\ * & -X \end{bmatrix} < 0.$$

In addition to this, the control gain matrix K is found by $K = YX^{-1}$.

3   Discretization Strategy

As explained in the introduction, in this paper, we propose to use the tensor product model transformation, with slight modifications, to approximate the $\hat{A}(\boldsymbol{\alpha})$ and $\hat{B}(\boldsymbol{\alpha})$ matrix functions in (3). In order to find a representation with a smaller number of vertices, we first define the matrix function

$$L(\boldsymbol{\alpha}) = [\hat{A}(\boldsymbol{\alpha}) \quad \hat{B}(\boldsymbol{\alpha})],$$

and approximate this matrix function instead. Note that the image space of $L(\boldsymbol{\alpha})$ is in $\mathbb{R}^{n \times (n+m)}$.

3.1   Sampling

Considering that we have r convex sum weights α_i taking values in $[0,1]$, in the usual tensor product model transformation, we would start by defining an hyper-rectangular sampling grid over the $[0,1]^r$ space, with p_i samples along the ith dimension (resulting in $\prod_{i=1}^{r} p_i$ samples). Each sample taken from the grid would be stored in a tensor $\mathcal{L} \in R^{p_1 \times \dots \times p_r \times n \times (n+m)}$. This approach would, however, lead to some problems, since it does not take into account that the α_i are convex weights and should always add up to one.

In that regard, we propose the following approach: if there are $r \geq 2$ different α_i weights, we define a grid with p points in $[0,1]$ for $r-1$ of these weights. In addition, we only take samples from values on this $r-1$ dimensional grid if their sum is less than one. The remaining convex weight (the one not defined on the grid) is found by subtracting the sum of the current grid point from one (so that the sum of the weights is one). In addition, we store these samples in a $\mathcal{L} \in \mathbb{R}^{\kappa \times n \times (n+m)}$ tensor, in which κ is the total number of valid samples taken, and $\mathcal{L}_{ijk}$ represents the element in row j and column k from sample i.

At this point, the matrix function can be represented as

$$L(\boldsymbol{\alpha}) \approx \mathcal{L} \times_1 w^T(\boldsymbol{\alpha})$$

in which the function $w^T(\boldsymbol{\alpha})$ is an interpolation function that assigns a convex weight to each sample depending on the current value of $\boldsymbol{\alpha}$. A nearest neighbor or a finite element interpolation would generate a suitable interpolation (though, it does not make much difference given we are not really interested in the approximation model found, but only on the convex vertices found).

3.2   HOSVD

By making use of Theorem 1, we can decompose tensor $\mathcal{L}$ by its HOSVD along its first direction (since we are not interested in decomposing the last two) and rewrite it as

$$\mathcal{L} = \mathcal{S} \times_1 U_1,$$

with $\mathcal{S} \in \mathbb{R}^{q \times n \times (n+m)}$ and $U_1 \in R^{\kappa \times q}$.

Matrix U_1 acts like a weight matrix, since we can rewrite the matrix function as

$$L(\boldsymbol{\alpha}) \approx S \times_1 \boldsymbol{w}^T(\boldsymbol{\alpha})U_1 = \boldsymbol{S} \times_1 \boldsymbol{w}_h^T(\boldsymbol{\alpha})$$

with $\boldsymbol{w}_h^T(\boldsymbol{\alpha}) = \boldsymbol{w}^T(\boldsymbol{\alpha})U_1$. One might be tempted to use the vertices in tensor $\mathcal{S}$ as the vertex matrices in (1). Note, however, that since the U_1 weight matrix is allowed to assume any values, even though the elements of $\boldsymbol{w}^T(\boldsymbol{\alpha})$ can be seen as convex sum weights, the elements of $\boldsymbol{w}_h^T(\boldsymbol{\alpha})$ cannot.

3.3   Convex Hull Manipulation

With that in mind, we now seek to find a transformation for the U_1 matrix and the corresponding transformation for the tensor $\mathcal{S}$. In the tensor product model transformation literature several properties are proposed for the weight matrices (which might be interesting for the final representation found). The mains ones are

- **Sum Normalization** (SN): every column of U_1 adds up to one;

- **Non Negative** (NN): there are no negative elements in U_1;

- **Inverse Normalized** (INO): at least one element of every column of U_1 is equal to zero;

- **Relaxed Normalized**} (RNO): the maximum value of every column of U_1 is the same;

- **Close to Normalized** (CNO): the simplex whose vertices are the unitary vectors is the smallest volume simplex that covers the vectors formed by the rows of U_1.

If the SN and NN properties are satisfied, we can guarantee that the transformed weight vector $\boldsymbol{w}_h^T(\boldsymbol{\alpha})$ elements can be regarded as convex sum weights. The other properties aim at finding a ``tight" representation (one in which the vertices found at the end represent the smallest uncertain set possible). In this work, we apply the SN-NN transformation [21], followed by the RNO-INO transformation [25], [26] and the CNO transformation [27].

We employ these transformations, because, as is known in the literature [30]-[33], the use of different representations usually makes a significant difference on the feasibility of LMI conditions (and usually the CNO transformation is the recommended one for the stabilization case).

In order to apply these transformations, we note that, if

$$\tilde{U}_1 = U_1 T_1$$

$$U_1 = \tilde{U}_1 T_1^{-1}$$

which means that

$$\mathcal{S} \times_1 U_1 = \mathcal{S} \times \widetilde{U}_1 T_1^{-1}$$

$$= (\mathcal{S} \times_1 T_1^{-1}) \times_1 \widetilde{U}_1$$

$$= \tilde{\mathcal{S}} \times \widetilde{U}_1$$

With that in mind, and $\widetilde{U}_1$ a CNO matrix, we can rewrite the matrix function approximation as

$$L(\boldsymbol{\alpha}) \approx \tilde{\mathcal{S}} \times_1 w^T(\boldsymbol{\alpha}) \widetilde{U}_1 = \tilde{\mathcal{S}} \times_1 \widetilde{w}_h^T(\boldsymbol{\alpha})$$

and the desired $\hat{A}_l$ and $\hat{B}_l$ in (1) can be extracted from the $\tilde{\mathcal{S}}$ tensor, with $\hat{A}_{i_{jk}}$ the element in $\tilde{\mathcal{S}}_{ijk}$ and $\hat{B}_{i_{jk}}$ the element in $\tilde{\mathcal{S}}_{ij(k+n)}$.

3.4   Numerical Example

We present two different examples and compare their results with the ones in [28]. The methods presented here were implemented in Matlab R2016 using YALMIP [29] and Mosek.

Example 1: Consider the mass, spring, damper system presented in [28, Example 1]

$$\dot{x} = A(c_1, c_2)x + Bu$$

with

$$A(c_1, c_2) = \begin{bmatrix} 0 & 0 & 1 & 0 \\ 0 & 0 & 0 & 1 \\ -c_1 & c_1 & -0.2 & 0.2 \\ c_1/2 & -\dfrac{c_1 + c_2}{2} & 0.1 & -0.15 \end{bmatrix}, \ B = \begin{bmatrix} 0 \\ 0 \\ 1 \\ 0 \end{bmatrix},$$

and $c_1 \in [1.6, 2.4], c_2 \in [6.4, 9.6]$ (leading to a continuous-time polytopic representation with 4 vertices). The goal in this example is to find an approximate discrete-time polytopic model, and use the conditions in Theorem 2 to find a stabilizing discrete-time controller for the system.

By employing the approach presented in this paper, with 20 points used in the discretization in each α_i used, we end up with 6 nonzero singular values from the HOSVD step, given by 91.429, 3.6143, 2.8729, 0.010767, 0.0021677, and 0.0012893. Another vertex system had to be considered in order to enforce the SN condition, leading to a model with 7 vertices. By making use of the CNO transformation, in order to assure better stabilization results, we arrive at a model with 7 vertices with

$$\widehat{A}_1 = \begin{bmatrix} 0.9031 & 0.0931 & 0.2816 & 0.018 \\ 0.0473 & 0.8496 & 0.009 & 0.2784 \\ -0.6201 & 0.5772 & 0.8486 & 0.1468 \\ 0.2961 & -0.9629 & 0.0734 & 0.8096 \end{bmatrix}, \tag{4}$$

$$\widehat{A}_2 = \begin{bmatrix} 0.8917 & 0.0999 & 0.2805 & 0.0189 \\ 0.0518 & 0.7322 & 0.0094 & 0.2664 \\ -0.6916 & 0.5959 & 0.8375 & 0.1531 \\ 0.3161 & -1,6783 & 0.0766 & 0.6941 \end{bmatrix}, \tag{5}$$

$$\widehat{A}_3 = \begin{bmatrix} 0.9375 & 0.0587 & 0.2851 & 0.0146 \\ 0.0304 & 0.8445 & 0.0073 & 0.2779 \\ -0.4045 & 0.3628 & 0.8819 & 0.1135 \\ 0.192 & -0.9982 & 0.0568 & 0.8043 \end{bmatrix}, \tag{6}$$

$$\widehat{A}_4 = \begin{bmatrix} 0.9242 & 0.0679 & 0.2837 & 0.0156 \\ 0.0361 & 0.7259 & 0.0078 & 0.2657 \\ -0.4878 & 0.4002 & 0.8690 & 0.1223 \\ 0.2213 & -1.7211 & 0.0611 & 0.6876 \end{bmatrix}, \tag{7}$$

$$\widehat{A}_5 = \begin{bmatrix} 0.9412 & 0.0535 & 0.2854 & 0.0141 \\ 0.0284 & 0.7960 & 0.0071 & 0.2729 \\ -0.3812 & 0.3236 & 0.8855 & 0.1085 \\ 0.1774 & -1.2986 & 0.0542 & 0.7565 \end{bmatrix}, \tag{8}$$

$$\hat{A}_6 = \begin{bmatrix} 0.9156 & 0.0784 & 0.2829 & 0.0166 \\ 0.0407 & 0.7886 & 0.0083 & 0.2722 \\ -0.5430 & 0.4755 & 0.8607 & 0.1324 \\ 0.2522 & -1.3398 & 0.0662 & 0.7495 \end{bmatrix}, \tag{9}$$

$$\hat{A}_7 = \begin{bmatrix} 0.8901 & 0.1033 & 0.2803 & 0.0191 \\ 0.053 & 0.7798 & 0.0096 & 0.2713 \\ -0.7015 & 0.6268 & 0.8360 & 0.1565 \\ 0.3268 & -1.3911 & 0.0783 & 0.741 \end{bmatrix}, \tag{10}$$

$$\hat{B}_1 = \begin{bmatrix} 0.0434 \\ 0.0008 \\ 0.2816 \\ 0.009 \end{bmatrix}, \hat{B}_2 = \begin{bmatrix} 0.0433 \\ 0.0008 \\ 0.2805 \\ 0.0094 \end{bmatrix}, \hat{B}_3 = \begin{bmatrix} 0.0436 \\ 0.0007 \\ 0.2851 \\ 0.0073 \end{bmatrix}, \tag{11}$$

$$\hat{B}_4 = \begin{bmatrix} 0.0435 \\ 0.0007 \\ 0.2837 \\ 0.0078 \end{bmatrix}, \hat{B}_5 = \begin{bmatrix} 0.0437 \\ 0.0006 \\ 0.2854 \\ 0.0071 \end{bmatrix}, \hat{B}_6 = \begin{bmatrix} 0.0435 \\ 0.0007 \\ 0.2829 \\ 0.0083 \end{bmatrix}, \tag{12}$$

$$\hat{B}_7 = \begin{bmatrix} 0.0433 \\ 0.0008 \\ 0.2803 \\ 0.0096 \end{bmatrix}. \tag{13}$$

By making use of Theorem 2, we get the control gains $K = \begin{bmatrix} -3.7189 & 10.5546 & -4.1497 & -2.4520 \end{bmatrix}$.

Figure 1 shows the system's closed loop behavior with $x_0 = \begin{bmatrix} 1 & -2 & 3 & -1 \end{bmatrix}^T$ and $\alpha = \begin{bmatrix} 0.366 & 0.0909 & 0.2718 & 0.2713 \end{bmatrix}^T$.
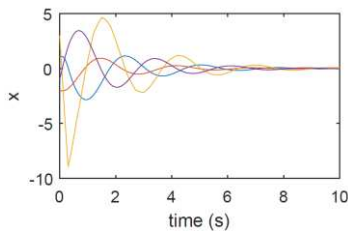
(a) States evolution over time   (b) Control input evolution over time
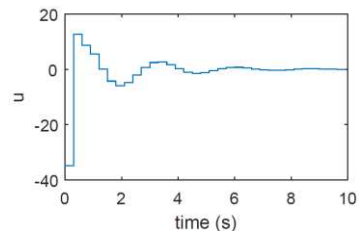
Figure 1
Closed loop behavior for the system in example 1

Example 2: Consider the 2 vertices system given in [28], described by

$$\dot{x} = \sum_{i=1}^{2} \alpha_i (A_i x + B_i \boldsymbol{u}).$$

with

$$A_1 = \begin{bmatrix} 1.8 & -0.8 \\ 3.1 & -2.15 \end{bmatrix}, A_2 = \begin{bmatrix} -a & -1.12 \\ 4.34 & -3.01 \end{bmatrix}$$

$$B_1 = \begin{bmatrix} -0.27 \\ 1.8 \end{bmatrix}, B_2 = \begin{bmatrix} -b \\ 2.4 \end{bmatrix}$$

The aim of this example is to search the parameter space of *a* and *b* and find the region under which we are able to find a stabilizing controller. We compare the region found with the one in [28] with l = 5. We make use of 100 sample points for α_1. We can see, from Figure 2, that, even though we make use of a simple condition, we are able to get better results than the ones in [28] with $l = 5$.
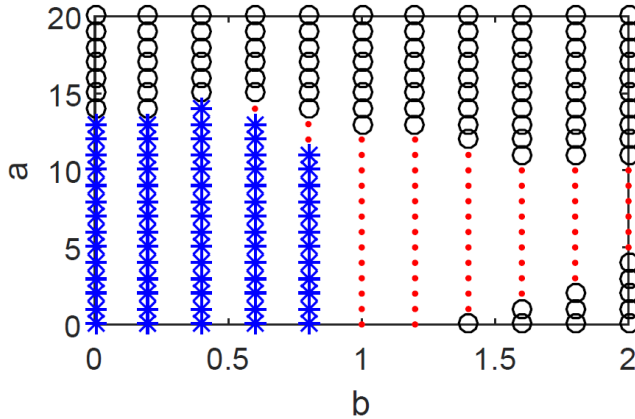
Figure 2

Stabilizable region for the *a* and *b* parameters in example 2. The asterisks determine the stabilizable region for [28] with a fifth order truncation. The asterisks and dots represent the region stabilizable for [28] with a fifth order truncation and linear search on the LMI conditions. The asterisks, dots and circles region represent the region stabilizable with the approach presented in this paper.

Conclusions and future works

This work proposed the use of the tensor product model transformation to approximate the matrix exponential function and find approximate uncertain discrete-time models for continuous-time uncertain systems with polytopic uncertainty. From the examples presented, we can see that the proposed methodology is a viable option, and allows the use of simpler LMIs for controller synthesis.

In the future, we aim to derive upper bounds on the approximation error during the sampling step of the tensor product model transformation and to make use of this upper bound in the control design in order to guarantee the continuous-time system stability when controlled by a digital controller tuned using the discrete-time model.

Referências

[1]   Y. Nesterov and A. Nemirovskii, Interior-Point Polynomial Algorithms in Convex Programming. Society for Industrial and Applied Mathematics, 1994

[2]   S. Boyd, L. E. Ghaoui, E. Feron, and V. Balakrishnan, Linear Matrix Inequalities in System and Control Theory. Society for Industrial and Applied Mathematics (SIAM), 1994

[3]   N. Vlassis and R. Jungers, "Polytopic uncertainty for linear systems: New and old complexity results," Systems & Control Letters, Vol. 67, pp. 9-13, 2014

[4]   T. Chen and B. A. Francis, Optimal Sampled-Data Control Systems. London, UK: Springer-Verlag, 1995

[5]   S. Hara, Y. Yamamoto, and H. Fujioka, "Modern and classical analysis/synthesis methods in sampled-data control — A brief overview with numerical examples," Proceedings of the 35th IEEE Conference on Decision and Control, Kobe, Japan, December 1996, pp. 1251-1256

[6]   P. Blackmore, D. Williamson, and I. Mareels, "Open-loop discretization methods for control systems design," International Journal of Control, Vol. 74, No. 15, pp. 1527-1542, 2001

[7]   T. Ono, T. Ishihara, and H. Inooka, "Design of sampled-data critical control systems based on the fast-discretization technique," International Journal of Control, Vol. 75, No. 8, pp. 572-581, 2002

[8]   L. S. Shieh, W. Wang, and G. Chen, "Discretization of cascaded continuous-time controllers and uncertain systems," Circuits, Systems and Signal Processing, Vol. 17, No. 5, pp. 591-611, October 1998

[9]   L. Hetel, J. Daafouz, and C. Iung, "LMI control design for a class of exponential uncertain systems with application to network controlled switched systems," American Control Conference, New York, NY, USA, July 2007, pp. 1401-1406

[10]   M. V. Kothare, V. Balakrishnan, and M. Morari, "Robust constrained model predictive control using linear matrix inequalities," Automatica, Vol. 32, No. 10, pp. 1361-1379, October 1996

[11]   S. Lee and S. Won, "Model Predictive Control for linear parameter varying systems using a new parameter dependent terminal weighting matrix,"

IEICE Transactions on Fundamentals of Electronics, Communications and Computer Sciences, Vol. E89-A, No. 8, pp. 2166-2172, 2006

[12]   N. Wada, K. Saito, and M. Saeki, "Model predictive control for linear parameter varying systems using parameter dependent Lyapunov function," The 2004 47th Midwest Symposium on Circuits and Systems, Vol. 53, No. 12, pp. 1446-1450, December 2006

[13]   M. Jungers, R. C. L. F. Oliveira, and P. L. D. Peres, "MPC for LPV systems with bounded parameter variations," International Journal of Control, Vol. 84, pp. 24-36, January 2011

[14]   M. F. Braga, C. F. Morais, E. S. Tognetti, R. C. L. F. Oliveira, and P. L. D. Peres, "Discretisation and control of polytopic systems with uncertain sampling rates and network-induced delays," International Journal of Control, Vol. 87, No. 11, pp. 2398-2411, November 2014

[15]   F. Amato, M. Mattei, and A. Pironti, "A note on quadratic stability of uncertain linear discrete-time systems," IEEE Transactions on Automatic Control, Vol. 43, No. 2, pp. 227-229, February 1998

[16]   M. C. de Oliveira, J. Bernussou, and J. C. Geromel, "A new discrete-time robust stability condition," System & Control Letters, Vol. 37, No. 4, pp. 261-265, July 1999

[17]   M. C. de Oliveira, J. C. Geromel, and J. Bernussou, "Extended H2 andH1 characterization and controller parametrizations for discrete-time systems," International Journal of Control, Vol. 75, No. 9, pp. 666-679, June 2002

[18]   G. Garcia, B. Pradin, S. Tarbouriech, and F. Zeng, "Robust stabilization and guaranteed cost control for discrete-time linear systems by static output feedback," Automatica, Vol. 39, No. 9, pp. 1635-1641, September2003

[19]   M. C. de Oliveira, R. C. L. F. Oliveira, and P. L. D. Peres, "A new method for robust Schur stability analysis," International Journal of Control, Vol. 83, No. 10, pp. 2181-2192, October 2010

[20]   K. J. A° stro¨m and B. Wittenmark, Computer Controlled Systems: Theory and Design. Englewood Cliffs, NJ: Prentice Hall Inc., 1984

[21]   Y. Yam, P. Baranyi, and C.-T. Yang, "Reduction of fuzzy rule base via singular value decomposition," IEEE Transactions on Fuzzy Systems, Vol. 7, No. 2, pp. 120-132, 1999

[22]   P. Baranyi, D. Tikk, Y. Yam, and R. J. Patton, "From differential equations to PDC controller design via numerical transformation, "Computers in Industry, Vol. 51, No. 3, pp. 281-297, 2003

[23]   P. Baranyi, Y. Yam, and P. V´arlaki, Tensor Product Model Transformation in Polytopic Model-Based Control. Boca Raton, FL: CRCPress - Taylor & Francis, 2013

[24]   L. De Lathauwer, B. De Moor, and J. Vandewalle, "A Multilinear Singular Value Decomposition," SIAM Journal on Matrix Analysis and Applications, Vol. 21, No. 4, p. 1253, 2000

[25]   P. Varkonyi, D. Tikk, P. Korondi, and P. Baranyi, "A new algorithm for RNO-INO type tensor product model representation," in 2005 IEEEInternational Conference on Intelligent Engineering Systems, INES'05. IEEE, 2005, pp. 263-266

[26]   P. Baranyi, "Output feedback control of 2-d aeroelastic system, "Journal of Guidance, Control, and Dynamics, Vol. 29, No. 3, pp. 762-767, 2006

[27]   V. C. S. Campos, F. Souza, L. A. B. Tôrres, and R. M. Palhares, "New stability conditions based on piecewise fuzzy Lyapunov functions and tensor product transformations," IEEE Transactions on Fuzzy Systems, Vol. PP, No. 99, pp. 1-1, 2013

[28]   M. F. Braga, C. F. Morais, E. S. Tognetti, R. C. L. F. Oliveira, and P. L. D. Peres, "A new procedure for discretization and state feedback control of uncertain linear systems," in 52nd IEEE Conference on Decision and Control, Dec 2013, pp. 6397-6402

[29]   J. Löfberg, "YALMIP: A toolbox for modeling and optimization in MATLAB," in Proceedings of the CACSD Conference, Taipei, Taiwan, 2004

[30]   P. Baranyi: „TP-Model Transformation-Based-Control Design Frameworks", Springer International Publishing Switzerland, 2016, p. 258 (eBook 978-3-319-19605-3, 978-3-319-19604-6, doi: 10.1007/978-3-319-19605-3, http://www.springer.com/gp/book/9783319196046)

[31]   A. Szollosi, P. Baranyi Influence of the Tensor Product Model Representation Of QLPV Models on The Feasibility of Linear Matrix Inequality, Asian Journal of control, 2016, pp 1328-1342

[32]   A. Szollosi, and P. Baranyi, Improved control performance of the 3-DoF aeroelastic wing section: a TP model based 2D parametric control performance optimization, Asian Journal of Control, Vol. 19, number 2, pp 450-466, 2017

[33]   A Szollosi, P. Baranyi „Influence of the Tensor Product Model Representation of qLPV Models on the Feasibility of Linear Matrix Inequality Based Stability Analysis", Asian Journal of Control, 2017 in print

Tensor Product Model-based Control Design with Relaxed Stability Conditions for Perching Maneuvers

Yingying Kan[1], Zhen He[1], Jing Zhao[2]

[1]College of Automation Engineering, Nanjing University of Aeronautics and Astronautics, No.29 Jiangjun Avenue, 211106, Nanjing, China, zdhzsy@nuaa.edu.cn, hezhen@nuaa.edu.cn

[2]School of Automation, Nanjing University of Posts and Telecommunications, No.66 Xin Mofan Road, 210003, Nanjing, China, zhaojing@njupt.edu.cn

Abstract: This paper proposed a control design approach based on tensor product models for perching maneuvers of fixed-wing aircraft. The highly nonlinear longitudinal dynamics of perching maneuvers is transformed into a tensor product model. The interpolation technique is investigated to reduce the conservatism of the convex tensor product model. The properties of the time derivatives of premise membership functions are utilized in the control design process to further reduce the control conservatism. The proposed method is demonstrated with simulation results.

Keywords: perching maneuvers; Tensor product model; Flight control; Parallel distributed compensation control

1   Introduction

Compared to rotorcraft, fixed-wing aircraft have the advantages of longer endurance, larger loading capacity and higher flight speed. However, the landing of a conventional fixed-wing aircraft usually needs a large space (e.g. a long runway), which restricts the application of fixed-wing aircraft. In nature, large birds could decelerate rapidly by performing a post-stall maneuver and eventually land on branches. Inspired by this kind of effective landing maneuver of large birds, a new landing approach for fixed-wing aircraft, i.e. the perching maneuver has been proposed and drawn more and more research attentions in recent years [1-5]. In the process of perching maneuver, a fixed-wing aircraft needs to emulate the landing maneuver of large birds, which involves rapidly decelerating by performing a very high angle-of-attack (AoA) flight and landing precisely at a prescribed perch point.

It is a challenging task to design a controller for fixed-wing aircraft performing perching maneuvers, for the aircraft dynamics is highly nonlinear and time-varying during high AoA maneuver. Studies on the control problem of perching maneuvers are relatively sparse. Stability analysis has been carried out by using contraction theory in [2]. It is shown that deviations in initial state variables will lead to trajectory divergence and prevent the aircraft from reaching the prescribed perch point [2]. In [6], a neighboring optimal control strategy has been used to cope with the perturbations from nominal trajectory. However, the simulation results show that the tolerant perturbations are too narrow [6]. In [5] and [7], a novel control synthesis approach known as LQR-Trees has been used to enlarge allowable perturbed initial conditions. In [2], a controller based on sliding-mode technique has been designed to guarantee successful perching maneuver under perturbed initial conditions.

The tensor product (TP) modeling method is a convenient and effective way to construct TP type polytopic model for nonlinear systems and therefore facilitated control design by enabling convex hull-based algorithms [8-11]. In this paper, the highly nonlinear dynamics of perching maneuvers is transformed into a linear parameter varying (LPV) model and then the corresponding TP modeling is carried out. In order to decrease the conservativeness of control design, the interpolation technique between two types of convex TP models has been investigated and the TP model with less conservativeness has been constructed. Based on the TP model, linear matrix inequality (LMI) stability conditions for the control design have derived and the system stability has been proved. In order to further reduce the conservatism of the controller, the control design process utilized the fuzzy Lyapunov functions and thusthe LMI stability conditions are more relaxed than conventional LMI stability conditions.

The paper is organized as follows: the dynamics and TP modeling of aircraft performing perching maneuvers is presented in Section 2; in Section 3, first a basic control scheme is designed and the conservatism of convex TP model is analyzed by using the interpolation technique; then parallel distributed compensation control design based on fuzzy Lyapunov functions is presented; simulation results are shown in Section 4; finally, the results of the research are concluded.

2   TP Modeling of Perching Maneuvers

This paper is focused on the longitudinal motion of perching maneuver, for this high AoA maneuver is mainly related to longitudinal variables. The longitudinal equations of motion (EOM) of fixed-wing aircraft performing perching maneuver are expressed in the wind axes as

$$\begin{cases} \dot{V} = (T\cos\alpha - D - mg\sin\gamma)/m \\ \dot{\gamma} = (T\sin\alpha + L - mg\cos\gamma)/mV \\ \dot{\alpha} = q - (T\sin\alpha + L - mg\cos\gamma)/mV \\ \dot{q} = M/I_y \\ \dot{x} = V\cos\mu \\ \dot{h} = V\sin\mu \end{cases} \tag{1}$$

where V, γ, α, q denote flight velocity, flight-path angle, angle of attack and pitch angle rate respectively; x and h represent horizontal displacement and altitude of the aircraft; m is the aircraft mass and I_y is the moment of inertia; T is the thrust; the lift L and the drag D are aerodynamic forces, and M is the aerodynamic moment.

The aerodynamic forces of the aircraft in the longitudinal plane can be written as

$$\begin{cases} L = \dfrac{1}{2}\rho V^2 S C_L \\ D = \dfrac{1}{2}\rho V^2 S C_D \end{cases} \tag{2}$$

where C_L and C_D denote the lift and drag coefficients of the aircraft respectively. ρ is the air density and S is the aerodynamic surface area of the aircraft. The aerodynamic behavior of aircraft during perching maneuvers is highly nonlinear. Combining the experimental and analytic results in [1, 2] and the plate model theory mentioned in [12], in this work the aerodynamic coefficients are given as follows:

$$\begin{cases} C_L = 0.8\sin(2\alpha) \\ C_D = 1.4(\sin\alpha)^2 + 0.1 \end{cases} \tag{3}$$

Assume that the aircraft uses an all-moving horizontal tail, so that it can acquire relatively large control moment even at low flight velocity. Then, the pitching moment is calculated as

$$M = -\frac{1}{2}\rho V^2 S_e l_e \begin{pmatrix} 0.8\cos\alpha\sin(2\alpha + 2\delta_e) + \\ 1.4\sin\alpha\sin^2(\alpha + \delta_e) + 0.1\sin\alpha \end{pmatrix} \tag{4}$$

where δ_e is the deflection angle of elevator, S_e represents the aerodynamic surface area of elevator and l_e denotes the distance from the aerodynamic center of elevator to the mass center of aircraft.

Let $X = [V, \gamma, \alpha, q]^T$ and $u = [T, \delta_e]^T$ and substitute the aerodynamic terms (2)-(4) into the equations of motion (1). Then the equations of motion (1) can be rearranged into two groups of equations as follows:

$$\dot{X} = f(X, u) \tag{5}$$

$$\begin{cases} \dot{x} = V \cos \gamma \\ \dot{h} = V \sin \gamma \end{cases} \tag{6}$$

where $f(\Box)$ is a nonlinear function vector, the specific form of which can be easily obtained from (1)-(4) and is not presented here for brevity.

The reference trajectory is assumed to be specified priori and described by (X_r, u_r), where $X_r = [V_r, \gamma_r, \alpha_r, q_r]^T$ and $u_r = [T_r, \delta_{er}]^T$, which satisfy $\dot{X}_r = f(X_r, u_r)$. Along the reference trajectory, the displacement variables x_r and h_r satisfy $\begin{cases} \dot{x}_r = V_r \cos \gamma_r \\ \dot{h}_r = V_r \sin \gamma_r \end{cases}$.

Then the control problem of perching maneuver is often treated as a trajectory tracking control problem, which means that a flight controller needs to be designed to make the actual states of the aircraft X and (x, h) to track the reference states X_r and (x_r, h_r) respectively.

Linearizing the nonlinear dynamics (5) along the reference trajectory and omitting the higher order terms would yield a LPV model, the system matrices of which are denoted as A and B. A and B depend on exogenous parameters (X_r, u_r). However, since (X_r, u_r) consists of six variables, it would be arduous to directly construct TP model. Considering that the variables in (X_r, u_r) are all functions of time, thus in the paper we express the system matrices A and B as functions of time and then we could construct the TP model by choosing the transformation space as $t \in [a_t, b_t]$. Thus the corresponding linearized model is as follows:

$$\Delta \dot{X}_r = \frac{\partial f}{\partial X}\bigg|_{\substack{X=X_r \\ u=u_r}} \Delta X_r + \frac{\partial f}{\partial u}\bigg|_{\substack{X=X_r \\ u=u_r}} \Delta u_r = \begin{bmatrix} A(t) & B(t) \end{bmatrix} \begin{bmatrix} \Delta X_r \\ \Delta u_r \end{bmatrix} \tag{7}$$

where $\Delta X_r = X - X_r$, $\Delta u_r = u - u_r$, $A(t) = \left. \dfrac{\partial f}{\partial X} \right|_{\substack{X=X_r \\ u=u_r}}$ and

$B(t) = \left. \dfrac{\partial f}{\partial u} \right|_{\substack{X=X_r \\ u=u_r}}$ .The   parameter   matrices $\left. \dfrac{\partial f}{\partial X} \right|_{\substack{X=X_r \\ u=u_r}}$ and $\left. \dfrac{\partial f}{\partial u} \right|_{\substack{X=X_r \\ u=u_r}}$ in   the

dynamics (7) depend on the variables along the reference trajectory and hence are time-varying.

Next, the TP modeling method is applied to (7) to construct the TP type ploytopic model of the perching maneuver. For the model (7), define the transformation space as $t \in \left[a_t, b_t \right]$. Discretize the space by a grid with the size of M, where M is a integer. Then the TP model transformation can be executed by using the TPtool Matlab toolbox [13]. The detailed procedure of this transformation method has been elaborated in the literatures [8-11]. The time-varying matrices in (7) can be approximated by a convex combination of linear-time-invariant (LTI) matrices, that is

$$\begin{bmatrix} A(t) & B(t) \end{bmatrix} = \sum_{i_t=1}^{J} w_{t,i_t}(t) \times \begin{bmatrix} A_{i_t} & B_{i_t} \end{bmatrix} \tag{8}$$

where A_{i_t} and B_{i_t} are constant matrices; w_{t,i_t} are weighting functions satisfying the following convex criteria [8]:

$$\begin{cases} \forall i_t, t : w_{t,i_t}(t) \in [0,1] \\ \forall i_t, t : \sum_{i_t=1}^{J} w_{t,i_t}(t) = 1 \end{cases} \tag{9}$$

3   Control Design with Relaxed Stability Conditions

3.1   Basic Controller Design and Conservatism Analysis of Convex TP Models

Before studying the conservatism reduction of the TP models, a basic controller needs to be designed to ensure the stability of the closed-loop system. Then, the conservatism of different TP models can be compared through the solvability of

the design conditions and the control performances. The structure of the basic controller is shown in Figure 1.
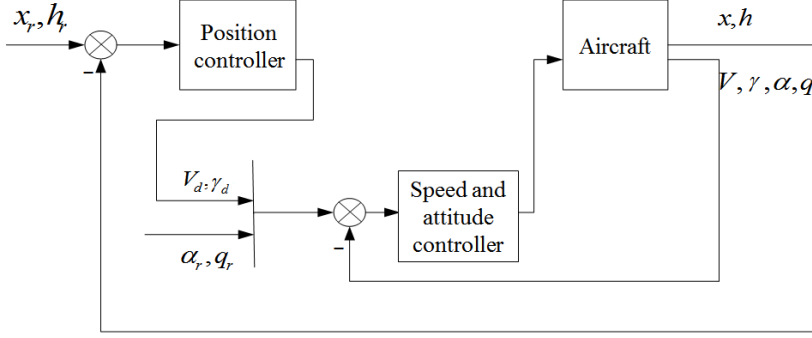
Figure 1

The basic controller structure

From (6) it can be known that the position tracking error satisfies the following relationship:

$$\begin{cases} \Delta \dot{x} = V \cos \gamma - V_r \cos \gamma_r \\ \Delta \dot{h} = V \sin \gamma - V_r \sin \gamma_r \end{cases} \tag{10}$$

where $\Delta x = x - x_r, \Delta h = h - h_r$. Suppose that the position tracking error is controlled by a proportional controller as

$$\begin{cases} \Delta \dot{x} = k_1 \Delta x \\ \Delta \dot{h} = k_2 \Delta h \end{cases} \tag{11}$$

However, the dynamics (11) cannot be implemented directly, for the actual flight speed V and the flight-path angle γ in (10) cannot responsed to commands immediately. Considering that the dynamics of position is slower than the flight speed and the flight-path angle, it is reasonable to utilize the flight speed and the flight-path determined from (10) and (11) (which are denoted as V_d and γ_d respectively) as the reference values for the actual speed and the flight-path angle. V_d and γ_d are calculated by

$$\begin{cases} V_d = \sqrt{(V_r \cos \mu_r + k_1 \Delta x)^2 + (V_r \sin \mu_r + k_2 \Delta h)^2} \\ \gamma_d = \arctan \left(\dfrac{V_r \sin \mu_r + k_2 \Delta h}{V_r \cos \mu_r + k_1 \Delta x} \right) \end{cases} \tag{12}$$

Denote $X_d = [V_d, \gamma_d, \alpha_r, q_r]$ and $\Delta X_d = X - X_d$. Then from (7) and (8), the dynamics of ΔX_d is obtained as

$$\Delta \dot{X}_d = \sum_{j=1}^{J} w_j \begin{bmatrix} A_j & B_j \end{bmatrix} \begin{bmatrix} \Delta X_d \\ \Delta u_r \end{bmatrix} \tag{13}$$

Note that the terms containing $(X_r - X_d)$ and its derivative in the dynamics of ΔX_d are neglected in (13). The speed and attitude controller is designed according to the parallel distributed compensation control scheme as follows:

$$\Delta u_r = \sum_{j=1}^{J} w_j K_j \Delta X_d \tag{14}$$

Substituting (14) into (13) yields

$$\Delta \dot{X}_d = \sum_{k=1}^{J} \sum_{j=1}^{J} w_j w_k (A_j + B_j K_k) \Delta X_d \tag{15}$$

The closed-loop TP model (15) can be rewritten into a compact form as

$$\Delta \dot{X}_d = S(p(t)) \Delta X_d \tag{16}$$

where $S(p(t)) = S \underset{n=1}{\overset{N}{)}} w_n(p_n(t))$ is the tensor expression of the coefficient matrices. Different types of convex weight functions can be chosen to derive TP model. Proper weight function type would decrease the conservatism of the system [11, 14-18]. Here the interpolation technique [11] is studied to obtain a TP model with less conservatism. The convex weight function types CNO and SNNN are considered and the corresponding convex hull expressions are as follows:

$$S(p(t)) = {}^{CNO}S \underset{n=1}{\overset{N}{)}} {}^{CNO} w_n(p_n(t)) \tag{17}$$

$$S(p(t)) = {}^{SNNN}S \underset{n=1}{\overset{N}{)}} {}^{SNNN} w_n(p_n(t)) \tag{18}$$

The discrete weighting functions of the two convex hulls as shown in (17) and (18) are interpolated as

$$^{I(\xi)} w_n^{D(\Omega,G)} = (1-\xi)^{SNNN} w_n^{D(\Omega,G)} + \xi^{CNO} w_n^{D(\Omega,G)} \tag{19}$$

where $\xi \in [0,1]$ is the interpolation coefficient and the superscript D means discrete weight function.

Then by using the pseudo tensor product model transformation, the interpolated convex hull can be obtained as

$$S(p(t)) = {}^{I(\xi)}S \sum_{n=1}^{N} {}^{I(\xi)}w_n(p_n(t)) \tag{20}$$

The gains of the parallel distributed compensation controller (14) need to be designed so that the closed-loop system is stable. Define a common Lyapunov function as $V = \Delta X_d^{\mathrm{T}} P \Delta X_d$. The following LMIs can be derived to ensure the stability of the closed-loop system:

$$
\begin{aligned}
& XA_j^T + A_j X + M_j^T B_j^T + B_j M_j < 0 \\
& XA_j^T + A_j X + XA_k^T + A_k X + M_k^T B_j^T + B_j M_k + M_j^T B_k^T + B_k M_j \le 0, \; j < k
\end{aligned}
\tag{21}
$$

where $k = 1, \ldots, J$, X is a positive definite symmetric matrix and $X = P^{-1}$, and M_k is a matrix with appropriate dimensions. The control gains are calculated as $K_k = M_k X^{-1}$.

In addition, pole placement techniques can be used to allocate closed-loop poles [19]. Define a pole region $\ell(\tau) = \{s \,|\, \mathrm{Re}(s) < -\tau < 0\}$ in the complex plane. The following LMIs guarantee that the closed-loop poles are located in region $\ell(\tau)$:

$$A_j X + X^T A_j^T + B_j M_k + M_k^T B_j^T + 2\tau X < 0, j,k = 1, \ldots, J \tag{22}$$

Solving the LMIs (21) and (22), the control gains in (14) can be determined as $K_k = M_k X^{-1}$, which guarantee both the stability and the pole location of the system. The maximum τ (which is denoted as $\tau_{\max}$) of a closed-loop system can be determined by iteratively solving the LMIs (21) and (22).

The conservatism of the convex hull (20) under different interpolation coefficients is analyzed by comparing the solvability of the above LMIs and $\tau_{\max}$. The relationship between the interpolation coefficient $\xi \in [0,1]$ and $\tau_{\max}$ is depicted in Figure 2. In Figure 2, the zero value of $\tau_{\max}$ means that the LMIs are not solvable in this case.
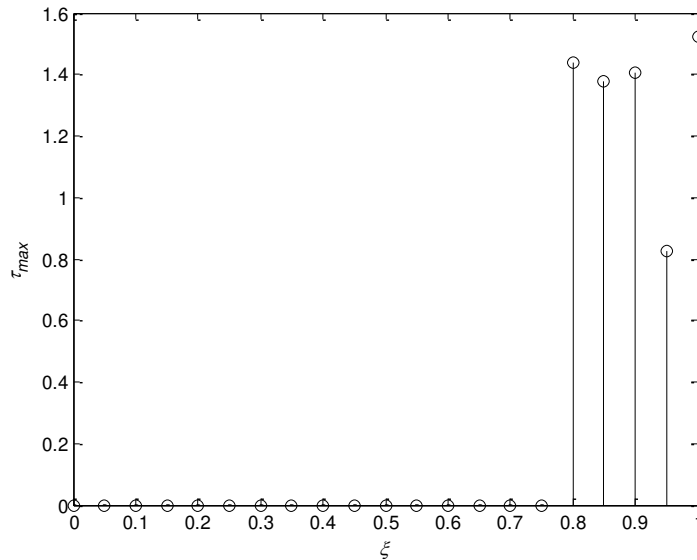
Figure 2

The relationship between ξ and τ_{max}

It can be seen from Figure 2 that the solvability of the LMIs are influenced by the interpolation coefficient ξ. When ξ is in the range of $[0.8,1]$, the LMIs (21) and (22) are solvable and the controller (14) can be obtained. In addition, τ_{max} also varies with ξ. The larger τ_{max} is, the faster the system responses. Thus, it is beneficial to choose the value of ξ corresponding to relatively large τ_{max} in the range of $[0.8,1]$. It is reasonable to think that the convex hull (20) under this chosen interpolation coefficient is less conservative.

3.2   Control Design Based on Fuzzy Lyapunov Functions

In section 3.1, the parallel distributed compensation controller (14) is designed by using common Lyapunov functions. The control design conditions (21) and (22) are derived in this way. However, control design based on common Lyapunov functions usually has strong conservatism. In order to further reduce the conservatism of the system, in this section the control design is based on fuzzy Lyapunov functions. By using fuzzy Lyapunov functions the properties of the time derivatives of premise membership functions can be exploited and therefore the LMI stability conditions can be relaxed [20-22].

The stability conditions for the perching maneuvers are presented in the following.

Consider the close-loop system (15). Assume that $\left| \dot{w}_\rho \right| \le \phi_\rho$, where ϕ_ρ is a positive real number and $\rho = 1,\ldots,J$. The closed-loop system is asymptotically stable if for some fixed $i = 1,\ldots,J$ and a scalar $\varepsilon > 0$ there exist positive definite

symmetric matrices S, Q_ρ and matrices $Z, Y_k, (k = 1, \ldots, J)$ satisfying the following LMIs:

$$Q_\rho > 0, \forall \rho \in \{1, \ldots, J\} \tag{23}$$

$$Q_\rho + S - Q_i \geq 0, \forall \rho \in \{1, \ldots, \ J\} - \{i\} \tag{24}$$

$$\begin{bmatrix} \tilde{Q}_\phi - A_j Z - Z^T A_j^T - B_j Y_j - Y_j^T B_j^T & * \\ Q_j - \varepsilon \left(A_j Z + B_j Y_j \right) + Z^T & \varepsilon \left(Z + Z^T \right) \end{bmatrix} < 0, j = 1, \ldots, J \tag{25}$$

$$\begin{bmatrix} \tilde{Q}_\phi - A_j Z - Z^T A_j^T - B_j Y_k - Y_k^T B_j^T & * \\ Q_j - \varepsilon \left(A_j Z + B_j Y_k \right) + Z^T & \varepsilon \left(Z + Z^T \right) \end{bmatrix} + \begin{bmatrix} \tilde{Q}_\phi - A_k Z - Z^T A_k^T - B_k Y_j - Y_j^T B_k^T & * \\ Q_k - \varepsilon \left(A_k Z + B_k Y_j \right) + Z^T & \varepsilon \left(Z + Z^T \right) \end{bmatrix} < 0$$
$$j < k, j, k = 1, \ldots, J$$
$$\tag{26}$$

where $\tilde{Q}_\phi = \pm \phi_i S + \sum_{\substack{\rho=1 \\ \rho \neq i}}^{J} \phi_\rho \left(Q_\rho + S - Q_i \right)$ with the symbol $\pm$ indicating that the

signs $+$ and $-$ must be tested.

The local gains can be obtained as $K_k = Y_k Z^{-1}$. The proof of LMI stability conditions (23)-(26) can be directly derived according to [22]. In LMIs (23)-(26), the values of i, ε and ϕ_ρ would influence the resulting control gains and need to be determined according to practical situation.

The controller designed by solving the LMIs (23)-(26) can guarantee the stability of the TP model. Consider that the approximation accuracy of TP model (15) is relatively high, and the time-varying model (7) can approximate the nonlinear model with relatively high accuracy if the aircraft operates near the reference trajectory. Thus, the designed controller is effective for the aircraft (described by the nonlinear model) if the aircraft operates near the reference trajectory.

4 Simulation Case

Simulations are carried out to demonstrate the effectiveness of the proposed control design method. Consider a fixed-wing aircraft with the main parameters as follows: $m = 0.8 \text{ kg}$, $I_y = 0.1 \text{ kg} \cdot \text{m}^2$, $S = 0.25 \text{ m}^2$ and $S_e = 0.054 \text{ m}^2$.

Considering the practical requirement that the thrust weight ratio of fixed-wing aircraft is less than 1 and the thrust should not below zero, the actuator constraint of the aircraft is set as $T \in [0, 7.8\text{N}]$. The transformation space of TP modeling is chosen as $t \in [0, 1.6\text{s}]$. Discretize the space by a grid with the size of $M = 100$. Then the TP model transformation can be executed by using the TPtool Matlab toolbox [13]. There are 12 nonzero singular values, the four biggest ones of which are kept. The weight functions are shown in Figure 3.
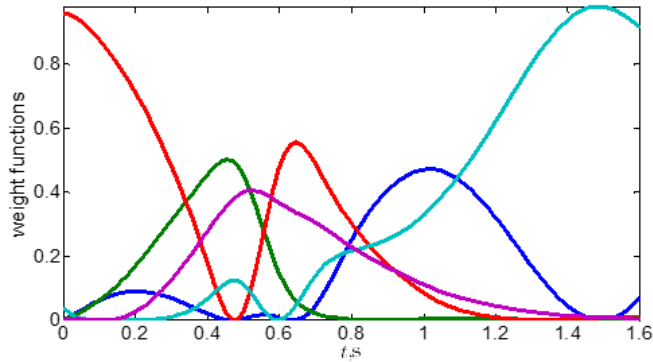
Figure 3

Weight functions

The position control gains in (11) are chosen as $k_1 = -2, k_2 = -8$. For the LMIs (23)-(26), the values of i and ε are chosen as $i = 5$ and $\varepsilon = 0.1$. The suprema of the time derivatives of premise membership functions are specified as:

$$\phi_1 = 2.1696, \phi_2 = 3.3704, \phi_3 = 5.2277, \phi_4 = 1.8306, \phi_5 = 1.6080$$

Then solve the LMIs (23)-(26) for the control gains in (14).

The initial reference states of the aircraft are set as: $V = 9.9736\text{m/s}$, $\mu = 0$, $\alpha = 0.2455rad$, $q = 0$, $x = 0$ and $h = 0$. Two kinds of simulation cases are carried out. In case 1, the initial deviation of flight speed is set as -1m/s, while in case 2, the initial deviation of flight speed is set as 1m/s. The initial error of angle of attack is set as $1°$.

In order to demonstrate the benefit of the proposed control scheme, the simulation results of the controller designed based on fuzzy Lyapunov function (the proposed control scheme) are compared with the simulation results of the controller designed based on common Lyapunov function.

First, consider the simulation case 1. The response curves of the state variables are shown in Figure 4. It can be seen from Figure 3 that, for both kinds of controllers, the angle of attack increases rapidly and the flight speed decreases from 9m/s to about 4m/s, which is relatively slow. Figure 5 shows the trajectory history of the aircraft. For both kinds of controllers, the actual trajectories can track the reference trajectory and the final position error is relatively small and acceptable

considering the size of the aircraft. However, as shown in Figure 6, the thrust command generated by the controller based on common Lyapunov function exceeds the constraint $T \in [0, 7.8N]$. Nevertheless, Figure 6 also shows that, for the controller based on fuzzy Lyapunov function, though the thrust and the elevator deflection do not converge to their reference curves, they are all kept within reasonable ranges. To some extent, this demonstrates that the proposed control design scheme for perching maneuvers is less conservative than the control design approach based on common Lyapunov functions. Thus, the simulation results demonstrate the effectiveness and benefit of the proposed controller.

The results of simulation case 2 are shown in Figure 7. It can be seen from Figure 7 that, similarly to the simulation case 1, the control command generated by the proposed controller is relatively mild, while the thrust command generated by the controller based on common Lyapunov function exceeds its constraint (in this case the thrust command is less than zero at the beginning period), though the response curves of the two kinds of controllers are similar. This verifies the benefit of using the proposed controller.
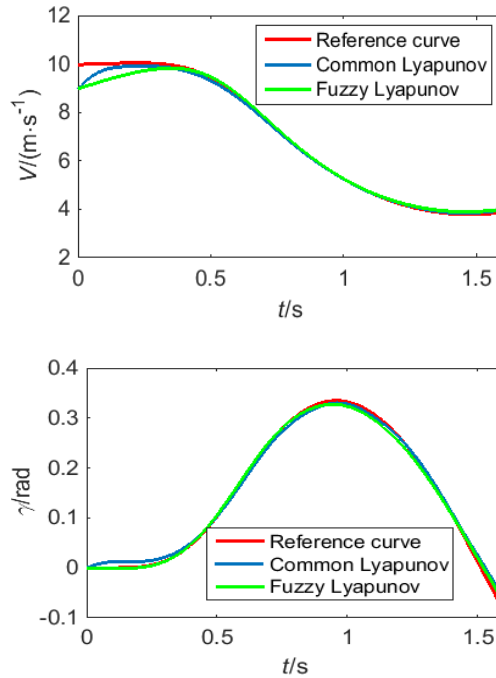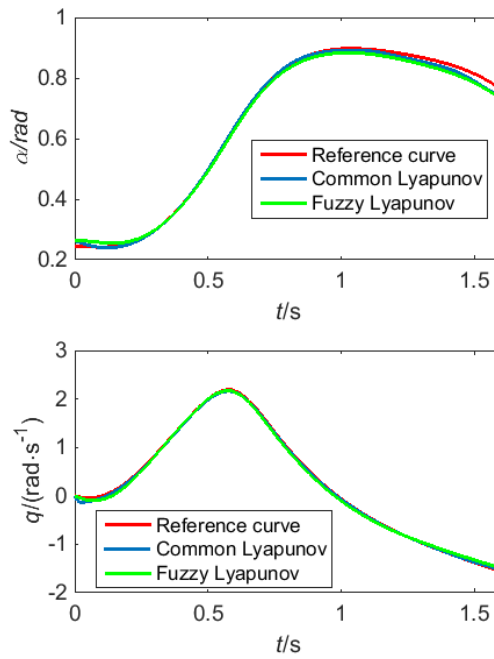
Figure 4
Response curves of the state variables in case 1
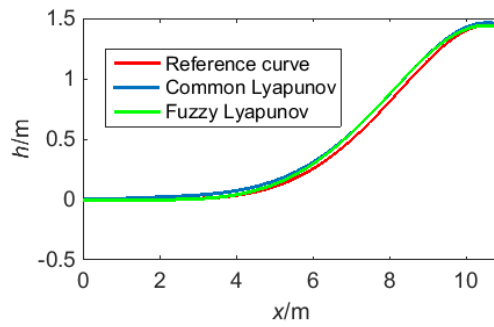
Figure 5
Trajectory history in case 1
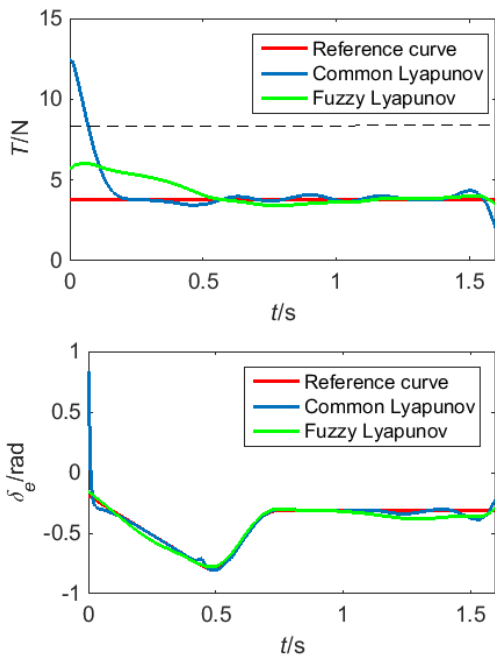
Figure 6

Control inputs in case 1
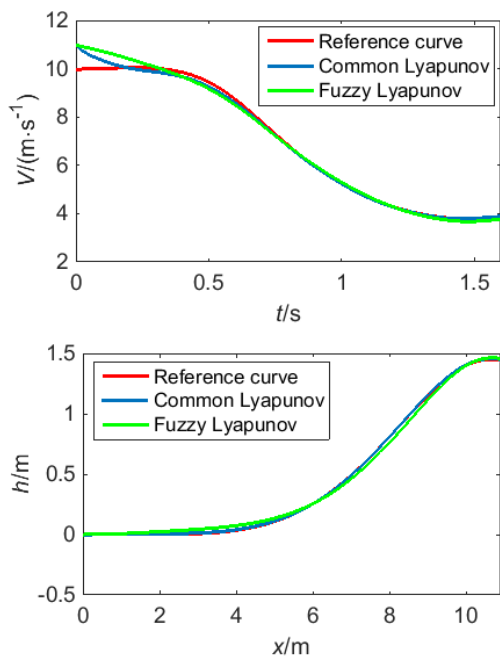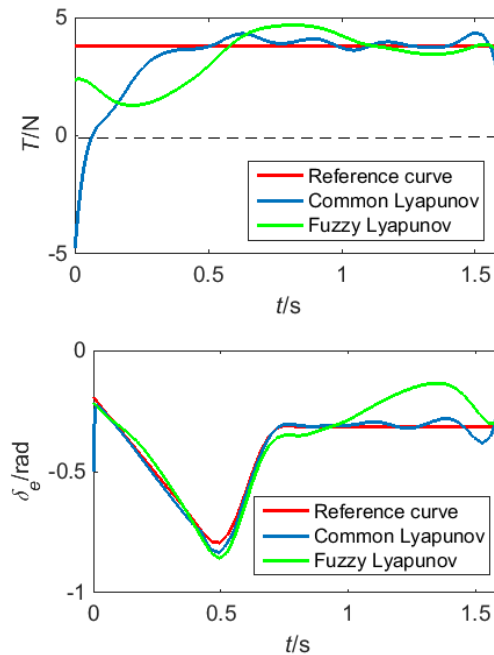
Figure 7
Response curves and inputs in case 2

Conclusions

In this paper, a tensor product model-based control design method is investigated for aircraft performing perching maneuvers. In order to decrease the conservativeness of control design, the interpolation technique between two types of convex TP models has been investigated and the TP model with less conservativeness has been constructed. The control design is carried out by using fuzzy Lyapunov functions, and the properties of the time derivatives of premise membership functions are considered in the design process. Therefore, the resulting LMI stability conditions are more relaxed than conventional LMI stability conditions. Simulation results show that the proposed control approach can ensure successful perching maneuvers, which demonstrates the effectiveness of the control design method. In addition, the simulation results of the proposed controller and the controller based on common Lyapunov function are compared, which demonstrates that the proposed controller is less conservative.

Acknowledgement

References

[1]   D. M. K. K. Venkateswara Rao, H. Tang, and T. H. Go, A parametric study of fixed-wing aircraft perching maneuvers, Aerospace Science and Technology, 42: 459-469, 2015

[2]   D. M. K. K. Venkateswara Rao, and T. H. Go, Optimization, stability analysis, and trajectory tracking of perching maneuvers, Journal of Guidance, Control, and Dynamics, 37(3): 879-888, 2014

[3]   M. AliKhan, N. K. Peyada, and T. H.Go, Flight dynamics and optimization of three-dimensional perching maneuver, Journal of Guidance, Control, and Dynamics, 36(6): 1791-1797, 2013

[4]   S. Regisford, and J. VanderMey, Perching a Minimally-Actuated Micro Air Vehicle, 51st AIAA Aerospace Sciences Meeting, Grapevine (Dallas/Ft. Worth Region), AIAA Paper 2013-0359, Jan. 2013

[5]   J. L. Moore, Robust post-stall perching with a fixed-wing UAV, Doctoral dissertation, Massachusetts Institute of Technology, 2014

[6]   S. Regisford, and Parry, An investigation into the use of neighboring optimal control in the solution of a perching problem, 51st AIAA Aerospace Sciences Meeting including the New Horizons Forum and Aerospace Exposition, Grapevine(Dallas/Ft. Worth Region), AIAA Paper 2013-0766, Jan. 2013

[7]   J. Moore, R. Cory, and R. Tedrake, Robust post-stall perching with a simple fixed-wing glider using LQR-Trees, Bioinspiration & biomimetics, 9(2): 1-15, 2014

[8]   P. Baranyi, TP model transformation as a manipulation tool for QLPV analysis and design. Asian Journal of Control, 17: 497-507, 2015

[9]   B. Takarics and P. Baranyi, Tensor-product-model-based control of a three degrees-of-freedom aeroelastic model. Journal of Guidance, Control, and Dynamics, 36: 1527-1533, 2013

[10]   P. Baranyi and B. Takarics, Aeroelastic wing section control via relaxed tensor product model transformation framework. Journal of Guidance, Control, and Dynamics, 37: 1671-1678, 2014

[11]   P. Baranyi, Y. Yam and P. Várlaki, Tensor product model transformation in polytopic model-based control. Boca Raton, Florida: CRC Press, 2013

[12]   R. E.Cory, Supermaneuverable perching, Doctoral dissertation, Massachusetts Institute of Technology, 2010

[13]   TPtool MATLAB Toolbox. Natick: MathWorks, MA, 2007

[14] P. Baranyi, The Generalized TP model transformation for T–S fuzzy model manipulation and generalized stability verification. Fuzzy Systems, IEEE Transactions on, 22: 934-948, 2014

[15] P. Baranyi, TP-Model transformation-based-control design frameworks. Springer International Publishing Switzerland, 2016 (doi: 10.1007/978-3-319-19605-3)

[16] A. Szollosi and P. Baranyi, Influence of the tensor product model representation of QLPV models on the feasibility of linear matrix inequality. Asian Journal of Control, 18(4): 1328-1342, 2016

[17] A. Szollosi and P. Baranyi, Improved control performance of the 3-DoF aeroelastic wing section: a TP model based 2D parametric control performance optimization. Asian Journal of Control, 19(2): 450-466, 2017

[18] A Szollosi and P. Baranyi, Influence of the tensor product model representation of qLPV models on the feasibility of linear matrix inequality based stability analysis, Asian Journal of Control, 2017 in print

[19] M. Chilali and P. Gahinet, H_∞ design with pole placement constraints: a LMI approach. IEEE Transactions on Automatic Control, 41: 358-367, 1996

[20] J. T. Pan, T. M. Guerra, S. M. Fei, et al. Nonquadratic stabilization of continuous T-S fuzzy models: LMI solution for a local approach. IEEE Transactions on Fuzzy Systems, 20(20):594-602, 2012

[21] B. J. Rhee, S. Won, A new fuzzy Lyapunov function approach for a Takagi--Sugeno fuzzy control system design. Fuzzy Sets & Systems, 157(9):1211-1228, 2006

[22] F. A. Faria, G. N. Silva, V. A. Oliveira, Reducing the conservatism of LMI-based stabilisation conditions for TS fuzzy systems using fuzzy Lyapunov functions. International Journal of Systems Science, 44(10): 1956-1969, 2013

Tensor Product Model-Based Control for Spacecraft with Fuel Slosh Dynamics

Hengheng Gong[1]**, Hang Sun**[2]**, Binglei Wang**[1]**, Yin Yu**[3]**, Zhen Li**[1,*]**, Xiaozhong Liao**[1]**, Xiangdong Liu**[1]

[1]School of Automation and Key Laboratory for Intelligent Control & Decision on Complex Systems, Beijing Institute of Technology, Beijing 100081, China.

[2]Shandong Institute of Aerospace Electronics Technology, Yantai, China.

[3]Science and Technology on Electronic Information Control Laboratory, Chengdu 610036, China.

Email: ghh9611@126.com; sunhang912@163.com; 1790261156@qq.com; yuyin206@163.com; zhenli@bit.edu.cn; liaoxiaozhong@bit.edu.cn; xdliu@bit.edu.cn.

[*]Corresponding author: zhenli@bit.edu.cn

Abstract: Large spacecrafts undertaking long-life mission greatly suffer from the nonlinear fuel slosh when altering the orbit or maneuvering, which leads to the downgrade on the performance and even stability of the body attitude control by unintentionally generating the huge disturbance thrust. In order to specifically address this solid-liquid coupling problem for a kind of spacecrafts when altering orbit, a nonlinear control method based on Tensor Product (TP) Model transformation is proposed to make a quick response control of the translational velocity vector and the attitude of the spacecraft. Based on the derived polytopic system from TP model transformation, the controller design can guarantee the robust against the uncertainties and disturbances for all system sets within the bounds. The proposed solution also offers an approximation tradeoff so that both the complexity of the TP model and the controller design can be dramatically minimized. The simulation results for spacecrafts with practical specification verify that the design method can make the spacecraft asymptotically stable and demonstrate the effectiveness of the proposed controller.

Keywords: Nonlinear control; TP model transformation; fuel slosh; high-order singular value decomposition.

1 Introduction

With the booming technology, the large spacecraft is undertaking more and more complicated applications with various kinds of higher requirements, which can be characterized by more on-orbit tasks and longer on-orbit time. In order to prolong

the lifetime of spacecraft and improve its stability, a large amount of liquid fuel must be carried. Hence, it will cause the fuel sloshing when the spacecraft alters the orbit or maneuvers with a partially full fuel tank. As a consequence, a disturbance torque on the spacecraft is generated by the fuel slosh. This solid-liquid coupling system presents the nonlinear and parameter time-varying characteristics. With the continuous consumption of fuel, the torque caused by slosh and the centroid offset could no longer be ignored for on-orbit tasks because the resultant huge jet thrust has an enormous impact on the stability of the attitude control, especially when the spacecraft alters its orbit. There are several typical failure experiences, which were caused by the fuel slosh [1].

To analyze and overcome this problem, the modeling is first of significance. The research on the fuel slosh model has two branches. The first one is based on the three-dimension models of various types [2, 3, 4, 5], and the second is focused on planar models [6, 7, 8, 9, 10, 11, 12, 13]. As for both of these models, the common purpose is to take place of the liquid by some masses. Thus, the dynamics can be described in an easier way. In terms of masses stated above, it can be further categorized into another two branches. For example, the slosh liquid is equivalent to a single pendulum in [2, 3, 5, 6, 8], and the other is using the mass-spring in [7, 9, 10, 11, 12, 13]. The accuracy of both analytical approaches was experimentally evaluated to estimate model parameters [15]. Currently, the problem regarding attitude maneuvers was addressed using different methods, for example, dynamic inversion and input shaping control method [2], various feedback control based on PID, linear quadratic regulator (LQR) and linear quadratic Gaussian (LQG) method [6, 7, 8, 10, 15]. Besides, a mechanical model was built based on Computational Fluid Dynamics (CFD) tools to estimate the propellant sloshing effect [11]. And a reduced-order observer was used in the full-state feedback in [12] for the estimation of the slosh states. The time-varying parameters were also considered in [13]. [16] presented a computational methodology based on Legendre's polynomials to predict the slosh and acoustic motion in nearly incompressible fluids in both rigid and flexible structures with free surface. [] However, most of these method mentioned above just designed the parameters by rule of thumb so that it was difficult to provide the best options. Besides, the computational efficiency is still a prominent issue due to the real-time numerical solving for some methods. Although some improvements have been made for the complicated application, some methods still cannot afford computational burdens for the spacecraft application because the spacecraft is significantly constrained by the on-board computational resources. Therefore, it is still desirable to develop a high efficient method in computational resources.

The tensor-product (TP) model transformation is an alternative way to solve the optimized nonlinear control problem in view of the nonlinear model transformation [17, 18, 19, 20, 21], which is a numerical method and based on the high-order singular value decomposition (HOSVD) [23, 24, 25]. Due to its universal approximation property, the TP model transformation is widely applied upon the original time varying nonlinear system. The resultant model is expressed in the convex combination form of the linear time invariant (LTI) systems. With the acquisition of the TP model, the subsequent linear controller design can be thus transformed to a convex optimization problem so that it can be numerically solved

based on a set of linear matrix inequalities (LMI). Since both the transformation and optimization can be carried out off-line in advance, the TP model transformation method is therefore effective in alleviating the on-line computation [26]. On the other hand, the number of vertices and approximation error of TP model transformation can be effectively adjusted by varying the number of retained singular values. Therefore, it can achieve a trade-off between approximation accuracy and complexity [27], which has been already used in many nonlinear controls [28, 26, 29, 30, 31, 32, 33, 34, 35, 36, 37, 38, 39, 40, 41]. Hence, it is efficient and easy to be implemented.

In this paper, the altering orbit and maneuvering in planar are taken into consideration at the same time with the huge torque in zero gravity environment. A state feedback controller based on Tensor-product (TP) model transformation is proposed for the control of the translational velocity vector and the attitude of the spacecraft. By means of the TP model transformation, the nonlinear slosh system model is transformed into the polytopic system, which can be treated as a linear convex-bounded uncertain system. Therefore, the nonlinear slosh control problem is accordingly converted into linear matrix inequality (LMI) problem based on the quadratic Lyapunov stability theory. The advantage of our solution is that the converted LMI problem can be effectively solved by convex optimization methods. In addition, the proposed controller design method is robust against the uncertainties and disturbances since the controller keeps valid for all the system sets within the convex-bounded system obtained by the TP model transformation.

The remaining part is organized as follows. In Section II, the mass-spring model is described and simplified by the elimination of a mass from [15]. The detailed TP model transformation for the nonlinear slosh system are formulated in section III. Section IV further gives the state feedback controller design and the solution via LMI. In Section V, the simulation example is presented to verify the effectiveness of the proposed control. Finally, Section VI concludes the paper.

2   The Solid-liquid Model of Fuel Slosh for Spacecrafts
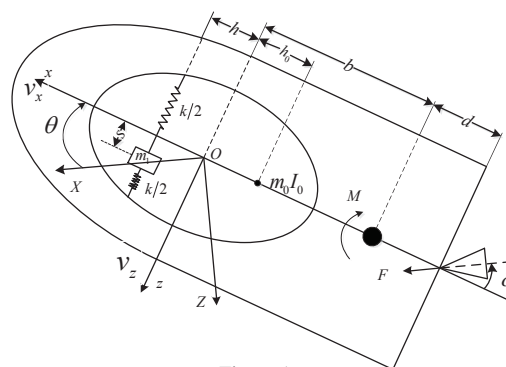

Figure 1
The slosh mass-spring model for a spacecraft

The maneuvering control problem is under study for the spacecraft with single fuel tank in a zero gravity environment during its altering orbit. By considering the

movement of the spacecraft on a plane, the spacecraft can be physically described as a mass-spring model to formulate the dynamics, which is indicated in Fig. 1.

In the axisymmetric model of Fig. 1, two coordinates of *Oxz*, *OXZ* are established as the body frame and orbit coordinate system, respectively, and θ denotes the attitude angle between these two frames. v_x, v_z are the axial and transverse components of the velocity of the center of the fuel tank. The tank with fuel is modeled by the mass-spring, which has two components, i.e., the fixed and slosh parts. The fixed part has the mass of m_0, whose moment of inertia is I_0, and the sloshed part is with the mass of m_1 joined to the tank by two springs, whose elastic coefficients are $k/2$. A restoring force $-ks$ acts on the mass m_1 whenever the relative position to the *z*-axis $s \neq 0$. The locations $h_0 > 0, h > 0$ are referenced to the center of the tank. A thrust F is produced by a gimballed thrust engine as shown in Fig. 1, where δ denotes the gimbal deflection angle and is considered as one of the control inputs. A pitching moment M is also available for the control purpose. There are some other constants in the problem statement such as the rigid spacecraft mass m, the moment of inertia I, the distance b between *z*-axis of the body coordinate and the spacecraft center of mass located along the longitudinal axis, the distance d from the gimbal pivot to the spacecraft center of mass, and the damping coefficient c of the spring.

Based on the formulation in [10], the equations of motion can be obtained as

$$(m+m_f)(\dot{v}_x + \dot{\theta}v_z) + mb\dot{\theta}^2 + m_1(s\ddot{\theta} + 2\dot{s}\dot{\theta}) = F\cos\delta \tag{1}$$

$$(m+m_f)(\dot{v}_z - \dot{\theta}v_x) + mb\ddot{\theta} + m_1(\ddot{s} - s\dot{\theta}) = F\sin\delta \tag{2}$$

$$\hat{I}\ddot{\theta} + m_1[s(\dot{v}_x + \dot{\theta}v_z) - h\ddot{s} + 2s\dot{s}\dot{\theta}] + mb(\dot{v}_z - \dot{\theta}v_x) = M + F(b+d)\sin\delta \tag{3}$$

$$m_1(\ddot{s} + \dot{v}_z - \dot{\theta}v_x - h\ddot{\theta} - s\dot{\theta}^2) + ks + c\dot{s} = 0 \tag{4}$$

where

$$\hat{I} = I + I_0 + mb^2 + m_0h_0^2 + m_1(h^2 + s^2), m_f = m_0 + m_1.$$

Because the thruster F is quite large during altering orbit, it is reasonable to ignore the fuel slosh dynamics along *x*-axis such as the second order terms in (1). Besides, it is further assumed that the axial acceleration term $\dot{v}_x + \dot{\theta}v_z$ is insignificantly changed since the θ and δ vary within a small range compared with the impact from the thruster F along *x*-axis [10]. Consequently, the equation of (1) becomes,

$$\dot{v}_x + \dot{\theta}v_z = \frac{F}{m+m_f}$$

Let

$$\begin{bmatrix} u_1 \\ u_2 \end{bmatrix} = D^{-1} \begin{bmatrix} F\sin\delta - m_1(\ddot{s} - s\dot{\theta}) \\ M + F(b+d)\sin\delta - m_1[s(\frac{F}{m+m_f}) - h\ddot{s} + 2s\dot{s}\dot{\theta}] \end{bmatrix}$$

where

$$D = \begin{bmatrix} m+m_f & mb \\ mb & \hat{I} \end{bmatrix}$$

By the transformation from (δ, M) to two new control inputs (u_1, u_2), the system(1)-(4) can be rewritten as,

$$\dot{v}_z = \dot{\theta} v_x(t) + u_1 \tag{5}$$

$$\ddot{\theta} = u_2 \tag{6}$$

$$\ddot{s} = -\omega^2 s - 2\xi \omega \dot{s} + s\dot{\theta}^2 - u_1 + h u_2 \tag{7}$$

where $\omega^2 = \frac{k}{m_1}, 2\xi\omega = \frac{c}{m_1}$, ω and ξ denote the undamped natural frequencies and damping ratios, respectively. Define the state variable $\boldsymbol{x} = \begin{bmatrix} \theta & \dot{\theta} & s & \dot{s} & v_z \end{bmatrix}^T$ and the whole system can be formulated by

$$\boldsymbol{x} = \boldsymbol{f}(\boldsymbol{x}, t) + \boldsymbol{b}(\boldsymbol{x}, t)\boldsymbol{u}, \tag{8}$$

where

$$\boldsymbol{f}(\boldsymbol{x}, t) = \begin{bmatrix} \theta \\ 0 \\ \dot{s} \\ -\omega^2 s - 2\xi \omega \dot{s} + s\dot{\theta}^2 \\ \dot{\theta} v_x(t) \end{bmatrix}, \text{ and} \tag{9}$$

$$\boldsymbol{b}(\boldsymbol{x}, t) = \begin{bmatrix} 0 & 0 \\ 0 & 1 \\ 0 & 0 \\ -1 & h \\ 1 & 0 \end{bmatrix}$$

With the model built above, the control objective is thus to design a nonlinear controller to accomplish a given planar maneuver. The equilibrium state $\boldsymbol{x}^{eq} = \begin{bmatrix} \theta^{eq} & 0 & 0 & 0 & v_z^{eq} \end{bmatrix}$ and v_x^{eq}. Without loss of generality, $v_z^{eq} = 0, \theta^{eq} = 0$, so the equilibrium point is $\boldsymbol{x} = \boldsymbol{x}^{eq} = \boldsymbol{0}, v_x = v_x^{eq}$.

3 TP Model Transformation for the Nonlinear Slosh System of Spacecrafts

This section transforms the nonlinear slosh system of spacecrafts into the polytopic system by using TP model transformation, based on which the nonlinear slosh control problem can be converted into linear matrix inequality (LMI) problem.

Consider the dynamical system modeled in state-space form

$$\dot{\boldsymbol{x}}(t) = \boldsymbol{A}(\mathbf{p}(t))\boldsymbol{x}(t) + \boldsymbol{B}(\mathbf{p}(t))\boldsymbol{u}(t) \tag{10}$$

where $\boldsymbol{u}(t) \in \mathbb{R}^l$ and $\boldsymbol{x}(t) \in \mathbb{R}^m$ are the input and state vectors, respectively. The system matrix is $\mathbf{S}(\mathbf{p}(t)) = \begin{bmatrix} \boldsymbol{A}(\mathbf{p}(t)) & \boldsymbol{B}(\mathbf{p}(t)) \end{bmatrix} \in \mathbb{R}^{m \times (m+l)}$, where $\mathbf{p}(t) \in \mathbb{R}^N$ is time varying in the N-dimension bounded space $\Omega \in \mathbb{R}^N$. Further, the parameter

$\mathbf{p}(t)$ may include some or all elements of $\boldsymbol{x}(t)$. Assume that there is a fixed polytope satisfying

$$\mathbf{S}(\mathbf{p}(t)) \in \{\mathbf{S}_1, \mathbf{S}_2, \ldots, \mathbf{S}_I\} = \{\sum_{i=1}^{I} \alpha_i S_i, \alpha_i \geq 0, \sum_{i=1}^{I} \alpha_i = 1\} \tag{11}$$

where the systems $\mathbf{S}_1, \mathbf{S}_2, \ldots, \mathbf{S}_I$ are the vertex systems of $\mathbf{S}(\mathbf{p}(t))$. When the values α_i are considered as the basis functions $w_i(\mathbf{p}(t))$,

$$\mathbf{S}(\mathbf{p}(t)) \approx \sum_{i=1}^{I} w_i(\mathbf{p}(t))\mathbf{S}_i.$$

With the approximation of $\mathbf{S}(\mathbf{p}(t))$ above, the dynamical system (10) takes the form

$$\dot{\boldsymbol{x}}(t) = \sum_{i=1}^{I} w_i(\mathbf{p}(t))(\boldsymbol{A}_i\boldsymbol{x}(t) + \boldsymbol{B}_i\boldsymbol{u}(t)) \tag{12}$$

When the basis functions are decomposed for all dimensions to get a high order approximate decomposition, the TP model takes the form as

$$\mathbf{S}(\mathbf{p}(t)) \approx \sum_{i_1=1}^{I_1} \sum_{i_2=1}^{I_2} \cdots \sum_{i_N=1}^{I_N} \prod_{n=1}^{N} w_{n,i_n}(p_n(t))S_{i_1,i_2,\ldots i_N} = \left(\mathscr{S} \boxtimes_{n=1}^{N} \boldsymbol{w}_n(p_n(t))\right) \tag{13}$$

where the values $p_n(t)$ are the elements of $\mathbf{p}(t)$ and normalized as below

$$\left\{\forall n, p_n(t) : \sum_{i_n=1}^{I_n} w_{n,i_n}(p_n(t)) = 1, \forall i, n, p_n(t) : w_{n,i}(p_n(t)) \geq 0\right\}.$$

Therefore, the system (10) can be transformed into

$$\dot{\boldsymbol{x}}(t) \approx \left(\mathscr{S} \boxtimes_{n=1}^{N} \boldsymbol{w}_n(p_n(t))\right) \begin{pmatrix} \boldsymbol{x}(t) \\ \boldsymbol{u}(t) \end{pmatrix}$$

Accordingly, the remaining objective comes to how to solve the tensor $\mathscr{S}$ and the vector $\boldsymbol{w}_n(p_n(t))$. Before the detailed demonstration of TP model transformation, various types of TP model will be discussed at first in the following subsection.

3.1   The Consideration of TP Model Types

The TP model for a given system is highly dependent on the construction of the weighting matrices regardless of the permutation of the vertices and the weighting functions. If satisfying the sum normalization (SN) and non-negative (NN) conditions, which ensure the convexity and are the necessities to the LMI-based methods, the TP model can be classified into the Normal (NO) type, close to the NO (CNO) type, the Inverted and Relaxed Normal (IRNO) type, and so on [22].

The feasibility of the LMIs solution is verified to be very sensitive to the structure of the TP model. It is obvious that the NO type is the most ideal candidate since it is as exact as the tight convex hull of the sampled system. However, it is impractical to obtain a strict NO result in the case of the limited number of the vertices. To address this issue, it is desirable to obtain a TP model in CNO type. However, the CNO variant of the TP model is again not unique and different CNO variants suffer from various degrees of conservativeness. Furthermore, in the case of INO-RNO type, it is guaranteed that the resultant vertex systems contributing in the convex combination have equal distance to the system matrix $\mathbf{S}(\mathbf{p}(t))$ in space $\mathbf{\Omega}$. Actually, the optimization for various types and their proper selection are still under discussion specific to different applications.

This paper focuses on the application of TP model transformation into the practical aerospace control system, which features in the nonlinear characteristics. The optimization for one certain TP model types is not the main focus. Therefore, the INO-RNO type is applied in this paper to carry out the TP model transformation due to its feasibility.

3.2   The Implementation of TP Model Transformation

By using the INO-RNO type TP model representation [22, 42], the polytopic approximation can be calculated in the following steps. Assume the parameter $\mathbf{p}(t)$ varies within the bounded space $\mathbf{\Omega} = [a_1 \quad b_1] \times [a_2 \quad b_2] \times \cdots \times [a_N \quad b_N] \subset \mathbb{R}^N$.

Step 1) Sampling the given functions over a hyper rectangular grid.

Define grid lines over Ω on each vectors to get an N dimensional hyper rectangular grid. A simplest way is to set the lines evenly spaced, $g_{n,m_n} = a_n + \frac{b_n - a_n}{M_n - 1}(m_n - 1), m_n = 1, 2, \ldots, M_n$. Then, calculate the system matrix $\mathbf{S}(\mathbf{p}(t))$ using the values sampled over the grid points $\mathbf{S}^D_{m_1, m_2, \ldots, m_n} = \mathbf{S}(\mathbf{p}_{m_1, m_2, \ldots, m_n}) \in \mathbb{R}^{m \times (m+l)}$. where $\mathbf{p}_{m_1, m_2, \ldots, m_n} = (g_{1, m_1}, g_{2, m_2}, \ldots, g_{N, m_N})$, and $\forall n : m_n = 1, 2, \ldots, M_n$. Next, using the tensor $\mathscr{S}^D \in \mathbb{R}^{M_1 \times M_2 \times \cdots \times M_N \times m \times (m+l)}$ to store the sampled value, $(\mathscr{S}^D)_{m_1, m_2, \ldots, m_n} = \mathbf{S}^D_{m_1, m_2, \ldots, m_n}$.

Step 2) Computing the vertex systems matrices.

The HOSVD is executed to decompose $\mathscr{S}$ as

$$\mathscr{S}^D = \mathscr{S} \boxtimes_{n=1}^N \mathbf{U}_n. \tag{14}$$

After the decomposition, the tensors $\mathscr{S} \in \mathbb{R}^{I_1 \times I_2 \times \cdots \times I_N}, \mathbf{U}_n \in \mathbb{R}^{M_n \times I_n}$ and $I_n = rank_n(\mathscr{S}^D) \leq M_n$, because of the ignorance of zero singular values. All the vertex systems $\mathbf{S}_{m_1, m_2, \ldots, m_n}$ can be obtained by using the processing according to the equation (13).

Step 3) Basis system normalization.

Normalize U_n to $\overline{U_n}$ for satisfying the following conditions, which is described by

$$\sum (\overline{U_n}) = 1_{J_n},$$
$$\overline{u}_{n, j_n, k_n} \geq 0,$$

where 1_{J_n} is J_n dimensional column vector with all entries being 1.

Step 4) Basis function.

The values of the basis functions sampled over the grid points can be obtained by comparing the equations of (13) and (14)

$$w_{n,i_n}(g_n, m_n) = (\mathbf{U}_n)_{m_n, i_n} \tag{15}$$

So far, the TP model transformation is completed. $w_{n,i_n}(g_n, m_n)$ is used to approximate the $w_{n,i_n}(p_n(t))$ over each subsection so that the bilinear approximation of $\mathbf{S}(\mathbf{p}(t))$ is achieved.

4   Slosh Controller Design

Based on the TP model transformation for the nonlinear slosh system, this section presents the corresponding controller design.

Lemma 1. *If a common matrix* $\mathbf{P} > 0$ *exists for all vertex systems with the condition*

$$A_r^T \mathbf{P} + \mathbf{P} A_r < 0, r = 1, 2, \ldots, R. \tag{16}$$

Then, the equilibrium of TP model is globally and asymptotically stable.

Theorem 1. *Consider the nonlinear system* (8) *and its polytopic approximation* (12)*, if there exist matrix* $\mathbf{X} > 0$ *and matrices* $\mathbf{M_r}$, $r = 1, 2, \ldots, R$ *solving the following linear matrix inequalities:*

$$-\mathbf{X} A_r^T - A_r \mathbf{X} + \mathbf{M}_r^T \mathbf{B}_r^T + \mathbf{B}_r \mathbf{M}_r > 0, r = 1, 2, \ldots, R \tag{17}$$

$$-\mathbf{X} A_r^T - A_r \mathbf{X} - \mathbf{X} A_s^T - A_s \mathbf{X} + \mathbf{M}_s^T \mathbf{B}_r^T + \mathbf{B}_r \mathbf{M}_s + \mathbf{M}_r^T \mathbf{B}_s^T + \mathbf{B}_s \mathbf{M}_r \geq 0, 1 \leq r < s \leq R \tag{18}$$

then the continuous system is globally and asymptotically stable at the equilibrium by using the control input:

$$\boldsymbol{u}(t) = - \left(\sum_{r=1}^{R} w_r(\mathbf{p}(t)) \mathbf{F}_r \right) \boldsymbol{x}(t), \tag{19}$$

where $\mathbf{F}_r = \mathbf{M}_r \mathbf{X}^{-1}$.

Proof:

By considering (19), (12) can be rewritten as

$$\dot{\boldsymbol{x}}(t) = \sum_{r=1}^{R} \sum_{s=1}^{R} w_r(\mathbf{p}(t)) w_s(\mathbf{p}(t)) (A_r - \mathbf{B}_r \mathbf{F}_s) \boldsymbol{x}(t). \tag{20}$$

With the assistance of defining a new matrix $\mathbf{G}_{r,s} = A_r - \mathbf{B}_r \mathbf{F}_s$, in order to satisfy the condition of *Lemma 1*, there must have $\mathbf{G}_{r,s}^T \mathbf{P} + \mathbf{P} \mathbf{G}_{r,s} < 0, r, s = 1, 2, \ldots, R$. However,

this is a sufficient but not necessary condition. By the dedicated consideration of the control and calculation time, (20) can be divided into two components

$$\dot{\boldsymbol{x}}(t) = \sum_{r=1}^{R} w_r(\mathbf{p}(t))w_r(\mathbf{p}(t))\boldsymbol{G}_{r,r}\boldsymbol{x}(t) + \sum_{r=1}^{R}\sum_{s=r+1}^{R} w_r(\mathbf{p}(t))w_s(\mathbf{p}(t))\left(\boldsymbol{G}_{r,s} + \boldsymbol{G}_{s,r}\right)\boldsymbol{x}(t).$$

The continuous system is globally and asymptotically stable in the large at the equilibrium if both parts satisfy *Lemma 1*. That is

$$\boldsymbol{G}_{r,r}^{T}\mathbf{P} + \mathbf{P}\boldsymbol{G}_{r,r} < 0, \tag{21}$$

and

$$(\boldsymbol{G}_{r,s} + \boldsymbol{G}_{s,r})^{T}\mathbf{P} + \mathbf{P}(\boldsymbol{G}_{r,s} + \boldsymbol{G}_{s,r}) < 0, \tag{22}$$

where $r = 1, 2, \ldots, R$ and $r < s \leq R$.

Hence, $\boldsymbol{F}_r$ needs to be further determined to satisfy the condition of *Lemma 1* regarding a common positive-definite matrix $\mathbf{P}$.

Define two new variables $\boldsymbol{X} = \mathbf{P}^{-1} > 0$ and $\boldsymbol{M}_r = \boldsymbol{F}_r\boldsymbol{X}$, and then multiply the inequalities of (21) and (22) on the left-hand side by $\boldsymbol{X}$, we can get

$$-\boldsymbol{X}\boldsymbol{A}_r^{T} - \boldsymbol{A}_r\boldsymbol{X} + \boldsymbol{M}_r^{T}\boldsymbol{B}_r^{T} + \boldsymbol{B}_r\boldsymbol{M}_r > 0, \tag{23}$$

$$-\boldsymbol{X}\boldsymbol{A}_r^{T} - \boldsymbol{A}_r\boldsymbol{X} - \boldsymbol{X}\boldsymbol{A}_s^{T} - \boldsymbol{A}_s\boldsymbol{X} + \boldsymbol{M}_s^{T}\boldsymbol{B}_r^{T} + \boldsymbol{B}_r\boldsymbol{M}_s + \boldsymbol{M}_r^{T}\boldsymbol{B}_s^{T} + \boldsymbol{B}_s\boldsymbol{M}_r \geq 0. \tag{24}$$

By means of the transformation from equations(21)-(22) to equations(23)-(24), the design is turned into an LMI problem,any other details could be found in [43]. The conditions are jointly convex in $\boldsymbol{X}$ and $\boldsymbol{M_r}$. Therefore, the positive-defined matrix $\boldsymbol{X}$ and $\boldsymbol{M_r}$ needs to be found in order to satisfy the conditions. Numerically, the computation of this problem can be efficiently solved by many available mathematical tools.

Remark. The main objective of this proposed control is to extend the practical application of TP model transformation into fuel slosh problem of spacecraft. Therefore, the simple model in [10] was applied. Although its polytopic model can be derived easily, the corresponding TP model transformation has more general application in practice. The design demonstrates the application of TP model transformation. It is also effective for the model more complex, e.g., multi-mass spring, which gives a higher accurate model information.

5   Verification with Numerical Simulation

The physical parameters of the spacecraft with fuel slosh used in this part are given in Table 1.

Table 1
Physical Parameters

Parameter	Value	Parameter	Value
m	$300kg$	F	$1200N$
m_0	$50kg$	b	$0.6m$
m_1	$20kg$	d	$0.4m$
h_0	$0.1m$	h	$0.15m$
k	$72N/m$	c	$8N \cdot m$
I	$500kg \cdot m^2$	I_0	$7.5N \cdot m^2$

And $f(x,t)$ in (8) can be rewritten as $f(x,t) = A(x,t)x$, where

$$A(x,v_x(t)) = \begin{bmatrix} 0 & 1 & 0 & 0 & 0 \\ 0 & s & -\dot{\theta} & 0 & 0 \\ 0 & 0 & 0 & 1 & 0 \\ 0 & s\dot{\theta} & -\omega^2 & -2\xi\omega & 0 \\ 0 & v_x(t) & 0 & 0 & 0 \end{bmatrix}.$$

So the system (8) becomes

$$\dot{x}(t) = A(x,v_x(t))x(t) + Bx(t). \tag{25}$$

Compared to the equation of (10), it is a special case with the constant matrix B. A simplified system matrix is chosen so as to reduce the computational burden by $S(\mathbf{p}(t)) = A(x,v_x(t))$, where $\mathbf{p}(t) = x_2, x_3, v_x(t)$.

As the $A(x,v_x(t))$ is a state-dependent matrix, this form won't be accompanied by an unique solution and there are many matrices matching the equation of (25). However, the selection of $A(x,t)$ will affect the controlled results and the computation complexity. Here, the value of $A(x,t)$ depends on three states, i.e., $\dot{\theta}$, s and $v_x(t)$.

As described in Section III, the first step is undertaken to sample the states above over a hyper rectangular grid. Here, give a rectangular grid in experience via many simulations.

$$s_i = -1 + 0.15i, \qquad\qquad i = 1,2,\ldots,13.$$
$$v_{x,j} = 10 + 20j, \qquad\qquad j = 1,2,\ldots,20.$$
$$\dot{\theta}_k = -2.2 + 0.2k, \qquad\qquad k = 1,2,\ldots,22.$$

It turns out that the ranks of all the three dimensions are 2. Thus, by removing all the zero singular values in the step 2 of the TP model transformation, 8 vertex systems are remained,

$$A_1 = \begin{bmatrix} 0 & 1 & 0 & 0 & 0 \\ 0 & -1 & 2.2 & 0 & 0 \\ 0 & 0 & 0 & 1 & 0 \\ 0 & 2.2 & -1.8 & -0.2 & 0 \\ 0 & 10 & 0 & 0 & 0 \end{bmatrix}, \quad A_2 = \begin{bmatrix} 0 & 1 & 0 & 0 & 0 \\ 0 & -1 & 2.2 & 0 & 0 \\ 0 & 0 & 0 & 1 & 0 \\ 0 & 2.2 & -1.8 & -0.2 & 0 \\ 0 & 390 & 0 & 0 & 0 \end{bmatrix},$$

$$
\boldsymbol{A}_3 = \begin{bmatrix} 0 & 1 & 0 & 0 & 0 \\ 0 & 0.95 & -2.2 & 0 & 0 \\ 0 & 0 & 0 & 1 & 0 \\ 0 & 2.09 & -1.8 & -0.2 & 0 \\ 0 & 390 & 0 & 0 & 0 \end{bmatrix}, \quad
\boldsymbol{A}_4 = \begin{bmatrix} 0 & 1 & 0 & 0 & 0 \\ 0 & 0.95 & -2.2 & 0 & 0 \\ 0 & 0 & 0 & 1 & 0 \\ 0 & 2.09 & -1.8 & -0.2 & 0 \\ 0 & 10 & 0 & 0 & 0 \end{bmatrix},
$$

$$
\boldsymbol{A}_5 = \begin{bmatrix} 0 & 1 & 0 & 0 & 0 \\ 0 & -1 & -2.2 & 0 & 0 \\ 0 & 0 & 0 & 1 & 0 \\ 0 & -2.2 & -1.8 & -0.2 & 0 \\ 0 & 10 & 0 & 0 & 0 \end{bmatrix}, \quad
\boldsymbol{A}_6 = \begin{bmatrix} 0 & 1 & 0 & 0 & 0 \\ 0 & -1 & -2.2 & 0 & 0 \\ 0 & 0 & 0 & 1 & 0 \\ 0 & -2.2 & -1.8 & -0.2 & 0 \\ 0 & 390 & 0 & 0 & 0 \end{bmatrix},
$$

$$
\boldsymbol{A}_7 = \begin{bmatrix} 0 & 1 & 0 & 0 & 0 \\ 0 & 0.95 & 2.2 & 0 & 0 \\ 0 & 0 & 0 & 1 & 0 \\ 0 & -2.09 & -1.8 & -0.2 & 0 \\ 0 & 390 & 0 & 0 & 0 \end{bmatrix}, \quad
\boldsymbol{A}_8 = \begin{bmatrix} 0 & 1 & 0 & 0 & 0 \\ 0 & 0.95 & 2.2 & 0 & 0 \\ 0 & 0 & 0 & 1 & 0 \\ 0 & -2.09 & -1.8 & -0.2 & 0 \\ 0 & 10 & 0 & 0 & 0 \end{bmatrix},
$$

$\boldsymbol{B}_{1-8} = \boldsymbol{B}$.

The coefficient functions w_r in equation (19) can be obtained by step 4 with 3 components ($w_r = w_s w_{v_x} w_{\dot{\theta}}$) as follows. And $\boldsymbol{F}_r = \boldsymbol{M}_r \boldsymbol{X}^{-1}$ can be accordingly computed
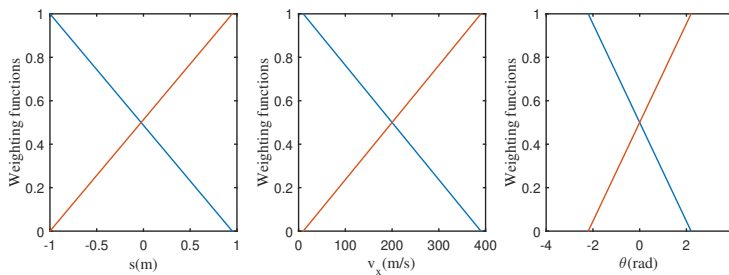
Figure 2
Three components of w_r.

by equations (23)-(24).

$$F_1 = \begin{bmatrix} 0.0394 & 22.7069 & -0.7180 & 0.3030 & 0.2137 \\ 0.1244 & 2.5719 & 4.4376 & 2.0346 & -1.1604 \end{bmatrix},$$

$$F_2 = \begin{bmatrix} 0.0324 & -4.9377 & -2.9289 & -0.6519 & 1.4266 \\ 0.1129 & 0.7964 & -3.9113 & -0.4062 & 1.2638 \end{bmatrix},$$

$$F_3 = \begin{bmatrix} 0.1002 & 406.0724 & 4.2298 & 14.7410 & 1.7203 \\ 0.2299 & 10.7266 & 15.7007 & 34.8356 & 2.1560 \end{bmatrix},$$

$$F_4 = \begin{bmatrix} 0.0933 & 378.4343 & 2.0207 & 13.7864 & 2.9328 \\ 0.2184 & 8.9377 & 7.3511 & 32.3958 & 4.5811 \end{bmatrix},$$

$$F_5 = \begin{bmatrix} 0.0389 & 23.5300 & -0.7281 & 0.1577 & 0.1643 \\ 0.1234 & 4.4683 & 4.4233 & 1.7040 & -1.2780 \end{bmatrix},$$

$$F_6 = \begin{bmatrix} 0.0333 & -4.0324 & -2.8251 & -0.4707 & 1.4099 \\ 0.1143 & 2.8825 & -3.6701 & 0.0050 & 1.2209 \end{bmatrix},$$

$$F_7 = \begin{bmatrix} 0.0997 & 406.9042 & 4.2245 & 14.5948 & 1.6669 \\ 0.2290 & 12.6282 & 15.6873 & 34.5060 & 2.0383 \end{bmatrix},$$

$$F_8 = \begin{bmatrix} 0.0940 & 379.2346 & 2.1306 & 13.9589 & 2.9087 \\ 0.2196 & 11.0320 & 7.5916 & 32.7891 & 4.5341 \end{bmatrix}.$$

By considering the influence of fuel burn into the parameters, the simulation time is chosen as 100 s and the altering thrust is stopped at 80 s. During this time slot, it is assumed that the fuel mass m_0 and m_1 are constant. Time responses shown in Fig. 3 to Fig. 5 correspond to the initial conditions of $\theta_0 = 0.55rad$, $\dot{\theta}_0 = 0$, $s_0 = 0.1m$, $\dot{s}_0 = 0$, $v_{z0} = 20m/s$. It can be seen from Fig. 3 and Fig. 4, the transverse velocity
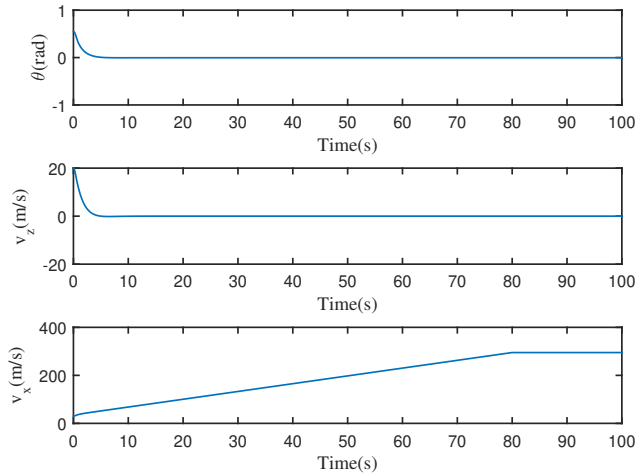
Figure 3
Time response of θ, v_z and v_x

v_z, the attitude angle θ, the slosh state s converge to the relative equilibrium at zero
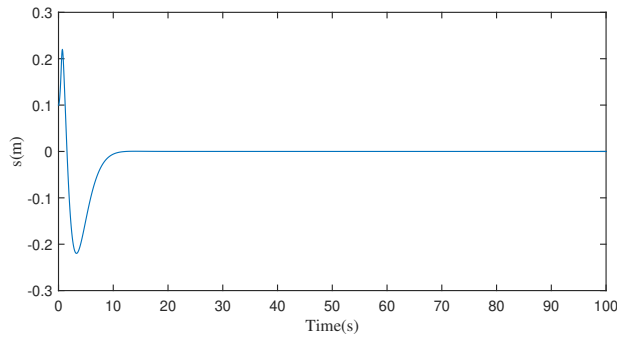
Figure 4
Time response of slosh state s.
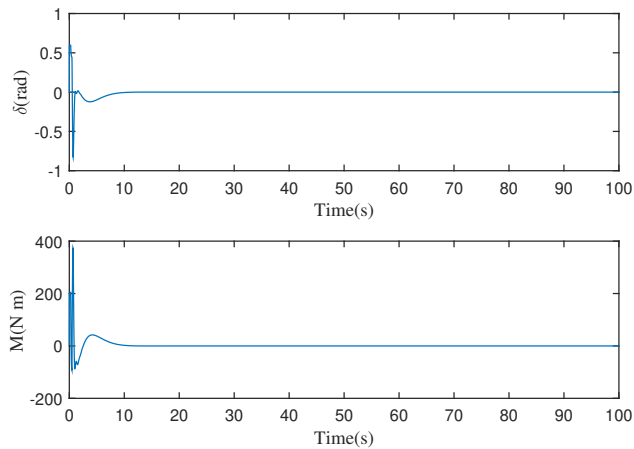
Figure 5
The inputs gimbal deflection angle δ and pitching moment M.

and v_x increases as an uniformly accelerated motion. During the orbital transfer, the controller can stabilize the spacecraft within a time as short as 15 seconds.

Furthermore, a nonlinear direct feedback controller is developed for the comparison in performance such as the response time and overshot, the details of which were summarized and can be referred in [8, 9, 10]. The corresponding direct feedback controller is designed as follows.

$$
\begin{aligned}
u_1 &= -2000 \left[5 \times 10^{-5} v_z - 0.002(s - h\dot{\theta}) \right], \\
u_2 &= -\frac{1}{10 - 0.002h^2} \left[80\theta + 1000\dot{\theta} + 5 \times 10^{-5} v_x v_z + \right. \\
&\quad \left. 0.002(hs\omega^2 + h\dot{s}\xi + s\dot{s}\dot{\theta} - h\dot{\theta}^2 s) \right].
\end{aligned}
\tag{26}
$$

The objective of the slosh controller is to alleviate the impact from the fuel slosh dy-
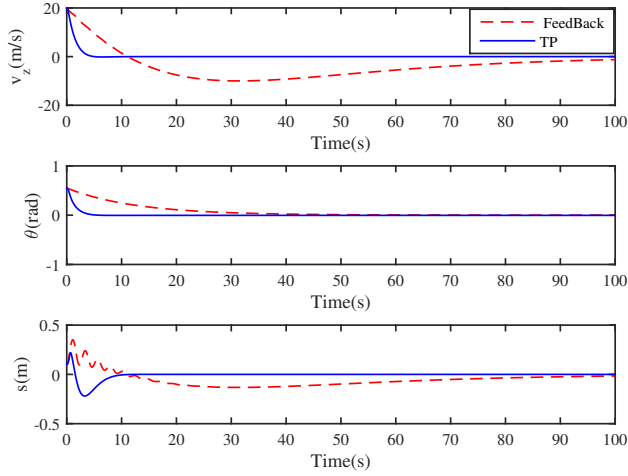
Figure 6
The comparison between the direct feedback and TP controller, where the red dashed curve is
corresponding to the direct feedback control and the blue solid one is for the TP control.

namics. Therefore, the response time (convergence) and overshot is of emphasis, the former of which determines how fast the controller eliminates the slosh dynamics. Besides, a slighter overshot (a relative deviation along z-axis) reflects the gradual mitigation by the controller although the fast response is always accompanied with the smaller overshot. The performance is plotted and compared in Fig. 6, which show that the state s (a relative deviation along z-axis) gets convergent within 10 seconds and its corresponding overshot is also smaller than the direct feedback control. Therefore, the proposed TP model-based control can achieve a faster response in convergence and slighter overshot so that the slosh dynamics can be effectively alleviated.

Conclusions

The paper proposes a numerical TP model transformation for space vehicles with fuel slosh. A state-dependent differential equation is firstly developed from the mass-spring model in zero gravity environment, which is transformed into the polytopic system and regarded as LMI problem. The advantage of our solution is that the converted LMI problem can be thus effectively solved by convex optimization methods. Based on the derived convex-bounded system, the controller design can always guarantee the robustness against the uncertainties and disturbances for all system sets within the bounds. Besides, this controller design is thus insusceptible to the time-varying parameters and coefficients seldom needs to be specially designed. Furthermore, the proposed TP model transformation offers an approximation tradeoff so that both the complexity of the TP model and the controller design can be dramatically minimized.

References

[1]   Shageer, H. and G. Tao, "Modeling and adaptive control of spacecraft with fuel slosh: overview and case studies," in Proc. AIAA Guidance, Navigation, and Control Conference, Hiton Head, South Carolina (2007).

[2]   Baozeng, Y. and Z. Lemei, "Hybrid control of liquid-filled spacecraft maneuvers by dynamic inversion and input shaping," AIAA J., vol. 52, no. 3, pp. 618–626 (2014).

[3]   Baozeng, Y. and Z. Lemei, "Heteroclinic bifurcations in attitude maneuver of slosh-coupled spacecraft with flexible appendage," J. of Astronautics, vol. 5, p. 007 (2011).

[4]   Ayoubi, M. A., F. A. Goodarzi and A. Banerjee, "Attitude motion of a spinning spacecraft with fuel sloshing and nutation damping," J. Astronaut. Sci. , vol. 58, no. 4, pp. 551–568 (2011).

[5]   Kang, J.-Y. and S. Lee, "Attitude acquisition of a satellite with a partially filled liquid tank," J. Guid. Control Dynam., vol. 31, no. 3, pp. 790–793 (2008).

[6]   De Souza, A. G. and L. C. de Souza, "Satellite attitude control system design taking into account the fuel slosh and flexible dynamics," Math. Probl. Eng., vol. 2014 (2014).

[7]   Hervas, J. R., M. Reyhanoglu, and H. Tang, "Thrust-vector control of a three-axis stabilized spacecraft with fuel slosh dynamics," in Proc. 13th International Conference on Control, Automation and Systems (ICCAS), pp. 761–766, IEEE (2013).

[8]   Reyhanoglu, M., "Modelling and Control of Space Vehicles with Fuel Slosh Dynamics, Advances in Spacecraft Technologies," Dr Jason Hall (Ed.), In-Tech (2011).

[9]   Reyhanoglu, M. and J. R. Hervas, "Nonlinear dynamics and control of space vehicles with multiple fuel slosh modes," Control Eng. Pract., vol. 20, no. 9, pp. 912–918 (2012).

[10]   Reyhanoglu, M. and J. R. Hervas, "Nonlinear control of space vehicles with multi-mass fuel slosh dynamics," in Proc. 5th International Conference on Recent Advances in Space Technologies (RAST), pp. 247–252, IEEE (2011).

[11]   Dong, K., N. Qi, J. Guo and Y. Li, "An estimation approach for propellant sloshing effect on spacecraft gnc," in Proc. 2nd International Symposium on Systems and Control in Aerospace and Astronautics, pp. 1–6, IEEE (2008).

[12] Hervas, J. R. and M. Reyhanoglu, "Observer-based nonlinear control of space vehicles with multi-mass fuel slosh dynamics," in Proc. IEEE 23rd International Symposium onIndustrial Electronics (ISIE), pp. 178–182, IEEE (2014).

[13] Hervas, J. R. and M. Reyhanoglu, "Control of a spacecraft with time-varying propellant slosh parameters," in Proc. 12th International Conference on Control, Automation and Systems (ICCAS), pp. 1621–1626, IEEE (2012).

[14] Mitra, S., P. Upadhyay and K. Sinhamahapatra, "Slosh dynamics of inviscid fluids in two-dimensional tanks of various geometry using finite element method," Int. J. Numer. Meth. Fl., vol. 56, no. 9, pp. 1625–1651 (2008).

[15] Reyhanoglu, M., "Maneuvering control problems for a spacecraft with unactuated fuel slosh dynamics," in Proc. IEEE Conference on Control Applications (CCA), vol. 1, pp. 695–699, IEEE (2003).

[16] Krishna Kishor, D., S. Gopalakrishnan and R. Ganguli, "Three-dimensional sloshing: A consistent finite element approach," Int. J. Numer. Meth. Fl., vol. 66, no. 3, pp. 345–376 (2011).

[17] P. Baranyi: "TP-Model Transformation-Based-Control Design Frameworks, Springer International Publishing Switzerland, 2016, p. 258. (eBook 978-3-319-19605-3, 978-3-319-19604-6, doi: 10.1007/978-3-319-19605-3, http://www.springer.com/gp/book/9783319196046)

[18] A. Szollosi, P. Baranyi Influence of the Tensor Product Model Representation Of QLPV Models on The Feasibility of Linear Matrix Inequality, Asian J. Control, 2016, pp 1328–1342

[19] A. Szollosi, and P. Baranyi, Improved control performance of the 3-DoF aeroelastic wing section: a TP model based 2D parametric control performance optimization, Asian J. Control, vol. 19, no. 2, pp 450-466, 2017

[20] A Szollosi, P. Baranyi "Influence of the Tensor Product Model Representation of qLPV Models on the Feasibility of Linear Matrix Inequality Based Stability Analysis , Asian J. Control, 2017, in print

[21] X. Liu, L. Li, L. Zhen, T. Fernando, and H. H. C. Iu, "Stochastic stability condition for the extended kalman filter with intermittent observations," *IEEE Trans. Circuits Syst. II, Exp. Briefs*, vol. 64, no. 3, pp. 334–338, March 2017.

[22] Baranyi, P., Yam Y. and Várlaki P., "Tp model transformation as a way to lmi-based controller design," Taylor & Francis, Boca Raton FL, pp. 248, 2013 (ISBN 978-1-43-981816-9).

[23] De Lathauwer, L., B. De Moor and J. Vandewalle, "A multilinear singular value decomposition," SIAM J. Matrix Anal. A., vol. 21, no. 4, pp. 1253–1278 (2000).

[24] Pan, J. and L. Lu, "Tp model transformation via sequentially truncated higher-order singular value decomposition," Asian J. Control, vol. 17, no. 2, pp. 467–475 (2015).

[25]   Baranyi, P., "The Generalized TP Model Transformation for TS Fuzzy Model Manipulation and Generalized Stability Verification" IEEE Trans. Fuzzy Syst., vol. 22, no. 4, pp. 934–948 (2014).

[26]   Baranyi, P., "Tensor product model-based control of two-dimensional aeroelastic system," J. Guid. Control Dynam., vol. 29, no. 2, pp. 391–400 (2006).

[27]   Baranyi, P., P. Korondi, R. J. Patton and H. Hashimoto, "Trade-off between approximation accuracy and complexity for ts fuzzy models," Asian J. Control, vol. 6, no. 1, pp. 21–33 (2004).

[28]   Baranyi, P., "Output feedback control of two-dimensional aeroelastic system," J. Guid. Control Dynam., vol. 29, no. 3, pp. 762–767 (2006).

[29]   Baranyi, P. and Takarics, B., "Aeroelastic Wing Section Control via Relaxed Tensor Product Model Transformation Framework" J. Guid. Control Dynam., vol. 37, no. 5, pp. 1671–1678 (2014).

[30]   Takarics and B., Baranyi, P., "Tensor-Product-Model-Based Control of a Three Degrees-of-Freedom Aeroelastic Model," J. Guid. Control Dynam., vol. 36, no. 5, pp. 1527–1533 (2013).

[31]   Petres, Z., P. Baranyi, P. Korondi and H. Hashimoto, "Trajectory tracking by tp model transformation: case study of a benchmark problem," IEEE Trans. Ind. Electron.,, vol. 54, no. 3, pp. 1654–1663 (2007).

[32]   Baranyi, P., "Tp model transformation as a manipulation tool for qlpv analysis and design," Asian J. Control, vol. 17, no. 2, pp. 497–507 (2015).

[33]   Campos, V. C. D. S., L. A. B. Tôrres and R. M. Palhares, "Revisiting the tp model transformation: Interpolation and rule reduction," Asian J. Control, vol. 17, no. 2, pp. 392–401 (2015).

[34]   P. Baranyi, Z. Petres, P. Korondi, Y. Yam and H. Hashimoto, "Complexity relaxation of the Tensor Product Model Transformation for Higher Dimensional Problems," Asian J. Control, vol. 9, no. 2, pp. 195–200 (2007).

[35]   D. Tikk, P. Baranyi and R. J. Patton, "Approximation Properties of TP Model Forms and its Consequences to TPDC Design Framework," Asian J. Control, vol. 9, no. 3, pp. 221–231 (2007).

[36]   Sz. Nagy, Z. Petres, P. Baranyi and H. Hashimoto, "Computational relaxed TP model transformation: restricting the computation to subspaces of the dynamic model," Asian J. Control, vol. 11, no. 5, pp. 461–475 (2009).

[37]   P. Baranyi, P. Korondi and H. Hashimoto, "Global Asymptotic Stabilisation of the Prototypical Aeroelastic Wing Section via TP Model Transfromation," Asian J. Control, vol. 7, no. 2, pp. 99–111 (2005).

[38]   X. Liu, L. Li, Z. Li, X. Chen, T. Fernando, H. H. C. Iu and G. He. "Event-trigger particle filter for smart grids with limited communication bandwidth infrastructure," IEEE Trans. on Smart Grid, vol. PP, no. 99, pp. 1-1 (2017).

[39]　S. Li, L. Li, Z. Li, X. Chen, T. Fernando, Herbert H. C. Iu, G. He, Q. Wang and X. Liu, "Event-trigger Heterogeneous Nonlinear Filter for Wide-area Measurement Systems in Power Grid," IEEE Trans. Smart Grid, vol. PP, no. 99, pp. 1–1 (2018).

[40]　B. Liu , Z. Li, X. Chen, Y. Huang and X. Liu, "Recognition and Vulnerability Analysis of Key Nodes in Power Grid Based on Complex Network Centrality," IEEE Trans. Circuits Syst. II, Exp. Briefs, vol. 65, no. 3, pp. 346–350 (2018).

[41]　Y. Yu, Z. Li, X. Liu, K. Hirota, X. Chen, T. Fernando, and H. H. Iu, "A nested tensor product model transformation," IEEE Trans. Fuzzy Syst., vol. PP, no. 99, pp. 1–1 (2018).

[42]　X. Liu, Y. Yu, Z. Li, and H. H. Iu, "Polytopic H_∞ filter design and relaxation for nonlinear systems via tensor product technique," Signal Process., vol. 127, pp. 191–205 (2016).

[43]　Tanaka K, Wang H O. Fuzzy Control Systems Design and Analysis: A Linear Matrix Inequality Approach [M]. John Wiley & Sons, Inc. 2002.

A State and Input Constrained Control Method for Air-Breathing Hypersonic Vehicles

Haoyu Du, Jie Yan, Yonghua Fan

Northwestern Polytecnical University
West Youyi Road 127, 710072, Xi'an city, Shaanxi, P.R.China
duhaoyu@mail.nwpu.edu.cn, jyan@nwpu.edu.cn, fanyonghua@nwpu.edu.cn

Abstract: Besides nonlinearity, high coupling and parameter uncertainties, the design of a hypersonic flight control system still faces challenges due to the unstable dynamics under various flight conditions and to the presence of state constraints required by a scramjet. This paper presents a state and input constrained control method for the longitudinal motion of an air-breathing hypersonic vehicle through combining tensor product (TP) model transformation and the command governor approach. This method consists of three steps. Firstly, the paper applies the tensor product (TP) model transformation, making the state space matrices depend on the vector θ of time varying parameters. Secondly, it uses LQ (Linear Quadratic) method to design a set of controllers in the vertex of the TP model, and then, the controllers are checked with the parallel distributed compensation (PDC) controller design framework to ensure global stability and improving control performance. Thirdly, it introduces a command governor (CG) device for command optimization, which modifies the command signal to avoid state and input violations. The significance of this method mainly lies in its capability to avoid excessive flight constraints under various flight conditions. In order to demonstrate the effectiveness of this method, we carried out numerical simulations of the air-breathing hypersonic vehicle in its climbing phase which has state constraints and actuator constraints.

Keywords: tensor product (TP) model; linear matrix inequalities (LMI); constrained control; parallel distributed compensation (PDC); command governor (CG)

1   Introduction

Air-breathing hypersonic vehicles (AHVs) receive great research attention because they present a more promising and economical technology for access to near space for both civilian and military applications [1-2], as witnessed by the success of NASA's scramjet-powered X-43A and X-51A. Compared with the traditional flight vehicles, the AHV flight control design still faces open challenges because the vehicle has high nonlinearity, inherently unstable and complex couplings and parametric uncertainties [3-7]. Most of the research

focuses on the cruising phase. When talking about maneuvering flight, another two aspects should be taken into consideration, the changing characteristics of the vehicle with various flight conditions and constrained flight status restricted by the requirements of the scramjet for safe running [8-12]. Therefore, pursuing an accurate varying model and designing a suitable constrained control method are key problems to be solved in the maneuvering phase.

In the past few decades, the linear parameter varying (LPV) control underwent huge development. Through obtaining parameter-dependent controller in the framework of linear matrix inequalities (LMI), the LPV control system is capable of gain-scheduling in real time with the measured or estimated parameters and ensuring the robust stability and satisfied performance of the control system. Among the various LPV modeling methods, the tensor product (TP) model transformation is very attractive, as it is convenient to be combined with the LMI-based control theory and has high accuracy [13-15]. These advantages have been taken to deal with extreme parameter variations caused by large flight envelope in flight control [9]. Together with the parallel distributed compensation (PDC) controller design, TP-based LMI controllers gain global stability in the area of parameter variation [16-17]. For air-breathing hypersonic vehicle control, flight status such as angle of attack and pitch rate must meet the restrictions by the scramjet. Otherwise, engine stall may fail the flight task. Focusing on state constrained flight control, researchers make great efforts [18]. The command governor approach gains a lot of attention in this field. The specific merit of this approach lies in handling constraints on both input and state-related variables without too many numerical burdens [19-20].

Motivated by the above, the paper addresses the command governor control method that incorporates the benefits of TP-based LPV control. To begin with, this paper transforms the state-space model of the plant by transforming a tensor product (TP) model into convex state-space TP model. Then, the control system is divided into two layers. The outer layer creates overload command for altitude tracking (which is not the focus of this paper). The emphasis lies in the design of inner layer design, which contains a command governor device and a set of LQ controllers. The aim of the inner loop is to improve the flight attitude control performance and implement the appropriate overload command without violating various restrictions. The values of the LQ controllers are checked by solving a set of LMIs generated by PDC technique according to desired specifications in all the TP-model vertex systems. As for the restrictions, the command governor device optimizes the overload command in every control period, which guarantees that all the related variables may not violate constraints. Finally, nonlinear numerical simulation results are provided to verify the effectiveness of the method.

2   Flight Model

With the nonlinear model for longitudinal dynamics of an AHV considered, the nonlinear equations of motion for velocity $V(meter/s)$, altitude $H(meter)$, flight-path angle $\gamma(rad)$, the angle of attack $\alpha(rad)$ and pitch rate $q(rad/s)$ are described as follows:

$$\begin{cases} \dot{h} = V\sin\gamma \\ \dot{\gamma} = \dfrac{L+T\sin\alpha}{mV} - \dfrac{g}{V}\cos\gamma \\ \dot{\alpha} = q - \dot{\gamma} \\ \dot{q} = \dfrac{M_z}{I_{zz}} \end{cases} \tag{1}$$

where m denotes the mass of the flight vehicle; T and L represent thrust and lift force; I_{zz} stands for the longitudinal moment of inertia; M_z is the pitch moment. The control input $u = [\delta_e]$, whose unit is rad.

The CFD results show the thrust coefficient C_T, the lift coefficient C_L, and pitch moment coefficient C_M are related to Mach (Ma) number, angle of attack (α) and elevator (δ_e). The forces and moments have the following forms:

$$L = 0.5\rho V^2 S C_L(Ma,\alpha,\delta_e)$$
$$M = 0.5\rho V^2 S c C_M(Ma,\alpha,\delta_e) \tag{2}$$
$$T = 0.5\rho V^2 S C_T(Ma,\alpha,\delta_T)$$

where ρ, S, c, δ_T stand for the air density, reference area, aerodynamic chord. The unit for L, T is Newton; the unit for M is Newton times meter.

The miscellaneous coefficients of the inner-loop control system, which involves the last two equations in Eq. (1), are simplified under the trimmed condition, while the state and input and output vectors are chosen as follows:

$x_s = [\alpha, q]^T, u = [\delta_e], y = [n_z]$, where n_z is the measured value of normal acceleration.

Small perturbation linearized equations of the flight attitude are derived as follows:

$$\begin{bmatrix} \dot{\alpha} \\ \dot{q} \end{bmatrix} = \begin{bmatrix} -\dfrac{0.5\rho V^2 S C_L^\alpha + T}{mV} & 1 \\ \dfrac{0.5\rho V^2 S c C_M^\alpha}{I_{ZZ}} & 0 \end{bmatrix} \begin{bmatrix} \alpha \\ q \end{bmatrix} + \begin{bmatrix} -\dfrac{0.5\rho V^2 S C_L^{\delta_e}}{mV} \\ \dfrac{0.5\rho V^2 S c C_M^{\delta e}}{I_{zz}} \end{bmatrix} \delta_e \tag{3}$$

$$n_z = [\frac{0.5\rho V^2 SC_L^\alpha}{mg} \quad 0]\begin{bmatrix} a \\ q \end{bmatrix} + [\frac{0.5\rho V^2 SC_L^{\delta_e}}{mg}]\delta_e . \tag{4}$$

$C_L^\alpha, C_L^{\delta_e}, C_M^\alpha, C_M^{\delta e}$ represent first order partial derivative of coefficients in Eq. (2). $C_L^\alpha, C_L^{\delta_e}, C_M^\alpha, C_M^{\delta e}$ vary with Ma and α; ρ changes with h, and V equals Ma times speed of sound. The equations (3) and (4) vary with $p(t) = [h, Mach, \alpha]$. We assume that all these parameters can be obtained in real-time (In fact, the Ma and h can be measured by sensors, while α should be estimated according to the inertial guidance system).

Eqs. (3) and (4) can be expressed in the LPV form:

$$\begin{cases} \dot{x}_s(t) = A_s(p(t))x_s(t) + B_s(p(t))u(t) \\ y(t) = C_s(p(t))x_s(t) + D_s(p(t))u(t) \end{cases} \tag{5}$$

$p(t) = [h(t), Ma(t), \alpha(t)]^T$ is the vector of varying parameters. The desired command values of the normal acceleration is denoted by $r(t) = [n_{zc}]$. The error integral equation is defined as follows:

$$e(t) = \int_0^t [r(t) - y(t)]d\tau \tag{6}$$

The augmented system is as follows:

$$\begin{bmatrix} \dot{x}_s(t) \\ \dot{e}(t) \end{bmatrix} = \begin{bmatrix} A_s(p(t)) & 0 \\ -C_s(p(t)) & 0 \end{bmatrix}\begin{bmatrix} x_s(t) \\ e(t) \end{bmatrix} + \begin{bmatrix} B_s(p(t)) \\ -D_s(p(t)) \end{bmatrix}u(t) + \begin{bmatrix} 0 \\ I \end{bmatrix}r(t) \tag{7}$$

$$y = n_z = \begin{bmatrix} C_s(p(t)) & 0 \end{bmatrix}\begin{bmatrix} x_s(t) \\ e(t) \end{bmatrix} + D_s(p(t))u(t) \tag{8}$$

This paper focuses on the climbing phase to do the flight maneuver. The higher altitude corresponds to a faster cruising velocity. In the climbing phase, its engine works in full mode (which means the ratio of air and oil should always be 1). The mission is to maneuver the cruising vehicle to a higher altitude as soon as possible, without violating any constraints. The longitudinal control system can be considered as a two-layered control system. The outer-loop control system determines a reference longitudinal acceleration n_{zc} based on the altitude error. The inner-loop control system regulates the vehicle's attitude to follow the reference signal using an elevator. Constraints exist in the angle of attack and pitch rate for the stable combustion of the scramjet. Constraints on the elevator prevent input saturation. These constraints can be represented by:

$$\alpha_{min} \leq \alpha(t) \leq \alpha_{max},$$
$$q_{min} \leq q(t) \leq q_{max}, \tag{9}$$
$$\delta_{e_{min}} \leq \delta_e(t) \leq \delta_{e_{max}}.$$

The attitude control should be quick and accurate with acceptable behaviours of the elevator. The paper uses the linear quadratic proportional plus integral (LQ-PI) controller to make the control performance satisfactory.

3 TP Transformation and Control Method

3.1 TP Transformation for the LPV Model

The LPV state-space model is given as follows:

$$\begin{cases} \dot{x}(t) = A(p(t))x(t) + B(p(t))u(t) \\ y(t) = C(p(t))x(t) + D(p(t))u(t) \end{cases} \quad y(t) \in \mathbb{R}^l \quad (10)$$

with input $u(t) \in \mathbb{R}^k$, output and state vector $x(t) \in \mathbb{R}^m$. The system matrix is written as

$$S(p(t)) := \begin{pmatrix} A(p(t)) & B(p(t)) \\ C(p(t)) & D(p(t)) \end{pmatrix} \in \mathbb{R}^{(m+k)\times(m+l)} \quad (11)$$

where $p(t) \in \Omega$ is a time-varying N-dimensional parametric vector with the hypercube $\Omega = [a_1 \quad b_1] \times [a_2 \quad b_2] \times L \times [a_N \quad b_N] \subset \mathbb{R}^N$.

The TP model transformation is capable of converting a model given by a set of continuous multivariable functions into a polytopic TP model. If a model is established with the relevant aerodynamic data, it still works by substituting the sampling data produced by functions with these data. In this way, the establised model can be transformed into products consisting of orthonormal one-variable weighting functions. Based on the concepts of higher-order singular value decomposition (HOSVD), these products are constructed into a tensor product structure according to the significance of each component. For more details, see Ref. [14].

In the qLPV plant, the system matrix $S(p(t))$ is transformed into the following polytopic TP model for parametric vector $p(t)$:

$$S(p(t)) = \sum_{i_1=1}^{I_1} L \sum_{i_N=1}^{I_N} \prod_{n=1}^{N} w_{n,i_n}(p_n(t)) S_{i_1 L\, i_N} \quad (12)$$

which stands for a parameter-dependent convex combination of linear time-invariant (LTI) system matrices, with the vertex systems $S_{i_1 L\, i_N} \in \mathbb{R}^{(m+k)\times(m+l)}$ and the weighting function $w_n(p_n(t))$. In Eq.(12), $p_n(t)$ stands for the n th parameter

in $p(t)$, with $n = 1, \text{L } N$. I_n represents the number of singular values kept in each $p_n(t)$. The number of vertices is $R = I_1 I_2 \text{L } I_N$. After this, the system $S(p(t))$ in Eq. (11) can be expressed by combining the R vertex in Eq. (12).

Based on the tensor product model transformation in a compact form, Eq. (12) can be rewritten as:

$$S(p(t)) = \mathbf{S} \overset{N}{\underset{n=1}{\otimes}} \mathrm{w}_n(p_n(t)) \tag{13}$$

which enables the application of matrix and tensor algebra methods. The $(N+2)$ dimensional coefficient of the core tensor $\mathbf{S} \in \mathbf{\textupipe}^{I_1 \times \text{L} \times I_n \times (m+k) \times (m+l)}$ is constructed from the LTI vertex systems S_{i_1, L, i_N} and the row vector $\mathrm{w}_n(p_n(t))$ that contains the one-variable weighting function $w_{n, i_n}(p_n(t))$, $i_n = 1\text{L } I_N$.

The weighting function satisfies the sum normalized, non-negative (SNNN) condition[14], which can be expressed as Eqs. (14) and (15):

$$\forall n, i_n, p_n(t) : w_{n, i_n}(p_n(t)) \in [0,1] \tag{14}$$

$$\forall n, i_n, p_n(t) : \sum_{i=1}^{I_n} w_{n, i_n}(p_n(t)) = 1. \tag{15}$$

In the following, we show that types of weighting functions can be modified by the TP model transformation:

Type 1: (the normality [NO] type). The resulting weighting functions satisfies the SNNN conditions, and the largest value of each function is 1.

Type 2: (the close-to-normality [CNO] type). The resulting weighting function satisfies the SNNN conditions, and the largest value of each function is 1 or close to 1.

Type 3: (the inverse normality [INO] type). The resulting weighting function satisfies the SNNN conditions, and the smallest value of all functions is 0.

For a CNO type TP model, some of its weighting functions can acquire 1, leading to $S(p(t))$ being exactly mapped into some of the vertex systems. Compared to other types, the CNO type, which yields a tighter convex hull, is generally best suitable for controller design [14, 21]. We adopt the TP model that uses the CNO type weighting function.

The systems in Eqs. (7-8) then can be rewritten with Eq. (10) to form the following:

$$x = [x_s \quad e]^T,$$

$$A(p(t)) = \begin{bmatrix} A_s(p(t)) & 0 \\ -C_s(p(t)) & 0 \end{bmatrix}, B(p(t)) = \begin{bmatrix} B_s(p(t)) \\ -D_s(p(t)) \end{bmatrix}, \tag{16}$$

$$C(p(t)) = \begin{bmatrix} C_s(p(t)) & 0 \end{bmatrix}, D(p(t)) = D_s(p(t))$$

The systems' core tensor $\mathbf{S}$ has the following structure:

$$\mathbf{S} = \begin{bmatrix} \mathbf{S}_A & \mathbf{S}_B \\ \mathbf{S}_C & \mathbf{S}_D \end{bmatrix} \tag{17}$$

$$\mathbf{S}_A = \begin{bmatrix} \mathbf{S}_{A_s} & \mathbf{0} \\ -\mathbf{S}_{C_s} & \mathbf{0} \end{bmatrix}, \mathbf{S}_B = \begin{bmatrix} \mathbf{S}_{B_s} \\ -\mathbf{S}_{D_s} \end{bmatrix}, \mathbf{S}_C = \begin{bmatrix} \mathbf{S}_{C_s} & \mathbf{0} \end{bmatrix}, \mathbf{S}_D = \begin{bmatrix} \mathbf{S}_{D_s} \end{bmatrix} \tag{18}$$

With this, we obtain the TP model-based LPV model in Eq.(7) as follows:

$$\begin{bmatrix} \dot{x}_s(t) \\ \dot{e}(t) \end{bmatrix} = \begin{bmatrix} \mathbf{S}_{A_s} \overset{N}{\underset{n=1}{\otimes}} \mathrm{w}_n(p_n(t)) & 0 \\ -\mathbf{S}_{C_s} \overset{N}{\underset{n=1}{\otimes}} \mathrm{w}_n(p_n(t)) & 0 \end{bmatrix} \begin{bmatrix} x_s(t) \\ e(t) \end{bmatrix} + \begin{bmatrix} \mathbf{S}_{B_s} \overset{N}{\underset{n=1}{\otimes}} \mathrm{w}_n(p_n(t)) \\ -\mathbf{S}_{D_s} \overset{N}{\underset{n=1}{\otimes}} \mathrm{w}_n(p_n(t)) \end{bmatrix} u(t) + \begin{bmatrix} 0 \\ I \end{bmatrix} r(t) \tag{19}$$

$$y = n_z = \begin{bmatrix} \mathbf{S}_{C_s} \overset{N}{\underset{n=1}{\otimes}} \mathrm{w}_n(p_n(t)) & 0 \end{bmatrix} \begin{bmatrix} x_s(t) \\ e(t) \end{bmatrix} + \begin{bmatrix} \mathbf{S}_{D_s} \overset{N}{\underset{n=1}{\otimes}} \mathrm{w}_n(p_n(t)) \end{bmatrix} u(t) \tag{20}$$

3.2 Designing LQ Controller in the PDC Framework

The LQ method is widely used in flight control because of its good performance without excessive input. However, it is difficult to ensure the stabilization of a large flight envelope even with a large number of controllers. This part of the paper introduces a new method for combining the LQ controller design with the PDC framework to ensure that the global and asymptotic stabiliy is within the whole flight envelope.

The PDC design technique determines one feedback to each vertex system
$$\mathbf{K} = PDC(\mathbf{S}, stability\_theorem) \tag{21}$$

Then define the control value as

$$u(t) = -\left(\mathbf{K} \overset{N}{\underset{n=1}{\otimes}} \mathrm{w}_n(p_n(t)) \right) x(t) \tag{22}$$

The control performance should be guaranteed by the selected "stability_theorem" in Eq. (21), which is a symbolic parameter specifying the stability criteria and the desired control performance predefined in terms of LMIs [23-24]. For example, the H_2 / H_∞ control performance and the pole placement can be considered through LMI-based stability theorems properly. We use the parallel distributed compensation method to guarantee the global asymptotic stability for a given dynamic system.

In order to have a direct link to the typical form of LMI-based stablity theorem, we define its indexing as follows:

$$S_r = \begin{pmatrix} A_r & B_r \\ C_r & D_r \end{pmatrix} = S_{i_1, \mathrm{L}, i_N} \tag{23}$$

where $r = ordering(i_1, \mathrm{L}, i_N)$ \hfill (24)

The term 'ordering' presents in the linear index equivalent to an N-dimensional array's index i_1, L, i_N, when the size of the array is $I_1 \times I_2 \times \mathrm{L} \times I_N$, its expression is:

$$\begin{aligned} r = {} & (i_{n+1}-1)I_{n+2}I_{n+3}\mathrm{L}\ I_N I_1 I_2 \mathrm{L}\ I_{n-1} + (i_{n+2}-1)I_{n+3}I_{n+4}\mathrm{L}\ I_N I_1 I_2 \mathrm{L}\ I_{n-1} \\ & +\mathrm{L}\ +(i_N-1)I_1 I_2 \mathrm{L}\ I_{n-1} + (i_1-1)I_2 I_3 \mathrm{L}\ I_{n-1} + (i_2-1)I_3 I_4 \mathrm{L}\ I_{n-1} \\ & +\mathrm{L}\ +(i_{n-2}-1)I_{n-1} + i_{n-1}. \end{aligned} \tag{25}$$

The basis functions can be defined according to the sequence of:

$$w_r(p(t)) = \prod_{n=1}^{N} w_{n,i_n}(p_n(t)) \tag{26}$$

Then the controller can be design with the Lyapunov stability theorems for global and asymptotic stability as follows:

Find $\mathrm{X} > 0$ and M_r satisfies:

$$-\mathrm{XA}_r^{\mathrm{T}} - \mathrm{A}_r \mathrm{X} + \mathrm{M}_r^{\mathrm{T}} \mathrm{B}_r^{\mathrm{T}} + \mathrm{B}_r \mathrm{M}_r > 0 \tag{27}$$

for all r and

$$-\mathrm{XA}_r^{\mathrm{T}} - \mathrm{A}_r \mathrm{X} - \mathrm{XA}_s^{\mathrm{T}} - \mathrm{A}_s \mathrm{X} + \mathrm{M}_s^{\mathrm{T}} \mathrm{B}_r^{\mathrm{T}} + \mathrm{B}_r \mathrm{M}_s + \mathrm{M}_r^{\mathrm{T}} \mathrm{B}_s^{\mathrm{T}} + \mathrm{B}_s \mathrm{M}_r > 0 \tag{28}$$

for $r < s \leq R$, except the pair (r, s) in which $w_r(p(t))w_s(p(t)) = 0, \forall p(t)$.

Finding a positive definite matrix X and M_r or determining that no such matrices exist is a convex feasibility problem. Using the powerful tools in MATLAB-LMI toolbox [25], this problem can be solved very efficiently. The feedback gains can form the solutions X and M_r as follows:

$$\mathrm{K}_r = \mathrm{M}_r \mathrm{X}^{-1} \tag{29}$$

Then, we can match the feedback $\mathrm{K}_{i_1, \mathrm{L}, i_N}$ from K_r with the $r = ordering(i_1, \mathrm{L}, i_N)$ and store these gains into tensor $\mathbf{K}$ of Eq. (21).

To solve the above problem, we design the controller with the LQ method and check the control system with the PDC framework to enssure the global and asymptotic stability. The performance index becomes:

$$J = \int_0^\infty (x^T Q x + u^T E u) dt \tag{30}$$

Q and E are symmetric positive definite matrices. By solving the LQ controller

for the vertex system in Eq. (16) with the algebra riccati equation, we obtain a set of controllers of K_r for the vertex system. Next, using Eq. (29), M_r can be expressed as follows:

$$M_r = K_r X \tag{31}$$

We substitute Eq. (31) into Eq. (27) and (28) and solve the new LMI problem; if there exists a matrix $X > 0$, we conclude that the control system satisfies global and asymptotic stability in the whole flight envelope. Then, the closed loop control system in Eqs. (19) and (20) can be implemented:

$$
\begin{bmatrix} \dot{x}_s(t) \\ \dot{e}(t) \end{bmatrix}
= \left\{ \begin{bmatrix} \mathbf{S}_{A_s} \underset{n=1}{\overset{N}{\otimes}} \mathrm{w}_n(p_n(t)) & 0 \\ -\mathbf{S}_{C_s} \underset{n=1}{\overset{N}{\otimes}} \mathrm{w}_n(p_n(t)) & 0 \end{bmatrix} + \begin{bmatrix} \mathbf{S}_{B_s} \underset{n=1}{\overset{N}{\otimes}} \mathrm{w}_n(p_n(t)) \\ -\mathbf{S}_{D_s} \underset{n=1}{\overset{N}{\otimes}} \mathrm{w}_n(p_n(t)) \end{bmatrix} \left(\mathbf{K} \underset{n=1}{\overset{N}{\otimes}} \mathrm{w}_n(p_n(t)) \right) \right\} \begin{bmatrix} x_s(t) \\ e(t) \end{bmatrix}
$$
$$
+ \begin{bmatrix} 0 \\ I \end{bmatrix} r(t) \tag{32}
$$

$$
y = n_z = \left\{ \begin{bmatrix} \mathbf{S}_{C_s} \underset{n=1}{\overset{N}{\otimes}} \mathrm{w}_n(p_n(t)) & 0 \end{bmatrix} + \begin{bmatrix} \mathbf{S}_{D_s} \underset{n=1}{\overset{N}{\otimes}} \mathrm{w}_n(p_n(t)) \end{bmatrix} \left(\mathbf{K} \underset{n=1}{\overset{N}{\otimes}} \mathrm{w}_n(p_n(t)) \right) \right\} \begin{bmatrix} x_s(t) \\ e(t) \end{bmatrix} \tag{33}
$$

As to the command signal of $r(t) = [n_{zc}]$, the closed-loop control system in Eq.(32) is obviously a Type-1 servo system. The static error is zero. In every sampling time, we derive the time-varying parameter vector $p(t)$ according to the flight condition. The closed-loop system can be determined with the value of $p(t)$.

3.3   Command Governor Design

The model derived from Eqs. (32) and (33) is in continuous form. The discretized model with the sampling time Ts can be expressed with the following equations:

$$x(t+1) = \Phi(p(\mathrm{t}))x(t) + G(p(\mathrm{t}))r(t)$$
$$y(t) = H_y(p(\mathrm{t}))x(t) \tag{34}$$

The matrix $\Phi(p(\mathrm{t})), G(p(\mathrm{t}))$ are the discretized relevant parts in Eq.(32), while the matrix $H_y(p(\mathrm{t}))$ is the discretized relevant part in Eq. (33), with $x = [x_s \quad e]^T$.

With the state and input constrained control problem considered, we choose the command governor method to modify the command signal $r(t)$ and substitute it with the closest value $g(t)$, thus meeting all the constraints in a long enough horizon. The system in Eq.(34) is modified as follows:

$$x(t+1) = \Phi(p(t))x(t) + G(p(t))g(t) + d(t)$$
$$y(t) = H_y(p(t))x(t) \tag{35}$$
$$c(t) = H_c(p(t))x(t)$$

where $t \in \phi_+ := \{0, 1, L\}$. $g(t)$ is the command governor (CG) action. A suitable command input, which, if no constraints were present, would coincide with the command reference $r(t)$. $d(t) \in \textrm{¡}^n$, discribes disturbance and $d(t) \in D \subset \textrm{¡}^d$; $y(t) \in \textrm{¡}^m$ describes the output, which is required to track the reference signal $g(t)$; $c(t) \in \textrm{¡}^c$ is the constrained vector. $H_c(p(t))$ represents the relationship between $c(t)$ and state vector $x(t)$. $c(t) \in C, \forall t \in \phi_+$ with C represents a specified convex and compact set. In the sequel, the following assumptions are made:

A1. Φ is a Schur matrix.

A2. The system in Eq. (35) is offset free, that is, $H_y(p(t))(I_n - \Phi(p(t)))^{-1}G(p(t)) = I_m$.

As to a Type-1 servo system, the A2 assumption is always satisfied.

Under these assumptions, given a constant command $g(t) \equiv \omega, \forall t$, the disturbance-free and steady-state solution of Eq. (35) is

$$\bar{x}_\omega := (I_n - \Phi(p(t)))^{-1}G(p(t))\omega,$$
$$\bar{y}_\omega := H_y(p(t))(I_n - \Phi(p(t)))^{-1}G(p(t))\omega, \tag{36}$$
$$\bar{c}_\omega := H_c(I_n - \Phi(p(t)))^{-1}G(p(t))\omega$$

The $\bar{x}_\omega, \bar{y}_\omega, \bar{c}_\omega$ means the steady value of $x(t), y(t), c(t)$ with a constant command $g(t) \equiv \omega, \forall t$, when the disturbance $d(t)$ is zero.

Consider the following Minkowski difference recursions on the constrained set:

$$C^0 := C, \quad C^k := C^{k-1} \sim H_c\Phi(p(t))^{k-1}D, \quad C^\infty := \bigcap_{k=0}^{k=\infty} C^k \tag{37}$$

The equations show that a CG device can be designed for the system in Eq. (12) and compute the action $g(\cdot)$ instantly and each time according to the convex optimization over a prediction horizon $k_0 \in \mathcal{\cancel{C}}_+$:

$$g(t) = \arg \min_{\omega \in V(x(t))} \|\omega - r(t)\|^2 \tag{38}$$

where

$$V(x) = \left\{ \omega \in W^\delta : \bar{c}(k, x, \omega) \in C^k, k = 0, \ldots, k_0 \right\} \tag{39}$$

with

$$W^\delta = \left\{ \omega \in \mathbf{R}^m : \bar{c}_\omega \in C^\delta \right\}, \quad C^\delta = C^\infty \sim B_\delta \tag{40}$$

$$\bar{c}(k, x, \omega) = H_c \left(\Phi(p(t))^{k-1} x + \sum_{i=0}^{k-1} \Phi(p(t))^{k-i-1} G(p(t)) \omega \right) \tag{41}$$

where B_δ a ball of radius δ centered at the origin, which covers the region where all constant virtual commands whose state evolution starts from the current x satisfy all the constraints during the transients, too. For computational details about Eq. (37), refer to Refs. [26-27].

In describing the current system, a small problem is that the $\Phi(p(t))$ used in the prediction sequel is a constant matrix, which, however, should be time-varying like $\Phi(p(t+k))$. Considering the computational efficiency and difficulties in solving complicated optimization problems, using $\Phi(p(t+k))$ instead of $\Phi(p(t))$ is impractical. Instead, a practical method is to increase the sampling frequency to reduce errors at the price of a moderate computational burden. With this method, a practical command governor device in the LPV form can be established. The following numerical simulations verify the effectiveness of this method.

4   Numerical Simulation

This section presents the simulation results to demonstrate the effectiveness of the proposed method for state and input constrained control of the AHV. Suppose that the AHV cruises with the velocity of 1522 m/s and the altitude of 20000 m. The cruise altitude of the maneuvering target changes to 21000 m. This orbital transfer capability is important because it improves the penetration probability and economical flight of the AHV. The initial attitude and angular velocity conditions are chosen as $\alpha_0 = 2 \deg, \gamma_0 = 0 \deg, q_0 = 0 \deg/s$. The attitude and input constraints are given as:

$$-4\,\text{deg} \le \alpha \le 6\,\text{deg}$$
$$-12\,\text{deg/ s} \le q \le 12\,\text{deg/ s} \tag{42}$$
$$-20\,\text{deg} \le \delta_e \le 20\,\text{deg}.$$

The AHV's TP model-based LPV model is established with discrete flight dynamic data; the velocity $\text{Ma} \in [5, 5.5, 6]$, the altitude $h \in [20, 21, 22, 23, 24, 25, 26]\,\text{km}$, and the angle of attack $\alpha \in [-6, -4, -2, 0, 2, 4, 6]\,\text{deg}$.

We utilize the tensor product transformation to establish the LPV models of the systems in Eq. (7)and (8). The rank of the discretized core tensor S results in 3,3,6 in the first, second and third dimensions; therefore, the $3 \times 3 \times 6 = 54$ vertex describes the exact polytopic TP model of the qLPV state-space model. To acquire the relaxed qLPV state-space model, we disposed of small singular values, which, in each dimension, take the following singular values:

Table 1

The comparison results on paris of singular values

Dimension $h(t)$:	18.8831	2.7874	1.217e-05			
Dimension $Mach(t)$:	18.7274	3.6515	0.5401			
Dimension $\alpha(t)$:	19.0624	0.7876	0.5556	0.1576	0.1054	0.0326

The singular values kept in each dimension are 2, 3, 4, then the relaxed TP model can be described with 24 vertexes.

The LTI vertex systems in Eq. (16) is given as follows:

$$A_{1,1,1} = \begin{pmatrix} -0.0023 & 1 & 0 \\ 0.3685 & 0 & 0 \\ -0.4149 & 0 & 0 \end{pmatrix}, B_{1,1,1} = \begin{pmatrix} -0.0007 \\ -1.4529 \\ -0.1188 \end{pmatrix}$$

$$A_{1,1,2} = \begin{pmatrix} -0.0033 & 1 & 0 \\ 0.4698 & 0 & 0 \\ -0.5941 & 0 & 0 \end{pmatrix}, B_{1,1,2} = \begin{pmatrix} -0.0008 \\ -1.6998 \\ -0.1379 \end{pmatrix}$$

$$A_{1,1,3} = \begin{pmatrix} -0.0030 & 1 & 0 \\ 0.0457 & 0 & 0 \\ -0.5344 & 0 & 0 \end{pmatrix}, B_{1,1,3} = \begin{pmatrix} -0.0006 \\ -1.3882 \\ -0.1137 \end{pmatrix}$$

$$A_{1,1,4} = \begin{pmatrix} -0.0026 & 1 & 0 \\ 0.4538 & 0 & 0 \\ -0.4631 & 0 & 0 \end{pmatrix}, B_{1,1,4} = \begin{pmatrix} -0.0006 \\ -1.3955 \\ -0.1141 \end{pmatrix}$$

(43)

g

g

g

$$A_{2,3,4} = \begin{pmatrix} -0.0008 & 1 & 0 \\ -0.2121 & 0 & 0 \\ -0.1018 & 0 & 0 \end{pmatrix}, B_{2,3,4} = \begin{pmatrix} -0.0004 \\ -0.5823 \\ -0.0479 \end{pmatrix}$$
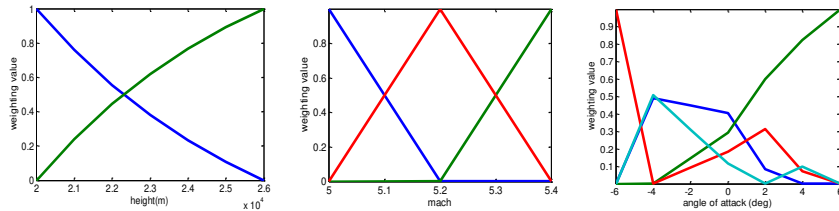

Figure 1

CNO-type scheduling parameter weighting functions for the established TP model

Then, we use the inner-loop control structure (shown in Figure 2) to realize offset –free command tracking.
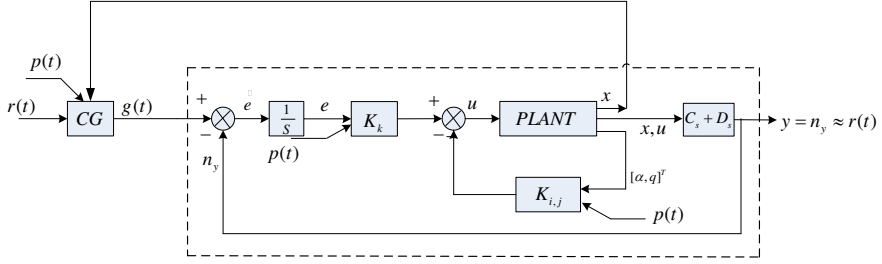
Figure 2

The Inner-loop control structure with command governor

Where the dash-line-surrounded part represents the primal controller. Using the LQ method shown in Eq. (30), we design the primal controller for vertex systems with Q and E as follows:

$$Q = \begin{bmatrix} 80 & 0 & 0 \\ 0 & 1.2 & 0 \\ 0 & 0 & 0.3 \end{bmatrix}, E = 3 \tag{44}$$

We gain the following vertex controllers:

$K(1,1,1) = [-5.3716, -0.6709, 0.3162]$

$K(1,1,2) = [-5.1731, -0.6289, 0.3162]$

$K(1,1,3) = [-5.1263, -0.6465, 0.3162]$

g   (45)

g

g

$K(2,3,4) = [-5.4605, -0.7560, 0.3162]$

Based on PDC theory, we use MATLAB LMI Toolbox to test the feasibility of Eqs. (27) and (28). The monitoring matrix is as follows:

$$X = \begin{bmatrix} 8.9962e-10 & -4.886e-09 & 5.6984e-09 \\ -4.0886e-09 & 3.9156e-08 & 5.4979e-09 \\ 5.6984e-09 & 5.4979e-08 & 1.1643e-07 \end{bmatrix} > 0 \tag{46}$$

The matrix indicates that the compensated LPV system is globally and asymptotically stable. Then the control value is computed according to Eq. (22):

$$u(t) = -(\sum_{i=1}^{2} \sum_{j=1}^{3} \sum_{k=1}^{4} w_{1,i}(h) w_{2,j}(Ma) w_{3,k}(\alpha) K_{i,j,k}) x(t) \tag{47}$$

The compensated system can be described as:

$$
\begin{bmatrix} \dot{x}_s(t) \\ \dot{e}(t) \end{bmatrix} =
$$

$$
\left\{ \begin{bmatrix} \mathbf{S}_{A_s} \sum_{i=1}^{2}\sum_{j=1}^{3}\sum_{k=1}^{4} w_{1,i}(h)w_{2,j}(Ma)w_{3,k}(\alpha)\mathrm{K}_{i,j,k} & 0 \\ -\mathbf{S}_{C_s} \sum_{i=1}^{2}\sum_{j=1}^{3}\sum_{k=1}^{4} w_{1,i}(h)w_{2,j}(Ma)w_{3,k}(\alpha)\mathrm{K}_{i,j,k} & 0 \end{bmatrix} + \right.
$$

$$
\begin{bmatrix} \mathbf{S}_{B_s} \sum_{i=1}^{2}\sum_{j=1}^{3}\sum_{k=1}^{4} w_{1,i}(h)w_{2,j}(Ma)w_{3,k}(\alpha)\mathrm{K}_{i,j,k} \\ \text{-}\mathbf{S}_{D_s} \sum_{i=1}^{2}\sum_{j=1}^{3}\sum_{k=1}^{4} w_{1,i}(h)w_{2,j}(Ma)w_{3,k}(\alpha)\mathrm{K}_{i,j,k} \end{bmatrix} \left(\mathbf{K} \sum_{i=1}^{2}\sum_{j=1}^{3}\sum_{k=1}^{4} w_{1,i}(h)w_{2,j}(Ma)w_{3,k}(\alpha)\mathrm{K}_{i,j,k} \right) \left. \right\} \begin{bmatrix} x_s(t) \\ e(t) \end{bmatrix}
$$

$$
+ \begin{bmatrix} 0 \\ I \end{bmatrix} g(t)
$$

$$
\tag{48}
$$

$$
y =
$$

$$
\left\{ \begin{bmatrix} \mathbf{S}_{C_s} \sum_{i=1}^{2}\sum_{j=1}^{3}\sum_{k=1}^{4} w_{1,i}(h)w_{2,j}(Ma)w_{3,k}(\alpha)\mathrm{K}_{i,j,k} & 0 \end{bmatrix} + \right.
$$

$$
\begin{bmatrix} \mathbf{S}_{D_s} \sum_{i=1}^{2}\sum_{j=1}^{3}\sum_{k=1}^{4} w_{1,i}(h)w_{2,j}(Ma)w_{3,k}(\alpha)\mathrm{K}_{i,j,k} \end{bmatrix} \left(\mathbf{K} \sum_{i=1}^{2}\sum_{j=1}^{3}\sum_{k=1}^{4} w_{1,i}(h)w_{2,j}(Ma)w_{3,k}(\alpha)\mathrm{K}_{i,j,k} \right) \left. \right\} \begin{bmatrix} x_s(t) \\ e(t) \end{bmatrix}
$$

$$
\tag{49}
$$

We translate the system in Eqs. (48) and (49) into its discrete form with the sampling time of 0.005s,

$$
x(t+1) = \Phi(p(\mathrm{t}))x(t) + G(p(\mathrm{t}))g(t) + d(t),
$$
$$
y(t) = H_y(p(\mathrm{t}))x(t)
\tag{50}
$$

We also transform $c = [\alpha \quad q \quad u]^T$ into constrained variables and describe it with the following state variables:

$$
c(t) = H_c x(t)
\tag{51}
$$

$$
H_c = \begin{bmatrix} 1 & 0 & 0 \\ 0 & 1 & 0 \\ \mathrm{K}_1 \underset{n=1}{\overset{N}{\otimes}} \mathrm{w}_n(p_n(t)) & \mathrm{K}_2 \underset{n=1}{\overset{N}{\otimes}} \mathrm{w}_n(p_n(t)) & \mathrm{K}_3 \underset{n=1}{\overset{N}{\otimes}} \mathrm{w}_n(p_n(t)) \end{bmatrix}
\tag{52}
$$

The $d(t)$ should be the model error, and its region is estimated to be within 0.02.

The nominal constraints are formulated into Eq.(42) and the command governor is design. Then, we design the outer-loop flight control system as the PD control of

height error. The total control system is depicted in Figure 3, with $K_h = 0.02$ and $K_d = 0.1$.
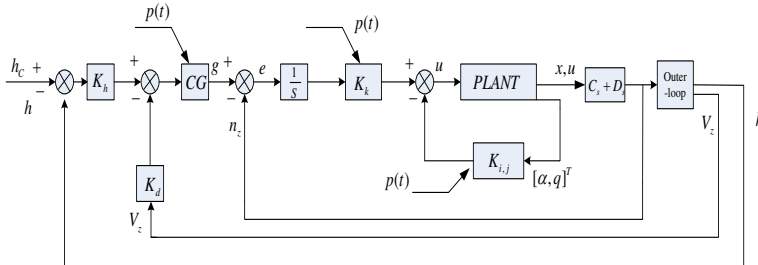

Figure 3

The Framework that includes both the inner and outer-loop control systems
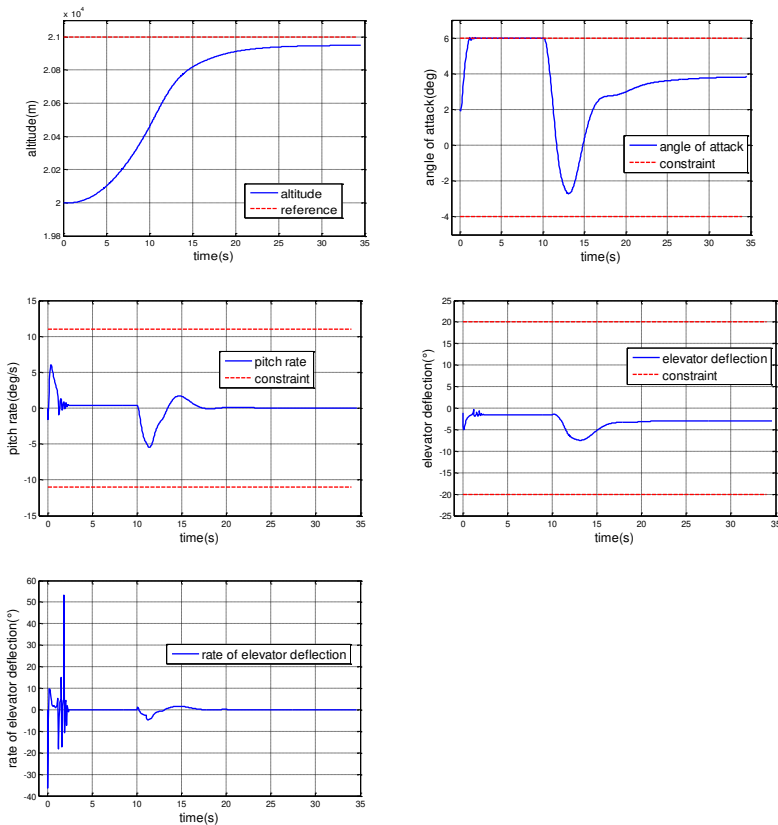

Figure 4

Simulation results

Figure 4 illustrates that the AHV climbs for 1km and shows that: the settling time is less than 20 seconds; the steady-state error is within 50 m; the angle of attack stays within -3 to 6 degrees; the pitch rate stays within -5.5 to 6.5 deg/s; the elevator deflection remains -7.5 to 0 degrees. All the constraints are satisfied. The rate of elevator deflection remains -37 to 54 deg/s, indicating that the control signal satisfies the actuator's constraints. The figure also shows that the angle of attack remains to be the maximum value available, namely for a period of almost 10 seconds when the climbing begins, which gains a maximum lift to accelerate the climbing. This is because when the climbing begins, the error of the command signal h_C and the measured altitude h is big and leads to the big normal overload command of the inner-loop control system. Then, the command governor modifies the overload command to a maximum degree that satisfies all the constraints. In this way, the best use is made of the angle of attack available to realize a quick climbing. When the error decreases and the climbing velocity increases, the AHV adjusts its angle of attack to track the desired altitude without overshoot. The final altitude is 20970 meters, indicating that the altitude tracking system. It is because the altitude tracking system has a steady error. This is because the altitude tracking system is a Type-0 servo system.

Conclusion

The purpose of this study is to demonstrate the successful application of a state and input constrained controller to designing an AHV's control system with a large flight envelope. Based on the TP transformation, the AHV's accurate qLPV model is established with the acceptable number of vertexes and therefore lightens the computational burden for model description and controller design. As to the controller design, the authors use the LQ method within the PDC framework,,thus obtaining a good control performance near all the vertexes and a global stability in the flight envelope. Together with command governor design, the AHV meets all the constraints in the climbing phase. At the beginning of the climbing phase, the flight makes the best use of maximal angle of attack available to climb quickly. The simulation results on the altitude tracking system demonstrate the effectiveness of the proposed state and input constrained control method.

Acknowledgement

References

[1]   C Mu, Z Ni, C Sun, H He: Air-Breathing Hypersonic Vehicle Tracking Control Based on Adaptive Dynamic Programming, IEEE Transactions on Neural Networks & Learning Systems, 28(3) pp. 584-598, 2016

[2]　D P Wiese, AM Annaswamy, JA Muse, MA Bolender: Adaptive Control of a Generic Hypersonic Vehicle, Aiaa Guidance, Navigation, and Control conference, Boston, MA, USA, pp. 19-22, 2013

[3]　X Yang, J Li, Y Dong: Flexible Air-Breathing Hypersonic Vehicle Control Based on a Novel Non-Singular Fast Terminal Sliding Mode Controland Nonlinear Disturbance Observer, Proceedings of the Institution of Mechanical Engineers Part G Journal of Aerospace Engineering, 231(11) pp. 2132-2145, 2016

[4]　L Fiorentini, A Serrani, MA Bolender, DB Doman: Nonlinear Robust Adaptive Control of Flexible Air-Breathing Hypersonic Vehicles, Journal of Guidance Control & Dynamics, 32(2) pp. 402-417, 2012

[5]　Z Guo, J Zhou, J Guo, J Cieslak, J Chang: Coupling Characterization-Based Robust Attitude Control Scheme For Hypersonic Vehicles, IEEE Transactions on Industrial Electronics, 64 (8) pp. 6350-6361, 2017

[6]　Y Wei, Y Chen, G Duan, W Liu: Reference Command Tracking of a Hypersonic Vehicle With Elastic Effects, Guidance, Navigation and Control Conference. China, pp. 1-6, 2016

[7]　Y Zhu, H Shen, Y Liu, G Zhang, Y Lu: Optimal Control and Analysis for Aero-Elastic Model ff Hypersonic Vehicle, Guidance, Navigation and Control Conference, China, pp. 1911-1915, 2016

[8]　X Tao, N Li, S Li: Multiple Model Predictive Control for Large Envelope Flight of Hypersonic Vehicle Systems, Information Sciences, 328(C):pp. 115-126, 2016

[9]　W Jiang, H Wang, J Lu, Z Xie: Hosvd-Based LPV Modeling and Mixed Robust H2/H∞ Control Design for Air-Breathing Hypersonic Vehicle, Journal of Systems Engineering and Electronics, 27(1), pp. 183-191, 2016

[10]　LI Gong Jun: Adaptive Tracking Control For Air-Breathing Hypersonic Vehicles With State Constraints, Frontiers of Information Technology and Electronic Engineering, 18(5):pp. 599-614, 2017

[11]　Zhu S, Li Y, Zhang J, Sun T: Characteristic Model-Based Robust Predictive Control for Reentry Hypersonic Vehicle with Constraints, Guidance, Navigation and Control Conference, China, pp. 634-639, 2016

[12]　Hao A, Xia H, Wang C: Barrier Lyapunov Function-Based Adaptive Control for Hypersonic Flight Vehicles, Nonlinear Dynamics, 88(3) pp. 1833-1853, 2017

[13]　P. Baranyi: TP-Model Transformation-Based-Control Design Frameworks, Springer International Publishing, Switzerland, pp. 258-260, 2016

[14]　P. Baranyi, Y. Yam, P. Várlaki: Tensor Product Model Transformation in Polytopic Model-based Control, Taylor&Francis, Boca Raton FL, pp. 248-250, 2013

[15]   P. Baranyi: The Generalized TP Model Transformation for TS Fuzzy Model Manipulation and Generalized Stability Verification, IEEE Transaction on Fuzzy Systems, 22(4) pp. 934-948, 2014

[16]   P. Baranyi: TP model transformation as a way to LMI based controller design, IEEE Transaction on Industrial Electronics, 51(2) pp. 387-400, 2004

[17]   P. Baranyi, D. Tikk, Y. Yam, R. J. Patton: From Differential Equations to PDC Controller Design via Numerical Transformation, Computers in Industry, 51(3) pp. 281-297, 2003

[18]   H Huang, Y Ke, W Qin: PD-RMPC for a Flexible Air-Breathing Hypersonic Vehicle with Input Saturation and State Constraints, Guidance, Navigation and Control Conference, Yantai, China, pp. 1224-1229, 2014

[19]   A Casavola, E Mosca: Bank-To-Turn Missile Autopilot Design via Observer-Based Command Governor Approach, Journal of Guidance Control & Dynamics, 27(4) pp. 705-710, 2004

[20]   A Casavola, E Mosca, D Angeli: Robust Command Governors for Constrained Linear Systems, Automatic Control IEEE Transactions on automatic control, 45(11) pp. 2071-2077, 2000

[21]   A Szollosi, P Baranyi: Improved Control Performance of The 3-Dof Aeroelastic Wing Section: a TP Model Based 2D Parametric Control Performance Optimization, Asian Journal of Control, 19(2) pp. 450-466, 2017

[22]   A. Szollosi, P. Baranyi: Influence of the Tensor Product Model Representation of QLPV Models on the Feasibility of Linear Matrix Inequality, Asian Journal of control, 18(4) pp. 1328-1342, 2016

[23]   B. Takarics, P. Baranyi: Tensor Product Model Based Control of a Three Degrees-of-Freedom Aeroelastic Model, Journal of Guidance, Control and Dynamics, 36(5) pp. 1527-1533, 2013

[24]   A. Szollosi, P. Baranyi: Improved control performance of the 3-DoF aeroelastic wing section: a TP model based 2D parametric control performance optimization, Asian Journal of Control, 19(2) pp. 450-466, 2017

[25]   P. Gahinet, A. Nemirovski, A. J. Laub, M. Chilali: LMI Control Toolbox, Math Works, 1995

[26]   Kolmanovsky I, Gilbert EG: Theory and computation of disturbance invariant sets for discrete-time linear systems, Mathematical Problems in Egineering,4(4) pp. 317-367, 1998

[27]   Artstein Z, Rakovi´c SV: Set-invariance under output-feedback: a set-dynamics approach, International Journal of Systems Science 42(4) pp. 539-555, 2011

Tensor Product Model Transformation based Parallel Distributed Control of Tumor Growth

Levente Kovács and György Eigner

Physiological Controls Research Center
Research and Innovation Center of Óbuda University
H-1034, Budapest, Bécsi út 96/B
{kovacs.levente,eigner.gyorgy}@nik.uni-obuda.hu

Abstract: The current work investigates tumor growth control under antiangiogenic targeted molecular therapy by use of Tensor Product (TP) transformation. During the dynamics of the tumor growth we have considered that the tumor volume $x_1(t)$ is measurable, while due to the lack of information about the second state $x_2(t)$ (the inhibitor level in the serum), we have developed an appropriate Extended Kalman Filter (EKF) to estimate it. We applied different quasi Linear Parameter Varying (qLPV) models during the design of the EKF and the controller. Tensor Product model transformation method completed with Linear Matrix Inequality based optimization have been applied to design the main controller. The reference signals were generated by trajectory tracking kind control based on Inverse Dynamic Control - Proportional Derivate compensator, applied it on the "simulated" (original) model. We did not consider any state disturbance. However, we have taken into account sensor noise in accordance with the properties of the model.

We have found that all of the control goals have been satisfied with the developed control framework: (i) the tumor volume was lower than 1 mm^3 at the end of the therapy; (ii) the developed models have approached each other with good accuracy; (iii) the totally injected inhibitor level was physiologically acceptable.

Keywords: Antiangiogenic Targeted Molecular Tumor Therapy, Tensor Model transformation, Linear Parameter Varying, Linear Matrix Inequality, Parallel Distributed Control

1   Introduction

Targeted Molecular Therapies (TMTs) are advanced tumor therapeutic possibilities which can be used beside the classical treatments (e.g. chemotherapy, radiotherapy, etc.). TMT drugs directly inhibit the specific biochemical pathways used by the different kinds of cancers in order for growing, proliferation and spreading [1, 2]. Hence, by TMTs more personalized treatment can be achieved focusing on the vital phenomena of the tumor and applying specific drugs [3]. The main benefits of TMTs are less damaging to the normal cells, causing less side effects, improving

the efficiency of regular therapies and improving the quality of life of the patients [2]. Among the several types of TMTs the mostly commonly used ones are the apoptosis inducers, gene expression inhibitors, signal transmission inhibitors and anti-angiogenic therapies [3].

Angiogen inhibitors are commonly used in modern medicine by targeting the so-called pro-angiogen factor, the vascular endothelial growth factor (VEGF) that indicates the endothelial proliferation leading to the formation of new blood vessels. The tumors produce VEGF in order to get new blood vessels through which they are able to get the nutrients for further growing. By inhibiting this molecular pathway, the new blood vessels formation phenomena can be decreased causing the "starvation" of the tumor [3–5]. The nature of this process is an excellent therapeutic target to be combined with control engineering methodologies optimizing the drug injection and therapy outcomes [6]. One of the most commonly used TMT drugs in case of angiogen inhibition is bevacizumab which is investigated in this study as well as the parametric identification done by the preparation of the applied model [7].

Similarly to other physiological control applications like diabetes or anesthesia [8–13] the control of tumor growth is challenging due to several unfavorable effects that should be taken into account. The nonlinear nature of the process completed with cross-effects, parameter and model uncertainties and time-delays increases the difficulty of the problem. Recently, several results appeared in the topic of antiangiogenic TMT control problem [6, 14–18].

The current work investigates the combined applicability of advanced control methodologies. One of the most promising ones is represented by the LPV framework, a useful technique to apply the well-developed linear control methods on the original nonlinear model without linearizing it [19]. The TP model transformation represents another solution that can be combined with LMI based optimization and can be done on LPV functions as well, making it possible to design TP-LPV-LMI kind controllers [20]. These kind of controllers have many beneficial properties: the parameter uncertainties and the nonlinearities can be embedded into the model making the designed controller robust against these effects. Furthermore, the control requirements can be formulated as LMIs, which can be taken into account during the design procedure in order to guarantee their satisfaction by the control action.

On the other hand, not all of the state variables of given models are available. One suitable solution to deal with this problem is definitely Kalman-filtering. The Extended Kalman Filter (EKF) represents an estimator designed for nonlinear systems that can be used effectively for highly nonlinear as well [21].

The paper is structured as follows: first, the minimal tumor growth model and the developed qLPV models are introduced. After, the controller design procedure is detailed including the TP model transformation, the LMI based optimization, the EKF design and the development of the reference subsystem. Finally, the results of the numerical simulations are presented, done in MATLAB environment.

2 Tumor Growth Models

2.1 The Examined Tumor Growth Model

The current study focuses on the minimal tumor growth model [22,23]. This second-order model includes two state variables: $x_1(t)$ [mm^3] for the tumor volume and $x_2(t)$ [mg/kg] as the serum inhibitor level:

$$\begin{aligned} \dot{x}_1(t) &= ax_1(t) - bx_1(t)x_2(t) \\ \dot{x}_2(t) &= -cx_2(t) + u(t) \end{aligned} \quad . \tag{1}$$

The control input is represented by the inhibitor intake $u(t)$ [mg/kg/day], while the output of the model is the $x_1(t)$ tumor volume – that is assumed to be measurable. Three scalar parameters determine the dynamic specificities of the model: a [1/day] is the tumor growth rate, b [kg/mg/day] is the inhibitor rate and c [1/day] is the inhibitor clearance rate. During our investigations the following dataset has been used: $[a, b, c]^\top = [0.27, 0.0074, \ln(2)/3.9]^\top$. These values are coming from parametric identification done on measurements from mice experiments related to C38 colon adenocarcinoma [22].

As a result, the model is a simple mathematical formulation of the phenomena. It is assumed that by using only antiangiogen inhibitor (e.g. bevacizumab [24]) the tumor volume can be maintained and decreased. In the lack of inhibitor, the $x_1(t)$ tumor volume grows limitlessly with the dynamics determined by a. The nontrivial equilibrium of the model can be calculated as follows:

$$\begin{aligned} 0 &= ax_{1,\infty} - bx_{1,\infty}x_{2,\infty} \\ 0 &= -cx_{2,\infty} + u_\infty \end{aligned} \quad , \tag{2}$$

from which $x_{1,\infty}$ and u_∞ becomes:

$$x_{2,\infty} = \frac{a}{b} \, , \tag{3a}$$

$$u_\infty = -c\frac{a}{b} \, . \tag{3b}$$

Hence, $x_{2,\infty}$ and u_∞ are independent from $x_{1,\infty}$. It is easy to see that $x_2(t) = a/b$ is needed to keep the tumor volume on a certain level and $x_2(t) > a/b$ should be used to decrease the $x_1(t)$. The belonging control signals are $u(t) = c \cdot a/b$ and $u(t) > c \cdot a/b$, respectively. These requirements have to be taken into account during the controller design.

It should be noted that a lower limit was applied against the tumor volume in all kind of models appearing in this study: $\min(x_1(t)) = \min(x_{1,ref}(t)) = \min(\hat{x}_1(t)) = 10^{-3}$ mm^3 – which is an approximation of the zero level. From the antiangiogenic TMTs point of view this is reasonable since the goal of these kinds of therapies are usually not to eliminate (kill) the tumor itself, but to keep its volume under a certain level [25].

2.2   The Reference Model

As it will be introduced later, the main goal of the control is to enforce the original nonlinear model to behave as a given – beneficiary selected – reference model. As $x_1(t)$ can be measured, a simple model was developed with decreasing state trajectory:

$$x_{1,nom}(t) = e^{(-\xi \cdot t)} \cdot x_{1,ref}(t_0) \ , \tag{4}$$

where ξ is a scalar and t represents the time. $x_{ref}(t_0)$ is the – known – initial value of the reference model which can be determined by exact measurement (if $x_1(t_0) = x_{1,ref}(t_0)$) or estimation (if $\hat{x}_1(t_0) = x_{1,ref}(t_0)$). This reference model will be used for trajectory determination during the controller design.

2.3   qLPV Model Development

In conformity with [26–28], the general state-space form of an LPV model is the following:

$$
\begin{aligned}
\dot{\mathbf{x}}(t) &= \mathbf{A}(\mathbf{p}(t))\mathbf{x}(t) + \mathbf{B}(\mathbf{p}(t))\mathbf{u}(t) \\
\mathbf{y}(t) &= \mathbf{C}(\mathbf{p}(t))\mathbf{x}(t) + \mathbf{D}(\mathbf{p}(t))\mathbf{u}(t) \\
\mathbf{S}(\mathbf{p}(t)) &= \begin{bmatrix} \mathbf{A}(\mathbf{p}(t)) & \mathbf{B}(\mathbf{p}(t)) \\ \mathbf{C}(\mathbf{p}(t)) & \mathbf{D}(\mathbf{p}(t)) \end{bmatrix} \\
\begin{pmatrix} \dot{\mathbf{x}}(t) \\ \mathbf{y}(t) \end{pmatrix} &= \mathbf{S}(\mathbf{p}(t)) \begin{pmatrix} \mathbf{x}(t) \\ \mathbf{u}(t) \end{pmatrix}
\end{aligned}
\tag{5}
$$

The considered vectors and parameter dependent matrices are: $\mathbf{x}(t) \in \mathbb{R}^n$ state vector, $\mathbf{u}(t) \in \mathbb{R}^m$ input vector, $\mathbf{y}(t) \in \mathbb{R}^k$ output vector, $\mathbf{A}(\mathbf{p}(t)) \in \mathbb{R}^{n \times n}$ state matrix, $\mathbf{B}(\mathbf{p}(t)) \in \mathbb{R}^{n \times m}$ input matrix, $\mathbf{C}(\mathbf{p}(t)) \in \mathbb{R}^{k \times n}$ output matrix, $\mathbf{D}(\mathbf{p}(t)) \in \mathbb{R}^{k \times m}$ feedforward matrix and $\mathbf{S}(\mathbf{p}(t)) \in \mathbb{R}^{(n+k) \times (n+m)}$ system matrix – the latter one is the so-called LPV function (inasmuch any of the state variables is involved as scheduling variable we call it quasi-LPV (qLPV) model and qLPV function [27]). The matrices in (5) are dependent from the $\mathbf{p}(t) \in \Omega^R \in \mathbb{R}^R$ parameter vector that consists of the so-called scheduling variables $p_i(t)$, namely, $\mathbf{p}(t) = [p_1(t) \dots p_R(t)]^\top$. The $\Omega = [p_{1,min}, p_{1,max}] \times [p_{2,min}, p_{2,max}] \times \dots \times [p_{R,min}, p_{R,max}] \in \mathbb{R}^R$ hypercube – a subspace of the $\mathbb{R}^R$ real vector space – is characterized by the extremes of the $p_i(t)$. As it will be seen in the subsequent sections, two different qLPV models have been developed and applied. In order to avoid any misunderstanding, alternative notations for the parameter vectors belonging to the qLPV model were used. In case of Model-I $\mathbf{q}(t) = q(t) \in \mathbb{R}^1$, while for Model-II this is $\mathbf{p}(t) \in \mathbb{R}^2$.

2.3.1   Model-I

We have selected the $q(t) = x_1(t)$ as scheduling variable from (1) which leads to the following qLPV model:

$$\dot{\mathbf{x}}(t) = \mathbf{A}_I(q(t))\mathbf{x}(t) + \mathbf{B}_I\mathbf{u}(t)$$
$$\mathbf{y}(t) = \mathbf{C}_I\mathbf{x}(t)$$
$$\mathbf{S}_I(q(t)) = \begin{bmatrix} \mathbf{A}_I(q(t)) & \mathbf{B}_I \\ \mathbf{C}_I & \mathbf{D}_I \end{bmatrix} = \begin{bmatrix} a & -bq(t) & 0 \\ 0 & -c & 1 \\ 1 & 0 & 0 \end{bmatrix} , \qquad (6)$$

where the I subscript is related to Model-I. In this case, $\mathbf{B}_I = \mathbf{B}$ and $\mathbf{C}_I = \mathbf{C}$ are equal to each other due to the lack of specific transformation – we only pointed out one state variable. The selected range for $q(t) is \{10^{-3}, \ldots, 5 \times 10^5\}$. The lower boundary is related to the aforementioned limitation against the tumor volume. The upper boundary is in conformity with our previous investigations [6]. Model-I was developed to support the EKF design and application as it will be introduced later.

2.3.2   Model-II

In order to apply state feedback kind controller without reference compensation, a corresponding qLPV model is necessary. The difference based control oriented qLPV models can be a solution for this issue [29]. In this case, the deviation between the states of the model to be controlled and from the states of a given reference system should be modeled, namely, the dynamics of the "state error". For the actual problem this means: $\Delta x_1(t) = x_1(t) - x_{1,ref}(t)$, $\Delta x_2(t) = x_2(t) - x_{2,ref}(t)$ and $\Delta u(t) = u(t) - u_{ref}(t)$. By this transformation the control goal is transformed as well: instead of reaching a certain value by the state variables the new control goal becomes – reaching zero level by the states over time. Hence, $\Delta\mathbf{x}(t) = [\Delta x_1(t), \Delta x_2(t)]^\top$, $\Delta\mathbf{x}(t) \to \mathbf{0}$, $t \to \infty$. In case of a state feedback kind controller this can be obtained, if we use the $\Delta\mathbf{r} = \mathbf{0}^{2\times 1}$ reference signal and the $\Delta\mathbf{x}(t)$ is compared to this zero reference. The derivation of the transformed differential equations is the following:

$$\begin{aligned}
\Delta\dot{x}_1(t) &= \dot{x}_1(t) - \dot{x}_{1,ref}(t) = ax_1(t) - bx_1(t)x_2(t) \\
&\quad - \big(ax_{1,ref}(t) - bx_{1,ref}(t)x_{2,ref}(t)\big) = \\
a\Delta x_1(t) &- bx_1(t)x_2(t) - bx_{1,ref}(t)x_{2,ref}(t) + 0 = \\
a\Delta x_1(t) &- bx_1(t)x_2(t) - bx_{1,ref}(t)x_{2,ref}(t) \\
&\quad + bx_1(t)x_{2,ref}(t) - bx_1(t)x_{2,ref}(t) = \\
(a &- bx_{2,ref}(t))\Delta x_1(t) - bx_1(t)\Delta x_2(t)
\end{aligned} \qquad . \qquad (7)$$

$$\begin{aligned}
\Delta\dot{x}_2(t) &= \dot{x}_2(t) - \dot{x}_{2,ref}(t) = -cx_2(t) + u(t) - \big(-cx_2(t) + u(t)\big) = \\
&\quad -c\Delta x_2(t) + \Delta u(t)
\end{aligned}$$

The state-space form of (7) will be the following:

$$\Delta\dot{\mathbf{x}}(t) = \mathbf{A}_{II}(\mathbf{p}(t))\Delta\mathbf{x}(t) + \mathbf{B}_{II}\Delta\mathbf{u}(t)$$
$$\Delta\mathbf{y}(t) = \mathbf{C}_{II}\Delta\mathbf{x}(t)$$

$$\mathbf{S}_{II}(\mathbf{p}(t)) = \begin{bmatrix} \mathbf{A}_{II}(\mathbf{p}(t)) & \mathbf{B}_{II} \\ \mathbf{C}_{II} & 0 \end{bmatrix} = \begin{bmatrix} a - bp_1(t) & -bp_2(t) & 0 \\ 0 & -c & 1 \\ 1 & 0 & 0 \end{bmatrix} . \tag{8}$$

The selected scheduling variables have been $p_1(t) = x_{2,ref}(t) \in \{a/b + 10^{-3}, \ldots, 10^4\}$ and $p_2(t) = x_1(t) \in \{10^{-3}, \ldots, 5 \times 10^5\}$ at which $\mathbf{p}(t) = [p_1(t), p_2(t)]^\top$. If the goal is to keep the tumor's level on a certain value, $x_2 = a/b$ should be reached via $u = c \cdot a/b$. Consequently, we have approached the a/b by $a/b + 10^{-3}$ in order to increase the numerical stability, further, to keep the controllability of Model-II. $p_{1,max} = 10^4$ is considered the maximum value which may occur [6], while $p_{2,min}$ and $p_{2,max}$ are the same as in case of q discussed in Model-I.

3 Control Design

3.1 TP Model Transformation and Control

By TP model transformation it was possible to convert the qLPV function into convex polytopic TP model form. The resulting TP model is able to describe the initial qLPV function and through the original nonlinear system with given accuracy. The usability of this tool has been proven several times for highly nonlinear systems (e.g. [20, 30–33]), what the physiological systems are in general [34]. Applying the TP model transformation on the qLPV function of (5), the following finite element convex polytopic TP model is obtained:

$$\begin{pmatrix} \dot{\mathbf{x}}(t) \\ \mathbf{y}(t) \end{pmatrix} = \mathbf{S}(\mathbf{p}(t)) \begin{pmatrix} \mathbf{x}(t) \\ \mathbf{u}(t) \end{pmatrix}$$
$$\mathbf{S}(\mathbf{p}(t)) = \mathscr{S} \underset{r=1}{\overset{R}{\boxtimes}} \mathbf{w}_r(p_r(t)) = \mathscr{S} \times_r \mathbf{w}(\mathbf{p}(t)) \tag{9}$$

The core tensor $\mathscr{S} \in \mathbb{R}^{I_1 \times I_2 \times \ldots \times I_R \times (n+k) \times (n+m)}$ consists of the $\mathbf{S}_{i_1,i_2,\ldots,i_R}$ LTI vertices. The $\mathbf{w}_r(p_r(t))$ weighting vector function consists of the $w_{r,i_r}(p_r(t))$ ($i_r = 1\ldots I_R$) continuous convex weighting functions. The convexity is held, if $\forall r, i, p_r(t):$

$$w_{r,i_r}(p_r(t)) \in [0, 1] \text{ and } \forall r, p_r(t) : \sum_{i=1}^{I_r} w_{r,i_r}(p_r(t)) = 1.$$

Different kinds of convex hulls can be applied during the TP model transformation. In this study the Minimal Volume Simplex (MVS) convex hull was considered that allows the use of the smallest convex hull inside Ω [35]. However, the TP model approximating the original model inside the Ω hypercube with certain accuracy depends on the applied sampling resolution in Ω [36]. The practical realization of the TP model transformation can be found in [20, 31, 36, 37].

In case of general state-feedback control, the control signal can be generated in the LPV case as follows [20, 27, 30, 31]:

$$\mathbf{u}(t) = -\mathbf{G}(\mathbf{p}(t))\mathbf{x}(t) \ , \tag{10}$$

if the case is $\mathbf{r}(t) = \mathbf{0}^{n \times 1}$ – which is in conformity with (8) and the used Model-II. In (10), the $\mathbf{G}(\mathbf{p}(t)) \in \mathbb{R}^{m \times n}$ is the parameter dependent controller gain. Consequently, the polytopic convex TP controller becomes:

$$\mathbf{G}(\mathbf{p}(t)) = \mathscr{G} \underset{r=1}{\overset{R}{\boxtimes}} \mathbf{w}_r(p_r(t)) = \mathscr{G} \times_r \mathbf{w}(\mathbf{p}(t)) \ . \tag{11}$$

As a result, the $\mathscr{G}$ feedback tensor consisting by $\mathbf{G}_{i_1, i_2, \dots, i_R}$ feedback gain matrices belongs to the given $\mathbf{S}_{i_1, i_2, \dots, i_R}$ LTI systems. The $\mathbf{w}_r(p_r(t))$ convex weighting functions are the same as in (7). Further derivations, explanations and case studies can be found in [32,35,36,38]. The TP model transformation has been successfully adopted and applied in many technical fields thanks to the continuous improvements in the recent times. New approaches have appeared regarding the computational improvements related to TP model transformation [39, 40]. The latest research explored that the LMI based controller design methods are sensitive to the applied convex hulls. Hence, the selection of the applicable convex hull manipulation and the convex hull candidate with respect to the LMI based controller design methods is a critical aspect [31, 41–43]. Effective convex hull manipulation techniques are introduced in [35, 44, 45]. The application of the TP model based control can be found both in physical control systems [46–59] and it was applied in case of physiological controls as well [60–66]. Many other important control approaches regarding the TP model transformation have been elaborated in [56, 67–74]

3.2   Linear Matrix Inequality based Optimization

In accordance with Lyapunov's direct method, an $\dot{\mathbf{x}}(t) = \mathbf{A}\mathbf{x}(t)$ system is stable if there exists a $V(\mathbf{x}) = \mathbf{x}^\top \mathbf{P}\mathbf{x}$ positive definite quadratic Lyapunov function and the $\dot{V}(\mathbf{x}) = \mathbf{x}^\top (\mathbf{A}^\top \mathbf{P} + \mathbf{P}\mathbf{A})\mathbf{x}$ is negative definite, namely, $\mathbf{A}^\top \mathbf{P} + \mathbf{P}\mathbf{A} < \mathbf{0}$ and $\mathbf{P} = \mathbf{P}^\top > \mathbf{0}$ [20, 75]. The $\dot{\mathbf{x}}(t) = \mathbf{A}(\mathbf{p}(t))\mathbf{x}(t) + \mathbf{B}(\mathbf{p}(t))\mathbf{u}(t)$ is the system equation of a general, polytopic system, where the $[\mathbf{A}(\mathbf{p}(t)) \ \mathbf{B}(\mathbf{p}(t))] = \sum_{r=1}^{R} w_r(\mathbf{p})[\mathbf{A}_r \ \mathbf{B}_r]$ are the polytopic vertices and $w_r(\mathbf{p})$ is the belonging convex weighting function [20]. By utilizing the $V(\mathbf{x}(t)) = \mathbf{x}^\top \mathbf{P}\mathbf{x} = \mathbf{x}^\top \mathbf{X}^{-1}\mathbf{x}$ Lyapunov function, the controller candidate becomes [36]:

$$\mathbf{u}(t) = \mathbf{M}(\mathbf{p}(t))\mathbf{X}^{-1}\mathbf{x}(t) = \sum_{j=1}^{J} w_j(\mathbf{p})\mathbf{M}_j \mathbf{X}^{-1}\mathbf{x}(t) \ . \tag{12}$$

By realizing the derivative of the Lyapunov function, the following term appears, where "Sym" acronym means symmetric:

$$\dot{V}(\mathbf{x}(t)) = \mathbf{x}^\top(t)\mathbf{X}^{-1} \cdot \mathrm{Sym}\big(\mathbf{A}(\mathbf{p})\mathbf{X} + \mathbf{B}(\mathbf{p})\mathbf{M}(\mathbf{p})\big) \cdot \mathbf{X}^{-1}\mathbf{x}^\top(t) \ , \tag{13}$$

The symmetric term can be described by using the polytopic weighting functions as follows:

$$\text{Sym}\big(\mathbf{A}(\mathbf{p})\mathbf{X}+\mathbf{B}(\mathbf{p})\mathbf{M}(\mathbf{p})\big) = \sum_{i=1}^{R}\sum_{j=1}^{R} w_i(\mathbf{p})w_j(\mathbf{p})\,\text{Sym}\big(\mathbf{A}_i\mathbf{X}+\mathbf{B}_i\mathbf{M}_j\big) < \mathbf{0} \ . \quad (14)$$

The $\mathbf{S}(\mathbf{p}(t)) = \text{Co}(\mathbf{S}_1,\mathbf{S}_2,\ldots,\mathbf{S}_R)$ and $\mathbf{G}(\mathbf{p}(t)) = \text{Co}(\mathbf{G}_1,\mathbf{G}_2,\ldots,\mathbf{G}_R)$ are polytopic structures – the "Co" acronym means convex combination. In this study, we have applied Parallel Distributed Compensation (PDC) type control. This is possible if the same $\mathbf{w}(\mathbf{p}(t))$ weighting functions are used (to describe the polytopic qLPV system and the controller) citeBaranyi:2013. As a result, LMI optimization can be used in order to design a quadratically stabilizing PDC for continuous polytopic systems [75]:

$$\begin{aligned}
&\mathbf{X} > \mathbf{0}, \\
&-\mathbf{X}\mathbf{A}_i^\top - \mathbf{A}_i\mathbf{X} + \mathbf{M}_i^\top\mathbf{B}_i^\top + \mathbf{B}_i\mathbf{M}_i > \mathbf{0}, \\
&-\mathbf{X}\mathbf{A}_i^\top - \mathbf{A}_i\mathbf{X} - \mathbf{X}\mathbf{A}_j^\top - \mathbf{A}_j\mathbf{X} + \mathbf{M}_j^\top\mathbf{B}_i^\top + \mathbf{B}_i\mathbf{M}_j + \mathbf{M}_i^\top\mathbf{B}_j^\top + \mathbf{B}_j\mathbf{M}_i \ge \mathbf{0}, \\
&i < j \le R \ \ s.t. \ \ \forall\mathbf{p}(t) : w_i(\mathbf{p}(t))w_j(\mathbf{p}(t)) = 0,
\end{aligned} \quad (15)$$

where $\mathbf{X}^{n\times n}$ is a positive definite and symmetric matrix, $\mathbf{M}_i^{m\times n}$ is the supplementary matrix and w_i and w_j are general polytopic weighting functions, respectively.

In accordance with [36, 75], the control gain is calculated as follows: $\mathbf{M}_i = \mathbf{G}_i\mathbf{X}$, thus, $\mathbf{G}_i = \mathbf{M}_i\mathbf{X}^{-1}$. As the level of injectable inhibitor level is limited – in conjunction with the physiological reality – an LMI constraint was applied on the control input to avoid the unrealistically high injections from the drug.

$$\begin{aligned}
&\min_{\mathbf{X},\mathbf{M}} \mu \\
&\mathbf{X} \ge \mathbf{I}, \\
&\begin{bmatrix} \mathbf{X} & \mathbf{M}^\top \\ \mathbf{M} & \mu^2\mathbf{I} \end{bmatrix} \ge \mathbf{0}
\end{aligned} \quad . \quad (16)$$

By using (16), the $\|\mathbf{u}(t)\|_2 \le \mu$ at $t \ge 0$ can be guaranteed. This is true if $\mathbf{x}(0)$ lies in the polytope, which needs that $\|\mathbf{x}(t_0)\|_2 \le 1$, as it is stated in [76]. We have considered the Model-II from (8) during the controller design via LMI optimization. Due to the constraint on $p_{1,min}$, the rank$(\mathscr{C}(\mathbf{A}_{II}(\mathbf{p}(t)),\mathbf{B}_{II})) = n = 2 \ \forall\mathbf{p}(t)$, namely, the controllability property of Model-II can be kept in the Ω parameter domain.

3.3   Extended Kalman Filter Design

The use of mixed continuous/discrete EKF is quite common regard to physiological applications, as the process to be estimated is continuous, however, the measurements are performed by discrete sensors [21, 77, 78]. During the EKF design we have applied the Model-I qLPV model. The assumed sampling time was considered $T = 1$ day in accordance with the model properties of (1).

Hence, the general system description regard to the EKF becomes [21]:

$$\begin{aligned}
&\dot{\mathbf{x}}(t) = f(\mathbf{x}(t),\mathbf{u}(t)) + \mathbf{w}(t), \quad \mathbf{w}(t) \sim \mathcal{N}(\mathbf{0},\mathbf{Q}(t)) \\
&\mathbf{y}_k = h(\mathbf{x}_k) + \mathbf{v}_k, \quad \mathbf{v}_k \sim \mathcal{N}(\mathbf{0},\mathbf{R}_k)
\end{aligned} \quad , \quad (17)$$

where $f = \mathbf{A}_I(\mathbf{p}(t))\mathbf{x}(t) + \mathbf{B}_I\mathbf{u}(t)$ is the system equation from (6) and $\mathbf{x}_k = \mathbf{x}(t_k)$. The $\mathbf{w}(t)$ represents the continuous disturbance, while $\mathbf{v}_k$ is the discrete noise signal. The h is the discrete sensor model and is equal to $h = C_I\mathbf{x}_k$ from (6) since the discretization does not modify the output model in this case.

Due to the properties of the original model no system disturbance was considered. From the design point of view that means $\mathbf{Q}(t) = \mathbf{0}^{n \times n}$. However, we assumed moderate measurement noise: $\mathbf{R}_k = \sigma^2 = 50^2$. The applied σ variance was arbitrarily selected – to be reasonable compared to the magnitude of the output.

The considered initial conditions have considered the followings: $\hat{\mathbf{x}}_{0|0} = \mathrm{E}\big[\mathbf{x}(t_0)\big]$ and $\mathbf{P}_{0|0} = \mathrm{Var}\big[\mathbf{x}(t_0)\big]$. The prediction phase of the mixed EKF is to solve the following differential equations with respect to Model-I:

$$\begin{aligned}\dot{\hat{\mathbf{x}}}(t) &= f(\hat{\mathbf{x}}(t), \mathbf{u}(t), q(t)) \\ \dot{\mathbf{P}}(t) &= \mathbf{F}(t)\mathbf{P}(t) + \mathbf{P}(t)\mathbf{F}^\top(t) + \mathbf{Q}(t)\end{aligned} \quad , \tag{18}$$

where $\hat{\mathbf{x}}(t_{k-1}) = \hat{\mathbf{x}}_{k-1|k-1}$, $\mathbf{P}(t_{k-1}) = \mathbf{P}_{k-1|k-1}$ and $\mathbf{F}(t) = \left.\dfrac{\partial f}{\partial \mathbf{x}}\right|_{\hat{\mathbf{x}},\mathbf{u}}$. The obtained results are applied in the updating phase of the EKF as follows: $\hat{\mathbf{x}}_{k|k-1} = \hat{\mathbf{x}}(t_k)$ and $\mathbf{P}_{k|k-1} = \mathbf{P}(t_k)$.

Consequently, the so-called Kalman gain is calculated as the first part of the updating phase:

$$\mathbf{K}_k = \mathbf{P}_{k|k-1}\mathbf{H}_k^\top (\mathbf{H}_k\mathbf{P}_{k|k-1}\mathbf{H}_k^\top + \mathbf{R}_k)^{-1} \quad . \tag{19}$$

here, the $\mathbf{H}_k = \left.\dfrac{\partial h}{\partial \mathbf{x}}\right|_{\hat{\mathbf{x}}_{k|k-1}}$. Finally, the last step of the EKF design and operation is the correction of the prediction with respect to the measurement by using the calculated Kalman gain:

$$\begin{aligned}\hat{\mathbf{x}}_{k|k} &= \hat{\mathbf{x}}_{k|k-1} + \mathbf{K}_k(\mathbf{y}_k - h(\hat{\mathbf{x}}_{k|k-1})) \\ \mathbf{P}_{k|k} &= (\mathbf{I} - \mathbf{K}_k\mathbf{H}_k)\mathbf{P}_{k|k-1}\end{aligned} \quad , \tag{20}$$

at which $\mathbf{I}$ is an identity matrix.

3.4   Design of the Reference Trajectories

In order to design the $u_{ref}(t)$ and the reference state trajectories $\mathbf{x}_{ref}(t)$, the so-called inverse dynamics compensation was applied (a widely used tool in robotics), and completed with proportional-derivative (IDC-PD) compensator [8, 79, 80].

In case of the IDC-PD compensator the first step is to determine the direct connection between the control signal and the controlled variable in order to map the control effect via the model; moreover, to determine the order of the control. In the current case, the $u(t)$ directly affects the $\ddot{x}_1(t)$ according to (1). Thus, it is possible

to define a suitable description for $\ddot{x}_1(t)$ – in our case (4) has applied. The next step is to elaborate the second derivative of (4):

$$
\begin{aligned}
x_{1,nom}(t) &= e^{(-\xi \cdot t)} \cdot x_{1,ref}(t_0) \\
\dot{x}_{1,nom}(t) &= -\xi e^{(-\xi \cdot t)} \cdot x_{1,ref}(t_0) \\
\ddot{x}_{1,nom}(t) &= (-\xi)^2 e^{(-\xi \cdot t)} \cdot x_{1,ref}(t_0)
\end{aligned}
\qquad . \tag{21}
$$

As a result, the general second order compensator can be written [80]:

$$
F(\ddot{z}_{nom}(t) - \ddot{z}(t)) + F_D(\dot{z}_{nom}(t) - \dot{z}(t)) + F_P(z_{nom}(t) - z(t)) \; , \tag{22}
$$

where F is the weighting parameter of the second derivative of the error function, F_D is the derivative weighting parameter of the first derivative of the error function, F_P is the proportional weighting parameter of the the error function, $z_{nom}(t)$ is the desired nominal state trajectory and $z(t)$ is the state variable to be controlled.

As the idea is to characterize the reference system, (1) is used to describe it:

$$
\begin{aligned}
\dot{x}_{1,ref}(t) &= ax_{1,ref}(t) - bx_{1,ref}(t)x_{2,ref}(t) \\
\dot{x}_{2,ref}(t) &= -cx_{2,ref}(t) + u_{ref}(t)
\end{aligned}
\qquad . \tag{23}
$$

Here the original system is considered as an exactly known and valid one. Naturally, different reference systems can be used that are able to describe the connection between the control signal and the variable to be controlled.

As the trajectory tracking is needed for $x_{1,ref}(t)$, the next step is to elaborate (22) for the current problem:

$$
\begin{aligned}
\ddot{x}_{1,ref}(t) = \quad & a\dot{x}_{1,ref}(t) - b\dot{x}_{1,ref}(t)\dot{x}_{2,ref}(t) = \\
& a\dot{x}_{1,ref}(t) - b\dot{x}_{1,ref}(t)(-cx_{2,ref}(t) + u_{ref}(t))
\end{aligned}
\tag{24}
$$

It is assumed that $F = 1$, which is a generally used consideration in the literature [79, 80]:

$$
\begin{aligned}
&\ddot{e}(t) + F_D\dot{e}(t) + F_Pe(t) = 0 \\
&(\ddot{x}_{1,nom}(t) - \ddot{x}_{1,ref}(t)) + F_D(\dot{x}_{1,nom}(t) - \dot{x}_{1,ref}(t)) + F_P(x_{1,nom}(t) - x_{1,ref}(t)) = 0 \\
&\Big(\ddot{x}_{1,nom}(t) - \big(a\dot{x}_{1,ref}(t) - b\dot{x}_{1,ref}(t)(-cx_{2,ref}(t) + u_{ref}(t))\big)\Big) + \\
&\qquad\qquad F_D(\dot{x}_{1,nom}(t) - \dot{x}_{1,ref}(t)) + F_P(x_{1,nom}(t) - x_{1,ref}(t)) = 0 \\
&u_{ref}(t) = \frac{\ddot{x}_{1,nom}(t) - a\dot{x}_{1,ref}(t) + b\dot{x}_{1,ref}(t)cx_{2,ref}(t)}{-b\dot{x}_{1,ref}(t)} + \\
&\qquad\qquad \frac{F_D(\dot{x}_{1,nom}(t) - \dot{x}_{1,ref}(t)) + F_P(x_{1,nom}(t) - x_{1,ref}(t))}{-b\dot{x}_{1,ref}(t)}
\end{aligned}
\qquad . \tag{25}
$$

We have considered a constraint for (22) taken from the assumption on $p_{1,min}$ and the limitation of the model described in (1) as detailed above (decreasing the tumor

volume, and keeping the controllability and numerical stability).

$$u_{ref}(t) = \begin{cases} c \cdot (a/b + 10^{-3}) & \text{if } u_{ref}(t) \leq c \cdot (a/b + 10^{-3}) \\ (25) & \text{otherwise} \end{cases} . \qquad (26)$$

To sum up, by using $u_{ref}(t)$ from (26) as the input of (23), the $x_{1,ref}(t)$ has similar behavior than $x_{1,nom}(t)$ from (21) – which leads to a smooth reference trajectory to be followed by the volume of the tumor as it is enforced by the TP-LPV-LMI controller via the control framework.

3.5   Final Control Structure

The final control structure is built up from two systems as it can be seen on Figure 1. The reference subsystem is responsible to generate the reference trajectories to be followed by the states of the original system via the control framework. It has to be pointed out that the $u_{ref}(t)$ design method and the reference model applied in the reference subsystem can be arbitrarily selected. The main limitation is that the $u_{ref}(t)$ realization should consider the constraints against the reference control signal described above and the applied reference model has to provide a close-to-accurate description about the connection between $u_{ref}(t)$ and $\mathbf{x}_{ref}(t)$.
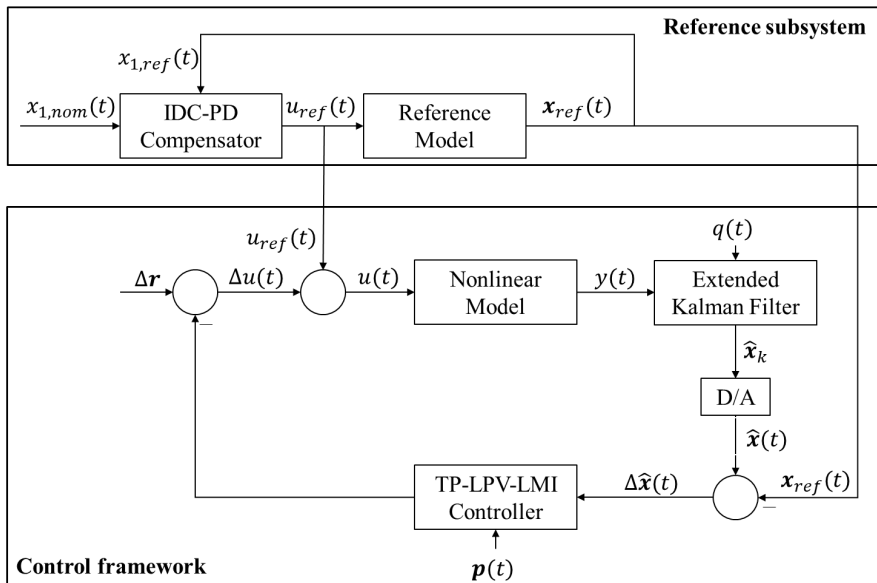

Figure 1
Structure of the control loop.

The control framework enforces that $\mathbf{x}(t) = \mathbf{x}_{ref}(t)$, $t \to \infty$. This is the same as $\Delta \mathbf{r} = \mathbf{x} - \mathbf{x}_{ref} = \mathbf{0}$. Due to the fact that $x_2(t)$ cannot be measured, it is provided by the EKF during the operation and $\hat{x}_2(t)$ is used for the difference generation.

4   Results of the Numerical Simulation

The realization of the control framework was done in the MATLAB framework using the forward method of Euler: $\mathrm{d}\mathbf{x}(t_0)/\mathrm{d}t \approx (\mathbf{x}(t_0 + T) - \mathbf{x}(t_0))/T$, where T represents the sampling time.

In accordance with the model properties we did not consider state disturbance neither at the EKF design nor at simulations. Therefore, we assumed that $d \equiv 0$. However, we assumed the presence of limited measurement noise with normal distribution: $v(t) \sim \mathcal{N}(0, 50^2)$ mm^3. We have taken into account this specificity during the EKF design and prepared the control framework for this action – moreover, the measurement noise only prevailed in $\hat{x}_1(t)$. By using the EKF, the noise appeared in the $u(t)$ – however, in an oppressed way.

A summary of the applied circumstances can be seen in Table 2. Since $x_1(t)$ have been considered as measurable, we assumed that $x_1(t_0)$ is available. On the other hand, $x_2(t_0) = 0$ represents that there is no inhibitor in the serum before the beginning of the therapy. The initial state variables of the EKF were selected by considering the previously mentioned facts: $x_1(t)$ is known and $x_2(t_0)$ is zero. We have applied $\hat{x}_1(t_0) = 30100$ mm^3 taking into account that there is a measurement noise from the beginning of the simulation. However, we have applied $x_{2,ref}(t_0) = a/b + 10^{-3}$ coming from the aforementioned fact in regards to $p_{1,min}$. Figure 2.

Table 1
Important indicators of the numerical simulations.

Notation	Value	Description
T	1 day	Sampling time
$O_{sampling}$	$[199, 199]^\top$	Sampling resolution of the TP model transformation in the Ω
$\mathbf{x}(t_0)$	$[30000, 0]^\top$	Initial values – original system
$\hat{\mathbf{x}}(t_0)$	$[30100, 0]^\top$	Initial values – EKF
$\mathbf{x}_{ref}(t_0)$	$[30100, 36.4875]^\top$	Initial values – reference system
$\mathbf{x}(t_{final})$	$[0.2949, 43.9637]^\top$	Final values – original system
$\hat{\mathbf{x}}(t_{final})$	$[19.0057, 43.9637]^\top$	Final values – EKF
$\mathbf{x}_{ref}(t_{final})$	$[0.3655, 43.9547]^\top$	Final values – reference system
$u(t_{final})$	8.618 mg/kg/day	Final value – realized control input
$v(t)$	$\sim \mathcal{N}(0, 50^2)$ mm^3	Measurement noise function

presents the variation of the state variables $\mathbf{x}(t)$ belonging to the original system (upper part), while the middle and lower sub-figures represent the output $y(t)$. The $\mathbf{x}(t)$ varies in accordance with the control law. At the beginning, the controller rapidly intervenes into the process and decreases the $x_1(t)$ under a certain level and later it enforces the system to approach the trajectories of the reference system. The middle figure shows the output $y(t)$ from day 0 to day 60. It demonstrates that the magnitude of the output is too high compared to the $v(t)$ and the measurement noise cannot be recognized on the signal. On the other hand, the lower figure presents the

output from day 60 to day 200 (end of the therapy). The effect of the noise is clearly visible in this case due to the comparable magnitudes of $y(t)$ and $v(t)$.
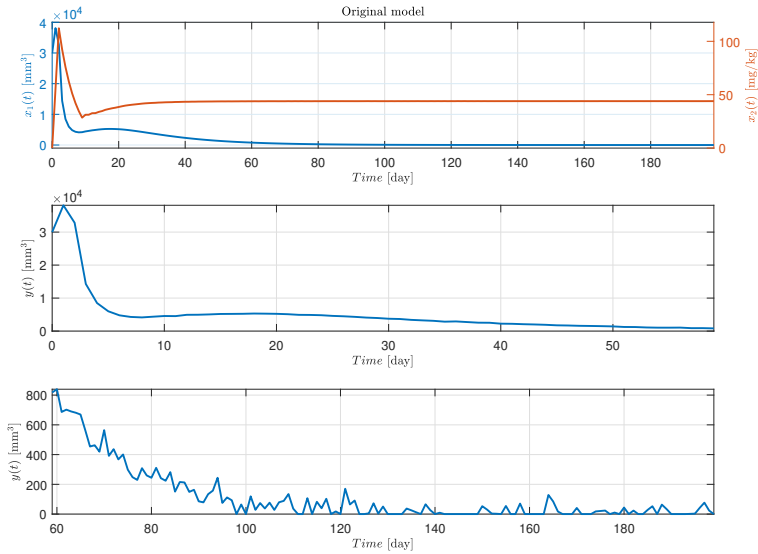

Figure 2
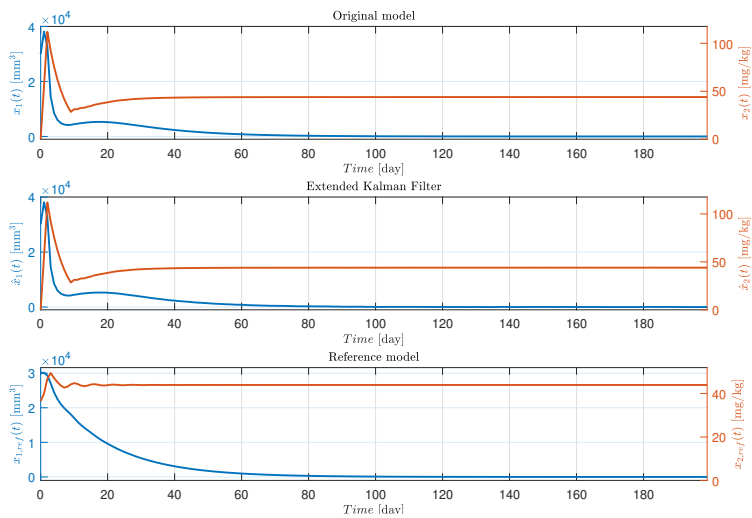Trajectories of the states and the output of the original nonlinear system.

Figure 3
Trajectories of the state variables.

The EKF approached the original model with high precision (Figure 3). The aim of the control, namely, $x_1(t_{final}) < 1$ mm^3 has been satisfied since, $x_1(t_{final}) = 0.2949$ mm^3.

Figure 4. shows the discrepancies between the states of the models. The initial state error between the original model and the EKF is $\mathbf{x}(t_0) - \hat{\mathbf{x}}(t_0) = [-100, 0]^\top$. As we mentioned, the measurement noise only reflects in the first state – in the output – of the EKF. The error rate can be measured by applying the two norm metric on the distance: $\|\mathbf{X}_1 - \hat{\mathbf{X}}_1\|_2 = 353.4982$ mm^3, $\mathbf{X}_1 = [\mathbf{x}_1(t_0), \mathbf{x}_1(t_1), \ldots, \mathbf{x}_1(t_{final})]$ and $\hat{\mathbf{X}}_1 = [\hat{\mathbf{x}}_1(t_0), \hat{\mathbf{x}}_1(t_1), \ldots, \hat{\mathbf{x}}_1(t_{final})]$. The obtained state error is small compared to occurred magnitudes of the tumor volumes. The EKF behaves as an optimal estimator from the second state point's of view since system disturbances has not been taken into consideration and sensor noise only reflects in the first state: $\|\mathbf{X}_2 - \hat{\mathbf{X}}_2\|_2 = 0$ mg/kg, $\mathbf{X}_2 = [\mathbf{x}_2(t_0), \mathbf{x}_2(t_1), \ldots, \mathbf{x}_2(t_{final})]$ and $\hat{\mathbf{X}}_2 = [\hat{\mathbf{x}}_2(t_0), \hat{\mathbf{x}}_2(t_1), \ldots, \hat{\mathbf{x}}_2(t_{final})]$.

Both the original model and the EKF have approached the states of the reference model with acceptable error rate within acceptable time horizon of the therapy. More precisely, the difference between $x_1(t)$, $\hat{x}_1(t)$ and $x_{1,ref}(t)$ was inside a range of 100 mm^3 after day 77 and continuously decreased until day 200. The deviation between $x_2(t)$, $\hat{x}_2(t)$ and $x_{2,ref}(t)$ was inside a range of 1 mg/kg after day 33 and continuously decreased until day 200.

Due to the small state error between the original and EKF states, the $\mathbf{x}_{ref}(t) - \hat{\mathbf{x}}(t)$ characterizes the $\mathbf{x}_{ref}(t) - \mathbf{x}(t)$ as well. Therefore, we only presented here the $\mathbf{x}_{ref}(t) - \hat{\mathbf{x}}(t)$. It is clearly visible that $\hat{\mathbf{x}}(t)$ appropriately approaches $\mathbf{x}_{ref}(t)$ over time. The state errors converge to zero, although the $\mathbf{x}_{ref}(t_{final}) - \hat{\mathbf{x}}(t_{final}) = [-18.6403, -0.0096]^\top$ due to the applied disturbance.
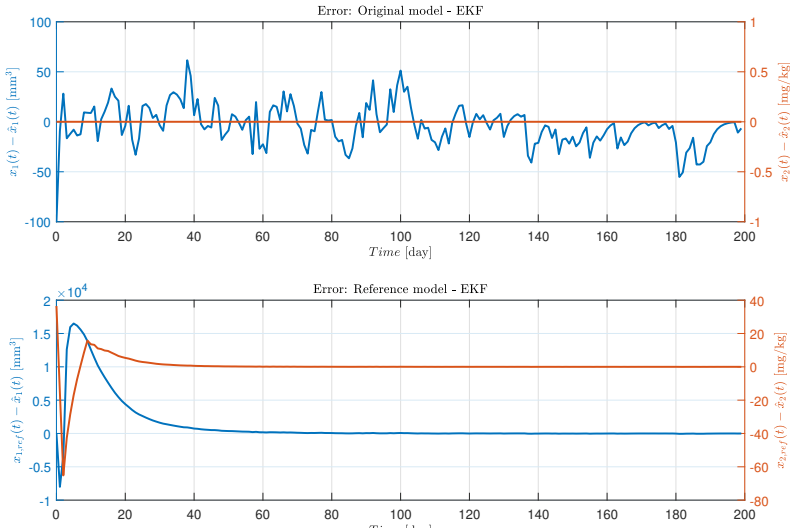

Figure 4
Deviations between the states of the models.

The comparison of the control signals can be seen in Figure 5. The upper subfigure belongs to the $u_{ref}(t)$ and it presents that the reference control signal varies accordingly based on the above defined constraints. What can be pointed out is the flat region from $2 - 5$ days that is the consequence of the constraint on $x_{2,ref}(t)$ coming from the already described model property: if we want to decrease the tumor volume, we need that $x_{2,ref}(t) > a/b$ which requires that $u_{ref}(t) > c \cdot a/b$.

There is the higher peak in $u(t)$ at the beginning which decreases to zero. This immediate action is a consequence of the applied state-feedback kind control due to the initial state discrepancy between $x_{2,ref}(t_0)$ and $\hat{x}_2(t_0)$. The $u_{ref}(t) - u(t) < 0.4$ mg/kg/h, $t > 20$. Small oscillations can be seen in $u(t)$ due to the effect of the EKF.

The calculation of the totally injected inhibitor is quite easy based on Euler's forward method. The IDC-PD compensator has calculated with a $\sum_{t=0}^{120} u_{ref}(t) \cdot T = 1567.7$ mg/kg, beside, the $\sum_{t=0}^{120} u(t) \cdot T = 1600.7$ mg/kg generated by the TP-LPV-LMI controller over the simulated time horizon, while $\sum_{t=0}^{120} \left(|u_{ref}(t) - u(t)| \right) = 163.9821$ mg/kg was the obtained difference within the time frame of the therapy.
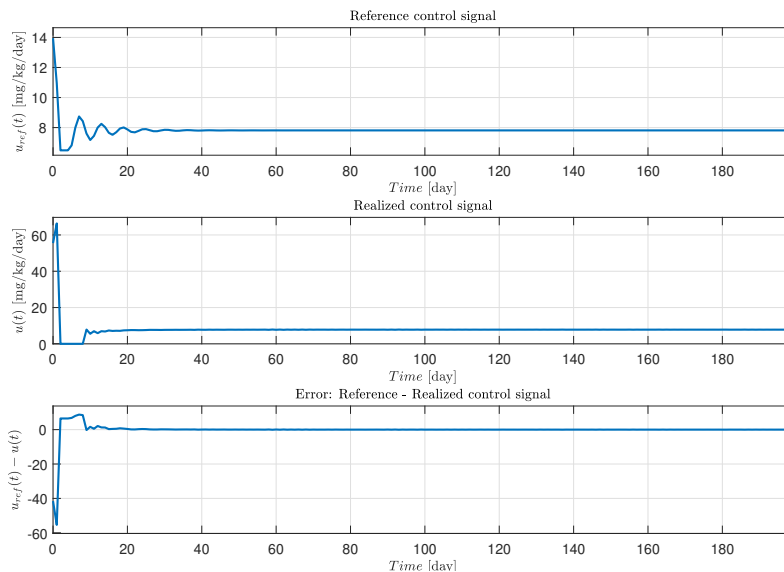

Figure 5
The reference and realized control signals.

Conclusions

The study details our latest achievements in regards to the control of tumor growth through antiangiogen therapy. Two qLPV models have been developed based on the

original nonlinear model. The Model-I has been applied during the EKF design and operation. The Model-II was used in order to design the difference based TP-LPV-LMI controller. A reference model has been also developed to describe the behavior of the first state – this was used during the reference trajectory generation.

The controller design was a complex procedure. First, we have applied TP model transformation on the Model-II. After, the control goals have been formalized by using LMIs. The procedure resulted the convex weighting functions and the controller vertices which built up the TP-LPV-LMI controller. We have developed a reference subsystem, as well based on IDC-PD kind compensator with the purpose of generation of the reference state variables and reference control input.

The developed control framework was tested on numerical simulations scenarios. We have found that the system performed well and all of the control goals have been satisfied. Not just the tumor volume was decreased under a certain level, but the original nonlinear model was enforced to behave as the reference model as well.

In the future we plan to analyze the performance of the developed solutions in case of state disturbances. Moreover, we will investigate other reference signal possibilities as well.

Acknowledgement

References

[1] P. Charlton and J. Spicer. Targeted therapy in cancer. *Medicine*, 44(1):34–38, 2016.

[2] K. Xing and S. Lisong. Molecular targeted therapy of cancer: The progress and future prospect. *Front Lab Med*, 1(2):69–75, 2017.

[3] N.S. Vasudev and A.R. Reynolds. Anti-angiogenic therapy for cancer: current progress, unresolved questions and future directions. *Angiogenesis*, 17(3):471–494, 2014.

[4] B. Al-Husein, M. Abdalla, M. Trepte, D.L. DeRemer, and P.R. Somanat. Anti-angiogenic therapy for cancer: An update. *Pharmacotherapy*, 32(12):1095–1111, 2012.

[5] Y. Kubota. Tumor angiogenesis and antiangiogenic therapy. *Keio J Med*, 61:47 – 56, 2012.

[6] J. Sájevicsé Sápi. *Controller-managed automated therapy and tumor growth model identification in the case of antiangiogenic therapy for most effective, individualized treatment*. PhD thesis, Applied Informatics and Applied Mathemathics Doctoral School, Óbuda University, Budapest, Hungary, 2015.

[7]   A.M.E. Abdalla, L. Xiao, M. Wajid Ullah, M. Yu, C. Ouyang, and G. Yang. Current challenges of cancer anti-angiogenic therapy and the promise of nanotherapeutics. *Theranostics*, 8(2):533–548, 2018.

[8]   J.K. Tar, J. Bitó, L. Nádai, and JA Tenreiro Machado. Robust fixed point transformations in adaptive control using local basin of attraction. *Acta Polytech Hung*, 6(1):21–37, 2009.

[9]   A. Dineva, J.K. Tar, A. Várkonyi-Kóczy, and V. Piuri. Adaptive controller using fixed point transformation for regulating propofol administration through wavelet-based anesthetic value. In *2016 IEEE International Symposium on Medical Measurements and Applications (MeMeA)*, pages 1–6. IEEE, 2016.

[10] L. Kovács. A robust fixed point transformation-based approach for type 1 diabetes control. *Nonlin Dyn*, 89(4):2481–2493, 2017.

[11] D. Copot, R. De Keyser, J. Juchem, and C.M. Ionescu. Fractional order impedance model to estimate glucose concentration: in vitro analysis. *Acta Polytech Hung*, 14(1):207–220, 2017.

[12] C. Ionescu, R. De Keyser, J. Sabatier, A. Oustaloup, and F. Levron. Low frequency constant-phase behavior in the respiratory impedance. *Biomed Signal Proces*, 6(2):197–208, 2011.

[13] C. Ionescu, A. Lopes, D. Copot, J.A.T. Machado, and J.H.T. Bates. The role of fractional calculus in modeling biological phenomena: A review. *Commun Nonlinear Sci*, 51:141–159, 2017.

[14] F.S. Lobato, V.S. Machado, and V. Steffen. Determination of an optimal control strategy for drug administration in tumor treatment using multi-objective optimization differential evolution. *Comp Meth Prog Biomed*, 131:51–61, 2016.

[15] D. Drexler, J. Sápi, and L. Kovács. Potential Benefits of Discrete-Time Controller-based Treatments over Protocol-based Cancer Therapies. *Acta Polytech Hung*, 14(1):11–23, 2017.

[16] J. Klamka, H. Maurer, and A. Swierniak. Local controllability and optimal control for amodel of combined anticancer therapy with control delays. *Math Biosci Eng*, 14(1):195–216, 2017.

[17] D.A. Drexler, J. Sápi, and L. Kovács. Modeling of tumor growth incorporating the effects of necrosis and the effect of bevacizumab. *Complexity*, 2017:1–10, 2017.

[18] D.A. Drexler, J. Sápi, and L. Kovács. Positive control of a minimal model of tumor growth with bevacizumab treatment. In *Proceedings of the 12th IEEE Conference on Industrial Electronics and Applications*, pages 2081–2084, 2017.

[19] L. Kovács. Linear parameter varying (LPV) based robust control of type-I diabetes driven for real patient data. *Knowl-Based Syst*, 122:199–213, 2017.

[20] P. Baranyi, Y. Yam, and P. Varlaki. *Tensor Product Model Transformation in Polytopic Model-Based Control*. Series: Automation and Control Engineering. CRC Press, Boca Raton, USA, 1st edition, 2013.

[21] M.S. Grewal and A.P. Andrews. *Kalman Filtering: Theory and Practice Using MATLAB*. John Wiley and Sons, Chichester, UK, 3rd edition, 2008.

[22] D. Drexler, J. Sápi, and L. Kovács. A minimal model of tumor growth with angiogenic inhibition using bevacizumab. In *SAMI 2017 - IEEE 15th International Symposium on Applied Machine Intelligence and Informatics*, pages 185 – 190. IEEE.

[23] D.A. Drexler, J. Sápi, and L. Kovács. Positive nonlinear control of tumor growth using angiogenic inhibition. *IFAC-PapersOnLine*, 50(1):15068–15073, 2017.

[24] Y. Akatsu, Y. Yoshimatsu, T. Tomizawa, K. Takahashi, A. Katsura, K. Miyazono, and T. Watabe. Dual targeting of vascular endothelial growth factor and bone morphogenetic protein-9/10 impairs tumor growth through inhibition of angiogenesis. *Cancer Science*, 108(1):151–155, 2017.

[25] J. Sápi, L. Kovács, D.A. Drexler, P. Kocsis, D. Gaári, and Z. Sápi. Tumor volume estimation and quasi-continuous administration for most effective bevacizumab therapy. *PLoS ONE*, 10(11), 2015.

[26] O. Sename, P. Gáspár, and J. Bokor. Robust control and linear parameter varying approaches, application to vehicle dynamics. volume 437 of *Lecture Notes in Control and Information Sciences*. Springer-Verlag, Berlin, 2013.

[27] A.P. White, G. Zhu, and J. Choi. *Linear Parameter Varying Control for Engineering Applicaitons*. Springer, London, 1st edition, 2013.

[28] C. Briat. Linear parameter-varying and time-delay systems. *Analysis, Observation, Filtering & Control*, 3, 2014.

[29] Gy. Eigner. *Closed-Loop Control of Physiological Systems*. PhD thesis, Applied Informatics and Applied Mathemathics Doctoral School, Óbuda University, Budapest, Hungary, 2017.

[30] P. Baranyi. *TP-model Transformation-based-control Design Frameworks*. Springer, 2016.

[31] P. Baranyi. Extension of the Multi-TP Model Transformation to Functions with Different Numbers of Variables. *Complexity*, 2018, 2018.

[32] L-E. Hedrea, C-A. Bojan-Dragos, R-E. Precup, R-C. Roman, E.M. Petriu, and C. Hedrea. Tensor product-based model transformation for position control of magnetic levitation systems. In *2017 IEEE 26th International Symposium on Industrial Electronics (ISIE)*, pages 1141–1146. IEEE, 2017.

[33] L-E. Hedrea, C-A. Bojan-Dragos, R-E. Precup, and T-A. Teban. Tensor product-based model transformation for level control of vertical three tank sys-

tems. In *2017 IEEE 21st International Conference on Intelligent Engineering Systems (INES)*, pages 000113–000118. IEEE, 2017.

[34] J.D. Bronzino and D.R. Peterson, editors. *The Biomedical Engineering Handbook*. CRC Press, Boca Raton, USA, 4th edition, 2016.

[35] J. Kuti, P. Galambos, and P. Baranyi. Minimal volume simplex (MVS) convex hull generation and manipulation methodology for TP model transformation. *Asian J Control*, 19(1):289–301, 2017.

[36] J. Kuti, P. Galambos, and P. Baranyi. Control analysis and synthesis through polytopic tensor product model: a general concept. *IFAC-PapersOnLine*, 50(1):6558–6563, 2017.

[37] P. Galambos and P. Baranyi. TP model transformation: A systematic modelling framework to handle internal time delays in control systems. *Asian J Control*, 17(2):1 – 11, 2015.

[38] P. Baranyi. The generalized TP model transformation for T–S fuzzy model manipulation and generalized stability verification. *IEEE T Fuzzy Syst*, 22(4):934–948, 2014.

[39] Sz. Nagy, Z. Petres, P. Baranyi, and H. Hashimoto. Computational relaxed TP model transformation: restricting the computation to subspaces of the dynamic model. *Asian J Control*, 11(5):461–475, 2009.

[40] J. Cui, K. Zhang, and T. Ma. An efficient algorithm for the tensor product model transformation. *Int J Control Autom*, 14(5):1205–1212, 2016.

[41] A. Szollosi and P. Baranyi. Influence of the Tensor Product model representation of qLPV models on the feasibility of Linear Matrix Inequality. *Asian J Control*, 18(4):1328–1342, 2016.

[42] A. Szollosi and P. Baranyi. Improved control performance of the 3-DoF aeroelastic wing section: a TP model based 2D parametric control performance optimization. *Asian J Control*, 19(2):450–466, 2017.

[43] A. Szollosi and P. Baranyi. Influence of the Tensor Product Model Representation of qLPV Models on the Feasibility of Linear Matrix Inequality Based Stability Analysis. *Asian J Control*, 20(1):531–547, 2018.

[44] P. Várkonyi, D. Tikk, P. Korondi, and P. Baranyi. A new algorithm for RNO-INO type tensor product model representation. In *2005 IEEE International Conference on Intelligent Engineering Systems, INES*, volume 5, pages 263–266, 2005.

[45] X. Liu, Y. Yu, Z. Li, Herbert H.C. Iu, and T. Fernando. An Efficient Algorithm for Optimally Reshaping the TP Model Transformation. *IEEE T Circuits-II*, 64(10):1187–1191, 2017.

[46] X. Liu, X. Xin, Z. Li, and Z. Chen. Near Optimal Control Based on the Tensor-Product Technique. *IEEE T Circuits-II*, 64(5):560–564, 2017.

[47] X. Liu, Y. Yu, Z. Li, and H. Iu. Polytopic H$_\infty$ filter design and relaxation for nonlinear systems via tensor product technique. *Signal Process*, 127:191–205, 2016.

[48] X. Liu, Y. Yu, H. Li, Z.and Iu, and Ty. Fernando. A novel constant gain Kalman filter design for nonlinear systems. *Signal Process*, 135:158–167, 2017.

[49] P.S. Saikrishna, R. Pasumarthy, and N.P. Bhatt. Identification and multivariable gain-scheduling control for cloud computing systems. *IEEE T Cont Syst T*, 25(3):792–807, 2017.

[50] G. Zhao, D. Wang, and Z. Song. A novel tensor product model transformation-based adaptive variable universe of discourse controller. *J Frankl Inst*, 353(17):4471–4499, 2016.

[51] W. Qin, B. He, Q. Qin, and G. Liu. Robust active controller of hypersonic vehicles in the presence of actuator constraints and input delays. In *2016 35th Chinese Control Conference (CCC)*, pages 10718–10723. IEEE, 2016.

[52] Q. Weiwei, H. Bing, L. Gang, and Z. Pengtao. Robust model predictive tracking control of hypersonic vehicles in the presence of actuator constraints and input delays. *J Frankl Inst*, 353(17):4351–4367, 2016.

[53] T. Wang and B. Liu. Different polytopic decomposition for visual servoing system with LMI-based Predictive Control. In *2016 35th Chinese Control Conference (CCC)*, pages 10320–10324. IEEE, 2016.

[54] T. Wang and W. Zhang. The visual-based robust model predictive control for two-DOF video tracking system. In *2016 Chinese Control and Decision Conference (CCDC)*, pages 3743–3747. IEEE, 2016.

[55] T. Jiang and D. Lin. Tensor Product Model-Based Gain Scheduling of a Missile Autopilot. *T Jpn Soc Aeronaut S*, 59(3):142–149, 2016.

[56] S. Campos, V. Costa, L. Tôrres, and R. Palhares. Revisiting the TP model transformation: Interpolation and rule reduction. *Asian J Control*, 17(2):392–401, 2015.

[57] S. Kuntanapreeda. Tensor Product Model Transformation Based Control and Synchronization of a Class of Fractional-Order Chaotic Systems. *Asian J Control*, 17(2):371–380, 2015.

[58] R-E. Precup, E.M. Petriu, M-B. Rădac, S. Preitl, L-O. Fedorovici, and C-A. Dragoş. Cascade Control System-Based Cost Effective Combination of Tensor Product Model Transformation and Fuzzy Control. *Asian J Control*, 17(2):381–391, 2015.

[59] P. Korondi. Tensor product model transformation-based sliding surface design. *Acta Polytech Hung*, 3(4):23–35, 2006.

[60] Gy. Eigner, I. Böjthe, P. Pausits, and L. Kovács. Investigation of the tp modeling possibilities of the hovorka t1dm model. In *2017 IEEE 15th International*

Symposium on Applied Machine Intelligence and Informatics (SAMI), pages 259–264. IEEE, 2017.

[61] Gy. Eigner, P. Pausits, and L. Kovács. Control of t1dm via tensor product-based framework. In *2016 IEEE 17th International Symposium on Computational Intelligence and Informatics (CINTI)*, pages 55–60. IEEE, 2016.

[62] Gy. Eigner, I. Rudas, A. Szakál, and L. Kovács. Tensor product based modeling of tumor growth. In *2017 IEEE International Conference on Systems, Man, and Cybernetics (SMC)*, pages 900–905. IEEE, 2017.

[63] L. Kovács and Gy. Eigner. Usability of the tensor product based modeling in the modeling of diabetes mellitus. *Manuscript in preparation*, 2016.

[64] Gy. Eigner, I. Rudas, and L. Kovács. Investigation of the tp-based modeling possibility of a nonlinear icu diabetes model. In *2016 IEEE International Conference on Systems, Man, and Cybernetics (SMC)*, pages 3405–3410. IEEE, 2016.

[65] L Kovács and Gy. Eigner. Convex polytopic modeling of diabetes mellitus: A tensor product based approach. In *2016 IEEE International Conference on Systems, Man, and Cybernetics (SMC)*, pages 003393–003398. IEEE, 2016.

[66] J. Klespitz, I. Rudas, and L. Kovács. LMI-based feedback regulator design via TP transformation for fluid volume control in blood purification therapies. In *2015 IEEE International Conference on Systems, Man, and Cybernetics (SMC)*, pages 2615–2619. IEEE, 2015.

[67] J. Kuti, P. Galambos, and Á. Miklós. Output Feedback Control of a Dual-Excenter Vibration Actuator via qLPV Model and TP Model Transformation. *Asian J Control*, 17(2):432–442, 2015.

[68] J. Pan and L. Lu. TP Model Transformation Via Sequentially Truncated Higher-Order Singular Value Decomposition. *Asian J Control*, 17(2):467–475, 2015.

[69] J. Matuško, Š. Ileš, F. Kolonić, and V. Lešić. Control of 3d tower crane based on tensor product model transformation with neural friction compensation. *Asian J Control*, 17(2):443–458, 2015.

[70] G. Zhao, H. Li, and Z. Song. Tensor product model transformation based decoupled terminal sliding mode control. *Int J Syst Sci*, 47(8):1791–1803, 2016.

[71] S. Chumalee and J. Whidborne. Gain-Scheduled H∞ Control for Tensor Product Type Polytopic Plants. *Asian J Control*, 17(2):417–431, 2015.

[72] R-E. Precup, C-A. Dragos, S. Preitl, M-B. Radac, and E-M. Petriu. Novel tensor product models for automatic transmission system control. *IEEE Syst J*, 6(3):488–498, 2012.

[73] R-E. Precup, M-Cs. Sabau, and E.M. Petriu. Nature-inspired optimal tuning of input membership functions of takagi-sugeno-kang fuzzy models for anti-lock braking systems. *Appl Soft Comput*, 27:575–589, 2015.

[74] R-E. Precup, R-C. David, and E.M. Petriu. Grey wolf optimizer algorithm-based tuning of fuzzy control systems with reduced parametric sensitivity. *IEEE T Ind Electron*, 64(1):527–534, 2017.

[75] K. Tanaka and H.O. Wang. *Fuzzy Control Systems Design and Analysis: A Linear Matrix Inequality Approach*. John Wiley and Sons, Chichester, UK, 1st edition, 2001.

[76] S. Boyd, L. El Ghaoui, E. Feron, and V. Balakrishnan. *Linear Matrix Inequalities in System and Control Theory*, volume 15 of *Studies in Applied Mathematics*. SIAM, Philadelphia, PA, June 1994.

[77] H. Musoff and P. Zarchan. *Fundamentals of Kalman Filtering: A Practical Approach* . American Institute of Aeronautics and Astronautics, 3rd edition, 2009.

[78] J. Hartikainen, A. Solin, and S. Särkkä. *Optimal Filtering with Kalman Filters and Smoothers a Manual for the Matlab toolbox EKF/UKF*. Aalto University, v1.3 edition, 2011.

[79] Y. Tagawa, J.Y. Tu, and D.P. Stoten. Inverse dynamics compensation via simulation of feedback control systems. *Proceedings of the institution of mechanical engineers, Part I: Journal of systems and control engineering*, 225(1):137–153, 2011.

[80] B. Siciliano, L. Sciavicco, L. Villani, and G. Oriolo. *Robotics–Modelling, Planning and Control. Advanced Textbooks in Control and Signal Processing Series*. Springer-Verlag, 2009.

Notations and Abbreviations

Table 2
General Phrases.

Abbreviation	Meaning
LTI	Linear Time Invariant
LTV	Linear Time Variant
LPV	Linear Parameter Varying
qLPV	quasi LPV
TP model	Tensor Product model
LMI	Linear Matrix Inequality
MVS	Minimal Volume Simplex
SVD	Singular Value Decomposition
HOSVD	Higher-Order SVD
EKF	Extended Kalman Filter

Table 3
Mathematical terms.

Notation	Meaning
$a, b, \ldots$	scalars
$\mathbf{a}, \mathbf{b}, \ldots$	vector
$\mathbf{A}, \mathbf{B}, \ldots$	matrices
$\mathbf{a}_i, \mathbf{b}_i, \ldots$	ith row vector of $\mathbf{A}, \mathbf{B}, \ldots$ matrices
$a_{i,j}, b_{i,j}, \ldots$	jth elements of the $\mathbf{a}_i, \mathbf{b}_i, \ldots$ row vectors
$\mathscr{A}, \mathscr{B}, \ldots$	tensors
$\mathscr{S} \overset{N}{\underset{n=1}{\boxtimes}} \mathbf{W}_n$	multiple tensor products,
	e.g. $\mathscr{S} \times_1 \mathbf{W}_1 \ldots \times_N \mathbf{W}_N$
$\mathbb{R}, \mathbb{C}, \ldots$	mathematical sets

MaxWhere VR-Learning Improves Effectiveness over Clasiccal Tools of e-learning

Balint Lampert, Attila Pongracz, Judit Sipos, Adel Vehrer, Ildiko Horvath

VR-Learing Research Lab, Apáczai Faculty, Széchenyi István University
Liszt F. u. 42, H-9022 Győr, Hungary

lampert.balint@sze.hu, pongracz.attila@sze.hu, sipos.judit@sze.hu,
vehrer.adel@sze.hu, horvath.ildiko@sze.hu

Abstract: The paper investigates how workflows can be communicated and shared through linguistic descriptions, digital content and technological tools. We focus primarily on the content and digital tools of e-learning and VR learning. However, the results of the paper can be applied to collaborative workflows in general. The paper compares the effectiveness of three techniques, ranging from well-known to radically new: classical e-mail / attachment based sharing, sharing through web interfaces (through a Moodle frontend), and sharing through a VR interface provided by a recently developed VR engine called MaxWhere. To this end, the paper introduces new methods and a new set of concepts for the purposes of benchmarking digital capabilities and user effectiveness within the domain of workflow sharing. The paper applies these concepts and methods to compare the use of the above listed technologies with the participation of 379 test subjects. Tests show that the users were able to complete the required workflow at least 50% faster in the MaxWhere 3D environment than in all other competing cases. The paper also proves that 3D environments are capable of providing users with a much higher level of comprehension when it comes to sharing and interpreting digital workflows.

Keywords: VR-learning; e-learning; Cognitive Infocommunications

1   Introduction

In the past decade, the everyday use of the Internet has become widespread in all areas of life, including education. However, the question of which digital tools can be used most effectively in education is still open to debate.

Many educators share their curriculum and learning material using e-learning tools, which can also be accessed by students having the required access privileges. Others prefer to simply share the learning materials through e-mail.

In the past few years, VR applications have been used in education primarily as tools for visualization. The MaxWhere VR platform for education was first released in 2016. Besides serving visualization purposes, MaxWhere's strength lies in its ability to present complete electronic notes on smart slides in 3D space. Through MaxWhere, a powerful combination of interactive 3D visualization, working environments fit to specific workflows and e-learning can be achieved.

The topic of the paper belongs to Cognitive Infocommunications [1, 2], where the blended cognitive capabilities of Human and IT solutions are investigated. Within this topic the paper focus in the research direction of VR-learning and papers investigating user experience in virtual 3D environments [3, 4,..,25].

The goal of this paper is to provide a systematic comparison among the three aforementioned techniques in education and in the sharing of collaborative workflows.

2 Properties and Definitions of Workflow and Digital Content Sharing

In this section, we provide definitions of key concepts relevant to digital content: its comprehensibility and accessibility as well as the various forms in which it can be shared. Further sections of the paper will provide evaluations of various digital tools and methodologies based on this nomenclature.

Definition 1: Digital element (DE)

A digital element is taken to mean a unit that has to be opened or loaded separately, in itself with an appropriate software.

Example 1: PDF files, PPT presentations, video files, content accessed through a specific URL (as a Moodle test or Google form), web apps (e.g. Octave Online), or source files that can be opened using an editor or IDE are all examples of digital elements. In the experiments described in the paper, the following digital elements will be used:

doc1.pdf, doc2.pdf, doc3.pdf

home page 1 at www.hp1.com

pres1.ppt, pres2.ppt

test1 at url www.test1.com es test2 at url www.test2.com

 video1.avi,

Definition 2: Digital content

Digital content are defined as a set of digital elements. Digital content can be quantified based on the number of digital elements contained in the content.

Example 2: If we consider the digital elements listed in example 1.1. to be the building blocks of a digital content, the size of the content will be 9 DEs.

Definition 3: Digital fragmentation (DF)

Digital fragmentation is a property of digital content that shows how many different formats are represented by the digital elements forming the content - i.e. how many different software tools are required to open or load them.

Remark: we regard digital elements that can be accessed on the web through a url as being different formats, even though all of them can be loaded using a web browser. For example, a web page or a Google Drive document or a Moodle test are three different formats, not one. The reason for this is that although all of the examples can be opened using a web browser, separate web apps are required to open all of them.

Example 3: The digital content referred to in the previous examples have a digital fragmentation of 5 DFs.

Defintion 4: Digital project

A digital project is a set of tasks that are to be carried out on a digital content.

Example 4: Consider the 5DF, 9DE digital content referred to in the previous examples. The tasks in a digital project associated with that content might be to fill out two questionnaires based on the information contained in the digital elements forming the content.

Definition 5: Digital workflow (DW)

Digital workflows determine the order in which individual digital elements are to be accessed or processed during the course of a digital project. We distinguish among the following types of digital workflows:

1st order (linear): The digital elements are to be accessed in a static and sequential order, one after the other

2nd order (loopy): There are loops in the order in which the digital elements are to be accessed, so that individual elements, or smaller sequences thereof, are to be accessed repetitively. Such loops can be characterized by length and number of repetitions.

3rd order (networked): Digital elements accessed during the project are structured as hierarchical loops, so that the project may contain subprojects of subprojects, and / or the ordering of digital elements may be different upon different repetitions of the loops.

4th order (algorithmic): It is possible that the project contains branches, so that different digital elements are accessed dynamically in an order that depends on information obtained during the project.

Example 5.1: The digital workflow is of the 1st order if the order in which the digital elements are accessed is static and sequential, e.g.:

doc1.pdf -- doc2.pdf -- pres1.ppt -- test1 -- doc3.pdf -- video1.avi -- pres2.ppt -- test2 -- homepage1

Example 5.2: The digital workflow is of the 2nd order if the order in which the digital elements are accessed has repetitions, loops, e.g.:

doc1.pdf -- doc2.pdf -- pres1.ppt -- test1   -- doc2.pdf -- pres1.ppt - test1 -- doc3.pdf -- video1.avi -- pres2.ppt -- test2 -- pres2.ppt -- test2 -- homepage1

akkor ezt a digitalis workflow-t 2 rendunek nevezzuk

Example 5.3: The digital workflow is of the 3rd order if the order in which the digital elements are accessed has hierarchical, embedded loops, e.g.:

doc1.pdf -- [doc2.pdf -- pres1.ppt -- test1] -- [doc2.pdf -- pres1.ppt - test1] -- (doc3.pdf -- video1.avi -- {pres2.ppt -- test2} -- {pres2.ppt -- test2} - [doc2.pdf -- pres1.ppt -- test1] -- [doc2.pdf -- pres1.ppt - test1] -- doc3.pdf -- video1.avi --{ pres2.ppt -- test2 }-- {pres2.ppt -- test2} - [doc2.pdf -- pres1.ppt -- test1   ] -- [doc2.pdf -- pres1.ppt - test1]--) -- [doc2.pdf -- pres1.ppt -- test1] -- doc3.pdf -- video1.avi --{ pres2.ppt -- test2} --{ pres2.ppt -- test2} - [doc2.pdf -- pres1.ppt -- test1] --[doc2.pdf -- pres1.ppt - test1] -- homepage1

where in reality

 [doc2.pdf -- pres1.ppt -- test1]

and

 {pres2.ppt -- test2}

can also be regarded as subprojects

Based on the definition, the workflow is also of the 3rd order if the repeating loops are not always the same

doc1.pdf -- doc2.pdf -- pres1.ppt -- test1   -- doc2.pdf -- pres1.ppt - test1 -- doc2.pdf -- -- test1 --   pres1.ppt - test1 -- doc3.pdf -- video1.avi -- pres2.ppt -- test2 -- pres2.ppt -- test2 -- homepage1

Example 5.4: if the order of access of digital elements depends on information obtained during the workflow (i.e. there are branches in determining access to digital elements), then the workflow is of the 4th order, as in the following case:

doc1.pdf -- doc2.pdf -- pres1.ppt -- test1

if test 1 was successful then -- doc3.pdf -- video1.avi -- pres2.ppt -- test2 -- homepage1

if test 1 was NOT successful then -- homepage1

we may have a further branch at test 2 that leads to an even more complicated chain.

Through examples 5.1 - 5.4, it is clear that as the order of the workflows grows, so it becomes more difficult to represent them. For example, the workflow in example 5.1 can be expressed as a list:

Step 1 -- doc1.pdf - click here to open

Step 2 -- doc2.pdf - click here to open

Step 3 -- pres 1.ppt - click here to open

Step 4 test1 - click here to open

step 5 doc3.pdf - click here to open

step 6 video1.avi - click here to open

step 7 pres2.ppt - click here to open

step 8 test2 - click here to open

step 9 homepage1 - click here to open

However, the workflows in examples 5.2 and 5.3 are already very difficult to convey using text, which makes the execution of such workflows even more difficult than purely justifiable by their order. In such cases, representation through a dashboard or 2D graphical UI can help a lot (see Figures 1-3).
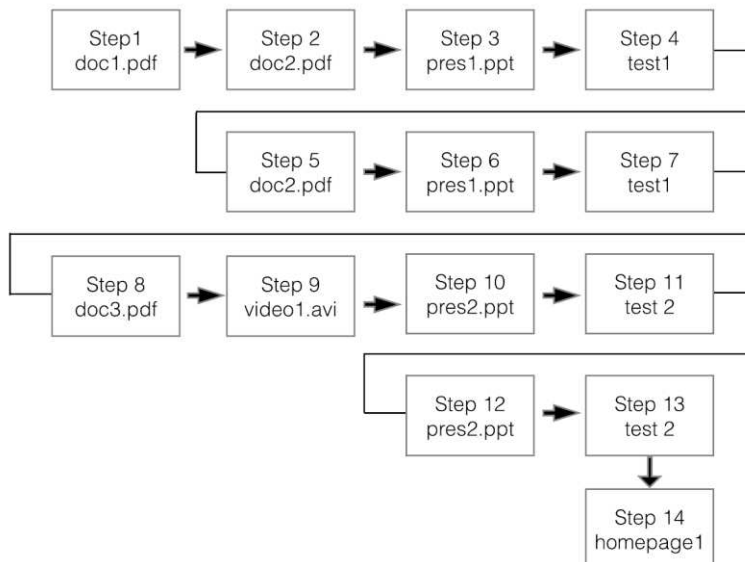

Figure 1
Workflow of the 2nd order, from example 5.2, as expressed using a process diagram
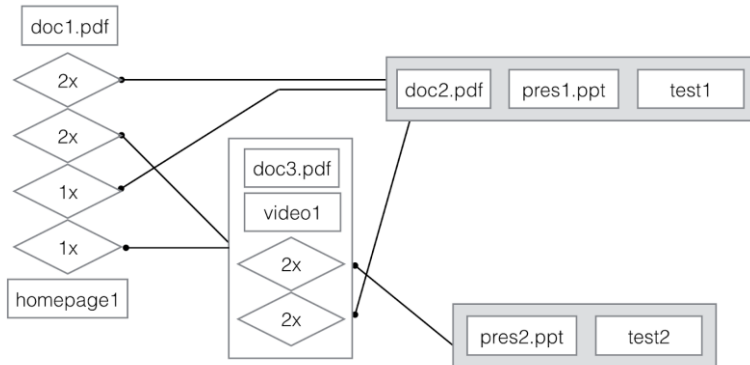
Figure 2
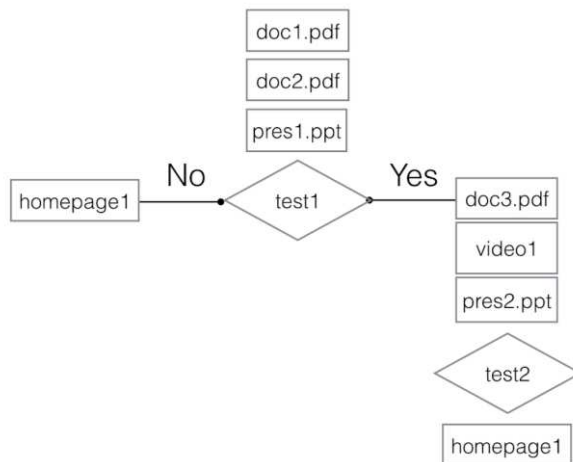Workflow of the 3rd order, from example 5.3

Figure 3
Workflow of the 4th order, from example 5.4, expressed using a process diagram

Based on the following, we make the following remarks in terms of accessibility and comprehensibility.

Lemma 1: Digital workflows of the 1st order can be conveyed well using text alone. Digital workflows of the 2nd order can be conveyed using text, but are better conveyed using a graphical process diagram. Digital workflows of the 3rd order are very difficult - if not impossible - to convey using text, depending on the complexity of the workflow. In more complex cases, the paths guiding the

workflow may even intersect and become entangled on the process diagram, making it difficult for humans to comprehend the diagram (see Figure 4, which shows that in such cases spatial diagrams may be used to good effect). In the case of digital workflows of the 4th order, where the workflows, in addition to being characterized by complex paths between the digital elements to be accessed, are also dynamic, no 2D graphical representation can be expected to work well, aside from the simplest of cases.

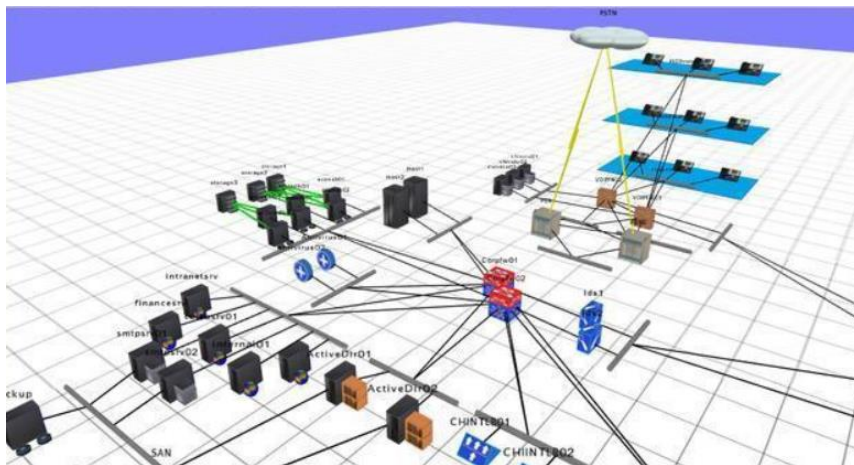All of the above observations are summarized in Table 1.

Figure 4
In more complex cases, loops in the workflow can better be represented in 3D space

Table 1
In the table, a value of 1 means that a digital workflow of the given order can be well represented in the given representation. A value of 0.5 means that although a digital workflow of the given order may be represented using the given representation, in more complex cases the representation cannot be expected to be effective. The letter X in the table symbolizes the fact that the given representation is not effective or cannot be used at all for a digital workflow of the given order.

DW	1	2	3	4
text based description	1	0,5	x	x
2D description	1	1	0,5	x
3D description	1	1	1	1

The comprehensibility of a digital workflow can be improved if the blocks in its representation can be clicked on and the corresponding digital elements open or load accordingly (or are already displayed alongside the blocks to begin with). The reason for this is that any ordering (even alphabetical ordering) of the digital elements that are independent of the representation itself will lead to the user

having to continually search for the element that needs to be accessed - a task that can be tedious and error-prone. Thus, it is worth distinguishing between representations in which the digital elements are embedded into the representation and those, in which, that are not.

Definition 6: Linked Digital Element (LDE)

A digital element is referred to as a Linked Digital Element (LDE) if it can be accessed by clicking on a link included in the representation (whether text-based or other) of the digital workflow.

Definition 7. Embedded Digital Element (EDE)

A digital element is referred to as an Embedded Digital Element (EDE) if it can be accessed without any additional interaction, together with the blocks corresponding to the digital elements within the representation of the digital workflow.

Example 7: Figure 5 shows an example of the block diagram with a pdf file, a video and an interactive application (Octave Online) providing real-time graphical output. All of the digital elements in the example are embedded into the representation of the workflow.

Based on the above, the following definition is formulated:

Definition 8: Digital comprehension (DC)

Digital comprehension is a qualitative concept that can be used to describe the quality of a representation with respect to a digital workflow. The following types of digital comprehension can be distinguished:

0th order: There is no ordering among the digital elements of the workflow.

1st order: There is a linear (sequential) ordering among the digital elements of the workflow, potentially supplemented with text descriptions.

2nd order: The linked digital elements of the digital workflow are ordered in 2D using icons on a dashboard. Relationships between the linked digital elements are represented in 2D and the icons representing the digital elements act as links to the elements.

3rd order: The order among the linked digital elements within the digital workflow is represented in a 3D space. The icons within the space are representations of the digital elements and links to them at the same time.

4th order: The digital elements and their relationships are represented in 3D space in a linked or embedded form - i.e. the digital elements are not only accessible through links but are also displayed continually as part of the visual description of the workflow.

Remark: there is no such representation as the embedded (EDE) form of 2nd order iconic dashboards. The reason for this is that in such cases, the running (embedded) applications cannot be effectively presented on a 2D monitor, so that the representation itself is already considered to be 3D; even if they are displayed on a flat screen, users need to access them via zoom in / out operations, and on a virtual canvas that is usually much larger than the 2D screen itself (for example, this is how Prezi software is able to call its presentations 3D).

Example 8: The text-based description of the digital workflow in example 5.6 has a digital comprehension (DC) of the 1st order. Figures 1, 2 and 3 show workflows of with a DC of the 2nd order. Figure 4 shows an example of a workflow with a DC of the 3rd order.

Figure 5
A workflow represented at a DC level of the 4th order, such that the digital elements are presented in 3D via running applications (EDE type elements).

Based on the above, the following relationship can be set up between digital comprehension and digital workflows.

Table 2
In the table, a value of 1 means that a representation with a digital comprehension of the given order can be used to represent a workflow of the given order effectively. A value of 0.5 means that although a representation with a digital comprehension of the given order may be used with respect to a given order of workflow, in more complex cases the representation cannot be expected to be effective. The letter X in the table symbolizes the fact that the given representation is not effective or cannot be used at all for a digital workflow of the given order.

DW	1	2	3	4
1 rendu DC	1	0,5	x	x
2 rendu DC	1	1	0,5	x
3 rendu DC	1	1	1	0,5
4 rendu DC	1	1	1	1

Definition 9: Digital guidance

none: *no guidance is applicable, or the representation of the digital content doesn't involve embedded digital elements (instead, the elements are provided through separate lists).*

sequential (DG-S): *The digital elements are traversed in sequential order. It is thus possible to jump between one element to the next in the context of a digital workflow.*

random access (DG-R - event/dynamic focus-driven): *One can switch between sequences of digital elements, and thus follow non-static sequences (for example, in the case of DWs of the 4th order).*

Example 9: Consider a DW of the 1st order represented with a DC of order 1, such that the digital elements are embedded using hyperlinks within the text. In this way, one can step forward and backward between digital elements using the page dn / page up keys.

In non-linear cases it is especially effective when users can jump, or branch in a random access fashion within a workflow represented in a 2D or 3D space (DW of the 4th order), such that the jumps are automatically adapted to the workflow.

Similar to table 1 and 2, it is possible to define a relation between digital guidances and digital workflows:

Table 3

Contains the result of comparing in pairs with the final result

DW	1	2	3	4
DG-S	1	1	0,5	x
DG-R	1	1	1	1

To summarize the above tables, it is clearly visible that a platform allowing for Digital Comprehension and Digital Guidance of the 4th order can be expected to be most effective in the transmission of even Digital Workflows of the 4th order, while a system capable of achieving a Digital Comprehension of only the 1st order (text-based) will be very limited in its ability to convey workflows.

For the sake of completeness, it is worth introducing a further two definition.

Definition 10: Digital complexity

Digital complexity describes the complexity of the mapping ("assignment") between digital elements. For example, if in order to fully interpret a digital element, the user has to access a further digital element, then the two are "assigned" to each other. Three different kinds of assignment can be distinguished:

i) one-to-one: refers to pairs of digital elements which are assigned to each other in both directions (i.e. the interpretation of each requires the other).

ii) one-to-many: refers to digital elements that can be interpreted only in the context of multiple other digital elements.

iii) many-to-many: refers to groups of digital elements that can be interpreted only in the context of (the same group of) multiple other digital elements.

Example 10: if a user needs to consult two digital elements in order to fill out a test, the digital complexity of the test is one-to-many.

Defintion 11

A digital map is the contextual system underlying digital elements, which in many cases coincides with the digital chain.

3   Comparison of Classical, e-learning and MaxWhere VR-based Learning Frameworks

In the following, we begin by outlining the 3 most common techniques used for sharing digital workflows. We then compare those techniques based on the conceptual framework outlined in earlier sections.

1. Classical - TXT based message

This technique consists of sending digital elements and digital content to a group of recipients as attachments to a text-based message, or as web links inside a text-based message (e.g. sent via e-mail or any kind of messenger application).

Because of the text-based medium it uses, the classical technique can be regarded as an example of Digital Comprehension of the 1st order. In the case of digital workflows conveyed through text, the associated digital elements cannot be integrated into the text (although links to web-based content can). Therefore, this approach can be referred to as having an LDE of 0.5. Correspondingly, it cannot be a part of a continuous guiding scheme, and therefore can be conceived of as representing a DG level of Not Applicable.

Lemma 3.1: The classical approach therefore can be characterized as having a DC of order 0, no EDE, an LDE of 0.5 and a DG of 'not applicable'.

2. Online interfaces such as Moodle

This technique consists of helping users access and / or download digital elements and digital content through an on-line web-based interface.

In the simplest of cases, the approach of using online interfaces can be equivalent to the classical approach (with the added quality of being web-based), such that

the task to be carried out is described using text, and the required digital elements are listed in some order at the end of the text.

At the same time, an important advantage of online interfaces is that links embedded into the text can be used to share not only digital elements that have a web-based url, but more generally any kind of digital format (EDE). Thus, the digital elements can be ordered inside the text as required by the digital workflow, and sequential DGs can be conveyed without a problem, as long as the digital elements are ordered and users are able to move between them using a scrolling operation or a specific combination of keys (e.g. page up and page dn).

Online interfaces are not amenable to the presentation of digital elements in a 2D process diagram. Thus, even if a digital workflow is presented through an image or a diagram, this solution can be regarded as only partial in view of the requirements of 2nd order DCs.

Lemma 3.2: As a result, online e-learning systems are typically capable of presenting DCs of the 1st order (complemented with LDE, DG-S), and can therefore be used to represent digital workflows of the 1st (and in some cases, 2nd) order.

3. The MaxWhere Operating System

From an IT perspective, the MaxWhere OS contains no digital elements. Instead, it gives users access to a single (pack or bundle) file, which can be loaded and which contains references to all of the digital elements that are in turn loaded recursively.

All digital content and elements thereof are displayed in thematic groups in 3D. Digital elements are displayed in smartboards, or opened using browser technology integrated into smartboards, hence the representation of the elements is of type EDE. In contrast, to text-based descriptions, the entire process underlying the workflow is in this case represented spatially, through digital elements that are laid out and opened in space.

Lemma 3.3 In summary, MaxWhere has the capability to represent workflows with a DC of the 4th order, with EDEs and DG-R - hence, it is suitable for the effective execution of DWs of the 4th order.

The following table summarizes the capabilities of classical, online web-based (e-learning) and MaxWhere operating system based approaches:

Table 4

Capabilities of classical, online web-based (e-learning) and MaxWhere operating system based approaches

DW	1	2	3	4	EDR	EDE
Classical	1	0.5	x	x	0.5	x
e-learning	1	1	0.5	x	1	x
MaxWhere	1	1	1	1	1	1

4   Experimental Evaluation of User Effectiveness

In this chapter, results of experimental evaluations are provided. The goal of these experiments was to investigate the effectiveness with which users can execute digital workflows shared through classical approaches, online interfaces and MaxWhere. The digital workflow used in the experiments was of the 1st order, with 11 DEs and a DC of type 5DF. The experiments were carried out on 379 students.

4.1   Digital Content

The digital content was comprised of 1 PowerPoint file, 1 PDF file, 1 video file, 4 webpages and a further 4 tests. From the point of view of digital complexity, the task involved both one-to-one and one-to-many relationships. Specifically, 1 (separate) test was to be filled out in the context of the PowerPoint file, the PDF file and the video file, respectively. A final test was given to users in the context of the 4 webpages. Therefore, the last test was characterized by a one-to-many relationship.

4.2   Digital Workflow

The key to solving the digital workflow effectively was the appropriate organization of the digital elements. Thus, users had to make sure that they could answer the questions on the first three tests based on the information contained in the PowerPoint file, the PDF file and the video file, respectively; and that they could answer the questions on the final test based on all 4 webpages provided to them in the context of that test. Since the task could be carried out by considering the digital elements in sequential order, the DW can be regarded as being of the 1st order. Naturally, the fact that in specific cases users could decide to go back to the previous digital elements for clarification does not mean that they are required to do so, and does not increase the order of the DW.

4.3   Sharing of the DW

Classic: one group of users received the DW based on the classical approach, through e-mail. The body of the email contained a textual description of the workflow, and the digital elements required for the workflow were attached to the e-mail. Finally, the webpages and tests were included as links at the end of the body of the email. The naming of the attachments and links were chosen to reflect the identity of the digital elements well.

Online interface: A second group of users received the DW on through the Moodle platform. Similar to the classic approach, the description of the workflow was text-based in this case as well. However, a simple form of digital guidance was also available to users in this case, given that each step within the description of the workflow included an embedded reference to the digital elements required for that step. As a result, users were able to perform the workflow step by step instead of first having to obtain a holistic overview of the workflow. In effect, the users' ability to scroll through the steps guaranteed a DG of type S in this case.

MaxWhere: Regardless of whether this group of users received the workflow on an online surface or through the classical approach, they could import the digital elements into MaxWhere, which then provided a spatial arrangement of EDEs in smartboards. In the case of the PowerPoint file, each slide was added to a separate smartboard. The tests were loaded in smartboards that were closest to the digital elements related to them. The MaxWhere Operating System also had built-in functionalities for S and R type DG, which could be made use of by the test subjects.

4.4   Experimental Procedure

In the classic case, test subjects received the workflow via e-mail or Facebook. The measurement of time to complete the workflow began when the e-mail or Facebook message was opened. In the case of the Moodle-based approach, the measurement of time began when the module for the workflow was opened. Finally, the same approach was used in the MaxWhere condition: the measurement of time began when users opened the e-mail containing the pack file for the workflow.

4.5   Details of Workflow Transmission

4.5.1   In the Classic Case, Test Subjects Received the Following e-mail

----

Dear Students,

Please take a look at the material listed under poinot A), and fill out the tests under point B) based on the material.

A. Materials on Google Drive and other webpages:

a. Click here:

https://drive.google.com/open?id=0By19Pc3VT68aOUZ2bGtKMGNSRzQ

1. Diasor.pptx

2. PDF-dokumentum.pdf

3. Video.mp4

b. Webpages:

https://drive.google.com/open?id=0By19Pc3VT68aNHRFY2Q2dUkzLU0

2. https://drive.google.com/open?id=0By19Pc3VT68abEIyWjJDblVyTW8

3. https://drive.google.com/open?id=0By19Pc3VT68aY21yWU0zc0FIc1U

4. https://drive.google.com/open?id=0By19Pc3VT68aLWRLUFBCZDI2dFE

B. Test forms:

https://docs.google.com/forms/d/e/1FAIpQLSdd8tF1R9pwmmwc-GqNrQvirnog8IgvTJmBbbrq90tBGbu8uw/viewform?usp=sf_link

https://docs.google.com/forms/d/e/1FAIpQLScNGnvtAEard6yfdpXGMw2lj6cGMoawZJ6kCvlriXUgseQG5A/viewform?usp=sf_link

https://docs.google.com/forms/d/e/1FAIpQLSdmeMFNDEFRTLEdfK5PTIy7uwZbQTwmKKddiYn9_q7_9X_CQg/viewform?usp=sf_link

https://docs.google.com/forms/d/e/1FAIpQLScEflnfw8bfla0Tw3gpY-kJATTOo1TvqVXLK5ng7rY0NWYGcg/viewform?usp=sf_l

Sincerely, ...

It is clear based on the above that the relationships between digital elements are not at all transparent. We used two different ways to add the digital content to the e-mail. In the first case we attached all files to the e-mail. In second case we put the link of the content located on the Google drive.

4.5.2   In the Case of the Online Interface, Test Subjects had to Open the Following Page

----

Dear Students,

Diasor

Please click on the "Diasor" link above, take a look at the slides and then answer the test questions that can be accessed through the following link:

https://docs.google.com/forms/d/e/1FAIpQLSdd8tF1R9pwmmwc-GqNrQvirnog8IgvTJmBbbrq90tBGbu8uw/viewform?usp=sf_link

PDF documentum

Please click on the "PDF-dokumentum" link above, take a look at the pdf file and then answer the test questions that can be accessed through the following link:

https://docs.google.com/forms/d/e/1FAIpQLScNGnvtAEard6yfdpXGMw2lj6cG MoawZJ6kCvlriXUgseQG5A/viewform?usp=sf_link

Video

Please click on the "Video" link above, watch the video and then answer the test questions that can be accessed through the following link:

https://docs.google.com/forms/d/e/1FAIpQLSdmeMFNDEFRTLEdfK5PTIy7uwZ bQTwmKKddiYn9_q7_9X_CQg/viewform?usp=sf_link

Please take a look at the following webpages:

https://drive.google.com/open?id=0By19Pc3VT68aNHRFY2Q2dUkzLU0

2. https://drive.google.com/open?id=0By19Pc3VT68abEIyWjJDblVyTW8

3. https://drive.google.com/open?id=0By19Pc3VT68aY21yWU0zc0FIc1U

4. https://drive.google.com/open?id=0By19Pc3VT68aLWRLUFBCZDI2dFE

Afterwards, please answer the test questions that can be accessed through the following link:

https://docs.google.com/forms/d/e/1FAIpQLScEflnfw8bfla0Tw3gpY-kJATTOo1TvqVXLK5ng7rY0NWYGcg/viewform?usp=sf_l

----

In this case, the order in which the sub-tasks were to be completed and the relevant digital elements to each sub-task were clearly delineated, therefore the workflow was supported by a DG of type S.

4.5.3   In the MaxWhere Case, Test Subjects Received the Following e-mail

_____

Dear Students,

Please open the following pack file using MaxWhere, and go through the space using the guiding functionality of MaxWhere. While doing so, please fill out the 4 tests included in the pack.

Sincerely,

4.6   Details of the Digital Elements

The PowerPoint file contained 14 slides. Each slide contained an image of a cat or a dog (see Appendix 1).

The PDF file contained 3 pages, each showing images of either a cat or a dog (see Appendix 2).

The video (30sec) contained a sequence of 5 static images, with one of them showing a dog (see Appandix 3).

Finally, each of the 4 webpages contained an image of a single animal -- either a cat or a dog (see Appendix 4).

4.7   Results of the Experiment

The number of students tested using the classical e-mail with attached content and with linked contennt, online platform and MaxWhere-based approach were 115, 77, 97 and 90 respectively.

Figures 6, 7 and 8 show the results of the test. The horizontal axes represent the time required to complete the test. The vertical axes represent the precentage of users corresponding to the given number of minutes.

The average and standard deviation of the time required to complete the workflow in each of the cases were:

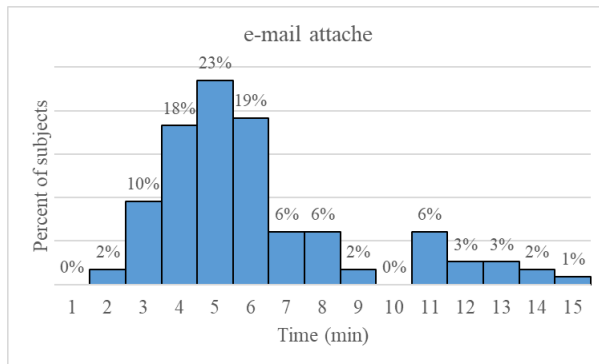|	
E-mail with attachment:	average: 6:42, standard deviation: 3:02
E-mail with Google Drive links:	average: 5:54, standard deviation: 1:39
Moodle	average: 6:42, standard deviation: 3:03
MaxWhere	average: 3:11, standard deviation: 0:46

Figure 6

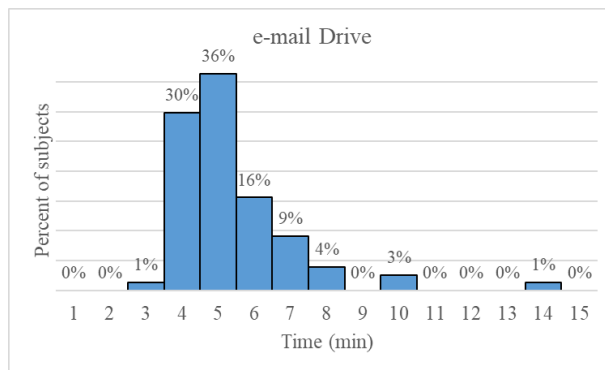Test in which files were sent via e-mail attachment.

Figure 7

Test in which digital content was sent through Google Drive links via e-mail
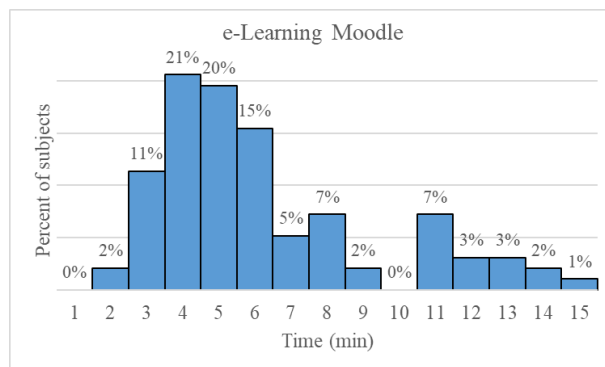

Figure 8

Test in which the digital workflow and digital content was shared through the Moodle e-learning
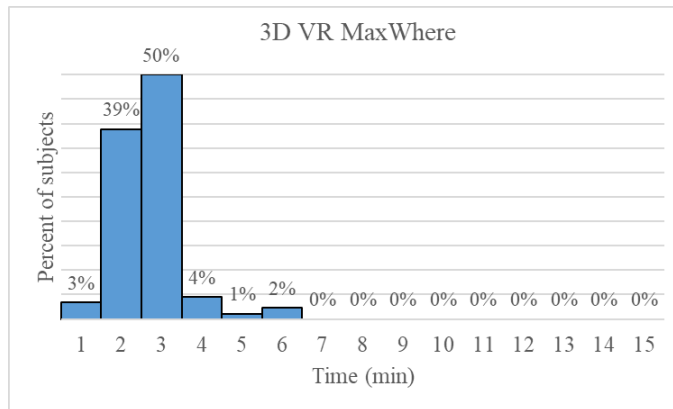framework

Figure 9

Test in which the digital workflow and digital content was shared through the MaxWhere 3D environment

Conclusions

This paper investigated how workflows can be communicated and shared through linguistic descriptions, digital content and technological tools. We focused primarily on the content and digital tools of e-learning and VR learning. However, the results of the paper can be applied to collaborative workflows in general. The results of the paper show that users of the MaxWhere VR environment could complete digital workflows in considerably less time (i.e., 50% faster) than using the more traditional (e-mail based and content management system based) approaches. It is also remarkable that the standard deviations of completion times are considerably smaller in the case where the MaxWhere-based approach was used. Although the reasons behind this observation may need to be clarified through further investigations, it nevertheless points to the conclusion that the whole process of comprehension is rendered clearer than usual in 3D environments capable of representing 4th order digital workflows with automatic guiding, as pointed out in the paper.

Acknowledgement

References

[1]   P. Baranyi, A. Csapo, Gy. Sallai, "Cognitive Infocommunications (CogInfoCom)", *Springer International Publishing* Switzerland, p. 191. (978-3-319-   19607   7, http://www.springer.com/us/book/9783319196077#aboutBook

[2]   P. Baranyi, Á. Csapó, "Definition and synergies of cognitive infocommunications." *Acta Polytechnica Hungarica* 9.1 (2012): 67-83

[3]   I. Horvath, "The edu-coaching method in the service of efficient teaching of disruptive technologies," *Springer book chapter*, *Cognitive Infocommunications and computing, in the Series of Topics in Inetelligent Engineering and informatics.* Accepted

[4]   M. Akçayır és G. Akçayır, „Advantages and challenges associated with augmented reality for education: A systematic review of the literature," *Educational Research Review,* , pp. 1-11, 2017

[5]   L. J. Ausburn és F. B. Ausburn, „Technical perspectives on theory in screen-based virtual reality environments: Leading from the future in VHRD," *Advances in Developing Human Resources,* pp. 371-390, 2014

[6]   E. Z. Borba és M. K. Zuffo, „Advertising Perception with Immersive Virtual Reality Devices," in *IEEE Virtual Reality (VR)*, 2017

[7]   T. Griffin, J. Giberson, S. H. M. Lee, D. Guttentag, M. Kandaurova, K. Sergueeva és F. Dimanche, „Virtual Reality and Implications for Destination Marketing," in *Tourism Travel and Research Association: Advancing Tourism Research Globally*, 2017

[8]   I. Horváth, „Innovative Engineering Education in the Cooperative VR Environment," *Cognitive Infocommunications (CogInfoCom), 2016 7th IEEE International Conference,* pp. 359-364, 2016

[9]   S. Jang, J. M. Vitale, R. W. Jyung és J. B. Black, „Direct manipulation is better than passive viewing for learning anatomy in a three-dimensional virtual reality environment," *Computers & Education*, pp. 150-165, 2017

[10]   H. Van Kerrebroeck, M. Brengman és K. Willems, „When Brands Come to Life: Experimental Research on the Vividness Effect of Virtual Reality in Transformational Marketing Communications," *Virtual Reality,* pp. 177-191, 2017

[11]   X. Zhang, S. Jiang, P. Ordóñez de Pablos, M. D. Lytras és Y. Sun, „How virtual reality affects perceived learning effectiveness: a task–technology fit perspective," *Behaviour & Information Technology,* pp. 1-9, 2017

[12]   J. Katona and A. Kovari, "A Brain–Computer Interface Project Applied in Computer Engineering," in *IEEE Transactions on Education*, Vol. 59, no. 4, pp. 319-326, Nov. 2016, doi: 10.1109/TE.2016.2558163

[13]   T. Ujbanyi, J. Katona, G. Sziladi and A. Kovari, "Eye-tracking analysis of

computer networks exam question besides different skilled groups," *2016 7th IEEE International Conference on Cognitive Infocommunications (CogInfoCom)*, Wroclaw, 2016, pp. 000277-000282., doi: 10.1109/CogInfoCom.2016.7804561

[14]   J. Katona, T. Ujbanyi, A. Kovari, "Investigation of the Correspondence between Problems Solving Based on Cognitive Psychology Tests and Programming Course Results," in *International Journal of Emerging Technologies in Learning*, Vol. 10, No. 3, pp. 62-65, 2015, doi: 10.3991/ijet.v10i3.4511

[15]   J. Katona, A. Kovari, "EEG-based Computer Control Interface for Brain-Machine Interaction," in *International Journal of Online Engineering*, Vol. 11, No. 6, pp. 43-48, 2015., doi: 10.3991/ijoe.v11i6.5119

[16]   J. Katona, T. Ujbanyi, G. Sziladi, A. Kovari, "Speed control of Festo Robotino mobile robot using NeuroSky MindWave EEG headset based Brain-Computer Interface," *2016 7th IEEE International Conference on Cognitive Infocommunications (CogInfoCom)*, Wroclaw, 2016, pp. 000251-000257, doi: 10.1109/CogInfoCom.2016.7804557

[17]   J. Katona, D. Peter, T. Ujbanyi and A. Kovari, "Control of incoming calls by a windows phone based brain computer interface," *2014 IEEE 15th International Symposium on Computational Intelligence and Informatics (CINTI)*, Budapest, 2014, pp. 121-125, doi: 10.1109/CINTI.2014.7028661

[18]   G. Sziládi, T. Ujbányi, J. Katona, "Cost-effective hand gesture computer control interface," *2016 7th IEEE International Conference on Cognitive Infocommunications (CogInfoCom)*, Wroclaw, 2016, pp. 000239-000243, doi: 10.1109/CogInfoCom.2016.7804555

[19]   J. Katona, "Examination and comparison of the EEG based Attention Test with CPT and T.O.V.A.," *2014 IEEE 15th International Symposium on Computational Intelligence and Informatics (CINTI)*, Budapest, 2014, pp. 117-120, doi: 10.1109/CINTI.2014.7028659

[20]   J. Katona, " Evaluation of The Neurosky MindFlex EEG Headset Brain Waves Data," *2014 IEEE 12th International Symposium on Applied Machine Intelligence and Informatics (SAMI)* Herl'any, Slovakia, 2014, pp. 91-94, doi: 10.1109/SAMI.2014.6822382

[21]   I. Horváth, "The IT device demand of the edu-coaching method in the education of engineering," 8th *IEEE Conference on Cognitive Infocommunications (CogInfoCom 2017)* pp. 000379-000384

[22]   I. Horváth, "Innovative engineering training, *Australian Journal of Intelligent*

Information Processing System, Vol. 14, No. 4

[23] I. Horváth, "Disruptive technologies in higher education," *7th IEEE Conference on Cognitive Infocommunications (CogInfoCom 2016)* 16-18 October, 10.1109/CogInfoCom.2016.7804574

[24] I. Horváth, "Digital Life," *IEEE Conference on Cognitive Infocommunications (CogInfoCom 2016)* 16-18 October, 10.1109/CogInfoCom.2016.7804575

[25] I. Horváth, "Innovative engineering education in the cooperative VR environment," *(CogInfoCom 2016),* 16-18 October, Wroclaw, Poland, pp. 000359-000364, doi: 10.1109/CogInfoCom.2016.7804576
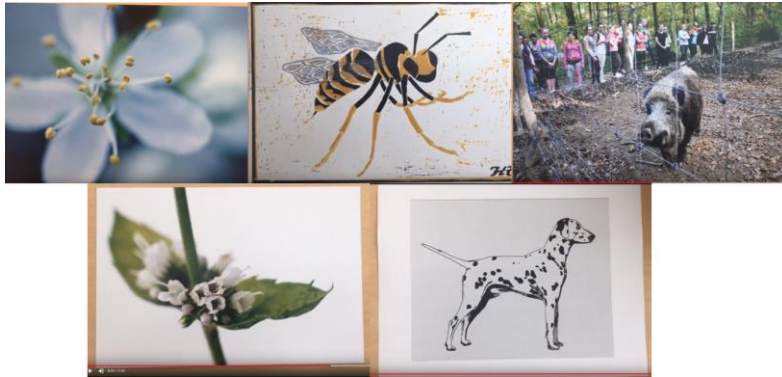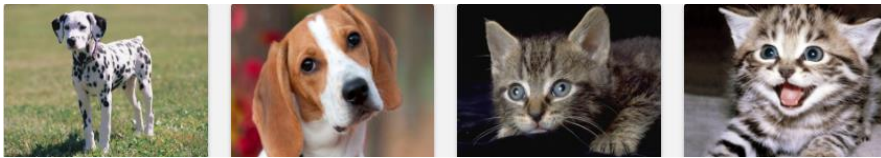
Appendix

Appendix 1. Slides
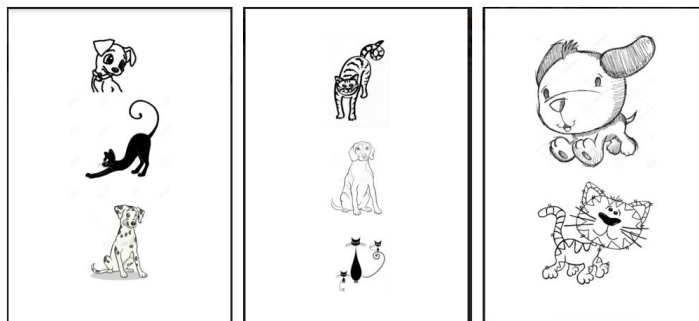
Appendix 2. Pages of the PDF file

Appendix 3. Content on the Video

Appendix 4. Webpages

Factors Contributing to the Enhanced Performance of the MaxWhere 3D VR Platform in the Distribution of Digital Information

Ildiko Horvath, Anna Sudar

VR-Learning Center, Széchenyi István University
Liszt F. u. 42, H-9022 Győr, Hungary

VR-Learing Research Lab, Apáczai Faculty, Széchenyi István University
Liszt F. u. 42, H-9022 Győr, Hungary

horvath.ildiko@sze.hu, sudar.anna@sze.hu

Abstract: The rapid evolution of information technology and of a new networked culture in the 21st Century has brought a new question to the forefront of scientific interest: the question of how new technologies influence the effectiveness with which humans are able to perform specific tasks. This paper presents an experiment contrasting traditional 2D interfaces and the MaxWhere 3D VR educational platform in order to shed light on how the effectiveness of various operations and workflows constituting the core of digital literacy has evolved in recent times. In order to draw specific conclusions, a new framework of concepts, qualitative and quantitative metrics and experimental procedures is proposed in the paper. The final goal of the proposed framework is to help evaluate the effectiveness of digital workflows. The results of the experiment, evaluated in terms of the proposed framework, point to the conclusion that when using MaxWhere instead of traditional 2D interfaces, users are able to accomplish the same digital workflows with 30% less user operations, and up to 80% less machine operations. Based on these results, the paper concludes that MaxWhere as an educational platform offers users a number of ways to accomplish tasks that would otherwise require extremely complicated digital workflows in more traditional 2D environments.

1   Itroduction

Today's generation of students are increasingly accustomed to the possibility of quickly accessing large amounts of digital information and, guided by their own internal motivation, to the practice of consuming this information in non-linear, often parallel ways. More and more new fields of science are appearing, among which the Cognitive Infocommunication (CogInfoCom) [1, 2] searching the trends of the progress in informatics calls the attention to the significance of the necessity

of access to infocommunication. With advances in technology, new forms of studying have also appeared. Students belonging to the generation of digital natives are generally less interested in the rote memorization of data and are instead motivated to explore a different way of internalizing new concepts. In short, their way of thinking is different. This conclusion is supported by the experience of many instructors, who often note that today's generation is simply unwilling to perform tasks that they see as unnecessary or uninteresting. For example, students today are often unwilling to engage with information that was sent to them using more traditional forms of communication, such as through e-mail attachments or through predominantly text-based e-learning platforms.

As an answer to this trend and in keeping with technological advances, the past few years have seen the appearance of numerous VR and AR applications in many areas of education. VR and AR technologies can be considered as entirely new forms of media that reflect a radically new way of viewing information that puts the dimensions of dynamics and intimacy to the forefront. A key example is the MaxWhere VR educational platform, the first release of which was made public in 2016. Besides their ease of use, an important advantage of MaxWhere's virtual spaces is that they allow information to be shared quickly and easily. In MaxWhere spacees, digital content is laid out in 3D space through a collection of SmartBoards, which helps users interpret the content and to navigate through it more effectively than with traditional (non-3D) approaches. A further important aspect is the ability of users to collaborate through MaxWhere. [3, 4,…10] Besides allowing for single-user workflows, MaxWhere's philosophy makes it possible to connect multiple users [11] and to enhance the effectiveness of their work by integrating all varieties of online collaborative tools.

The main goal of this study is to systematically compare the effectiveness of digital workflows when content is shared through classical text-based methods (e.g. e-mail and attachments), 2D content management systems (e.g. Moodle) and the MaxWhere 3D VR platform. All comparisons are made based on a novel framework that focuses on both quantitative and qualitative assessments of user interactions required for the completion of digital projects within different computational environments.

2   Properties and Definitions

In this section, key terms and properties are defined based on which the comprehensibility, effectiveness and adequacy of various content sharing approaches (i.e., classical e-mail attachments, 2D e-learning content management solutions and the MaxWhere 3D VR platform) can be compared. In the following sections, these terms and properties will be used to elucidate the effectiveness of the user interactions required to carry out digital workflows.

1) Machine Operations (MO)

A machine operation is a functional relationship, i.e. mapping between a user command (e.g. selection, click, typed command) and a pre-defined process that is executed by the machine in response to that command. Examples include the loading of a specific content, the deletion of a specific content, etc. The metric of MO is machine time.

In the following, user operations will be at the center of focus. From the perspective of our analysis, it is important to clarify that only those user operations will be considered that induce machine operations.

2) Elementary operations (EO)

An elementary operation is a simple interaction from the user that triggers the execution of a pre-defined process from the machine. Its unit is defined as 1 EO.

In this interpretation, examples of elementary operations include:

i) a single click to select an item

ii) a double click to select an item

iii) a key press

iv) an inversion of the click/select operation (i.e., release of a mouse button or a key at the appropriate place and/or time)

v) a press / push (push = long press) of a key or mouse button

vi) the Scroll up / down operation

From here on, each of these elementary operations will be regarded as having a complexity of 1 EO.

3) Complex operations (CO)

A complex operation is one that consists of more than 1, but at most 3 EOs that are performed in coordination.

For example, copying through the "Ctrl+C" key combination requires a click (to select) and the pressing of two keys to copy and paste. Similarly, the well-known drag-and-drop operation consists of a select EO, a push and an inverse click. Based on these examples, we propose to set up an equivalence between the metrics 1 CO and 3 EO.

4) Navigation-based elementary operations (Mouse – Nav & Click)

An elementary operation is navigation-based if it is performed not using a keyboard but using a mouse and a visual representation on the screen (such as a virtual keyboard). For example, file selection operations from a file manager involve moving a cursor to the right location and then performing the remaining operations – hence the sequence of operations is initiated by navigation.

In the investigations conducted in this paper, navigation-based elementary operations (NBEO) shall be considered as having a complexity of 1.5 elementary operations (1 NBEO = 1.5 EO), in recognition of the fact that NBEOs include the added complexity of the user having to navigate to the intended location on the screen.

5) Ordering operations (OO)

An ordering operation is a sequence of elementary and complex operations performed with the goal of improving the comprehensibility of digital content, and users' ability to navigate and comprehend it. An example of an ordering operation is when users arrange multiple windows on different parts of their screen to be able to shift their attention between them. Doing this consists of repositioning and resizing each window (the repositioning operation itself consists of dragging the window to the intended location, while the resizing operation consists of dragging at the corner of the window at least once and stretching both sides of the window to their final horizontal position). Thus, the complexity of such an operation would be at least 1 EO + 1NBEO + 2 NBEO = 5.5 EO per window, though in practice it often reaches the complexity of 7 EO, as users often chose to stretch the window on all 4 sides, and / or may have to iteratively improve on the entire ordering operation.

Motivated by the above example, we adopt the equivalence of 1 EO = 5.5 OO in this paper.

Remark: It is noteworthy that the manufacturers of modern operating systems seem to have recognized how tedious it is to multitask using their products and have therefore in the past few years begun to offer their clients alternative solutions. Based on the following examples, it is, however, clear that in many cases such solutions require either the installation of a separate display, or are constrained in their applicability to individual software solutions:

- The window placement assistance functionality of Windows 10 automatically positions the edge of the window to the edge of the screen, making for a more comfortable experience. Then, when the window is moved to the left or to the right, the operating system ensures that the window fills out half of the available screen space. This solution can also be used with multiple monitors, when the display is extended, such that two windows can be easily laid out on each physical display, allowing for a total of 4 windows. This functionality can also be triggered using the Windows + left (or right) arrow key.

- Mac OS users have the option to pull a window either to the left or to the right side of the screen by clicking on and holding down the green icon on the top left of the toolbar. The same operation can be repeated on the other side of the screen, allowing for two windows to be displayed simultaneously.

These two solutions represent all that can be achieved in terms of simultaneous window display on today's leading desktop operating systems.

6) High distraction operations (HDO) – loading / opening operations

Operations that are initiated by users through an EO or CO, but which also incur a period of waiting time are considered high distraction operations. Examples of such operations include file downloads, file open operations in specific applications, file compression, etc.

7) High alternation operations (HAO)

High alternation operations involve the user's having to alternate back and forth between multiple windows to carry out the required digital workflow. Once the required windows are opened, 1 HAO must be taken to correspond to 1 navigation based EO, which in turn corresponds to 1.5 EO based on the earlier discussions. As a result, 1 HAO may in a practical sense be considered as being equivalent to 1.5 EO.

At the same time, it is important to note that an HAO involves a complete change of screen content, which, in addition to the 1.5 EO it is equivalent to, also results in considerable (passive) brain activity associated with the changes in perceptual input and information processing activity thereby triggered. This fact alone motivates the use of the metric of 1 HAO instead of 1.5 EO whenever it is worth emphasizing this added complexity in cognitive load (CL). Another alternative is to use the equivalence 1 HAO = 1.5 EO + 1 CL.

8) Analog overview capability / capacity

The capability and capacity of a piece of software used for digital work to provide an overview of the entire digital content involved in workflow. In the remainder of this paper, our goal is to investigate the availability and degree of this capacity in relation to different forms of digital work.

Further concepts that are made use of in the paper, but are not central to the focus of the comparative analyses performed include [12]:

9) Digital element (DE)

A digital element is taken to mean a unit that has to be opened or loaded separately, in itself with an appropriate software.

10) Digital content

Digital content is defined as a set of digital elements. Digital content can be quantified based on the number of digital elements contained in the content.

11) Digital project

A digital project is a set of tasks that are to be carried out on a digital content.

12) Digital workflow (DW)

Digital workflows determine the order in which individual digital elements are to be accessed or processed during the course of a digital project. We distinguish among the following types of digital workflows:

- 1st order (linear): The digital elements are to be accessed in a static and sequential order, one after the other.

- 2nd order (loopy): There are loops in the order in which the digital elements are to be accessed, so that individual elements, or smaller sequences thereof, are to be accessed repetitively. Such loops can be characterized by length and number of repetitions.

- 3rd order (networked): Digital elements accessed during the project are structured as hierarchical loops, so that the project may contain subprojects of subprojects, and / or the ordering of digital elements may be different upon different repetitions of the loops.

- 4th order (algorithmic): It is possible that the project contains branches, so that different digital elements are accessed dynamically in an order that depends on information obtained during the project.

13) Digital Guidance (DG)

Digital guidance is taken to mean a process that unambiguously drives the user's attention during the digital workflow and thus reduces (partially, or to 0) the time required for searching for and finding the relevant digital content. It is possible to distinguish among three forms of digital guidance as follows:

- none: no guidance is applicable, or the representation of the digital content doesn't involve embedded digital elements (instead, the elements are provided through separate lists).

- sequential (DG-S): The digital elements are traversed in sequential order. It is thus possible to jump between one element to the next in the context of a digital workflow.

- random access (DG-R - event/dynamic focus-driven): One can switch between sequences of digital elements, and thus follow non-static sequences (for example, in the case of DWs of the 4th order).

3 Classical, e-Learning and MaxWhere 3D VR Digital Work Environments

In this section, the 3 working environments and digital workflow management techniques under comparison are introduced. Based on their interpretation, they are first contrasted based on the conceptual framework presented earlier, i.e. the

concepts of digital content, digital workflow and digital guidance are taken as input factors that influence the applicability of the different work environments in different scenarios. The perspective of user operations and complexities thereof are also taken into account based on earlier discussions.

3.1.   Work Environments Considered in the Experiment

Three different work environments were considered as follows:

1. **Classical** - **TXT based message.** In this approach, the digital workflow and digital content was shared through a text-based message and attachments to the message (via e-mail, Facebook Messenger or other means of text-based communication). Digital content available through the Web were shared not as attachments, but as links inside the messages themselves.

   Because this method of sharing is primarily text-based, the digital workflow carried out can be considered as providing a degree of comprehension of the first order (linear). In addition, since the digital elements sent as attachments cannot be embedded into the text message itself – but those elements that are available on the web can be included as web urls – the digital elements can be partly linked (hence the approach has an LDE, or Linked Digital Element count of 0.5). Finally, the method can involve no form of digital guidance (its DG type is none).

2. **Online e-Learning platform – MOODLE.** In this approach, both the description of the workflow and the digital content (or links to its digital elements) are shared on an online, web-based interface.

   Remark: In the simplest case this approach can be equivalent to the classical text-based approach, if the web-based interface consists of a separate description of the workflow, with links to the associated digital elements at the bottom of the description. However, a crucial advantage of online e-learning environments compared to the text-based approach with attachments is that it can include embedded digital elements within the text – and not just web-based urls, but also images, links to files uploaded to the e-learning server, etc. As a result, the digital elements belonging to the workflow can at least be referenced in order and at the place where they are needed (i.e., a sequential form of digital guidance is possible). Instructors who are well-versed in the use of e-learning environments often prefer to make use of this opportunity. As a result, online e-learning interfaces can be seen as providing a digital comprehension of the second order, and a digital guidance of the sequential type (DG-S), and is, therefore, suitable for carrying out digital workflows of the 2nd – or in some cases, 3rd order.[12]

3. **MaxWhere operating system.** MaxWhere is a novel solution that represents a radically new approach. For the purposes of this study, content associated with

MaxWhere was shared through a single pack file sent via e-mail. Similarities with the classical text-based approach end there: the pack files themselves cannot be regarded as digital elements in the classical sense; instead, they are better conceived of as archives that contain all digital content required for the workflow, combined with the digital guidance required to carry it out. Once imported into MaxWhere, the contents of the pack file are loaded in the SmartBoards that are laid out in 3D space. Those SmartBoards that correspond to cloud-based software will contain the web-based interface of the relevant software (hence, MaxWhere implements embedded digital elements). The steps of the digital guidance included in the pack file support the effectiveness of the digital workflow in an important sense.

From the user's perspective, importing a pack file requires 1 complex operation, and 1 machine operation which actually loads the file. In contrast to the classical text-based and the e-learning interface based approaches, MaxWhere provides a complete representation of the workflow in 3D. As a result, MaxWhere supports a digital comprehension of the 4th order, and a random access type of digital guidance (DG-R).

3.2   Key Elements of the Experiment

The experiment involves the comparison of three different workflow sharing techniques and work environments. In all three cases, the same digital content and workflow was used.

3.2.1   Digital Content

The digital content was comprised of 1 PowerPoint file, 1 PDF file, 1 video file, 4 webpages and a further 4 test questionnaires.

From the point of view of digital complexity, the task involved both one-to-one and one-to-many relationships. Specifically, 1 (separate) test was to be filled out in the context of the PowerPoint file, the PDF file and the video file, respectively. A final test was given to users in the context of the 4 webpages. Therefore, the last test was characterized by a one-to-many relationship.

Details of the digital content:

In the experiment, special emphasis was on making sure that none of the tasks involved background knowledge or computer usage skills that could skew the interpretation of the results. To this end, all of the tasks were very simple and consisted of counting the number of cats and dogs appearing in different digital documents. It was our hope that the simplicity of the tasks would ensure that the interpretation of the results would be clear-cut and the results comparable.

The PowerPoint file contained 15 slides. Each slide contained an image of a cat or a dog. The PDF file contained 2 pages, each showing images of either a cat or a dog. The video contained a sequence of static images, with one of them showing a dog. Finally, each of the 4 webpages contained an image of a single animal – either a cat or a dog.

3.2.2   Digital Workflow

The key to solving the digital workflow effectively was the appropriate organization of the digital elements. Thus, users had to make sure that they could answer the questions on the first three test questionnaires based on the information contained in the PowerPoint file, the PDF file and the video file, respectively; and that they could answer the questions on the final test based on all 4 webpages provided to them in the context of that test.

Because the task could be carried out by considering the digital elements in sequential order, the DW can be regarded as being of the 1st order. Naturally, the fact that in specific cases users could decide to go back to the previous digital elements for clarification does not mean that they are required to do so, and therefore does not increase the order of the DW.

Methods of sharing digital workflows

The experimental conditions were different in terms of the way in which digital workflows were shared.

1. Classical: one group of users received the DW based on the classical approach, through e-mail. The body of the email contained a textual description of the workflow, and the digital elements required for the workflow were attached to the e-mail. Finally, the webpages and tests were included as links at the end of the body of the email. The naming of the attachments and links were chosen to reflect the identity of the digital elements well.

2. Online e-Learning felület: A second group of users received the DW on through the Moodle platform. Similar to the classic approach, the description of the workflow was text-based in this case as well. However, a simple form of digital guidance was also available to users in this case, given that each step within the description of the workflow included an embedded reference to the digital elements required for that step. As a result, users were able to perform the workflow step by step instead of first having to obtain a holistic overview of the workflow. In effect, the users' ability to scroll through the steps guaranteed a DG of type S in this case.

3. MaxWhere: Regardless of whether this group of users received the workflow on an online surface or through the classical approach, they could import the digital elements into MaxWhere, which then provided a spatial arrangement of EDEs in smartboards. In the case of the PowerPoint file, each slide was added

to a separate smartboard. The tests were loaded in smartboards that were closest to the digital elements related to them. The MaxWhere Operating System also had built-in functionalities for S and R type DG, which could be made use of by the test subjects.

Details on the transmission of digital workflows:

In the **classic** case, test subjects received the workflow via e-mail or Facebook. The measurement of time to complete the workflow began when the e-mail or Facebook message was opened. In the case of the Moodle-based approach, the measurement of time began when the module for the workflow was opened. Finally, the same approach was used in the MaxWhere condition: the measurement of time began when users opened the e-mail containing the pack file for the workflow.

Dear Students,

Please take a look at the material listed under poinot A), and fill out the tests under point B) based on the material.

A. Materials on Google Drive and other webpages:

a. Click here:

https://drive.google.com/open?id=0By19Pc3VT68aOUZ2bGtKMGNSRzQ

1. Diasor.pptx

2. PDF-dokumentum.pdf

3. Video.mp4

b. Webpages:

https://drive.google.com/open?id=0By19Pc3VT68aNHRFY2Q2dUkzLU0

2. https://drive.google.com/open?id=0By19Pc3VT68abEIyWjJDblVyTW8

3. https://drive.google.com/open?id=0By19Pc3VT68aY21yWU0zc0FIc1U

4. https://drive.google.com/open?id=0By19Pc3VT68aLWRLUFBCZDI2dFE

B. Test forms:

https://docs.google.com/forms/d/e/1FAIpQLSdd8tF1R9pwmmwc-GqNrQvirnog8IgvTJmBbbrq90tBGbu8uw/viewform?usp=sf_link

https://docs.google.com/forms/d/e/1FAIpQLScNGnvtAEard6yfdpXGMw2lj6cGMoawZJ6kCvlriXUgseQG5A/viewform?usp=sf_link

https://docs.google.com/forms/d/e/1FAIpQLSdmeMFNDEFRTLEdfK5PTIy7uwZ
bQTwmKKddiYn9_q7_9X_CQg/viewform?usp=sf_link

https://docs.google.com/forms/d/e/1FAIpQLScEflnfw8bfla0Tw3gpY-
kJATTOo1TvqVXLK5ng7rY0NWYGcg/viewform?usp=sf_l

Sincerely, …

[12]

Remark: Due to its digital comprehensibility level of order 1, instructors using
the classic approach are extremely cautious in the way they formulate the task to
be completed. Accordingly, the above description is quite detailed. At the same
time, it is also clear that the mapping between tasks and digital content cannot be
made as clear in the classical approach as in the other approaches treated in this
paper. Thus, despite the instructors' best intention, the test subjects in this
condition were forced to figure out on their own which digital content
corresponded to which sub-task. This is the ultimate reason why there can be no
digital guidance associated with this approach (the type of digital guidance is
'none').

In the case of the **online Moodle interface**, test subjects had to open the following
page:

The translation of the message is as follows:

Dear Students,

Diasor

Please click on the "Diasor" link above, take a look at the slides and then answer the test questions that can be accessed through the following link:

https://docs.google.com/forms/d/e/1FAIpQLSdd8tF1R9pwmmwc-
    GqNrQvirnog8IgvTJmBbbrq90tBGbu8uw/viewform?usp=sf_link

PDF documentum

Please click on the "PDF-dokumentum" link above, take a look at the pdf file and then answer the test questions that can be accessed through the following link:

https://docs.google.com/forms/d/e/1FAIpQLScNGnvtAEard6yfdpXGMw2lj6cG
MoawZJ6kCvlriXUgseQG5A/viewform?usp=sf_link

Video

Please click on the "Video" link above, watch the video and then answer the test questions that can be accessed through the following link:

https://docs.google.com/forms/d/e/1FAIpQLSdmeMFNDEFRTLEdfK5PTIy7uwZ
bQTwmKKddiYn9_q7_9X_CQg/viewform?usp=sf_link

Please take a look at the following webpages:

https://drive.google.com/open?id=0By19Pc3VT68aNHRFY2Q2dUkzLU0

2. https://drive.google.com/open?id=0By19Pc3VT68abEIyWjJDblVyTW8

3. https://drive.google.com/open?id=0By19Pc3VT68aY21yWU0zc0FIc1U

4. https://drive.google.com/open?id=0By19Pc3VT68aLWRLUFBCZDI2dFE

Afterwards, please answer the test questions that can be accessed through the following link:

https://docs.google.com/forms/d/e/1FAIpQLScEflnfw8bfla0Tw3gpY-
kJATTOo1TvqVXLK5ng7rY0NWYGcg/viewform?usp=sf_l

Remark: In this case, the order in which the sub-tasks were to be completed and the relevant digital elements to each sub-task were clearly delineated, therefore the workflow was supported by a DG of type S.

In the **MaxWhere** case, test subjects received the following e-mail

----

Dear Students,

Please open the following pack file using MaxWhere, and go through the space using the guiding functionality of MaxWhere. While doing so, please fill out the 4 tests included in the pack.

Sincerely,

----

4   Evaluation and Comparison of User Effectiveness

This section examines the classical, e-learning based and MaxWhere based techniques in terms of user effectiveness. Following the principle of Forward Analysis, the experimental model is set up incrementally, with newer explanatory variables added step by step. The starting point of the model is provided by 2D spaces.

At the center of focus are the user operations required to carry out the digital workflow / project. Different work environments necessitate different kinds of operations, which can be contrasted based on the framework introduced earlier in this paper, i.e. based on elementary operations and high distraction / high alternation operations.

4.1   Detailed Comparison of Actual User Operations Carried Out

When the classical e-mail based approach is adopted, users have to carry out the following operations:

1.   Open the e-mail

    1 EO (click) + 1 HDO (as the e-mail loads),

2.   Load 4 webpages directly + open 4 tests directly

    4 Navigation-based EO + 4 HAO + 4 HDO = 4*1.5 EO+ 4*1.5 EO+4 HDO = **12 EO + 4HDO**

3.   Download files from e-mail:

Navigation within file manager requires, on average 4 Navigation-based EO (click) = 4*1.5 EO = **6 EO** (drive link + 3 files in the file manager), and 3 ppt+pdf+video downloaded (clicks on 3 files) and **3 HDO** associated with the files loading.

4.   Open webpages: 4 Navigation-based EO +4 HAO + 4 GM+4 HDO = 4*1.5 EO + 4*1.5

EO + 4GM + 4 HDO =**12 EO + 4HDO**

5.   Alternate between digital elements at least: 8 HAO + 8 HDO= 8*1.5 EO +8 HDO= **12EO+8HDO**

6.   Peruse PPT file 15 EO, **or** in the slide arrangement view 2 EO +1EO (scrolling). A conservative estimation would be: **3 EO**

7.   Peruse PDF file **1EO** (scroll down or page down)

8   Watch video **1EO**

9.   Fill out tests 1-4: 6EO*4=**24EO**

Total: 72 EO + 20 HDO

When the **Moodle-based approach** is used, carrying out the workflow consists of first making the content available to the students through Moodle. Then:

1   Students signed on to the Moodle platform.

2.   Upon the instructor's START signal (at which point time measurement began), students began working at the same time, without any intervention from the instructor or help from fellow students.

3.   Time measurement was stopped when the students completed the 4th test questionnaire and clicked on the SUBMIT / STOP button.

Remark: The task given to test subjects through Moodle was as follows. After the test subjects perused the "educational material," they had to fill out 4 different questionnaires, each corresponding to one of the 4 different types of digital elements (slide show, document, video, webpages). While completing the task, test subjects adopted different approaches. Some of them chose to open the files directly from the Moodle link and to peruse their contents immediately (direct open + "linear view"), while others chose to first download all of the files, and to then peruse their contents (download + "non-linear view"). In terms of selection and download operations, the two approaches were equivalent. The steps involved in the workflow are as follows:

1.   Download educational material and tests: 10 Navigation-based EO (PPT 2, the rest) +

9HDO = 15EO+9HDO

2. Alternate between educational material and tests at least: 8 HAO =8*1.5EO = **12 EO**

3. Peruse PPT 15 EO, **or** slide arrangement view **2 EO +1EO** (scroll down)

4. Peruse PDF **1EO** (scroll down or page down).

5. Watch video **1EO**

6. Fill out tests 1-4: 6EO*4=**24EO**

Total: 55 EO + 9 HDO

MaxWhere

1.   Open e-mail: 4 EO + 1 HDO

2   Download 1 file: 1 Navigation-based EO +1 HDO =1.5 EO+1HDO

3   Open MaxWhere space: 2 EO +1 HDO

4   Load pack file: 4 EO +1 HDO

5. Peruse slideshow: 1 CO (egér analóg, vagy ugrás, 1 CO=3EO)

6. Fill out tests 1-4 6 EO *4 =24 EO

7. PDF: Turn to pdf 1 EO, Select PDF, Scroll through PDF 2 EO

8. Video: Turn to video, start video: 2EO

9   Webpages: move to webpages 1 CO(=3EO)

Total: 45 EO + 4 HDO

The workload placed on users by the three approaches is visualized in Table 1 and Table 2.

From the considerations and data provided above, it should be empirically clear why MaxWhere's approach represents a 37.5% decrease in elementary operations and an 80% decrease in machine operations as compared to the traditional e-mail and attachment based approach. Also, it should be clear why MaxWhere is also superior to the various 2D e-learning interfaces such as Moodle, i.e. through an 18% improvement in elementary operations, and a 55.5% improvement in machine operations.

Table 1

	Classical TXT + attachment	Moodle e-learning	MaxWhere
EO	72	55	45
HDO	20	9	4

Table 2
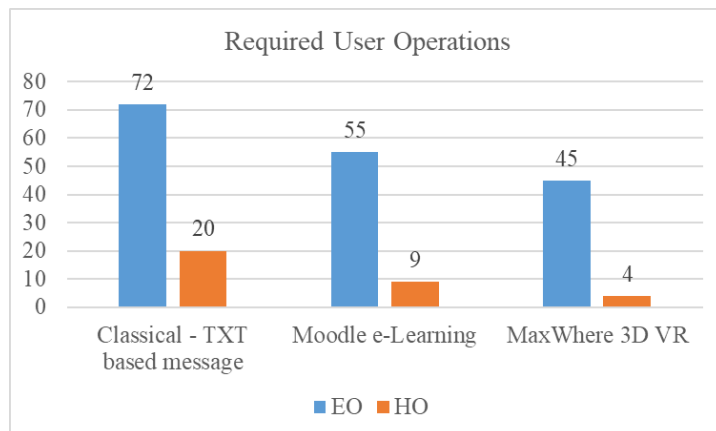
5   New User Capabilities Introduced by MaxWhere as Viewed from 2D Work Environments

The empirical observations provided above strongly suggest that MaxWhere can provide huge benefits over classical approaches in terms of user workload, ease of access to and comprehensibility of novel information.

In this section, the principle of Backward Analysis is adopted in order to examine how the operations that can be carried out in the MaxWhere 3D VR platform can be emulated in a strictly 2D environment.

It is shown in this section that MaxWhere provides a number of new user capabilities which are not available in classical 2D work environments – for the purposes of this study, in the Windows operating system. This fact alone motivates the application of the Backward Analysis principle, to see how the everyday use of MaxWhere can at least be emulated on 2D platforms. This approach has value in the sense that it matters whether one chooses to look at how a workflow carried out in 1D MS DOS can be carried out using Windows, or whether one instead chooses to look at how a workflow carried out using Windows could be carried out if only MS DOS were available (clearly it may be the case that the functional capabilities of Windows form a superset of those of MS DOS; and while in the case of Forward Analysis, we might conclude that a task can be carried out more easily in Windows, in the case of Backward Analysis it may also be additionally possible to conclude that it is nearly impossible to conceive of how a mundane task in Windows could be carried out on older, 1D platforms).

The comparative analysis performed in this section focused on the user operations required in order to carry out the digital workflow considered in the previous section.

First, we consider the possibilities provided by MaxWhere which support information processing (i.e. access to and comprehension of information).

Capabilities for Digital Guidance and Analog Overview

In MaxWhereben, the workflow under consideration can be carried out through the following operations:

1.   Open e-mail:4 EO + 1 HDO

2.   Download pack file: 3 EO +1 HDO

3.   Open MaxWhere space: 2 EO +1 HDO

4.   Load pack file: 4 EO +1 HDO

        Total: 13 EO + 4 HDO

5.   Access ordered overview of digital elements

A key advantage of the MaxWhere 3D VR platform over other solutions is its maximal support for Digital Guidance. This means that when loading a pack file, users also automatically get access to a logically ordered presentation of the digital content belonging to the workflow. As a result, all slides, PDF files, videos, webpages and questionnaires can be presented in the order that best facilitates the completion of the workflow. It can hardly be overemphasized that in this case, users have to perform **zero** operations to display the content. As a matter of fact, all operations that have to be carried out have to do with moving the mouse and performing clicks once in a while in order to focus on various digital elements that are laid out in 3D space and in thematic groups. The way in which these mouse operations function can be characterized as a capability for analog overview, meaning that it provides a capability for free-flowing navigation as opposed to enabling only discrete jumps in space. All of this helps users in comprehending complex digital content in its full breadth and is well suited for supporting new generations of digital natives in multitasking.

Besides greatly simplifying the necessary user interventions, MaxWhere also represents a huge improvement (compared to 2D operating systems) in the sharing of information, by alleviating the need for constant switching / alternation between application windows that are situated side by side (or, from most users' perspective, behind one another).

Figure 1 serves to highlight the above observations, by showing how the information that is needed at any given time can be quickly obtained as a result of the spatial arrangement of the content.

In terms of content organization, the workflow consisted of 4 well-separated logical groups of digital content.
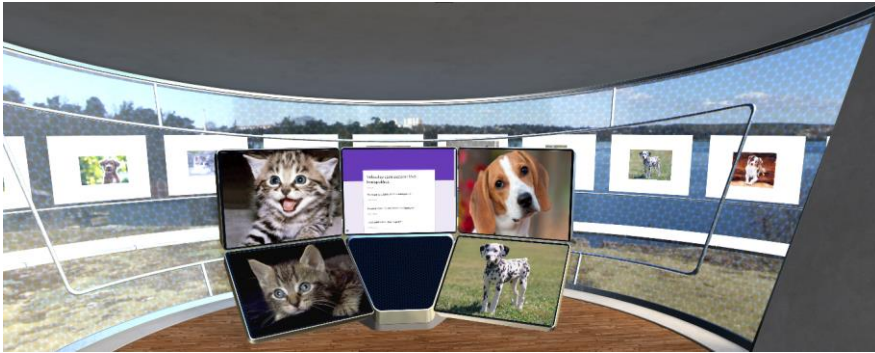

Figure 1
Information sharing in MaxWhere

1. Digital Content: PPT slides (14 slides) + questionnaire

Figure 2
PPT slides and corresponding questionnaire in MaxWhere

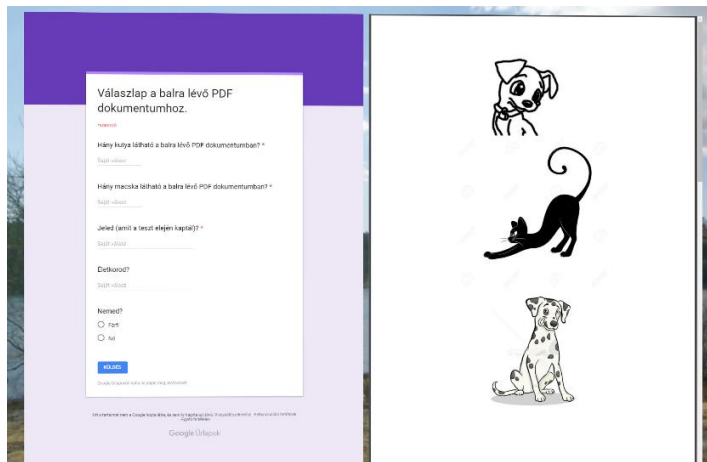2. Digital Content: PDF + questionnaire

Figure 3
PDF file and corresponding questionnaire in MaxWhere

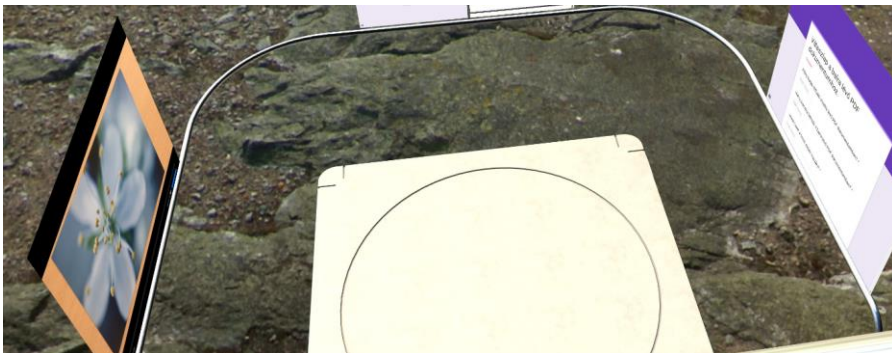## 3. Digital Content: video + questionnaire

Figure 4
Video file and corresponding questionnaire in MaxWhere

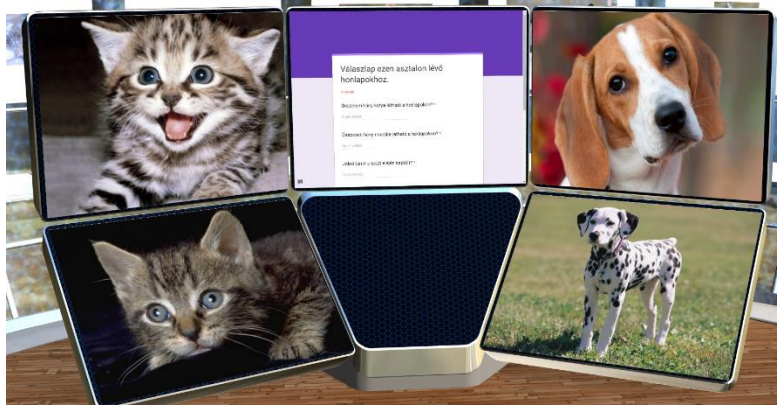## 4. Digital Content: web pages + questionnaire

Figure 5
Web pages and corresponding questionnaire in MaxWhere

Following the visual overview of content arrangement, we return to the quantitative assessment of user workload that would be associated with the same workflow in a 2D operating system (in our case, Windows), carried out in a similarly efficient and effective way (i.e. by making use of the limited possibilities of the OS for 2D spatial arrangement of windows to fill out the questionnaires correctly). In the assessment, attention is given not only to the elementary, complex and high distraction / high alternation operations considered earlier (though such operations, especially the high alternation and ordering operations will be of particular interest), but also to the effects of the availability or non-availability of Digital Guidance and Analog Overview capabilities.

For the sake of clarity, the quantitative assessment is broken down into parts based on the digital content types introduced in the earlier figures. The grand total of the assessment will also be provided in terms of elementary operations for better interpretability.

1. Comprehensible ordering of digital content in a 2D operating system:

    1 NBEO (opening of test questionnaire) = 1.5 EO

    14x (once per slide) – cycle

    1 NBEO (opening of PPT file) = 1.5 EO

    2 EO (selection of reading view)

    1 OO (setting of window size and location within ordering) = 5,5 EO

    End of cycle

    2 HAO = 2*1.5 EO and 2 CL

    Total number of operations with direct results: 1.5EO+14*9 EO+3 EO + 2CL

Operations carried out without direct results: 1OO = 5,5 EO

Total: 136 EO + 2 CL

The test questionnaire sent as part of a Google Document is not displayed while its window is being resized. Therefore, its ordered presentation does not improve the comprehensibility of the digital content. It is important to note that when ordering PPT slides that contain many slides in such a way, the recognizability of the information is greatly reduced. Therefore, the benefits of the ordering are partially eclipsed. The comprehensibility of PPT-related information and test questionnaire was quantified based on the following considerations: a total number of 15 digital elements were to be displayed, however, the Google Drive questionnaire could not be visualized with the aspect ratio available, hence only 14 PPT slides could be presented at the given time. Thus, the Analog Overview capability of the software in terms of the first (PPT-related) digital content was 93% (14 / 15).

User time ~ 6 minutes

The PPT file was opened in around 15 seconds.

The resizing of each PPT slide and its placement in the appropriate location on the screen took experienced users about 25 seconds on average. For 14 slides, this resulted in a total time of 5 minutes and 50 seconds.

2. Comprehensible ordering of digital content in a 2D operating system:

2 NBEO (opening of PDF file and test questionnaire) = 2*1.5 EO = 3 EO

1 OO (setting of- window size and location within ordering) = 5,5 EO

2 HAO – alternation between PDF file and Google Drive = 2*1.5 EOésCL= 3 EO és 2 CL

1 OO – positioning of Google Drive test questionnaire = 5,5 EO

Total number of operations with direct results: 17 EO + 2 CL

Total: 17 EO + 2 CL

In this case, MaxWhere's Analog Overview capability could be emulated by the user scrolling through the test questionnaire.

User time ~ 1 minute

The PDF file was opened in around 20 seconds

Resizing and positioning of PDF file took around 20 seconds

Resizing and positioning of Google Drive test questionnaire took around 20 seconds

3. Comprehensible ordering of digital content in a 2D operating system:

    2 NBEO (opening of video file and test questionnaire) = 2*1.5 EO = 3 EO

    1 OO (setting of window size and location within ordering) = 5,5 EO

    2 HAO – alternation between video file and Google Drive = 2*1.5 EO + 2 CL = 3 EO+ 2 CL

    1 OM – positioning of Google Drive test questionnaire = 5,5 EO

    Total number of operations with direct results: 17 EO + 2 CL

    Total: 17 EO + 2 CL

    In this case as well, MaxWhere's Analog Overview capability could be emulated by the user scrolling through the test questionnaire.

    User time ~ 55 seconds

    The video file was opened in around 15 seconds

    Resizing and positioning of video file took around 20 seconds

    Resizing and positioning of Google Drive test questionnaire took around 20 seconds

4. Comprehensible ordering of digital content in a 2D operating system:

    5 NBEO (opening of 4 webpages and the test questionnaire) = 5*1.5 EO = 7,5 EO

    4 OO (setting of window size and location within ordering) = 4* 5,5 EO = 22 EO

    1 OO (setting of test window size and location = 5,5 EO

    1 HAO (switching to the test) = 1.5 EO+ CL

    Total number of operations with direct results: 36,5 EO + 1 CL

    Total: 36,5 EO + 1 CL

    User time ~ 1 minute and 40 seconds

    The webpages were opened in around 4x5 = 20 seconds

    Resizing and positioning of webpages took around 4x15 seconds = 1 minute

    Resizing and positioning of Google Drive test questionnaire took around 20 seconds

    Remark: The 4 webpages could be placed on a single screen only if the physical size of the display was sufficiently large. The test questionnaire itself had to be filled out separately.

As they were filling out the test questionnaires, users had to perform at least 8 high alternation operations. If at any time the users forgot the following question and had to return to the test form, this resulted in more context switches. In the worst-case scenario, a total number of 32 high alternation operations had to be performed for the 4 test questionnaires.

The results of the quantitative investigation are summarized in Table 3.

Table 3

User workload	2D platform (Windows)	MaxWhere 3D VR platform
Elementary operations	**206,5**	**0**
Cognitive Load	**7**	
Analog Overview effectiveness (%)	**98%**	**100%**
Time spent to guarantee comprehensibility	**575 s = 9 minutes 35 seconds**	**0 s**

6 Radically New User Capabilities Introduced by MaxWhere

Among MaxWhere's capabilities not considered in this paper, it is worth mentioning a few that can in addition be of particular use when the goal is to improve learning and working processes:

1. Ability to handle 3D objects:

    a. Visualization of 3D objects.

    b. Presentation of 3D simulations.

2. Possibility of modifying / moving the view in special ways not supported by 2D graphical environments:

    a. Analog rotation around the camera view.

    b. Analog orbiting around selected objects as center points.

    c. Analog "swimming"/"flying" in 3D space.

    d. Analog zooming towards and back from specific objects.

The key advantages of the MaxWhere 3D VR platform as an educational tool are highlighted in Table 4.

Table 4

	Offered by MaxWhere 3D VR platform	Offered by 2D operating systems	Can it be implemented in 2D and to what extent?
Visualization of 3D objects	yes	no	no
3D simulations	yes	no	no
Zoom-in and zoom-out at a wide range of resolutions	yes	no	no
Analog movements similar to physical movement using the mouse	yes	no	Partly through key combinations, slow solution
Digital Guidance without added explanations	yes	no	With much added time and energy
Analog Overwiew	yes	no	With much added time and energy
Multitasking	yes	no	With much added time and energy
Access to digital content independent of time and space	yes	partly	Through the use of a separate software environment

Conclusions

Based on the comparative study presented in this paper, it can be concluded that the MaxWhere 3D VR platform allows for information to be shared and understood more quickly than when using its 2D counterparts. Further, these advantages of MaxWhere are multiplied when the goal is to carry out a workflow in the most time-effective way possible based on the shared content. MaxWhere's capabilities towards helping knowledge sharing and comprehension in education are much broader in scope than the capabilities of today's leading 2D graphical user interfaces. The operations that can be and are carried out in MaxWhere during everyday use of the platform are highly time-consuming at best (and sometimes nearly impossible to carry out) using traditional 2D solutions. MaxWhere represents a 30% improvement in number of elementary operations needed to be carried out, and an 80% improvement in number of machine operations needed to be carried out when compared with its 2D alternatives.

References 10 pt

[1]   Baranyi P. and Csapo A. and Sallai G. (2015): Cognitive Infocommunications (CogInfoCom), Springer International Publishing Switzerland,   p.   191   (978-3-319-19607-7, http://www.springer.com/us/book/9783319196077#aboutBook

[2]   Baranyi Infocommunications, (ISSN 1785-8860) P. and Csapo Acta A. Polytechnica Hungarica (2012): Definition and Vol Synergies 9, of No 1. pp. 67-83 Cognitive

[3]   I. Horvath, "The edu-coaching method in the service of efficient teaching of disruptive   technologies,"   Springer   book   chapter,   Cognitive Infocommunications and computing, in the Series of Topics in Inetelligent Engineering and informatics. Accepted

[4]   M. Akçayır és G. Akçayır, „Advantages and challenges associated with augmented reality for education: A systematic review of the literature," Educational Research Review, pp. 1-11, 2017

[5]   L. J. Ausburn és F. B. Ausburn, „Technical perspectives on theory in screen-based virtual reality environments: Leading from the future in VHRD," Advances in Developing Human Resources, pp. 371-390, 2014

[6]   E. Z. Borba és M. K. Zuffo, „Advertising Perception with Immersive Virtual Reality Devices," in IEEE Virtual Reality (VR) 2017

[8]   I. Horváth, „Innovative Engineering Education in the Cooperative VR Environment," Cognitive Infocommunications (CogInfoCom) 2016 7th IEEE International Conference, pp. 359-364, 2016

[9]   S. Jang, J. M. Vitale, R. W. Jyung és J. B. Black: „Direct manipulation is better than passive viewing for learning anatomy in a three-dimensional virtual reality environment," Computers & Education, pp. 150-165, 2017

[10]   Z. Kvasznicza:" Teaching electrical machines in a 3D virtual space", 8th IEEE International Conference on Cognitive Infocommunications, Debrecen, 2017

[11]   P. Galambos at all.: "Future Internet-based Collaboration in Factory Planning", Acta Polytech. Hung. 11. 7, 2014

[12]   B. Lampert, A. Pongrácz, J. Sipos, A, Vehrner, I. Horváth: "MaxWhere VR-learning improves effectiveness over clasiccal tools of e-learning, Acta Polytech. Hung. Accepted

2D Advertising in 3D Virtual Spaces

Borbála Berki

Széchenyi István University, Multidisciplinary Doctoral School of Engineering Sciences; Egyetem tér 1, H-9026 Győr, Hungary
berki.borbala@sze.hu

Abstract: 2D advertising in VR is more effective than in the classic banner ad format, our study confirms that ads in VR evoke better memory, namely more participants remembered the advertisement displayed in VR than the web-based ad. Advertising in virtual realities does not have to mean a virtual space exclusively dedicated to the promoted product. It can be a 2D ad inserted in the virtual space. It differs from the classic web-based ads, as it is not inserted in the content of a webpage, but stands alone in a virtual space. In this paper, we show a comparison of the classic banner ads, and 2D ads placed in a 3D virtual world. The effectiveness of the VR advertisement is higher than the classic web-based ads. In our experiment 22 people were involved. As the virtual space, we used the MaxWhere virtual platform, where the participant's task was to read four online articles. In one condition four banner ads were placed on each webpage, in the other condition, the advertisement was placed in the virtual space. Then, they answered questions about the article and the advertisement.

Keywords: virtual reality; MaxWhere; advertisement; internet advertising; marketing

1   Introduction

Throughout history advertising has appeared on various platforms to reach wide audience and to obtain attention to the promoted product. From the sales messages written on Egyptian papyrus, through the 19th Century's image with slogan style, advertisements have changed in many different ways, to find the most efficient forms to influence the consumers. Nowadays, the TV ads and online advertising are the focus of the advertising industry. As the interest in virtual realities increases, advertisers tend to focus on this new media to exploit its potentials.

1.1   Classic Web-based Advertising

Along with the increase in the number of Internet users around the world, online ads became a more and more important part of the advertising industry. In the first half of 2017, the digital advertising revenues in the United States reached $40.1

billion, which means a unique 22.6% growth in one year [1]. Correspondingly, we can find several advertisements in almost every kind of website. For example, when you read an online newspaper you can see banner ads at the top and/or at the bottom of the article or maybe at the sidebar or they use pop-ups in a new window. You can also meet with short commercials wedged in between two videos. Various forms of advertisements appeared along with the growing of the internet, but here is a general definition from Louisa Ha for the online advertising: Deliberate messages placed on third-party websites including search engines and directories available through Internet access [2]. In this paper, we focus on banner ads and do not cover the topics of social media ads.

All form of online advertising spring from print advertising, therefore they have a lot of similarities in terms of arrangement, text and graphic design. However, online advertising pushes the advantages of the digital world and supplements the still pictures with hyperlinks, various animations and sound effects to capture the attention of the consumers. One of the most common formats of online ads is banner ads, where the advertiser pays for space on one or more online pages to display a static or linked banner or logo [1]. These ads are examined in various studies [2] [3] [4] [5]. People have different attitudes to different ad formats, but it seems that consumers attribute the highest information factor to banner ads, and the highest overall positive attitude [4].

The effectiveness of an advertisement also depends on the media credibility and content congruence with the webpage. The online market requires consumers to make decisions about products without commonly used first-hand, physical experiences. Therefore, credibility has a greater role in online marketing than in traditional advertising industry. As advertisements never appear alone, they are embedded in non-advertising content; their reliability is judged on the base of the website and advertiser credibility. Banner ads on credible sites produce a more positive advertising outcome. The content compatibility means that the advertised product matches the website content thus consumers find it more interesting and useful [6]. Yet, this overall positive attitude is not toward the ad itself, but toward the brand and purchase intent [7].

As can be seen, the classic web-based advertisement is a widely examined subject since not only academics but practitioners are also concerned to find the most effective methods. Classic web-based advertisements share some common features, including embeddedness, which can be interpreted as they are always breaking the content, even the related ones. This can be a disadvantage as it can irritate the users and evokes ad avoidance.

Irritation is another contributing factor in advertising effectiveness. It is important to realize that advertisements can evoke a strong resistance from users as they typically try to block or just ignore them. When an individual is attempting to carry out a specific goal, the appearing advertisement is perceived as an aggravation, particularly by those users who understand the online persuasion

strategies (larger sizes, animations) [8]. Banner ads are generally displayed on the periphery; they do not interrupt directly the activity of web viewers. In contrast, pop-up ads are one of the most irritating web-based advertisement forms. According to the Interactive Advertising Bureau's definition, pop-up ads (or formally interstitials) are advertisements that appear in a separate window which automatically loads over an existing content window [1]. Therefore, users are forced to react to these commercial messages. For this interruption, the individuals can respond cognitively, affectively or behaviorally, which can be both positive and negative for the advertiser. A positive effect could be that because of this unexpected interruption, users will have greater processing and increased memory for the pop-up advertisement [6]. On the other hand, interstitials cause a negative attitude formation which can lead to the avoidance of the ads [9].

Why do consumers find only some advertising irritating and not all of them? The answer is the so-called intrusiveness: the interruption of editorial content [9]. This sounds a bit controversial, as the first objective of advertising is to get noticed, to be as salient as possible, thus interruption of editorial content should be a key characteristic of all advertisement. Whereas ads were related to the web user's task, they were perceived less intrusive [9]. The evoked negative attitudes and reactance could result in ad avoidance and feeling of irritation. Reactance theory is a social psychological theory which describes the human behavior as a response to the perceived loss of freedom in an environment. When an individual feels that his opportunities or freedom narrows, the reactance helps to re-establish the control of a situation and a sense of freedom [10]. This reactance is also present in advertising. Consumers actively interpret advertisements and react against the threats of persuasion. As ads are perceived less intrusive when related to the web user's task, the same manner, the more value is perceived in an ad (more information or entertainment) and it is evaluated as less intrusive. On the other hand, keep in mind that most consumers do not see high entertainment or information value of web-based advertisements. [6]. Avoidance is not a necessary consequence of an intrusive advertisement, the degree to which an ad is judged to be intrusive is more important [6]. The degree of this reactance depends on the importance of the threatened behavior, the severity of the threat, whether the threat affects other freedoms and whether the person ever actually enjoyed that freedom [10].

As described previously, advertisers tend to find new ways and new media to deliver their commercial messages to potential consumers. Virtual reality is a fast-growing field, where advertisers are trying to find more effective ways of advertising.

1.2   MaxWhere VR

The development of operating systems has a huge impact on the effectiveness of using a computer. From DOS, operated by text-based commands to the GUI (Graphical User Interface), like Windows OS, the ease of use evolved remarkably fast. The use of visual metaphors instead of the linguistic commands allowed more intuitive interactions with computers for a wider range of users. Displaying graphics, color pictures, videos became an essential feature; as did the option of multitasking by switching between different windows. The biggest advantage is that cognitive load was reduced during performing a task. The MaxWhere VR environment attempts to make a further step in this process to expand intuitive interactions from two dimensions to 3D. Along with the transformation of operating systems, information pressure is also increasing. To digest this incredible amount of data we can benefit from the possibilities of the 3D visualization, which enable an even more intuitive interaction with any data, even with advertisements. Fundamentally advertisements are visual constructs, but can take advantage of 3D too. For example, a better memory of ads if they are placed in the space or users can create expectations about ads.

A similar change can be observed between 2D and 3D browsing. In a classic 2D, browser tabs cover each other, tab organizing is uneasy and all the tab has the same size irrespective of its content. In contrast, browsing in 3D can create a transparent and clear overview of all tabs, users can organize and group the tabs according to their desires. The tabs can have different size; a bigger tab for a calendar with a month view and a narrower for a chat tab. In 3D the tabs do not cover each other (Figure 1).

Figure 1
Grouping of webtables in MaxWhere VR

Advertisements can benefit from a context-based placement [6], which can be implemented more effectively in a 3D environment. In shared virtual spaces they can be more personalized according to the target group. If everyone in the group could be interested, the ad is placed in a big webtable in the central part. If it is interesting for just one individual of the group then it could be displayed on a smaller personal advertisement area.

The most important differences between classic web-based and VR advertisement are that they differ in both modes of delivery and in the target audience. While the web advertisements have more written parts and designed for those who run a content-oriented information search, in a virtual environment, the users are more image and entertainment-oriented [11].
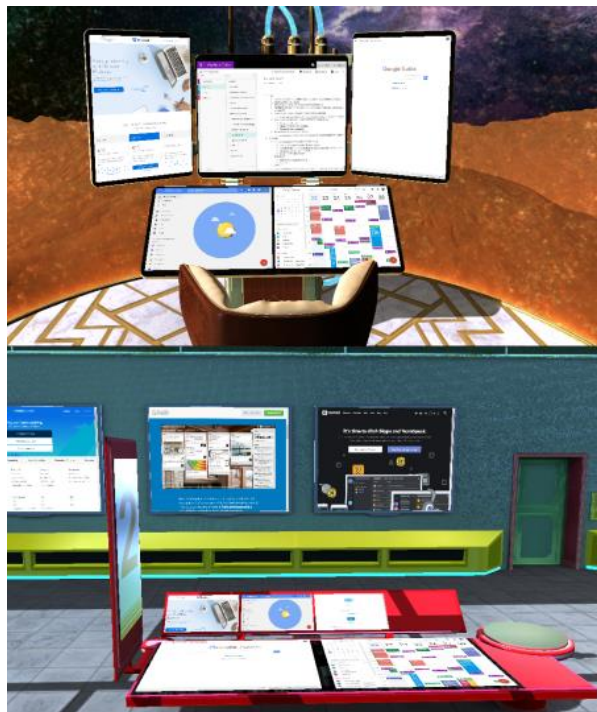

Figure 2
Webtables in different MaxWhere spaces

In our experiment, we used the MaxWhere VR engine. This is an innovative desktop based VR environment that integrates the opportunities provided by web technologies (HTML5, JavaScript, CSS) and 3D graphics with spatial metaphors. MaxWhere was developed by Mistems Ltd., with support in content creation from the Széchenyi István University. A great advantage of this environment is the user-friendly solutions, like the simple navigation in the space with a keyboard,

and the easy content upload, and management. All content is displayed on webtables, which are mostly landscape format with the widely used 4:3 proportion. On these smarttables, the user can display any web pages, cloud-based applications, real-time communication programs and PDF documents, images, videos and audio files from the PC (Figure 2). The user only writes the address to the address bar of the webtable. In a word, in this VR environment, the Internet literally surrounds the user [12] [13].

In the field of the VR-based education, along with other software, the MaxWhere VR has been used in scientific research [12] [13] [14] [15] [16] [17] [18] [19] [20], and also used for virtual reconstruction of historical buildings [21].

We used the MaxWhere VR in our experiment because it enables to place the advertisements in the space, like in a real world, they stand alone and they are not embedded in content, like in web pages.

2   Aim of the Study

The aim of our study was to compare the advertisement effectiveness of 2D ads in VR and in classic web-based form. We suppose that advertisements placed in a virtual space are more effective than ads placed on websites. As a measure of the effectiveness, we have taken the memory performance of the subjects, more precisely the number of participants who could recall the advertisement. To test our hypothesis we used a between-subject design; namely we divided the participants into two group to test simultaneously the ad effectiveness of advertisements in VR and in the classic web-based form. Our hypothesis was that in the VR group more individuals will remember that they have seen an advertisement than in the other group.

2.1   Contrast to Other VR Advertising Research

Advertisers use different methods to evoke the attention of customers. A widespread VR advertising method is to create virtual experiences, where users can get a kind of first-hand information about the product, before the acquisition [26]. As an illustration, we can take destination marketing, as a promotion tool, advertisers try to encourage real-life tourism visits by offering VR experiences. In this field, the visual imagery is essential to focus attention on to a special destination [27]. Another type of VR marketing method is the avatar-based advertising, where an attractive avatar gives information about a product or helps to choose an item in a virtual store. The effectiveness of these different advertisements depends on several factors, for example, the physical attractiveness of a spokes-avatar is a mediating factor [25]. But what are the most important

success factors in virtual worlds? According to Tikkanen and his colleagues, the value for customers, the community management, and highly interactive applications can be the biggest advantages [26].

Three dimensional is a key feature in virtual realities, which has been already established by advertisers. They realized that in an online shopping environment the 3D images are more persuasive for any customer. There are of course some differences regarding the type of product: in the case of geometric products (e.g.: watch) there is an even greater effect of 3D than in a case of a material product (e.g.: jacket) [27] [28]. The user's individual characteristics are also an important factor: if a person has a high need for touch, to decide, this user is less impressed by the 3D version of a jacket, than another consumer who does not feel this need to touch a product before purchasing [27]. Another characteristic of the 3D display is that it enhances the sense of presence in a virtual space and influence the product knowledge and purchase intention. This greater sense of presence is irrespective of the type of product (geometric or material) [29]. These examples are part of informational advertising, where the emphasis is on the details and knowing the product.

In contrast, the transformational advertisements are those, in which the emphasis is on the experience of using the product. For example, an advertisement showing a person feeling adventurous and lively when using a product. This type of ad influences the attitude toward the advertisement and the brand. These transformational ads were found more efficient when they were shown in 3D via a cardboard-type head-mounted device than showed in 2D [29]. In destination marketing, the VR-based advertisement generated more emotions toward the destination and the individuals found it more engaging [23].

The exposure effect is a well-known psychological effect which means that customers misattribute the increase of accessibility of a brand as liking of the brand. In other words, if an individual is exposed to an advertisement or a product, they see it regularly, they are going to interpret this, as they like the product [30]. Another advantage of product placement is that it could enhance the feeling of realism of the virtual space. Correspondingly, there are more ads for real products than for fictitious products in a video game, as this also can increase the sense of presence in this alternative reality [11]. Another advantage of the product placement is that it is less obtrusive. Namely, the media users are less likely to develop the above-mentioned psychological reactance toward the ad [6]. On the contrary, when product placement is compared with billboard placement in virtual realities, the object and brand recall for products advertised on billboards were greater than the product placement [31].

The presence, the feeling of immersion is the individual subjective feeling of being in the displayed virtual world. This presence could be a mediator between the ad format (2D or 3D) and the advertisement effectiveness [27] [32]. This

presence and high immersion also could evoke the affective engagement of the users [31].

The type of VR device also plays an important role in the effectiveness of an advertisement. A head-mounted device or a CAVE (cavern automatic virtual environment) can create a higher sense of presence as they are a more immersive system than a desktop monitor but this doesn't mean that the advertising is more efficient there. Moreover, better memory recall and more efficient brand advertising result were found in the case of a VR displayed on a desktop monitor. Another interesting remark of this research is that in the immersive system the location of an advertisement was more important than its actual size [33].

To sum up prior researches focused on the effects of the 3D visualization of advertisements [26] [27] [28], or virtual prototypes [11] [31], but rarely focused on the comparison between the classic web-based and VR-based 2D advertisements.

3   Methods

3.1   Subjects

In our experiment 22 individuals participated (18 male, 4 female; mean age: 23.45 years (SD:2.26)). All subjects had a basic knowledge of the MaxWhere software. Individuals participated voluntarily in the study. The whole experiment was conducted in Hungarian, all participants were native Hungarian speakers. Twelve participants were in the VR group, ten in the classic web-based ad group.

3.2   MaxWhere Space

To compare the efficiency of the advertisement in virtual spaces and the advertisements on web pages, we used the MaxWhere VR environment because it enables displaying both web pages and advertisements. The MaxWhere Environment 1.4.x software [34] is developed for visualization of 3D graphical templates and user contents. The 3D graphical templates are integrated parts of the software. All used computers matched the system requirements of the MaxWhere software: MS Windows 7 or newer (system memory: min. 8 GB; min. free storage: 2 GB, min. GPU: Intel HD Graphics 4400 or newer), MacOS System (memory: minimum 8 GB, min. free storage: 2 GB; GPU: Intel Iris graphics 6100 or newer).

For the experiment, we used the CogInfoCom17 space (artist: G. Kovács; FIEK program at SZIU), which is a special version of the Lecture Space SZIU. This space was designed for lectures, homework, and presentations. We used the central area, the original personal corner, and information desk to display the contents of the experiment.

3.3   Procedure

We used a between-subject experimental design to compare the results of the participants of different groups. Individuals were randomly assigned to one of the two conditions (classic web-based or VR advertisement). The web-based advertisement group saw four online articles in the central area of the virtual space. All articles contained a banner ad on the right side of the page. The same advertisement on all four sites (Figure 3). In the two conditions, the total area of advertisements was equaled.

Figure 3
Classic web-based advertisements

The individuals in the VR advertisement group saw the same four articles with the same spatial layout, but without the banner ads. For this group, the advertisement was displayed on a separate webtable, among the four articles (Figure 4). The surface of the advertisements was the same in both conditions.

Figure 4
VR based advertisement

During the experiment, the participants filled an online questionnaire, placed in the MaxWhere VR space. This questionnaire was the same for every individual regardless of the experimental group. The questionnaire contained all the instructions to fulfill the experiment. On the first page, they read a short description of the whole task (without any references to the aim of the study) and with a click, they indicated their willingness to participate in the study. Then they had to answer general questions about the four articles displayed on the central area. Then they had to import another pack (pack is an archive file that can be exported from the MaxWhere environment and contains copies of and/or references to User content as well as an optional list of 3D positions and orientations pertaining to the 3D template [34]). Then all the previous content (except for the questionnaire) were replaced with pictures. For checking whether the participants made this import, the next question was about the picture. Then they were asked if they remember any advertisement in the virtual space. If they answered yes, they were asked to write as many details as they can about the advertisement (brand, product, colors, slogan, etc.) and answered some basic demographical question.

Figure 5
Online questionnaire inserted in the VR environment for all participants

4   Results

In the statistical analysis we included only the results of those participants who answered positively to the questions about the articles, therefore 22 individuals' results were analyzed, from the original 27 participants.

Our hypothesis was that those individuals will recall the advertisement, who have seen it in the VR space, and not in the articles. To compare the memory performance of the individuals in the two group we used the Fisher's Exact Test. The null hypothesis of the test was that the proportion of the remembering participants in the two group are equal. At the cut point of 0.05, we want to test whether any observed difference of the proportions is significant. The results indicated a significant difference in the memory performance between the VR group with a prevalence of 91.67% (11/12), compared to 40% (4/10) in the classic web-based group (p=0.02). Which means that we can reject the null hypothesis, and assume that the proportion of the individuals who remember the advertisement is different in the two group.

The free recall test (Table 1) revealed that if an individual remembered the advertisement, then most of them could recall the promoted product and the brand. They also tried to recall the colors of the advertisement, but mostly they attributed the color of the brand to the color of the product. In this comparison, there was no statistically significant difference between the performance of the VR based and web-based group.

Table 1
Results of the free recall and the corresponding p-value of the Fisher's Exact Test

	VR	Classic web-based	p-value of Fisher's Exact Test
Ad	11/12	4/10	0,02
Product	10/12	4/4	1
Brand	9/12	¾	1
Colors of the ad	4/12	0/4	0.52
Color of product	0/12	0/4	1
Slogan	1/12	0/4	1

5   Discussion

Our aim was to compare the classic web-based and VR based 2D advertisements, its effectiveness. According to our results, if a 2D advertisement is placed directly in a 3D virtual space, users are more likely to recall the advertisement and the advertised product, compared to an advertisement inserted in a website. If a participant could recall the advertisement, the results of the free recall test do not show any differences in the recall of its details. This can be the effect of the location of the ads. People tend to block and avoid ads in everyday life. Accordingly, they could learn not to pay attention to the banner ads, displayed on many different websites. However, in the VR advertisement, the ad is placed between the different contents and not inside them and participants did not use this avoiding behavior. To sum up, this different layout could increase the effectiveness of a 2D advertisement. The recall performance in the VR advertisement group resembles the billboard advertisements effectiveness in the experiment of Grigorovici and Constantin [31], where they found that billboard advertisements in a low arousing 3D virtual world are more effective than product placements.

Immersion and presence are key factors in the research of VR. The feeling of presence influences how ad format (2D or 3D) effects advertising effectiveness [27] and high presence increases the recall of advertisements [32]. In our experiment participants in both groups used the same VR environment, then the feeling of immersion and presence probably do not differ in the two groups. We did not measure the presence directly thus this limits our conclusions. The difference between the performance in the two group is not because of the novelty effect of the virtual space, or the feeling of the presence, but the different layout of the two advertisements.

These results show, that advertisers do not have to design an own virtual space to create an experience with the product like in transformational marketing, but with the classic banner ad style advertisement, they can reach a more effective advertisement if they place it in a 3D virtual space instead of a classic website. Moreover, the media credibility which is a crucial question in online marketing [7], is already given, as the users already have chosen the software and all the contents are selected by themselves, presumably they evaluate as credible sites.

For further researches, we would like to use more Likert-scale questions, for example, to indicate the degree of the strength of the memory of advertisement or to indicate the level of irritation when they see these ads. Future research should investigate whether these effects appear in the case of animated, pop-up, and video ads too.

Conclusions

2D advertising in VR is more effective than in the classic banner ad format, our study confirms that ads in VR evoke better memory, namely more participants remembered the advertisement displayed in VR than in the web-based ad.

Acknowledgement

References

[1]   Interactive Advertising Bureau, "IAB Internet Advertising Revenue Report," December 2017 [Online] Available: https://www.iab.com/wp-content/uploads/2017/12/IAB-Internet-Ad-Revenue-Report-Half-Year-2017-REPORT.pdf. [Accessed 02. 01. 2018.]

[2]   L. Ha, „Online Advertising Research in Advertising Journals: A Review," *Journal of Current Issues & Research in Advertising,* pp. 31-48, 2008

[3]   H. Li és J. L. Bukovac, „Cognitive Impact of Banner Ad Characteristics: An Experimental Study," *Journalism & Mass Communication Quarterly,* pp. 341-353, 1999

[4]   K. S. Burns és R. J. Lutz, „The Function of Format: Consumer Responses to Six On-line Advertising Formats," *Journal of Advertising,* pp. 53-63, 2006

[5]   W. Flores, J.-C. V. Chen és W. H. Ross, „The Effect of Variations in Banner Ad, Type of Product, Website Context, and Language of Advertising on Internet Users' Attitudes," *Computers in Human Behavior,* pp. 37-47, 2014

[6]   S. M. Edwards, H. Li és J.-H. Lee, „Forced Exposure and Psychological Reactance: Antecedents and Consequences of the Perceived Intrusiveness of Pop-Up Ads," *Journal of Advertising,* pp. 83-95, 2002

[7]   S. M. Choi és N. J. Rifon, „Antecedents and Consequences of Web Advertising Credibility: A Study of Consumer Response to Banner Ads," *Journal of Interactive Advertising,* pp. 12-24, 2002

[8]   S. Rodgers és E. Thorston, „The Interactive Advertising Model: How users Perceive and Process Online Ads," *Journal of Interactive Advertising,* pp. 41-60, 2000

[9]   L. Ha, „Advertising Clutter in Consumer Magazines: Dimensions and Effects," *Journal of Advertising Research,* pp. 76-85, 1996

[10] J. W. Brehm, A Theory of Psychological Reactance, Oxford, England: Academic Press, 1966

[11] P. G. Lindmark, „A Content Analysis of Advertising in Popular Video Games," ETD Archive, 2011

[12] I. Horváth, „Innovative Engineering Education in the Cooperative VR Environment," in *7th IEEE International Conference on Cognitive Infocommunications (CogInfoCom)*, Wroclaw, 2016

[13] I. Horváth, *Teaching Disruptive Technologies in a Virtual Educational Environment Using the Edu-Coaching Method* (Ph.D. Dissertation) 2017

[14] I. Horváth, „Disruptive technologies in higher education," in *th IEEE International Conference on Cognitive Infocommunications (CogInfoCom)* Wroclaw, 2016

[15] G. Csapó, „Sprego virtual collaboration space," in *8th IEEE International Conference on Cognitive Infocommunications (CogInfoCom)* Debrecen, 2017

[16] G. Csapó, „Sprego virtual collaboration space: Improvement guidelines for the MaxWhere Seminar system," in *8th IEEE International Conference on Cognitive Infocommunications (CogInfoCom)* Debrecen, 2017

[17] K. Biró, G. Molnár, D. Pap és Z. Szűts, „The effects of virtual and augmented learning environments on the learning process in secondary school," in *8th IEEE International Conference on Cognitive Infocommunications (CogInfoCom)* Debrecen, 2017

[18] I. Horváth, „The IT device demand of the edu-coaching method in the higher education of engineering," in *8th IEEE International Conference on Cognitive Infocommunications (CogInfoCom)* Debrecen, 2017

[19] Z. Kvasznicza, „Teaching electrical machines in a 3D virtual space," in *8th IEEE International Conference on Cognitive Infocommunications (CogInfoCom)* Debrecen, 2017

[20] G. Bujdosó, O. C. Novac és T. Szimkovics, „Developing cognitive processes for improving inventive thinking in system development using a collaborative virtual reality system," in *8th IEEE International Conference on Cognitive Infocommunications (CogInfoCom)* Debrecen, 2017

[21] A. Gilányi, G. Bujdosó és M. Bálint, „Presentation of a medieval church in MaxWhere," in *8th IEEE International Conference on Cognitive Infocommunications (CogInfoCom)* Debrecen, 2017

[22] W. W. Kassaye, „Virtual Reality as Source of Advertising," *Journal of Website Promotion,* pp. 103-124, 2007

[23] T. Griffin, J. Giberson, S. H. M. Lee, D. Guttentag, M. Kandaurova, K. Sergueeva és F. Dimanche, „Virtual Reality and Implications for Destination Marketing," in *Tourism Travel and Research Association: Advancing Tourism Research Globally*, 2017

[24] S.-A. A. Jin és J. Bolebruch, „Avatar-Based Advertising in Second Life: the Role of Presence and Attractiveness of Virtual Spokesperson," *Journal of Interactive Advertising,* pp. 51-60, 2009

[25] H. Tikkanen, J. Hietanen, T. Henttonen és J. Rokka, „Exploring Virtual Worlds: Success Factors in Virtual World Marketing," *Management Decision,* pp. 1357-1381, 2009

[26] Y. K. Choi és C. R. Taylor, „How Do 3-dimensional Images Promote Products on the Internet?," *Journal of Business Research,* pp. 2164-2170, 2014

[27] S. Debbabi, M. Daassi és S. Baile, „Effects of Online 3D Advertising on Consumer Responses: the Mediating Role of Telepresence," *Journal of Marketing Management,* pp. 967-992, 2010

[28] H. Li, T. Daugherty és F. Biocca, „Impact of 3-D Advertising on Product Knowledge, Brand Attitude, and Purchase Intention: The Mediating Role of Presence," *Journal of Advertising,* pp. 43-57, 2002

[29] H. Van Kerrebroeck, M. Brengman és K. Willems, „When Brands Come to Life: Experimental Research on the Vividness Effect of Virtual Reality in Transformational Marketing Communications," *Virtual Reality,* pp. 177-191, 2017

[30] R. B. Zajonc, „Attitudinal Effects of Mere Exposure," *Journal of Personality and Social Psychology,* pp. 1-27, 1968

[31] D. M. Grigorovici és C. D. Constantin, „Experiencing Interactive Advertising Beyond Rich Media," *Journal of Interactive Advertising,* pp. 22-36, 2004

[32] C.-J. Keng és H.-Y. Lin, „Impact of Telepresence Levels on Internet Advertising Effects," *CyberPsychology & Behavior,* pp. 82-94, 2006

[33] E. Z. Borba és M. K. Zuffo, „Advertising Perception with Immersive Virtual Reality Devices," in *IEEE Virtual Reality (VR)* 2017

[34] "http://www.maxwhere.com/" [Online] [Accessed 11 October 2017]

Towards a Modern, Integrated Virtual Laboratory System

Tamás Budai, Miklós Kuczmann

Department of Automation, Széchenyi István University
Egyetem tér 1, H-9026 Győr, Hungary
budai.tamas@sze.hu; kuczmann@sze.hu

Abstract: The aim of this paper is to give an overview on virtual and remote laboratory systems and to evaluate current solutions focusing on feasibility and applicability in higher education. Based on the conclusions of this evaluation, a new set of requirements are established against a modern virtual laboratory system. Finally, an overview of state of the art infocommunication technologies, including cognitive infocommunication are presented, which can help create high user experience in the new virtual laboratory environment.

Keywords: virtual; laboratory; system; overview; design

1 Introduction

In the past decade distance learning or e-Learning has matured and now a widely used form of higher education worldwide. Most of these systems only provide a platform to give access to static content like textbooks and other course materials. Nowadays remote and virtual laboratories are also widespread, especially in engineering disciplines [1] [2], where laboratory exercises are playing a key part, helping students to connect lexical knowledge to the real world. These systems provide interactive learning tools which can complement the lectures in the classroom.

In the first part, a short discussion on the benefits and drawbacks of virtual and remote laboratories is presented. The terms remote and virtual are often used inconsistently in literature, therefore a clarification on the definition of these two is necessary [3]. In the second part the overview of the current state of remote and virtual laboratories is presented and a set of example systems are then analyzed to identify key factors that must be taken into account when evaluating a virtual laboratory system. After the overview and evaluation is complete the results and experiences are summarized. Finally, based on these results and by utilizing state of the art infocommunication technologies, a possible new way is proposed on how to implement modern virtual laboratories.

2   Remote and Virtual and Laboratories

The two common types of online laboratory systems are remote and virtual laboratories. From the perspective of the end-users, these look very similar, by providing an online service, which is available via either a website or a client application, but has a very important difference in their backend.
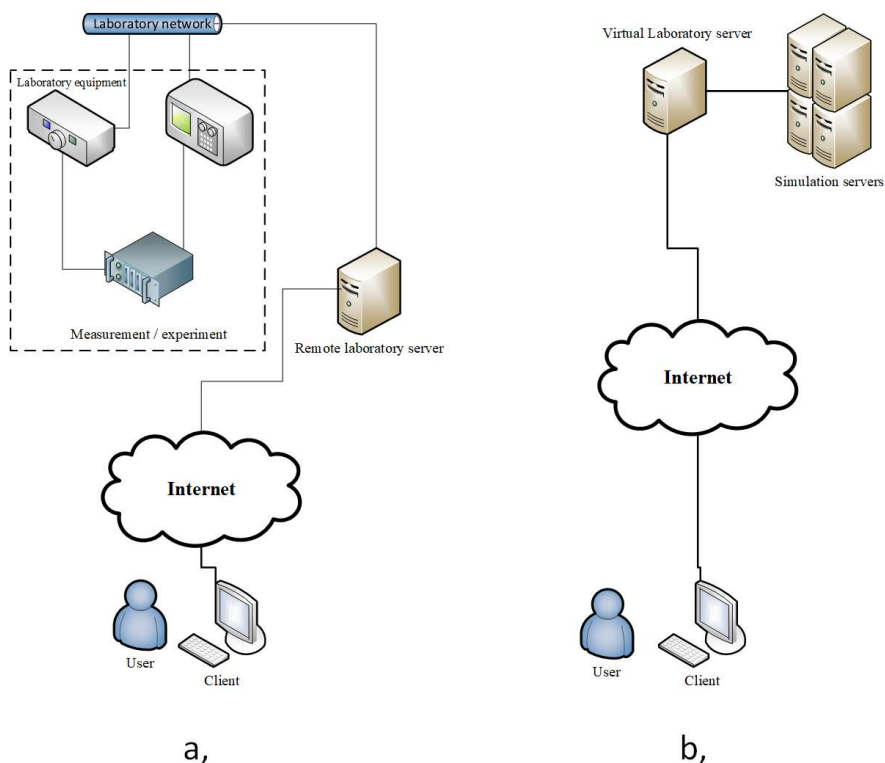

Figure 1

Figure 1 shows the main difference between remote (Fig. 1a) and virtual (Fig. 1b) laboratories. In a remote laboratory all the hardware components (e.g. measurement equipment) physically exist somewhere in the institution. By connecting this equipment to the network, the relevant part of the experiment can be controlled and examined by students from a remote location. On the other hand, in a virtual laboratory all of the above components are entirely simulated by software and can be accessed remotely by users. Distinguishing by their purpose of use, remote laboratories are both used in collaborative research and education. Virtual laboratories on the other hand are mostly suitable for education.

Beside these differences, the two have many common features, therefore for the first time comparison of remote and virtual laboratories will be treated as one category.

2.1   Advantages of Remote and Virtual Laboratories

From the perspective of the university and the professor, a virtual or remote laboratory provides the possibility to break out from the physical constraints of a traditional laboratory and make the exercises available to a wider audience of students. Because all of these labs involve infocommunication technology, it is possible to track student behavior and collect statistics, which can be used to generate useful feedback on the effectiveness of a given virtual or remote laboratory and can be used to pinpoint problems with a given material.

From the perspective of the students, the most appealing advantage is the ability to do the experiment in a self-paced manner and that the lab is accessible anytime from anywhere.

2.2   Disadvantages of Remote and Virtual Laboratories

One disadvantage of virtual and remote laboratories is the lack of hands-on contact with devices and equipment, therefore a virtual or remote laboratory does not improve manual skills i.e. dexterity, which is necessary to achieve the same experiment result when working with real-life equipment. This effect can be reduced to an extent by using high fidelity 3D models of the equipment.

Another disadvantage comes from the fact that the virtual environment is similar to video games. Students tend to look at the virtual experiment as a game, therefore they lose the sense of seriousness. In remote laboratories, students are unable to cause damage by making mistakes, because all controlled components have limits predefined and checked by the environment. These labs do not require the same level of discipline and caution that is necessary to do the same experiment in a traditional laboratory in a safe manner.

2.3   Advantages of Virtual Laboratories

A large number of laboratory experiments are either dangerous or involve expensive equipment, therefore a supervisor must be present in the laboratory and the necessary theoretical knowledge of the student must be tested before they can start the experiment. These two factors rule out the possibility to simultaneously do the experiment and gain theoretical knowledge in a learning-by-doing manner for the student.

In a virtual laboratory, students can conduct experiments in a safe manner and the virtual laboratory can simulate extreme conditions, like altered gravity or very high ambient temperature, which would be impossible or very expensive to do in a traditional or remote laboratory.

The absence of actual equipment (hardware) means the number concurrent labs are only limited by system resources, the virtual hardware does not age nor wear out, which means lower operational costs. It is also cheaper to establish a new experiment, because there is no need to buy new equipment.

2.4   Disadvantages of Virtual Laboratories

The only real disadvantage of a virtual laboratory over a remote one comes from the fact that a remote lab is backed by real hardware and therefore it produces all the behavior of that hardware without the need to create complex mathematical models that can never take into account all details of a real, existing physical system. Fortunately, the impact of this disadvantage depends on the use case of the laboratory system. The precision that a mathematical model can achieve is, most of the time, adequate for the purpose of education and demonstration. However, it is important to keep in mind that the model and the simulation must be sophisticated enough to cover all the important aspects of the given experiment: it is important to correctly model the phenomena that is the subject of the given lab (e.g.: precision of a measurement equipment is affected by the ambient temperature).

3   Overview and Evaluation

3.1   Current State of Virtual Laboratories

Since virtual laboratories have numerous advantages over traditional and remote labs, virtual laboratory design and development became a widely researched topic in the past few years. Many research groups, universities and even members of the industry developed their own virtual laboratories, covering a very wide area of disciplines [4] [5] [6]. In current scientific literature, two major categories of virtual laboratories can be distinguished.

In the first category [4] [7] **Error! Reference source not found.**[8], there is virtual laboratory implementations that were designed and suitable for a single specific purpose, i.e. for a single experiment. These implementations do not employ systematic approaches on design, e.g. does not take into account the re-

usability or different components. Instead, the focus is on the experiment itself and the software components that are already playing a role in this experiment is also used to implement the necessary services for the remote laboratory, e.g. the webserver. Most of the time, this approach yields quick results because the teacher or researcher are already familiar with the software, but in the long run it is a source of multiple problems. First, the software, which is perfectly suitable for the experiment, e.g. LabVIEW or Matlab may contain a module to implement a webserver. However, these were not designed to handle the challenges, e.g. a large number concurrent requests that webserver software was designed for. Second, it is impossible to integrate these components with external services, like authentication and authorization, accounting, and data storage. Third, it is very hard to create a consistent user interface for the end-users of the system.

In the second category [9] [10], there are proposed virtual laboratory system designs, some of them with reference implementations, which were created by following a systematic design approach, employing design patterns and best practices from the field of web-development. This approach successfully eliminates the problems mentioned in the first category. However, it poses a new requirement against the teams who want implement a new experiment, namely that they have to learn the usage of new tools that are specific to web-development. In engineering disciplines, this is often not a problem because teachers already have some knowledge and expertise in this area. However, in other disciplines, e.g. astrology, chemistry and medicine, where virtual laboratories are also very useful, this problem makes it hard to involve teachers in creating new virtual experiments.

Recently it is a subject of active research to fill the gap between this two categories [11] [12]. Therefore, these are still only suitable to a specific set of experiments or rely on software components that were not designed for the given purpose.

3.2 A New Perspective on Virtual Laboratories

In order to ensure the usability of different virtual laboratories, members of the scientific community – who are also users of these systems – conducted assessment, most of the time focusing either on the didactic aspects, i.e. how the usage of virtual laboratory increased student's grades or on the implementation aspects, i.e. the used software components. The most common assessment method involves surveying teachers and students on subjective indicators and processing the accumulated data with statistical methods. In a number of these articles, some assumptions can be found on which characteristics of a virtual laboratory are the most influential on the didactic success of the laboratory. However, there is no effort to evaluate these systems from the synergic point of cognitive infocommunication [13] [14].

In order to have a better picture on what makes a virtual laboratory system successful, it is necessary to link the cognitive process of learning and the virtual laboratory as an infocommunication system together. This can be done by evaluating virtual laboratories from the point of view of the participants, i.e. the communicating parties. This can help identify the key factors that must be taken into account when designing a new virtual laboratory system.

The aim of a traditional laboratory course is to complement theoretical knowledge, gained through lectures. The participating parties are the institution, i.e. the university, the teacher or laboratory supervisor and the student.

The virtual laboratory can be described as an infocommunication system, which is used by teachers to create virtual experiments and learning materials and by students to gain knowledge through these virtual experiments.

In the virtual laboratory, the teacher or supervisor is not present during the experiment; instead the necessary guidance is presented in the experiment description. Teachers create these descriptions and additional help materials to give the narrative during the virtual experiment. In this way, many students can do the same experiment in the same time, in a self-paced manner.

The aspects of evaluation, described in previous works [1] [2] [15] can be extended with the cognitive aspect as the following.

Aspects of the evaluation from the point of the university and the teachers:
- Technical: How hard is the installation of the virtual laboratory system? How complicated is the process to implement a new experiment? Which software tools or programming languages are supported to implement the simulation?
- Economical: what are the development and operation costs of the virtual laboratory system?
- Cognitive: is a virtual lab suitable for the current topic or concept? Is the user interface consistent and easy-to-use? Is it possible to present all related materials, like help docs and textbooks on a single user interface?

Aspects of the evaluation from the point of view of the student:
- Technical: what are the system requirements of the virtual lab? How complicated is it to access the virtual lab? Is it necessary to install new software?
- Cognitive: Is the virtual laboratory an effective tool to learn? How hard is it to gather all the related information to do the experiment? Is the provided narrative in the laboratory self-contained, and adequate to do the experiment?

3.3　Evaulation

In order to give an overview of the current state of virtual laboratories, several implementations were evaluated, based on the new, cognitive aspects. Since many these implementations are based on a similar design, the systems below were selected to illustrate the distinctive features that were identified during the evaluation.

3.3.1　Weblab Deusto

The Weblab Deusto [15] project is a joint effort to give access to real laboratory equipment over the internet for research and educational purposes. It can be categorized as is a remote laboratory system.

From the cognitive aspect, the learning materials in Weblab Deusto are presented on a web-based user interface. It is designed in a way that the relevant and related materials are not presented on the same interface as the remote interface of the experiment. Because of this, the description of the remote experiment and other learning materials must be gathered and accessed separately by the users.

3.3.2　VISIR

The Virtual Systems in Reality (VISIR) [11] project aimed to establish a remote laboratory for remote wiring and measurement of electronic circuits on breadboard.

The system design of this remote laboratory follows a modular approach. The measurement equipment used for the experiment is connected to a laboratory server, that is connected to a webserver.

The user interface is web-based and has similar features as a Learning Management system. This allows tutors to create courses, experiment descriptions and additional materials for the experiment with a familiar toolset. However, the experiment itself needs to be implemented by hand, with a specific toolset, using a separate user interface.

3.3.3　VEMA

Virtual Electric Manual or VEMA [5] is a Virtual Learning Environment, designed with focus on a high level of realism, in order to create an immersive experience.

From the cognitive aspect, the resemblance between real measurement equipment and the 3 dimensional model representation in the virtual environment helps students to connect the knowledge gained through the virtual experiment to the real world. This approach is promising; however a great amount of manual labor is required to create these high fidelity 3D models.

3.3.4   LDH vLab

This virtual laboratory aims to implement a web-based lesson to teach lactate dehydrogenase (LDH) enzyme kinetics to 2nd-year biochemistry students [6].

The virtual laboratory is accessible through a web-based user interface. This interface is designed in a way that the description of the experiment and related materials are presented side-by-side with the experiment itself. This reduces the amount of context switching that are necessary to finish the experiment. As described in [6], the overall experience of students was positive, but some of them experienced technical issues which perplexed the learning process.

4   Design of a New Virtual Laboratory Environment

4.1   Frontend

Looking at existing virtual laboratory implementations [1] [16] and considering the disadvantages of virtual laboratories, it is apparent that there is no consistency in the presentation layer, i.e. in user interfaces. From this problem, the first requirement can be defined as the following; the main user interface, including the administration interface for teachers and the user interface for students must be consistent and intuitive.

The second requirement, which comes from the cognitive aspect is to minimize the necessary context switches during the experiment, i.e. present all relevant and related material on a single user interface.

Nowadays the majority of students mainly use smartphones and tablets to gain access to web services instead of desktop and laptop computers, it is necessary to support these devices.

4.1.1   Web-based Client

In order to fulfill this requirement the current best practices from the field of web user interface design should be utilized. As [15] points out, many software components can be used. Therefore, it is advised to avoid technologies like Flash and Java, as the majority of mainstream web services do nowadays because of their many practical problems, like security and the lack of cross-platform operation.

The proposed web-based client interface should use modern web technologies like HTML5 and JavaScript [5] [12] [17]. This way it can be ensured that the user interface can be used in any modern web browser, which is already installed on

end-user devices like smartphones and tablets. This also ensures that on desktop PCs, the virtual laboratory can be used without the need to install additional software [15].

This approach also enables the usage of modern frameworks, which helps create an intuitive, self-explanatory interface because most of the UI components can be found in other popular web applications, which students already use on a daily basis [18].

4.1.2   3D Client Application

The proposed desktop client for the virtual laboratory system is based on the MaxWhere [19] framework. MaxWhere is a unique VR framework (engine) that is programmable through JavaScript and allows for building 3D, VR applications in which the conventional web content is fully associative with the 3D, VR world. MAXWHERE provides a JS API called WOM (Where Object Model) that implements similar functionality for VR as the DOM does in web browsers.

The ability to manipulate the models of the 3D space from the programming environment makes it easy to create high fidelity, interactive 3D models which can help students to understand complex 3D structures more easily [20].

The ability to load webpages inside the 3D environment makes MaxWhere a good choice to build upon because the same web-based user interface of the system can be used in the desktop client. This reduces the development effort and also ensures that user interfaces are consistent across the web and desktop clients. Another advantage of this ability is that by using multiple web browser windows placed in a 3D environment, all relevant content - e.g. lecture notes and description of the experiment - can be presented to the user in a single space [21] [22]. Students can also use these web browsers to open relevant and useful web-based products, e.g. their webmail client, online video materials and the university LMS website in this environment [23]. This highly reduces the amount of context switches, i.e. changing between different windows to complete a virtual experiment and helps students to focus on learning.

4.2   Backend

The recent trend in large-scale web-based software development and operation is to change the architecture from a monolithic service to microservices [24]. This trend induced the development of new tools to cover all the operation tasks from deployment to management, backup and monitoring. Nowadays the microservice ecosystem reached a maturity level that is considered ready for day-to-day business operation. Therefore, the new system should be composed of a set of modular microservices. This way it is straightforward to create scalable virtual laboratories and all the necessary tools are available to operate it.

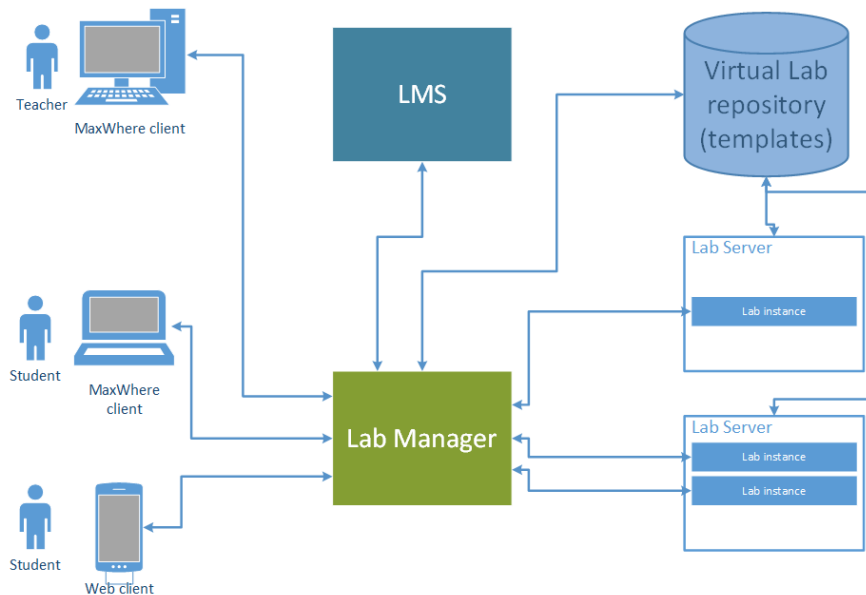Figure 1 shows the general overview of the proposed new architecture.

Figure 1

High level architecture of the virtual laboratory framework

4.2.1 Laboratory Manager

The core component of the new design is the Laboratory manager. It should provide the web server service, to serve the web application to clients. It should handle the authentication and authorization of clients with the help of the Learning Management System of the university, and it should handle the deployment, management and monitoring of the virtual laboratory instances.

Each of these roles require complex functionality, which means that the Laboratory Manager should be modular, as mentioned earlier, in order to scale well with the increasing number of concurrent users.

4.2.2 Virtual Lab Repository

The Virtual Lab repository stores all necessary assets of a virtual laboratory, like textual descriptions, source code or input files of the simulation and virtual laboratory templates. A virtual laboratory template should contain all the properties of a given laboratory, requirements of the simulation in terms of software components and system resources, and a recipe which describes the deployment and execution of the simulation.

This way, teachers can create different laboratories in a very rapid way, because several assets can be re-used for multiple laboratories and different learning narratives can be defined in the same virtual space.

The Laboratory Manager uses these templates to create, deploy and execute virtual laboratory instances.

4.3   Integration with Simulation Software Tools

The main part of a virtual laboratory is the simulation that calculates the actual state of the virtual environment. Therefore, in order to use a virtual laboratory one must run this simulation somewhere. There are two major problems regarding simulation that must be taken into account. First, as the complexity of the laboratory exercise rises, the simulation can quickly get very resource heavy in terms of CPU and memory. Second, these simulations are often implemented using different software packages and libraries, with very different system requirements [25], like the type and version of the operating system.

4.3.1   Local and Online Operation Modes

The straightforward solution for the first problem would be to raise the system requirements of virtual laboratory. However, this procedure would effectively shut out a large number of students from the virtual laboratory. In order to solve this problem, the system should be designed following the client-server model. In this way, the virtual laboratory can operate in two different ways based on the system resource requirement of a given simulation.

First, simulations with low resource requirements can be executed on the local machine and the calculated data is then transmitted to the client via a local interface without the need of a network connection. It is important to note that in this mode all software components must be run on the client machine; therefore, it is only suitable to a reduced set of simulation software. This operation mode is called *local mode*.

Second, simulations with high resource requirements can be executed on a remote server [26] and the calculated data is then transmitted to the client via the network. This operation mode is called *online mode*.

4.3.2   Standard Simulation Software Interface

The solution for the second problem would be to set up a list of simulation software and libraries which the teacher can choose from when implementing the virtual experiment. However, in this case the teacher is required to re-implement simulations that are already implemented in software that is not part of the list.

Instead, the new system should establish a new interface to exchange input and output data with the simulation software. This can be used to create wrappers for different simulators.

4.4   Integration with Learning Management Systems

The new system should be able to be integrated with widely used Learning Management Systems, like Moodle [15] [27]. The Laboratory Manager should use the LMS to authenticate and authorize teachers and students. It should be able to logically connect virtual laboratory exercises, defined by the teacher in the LMS and in the Manager. This way, the different interactions in a virtual laboratory can be defined as course requirements in the LMS. For example, the completion if a virtual laboratory can be set up as an obligatory requirement to pass a given course. In order to fulfill this requirement, the Manager should be able to collect and log the interactions of students in virtual laboratories. This can be achieved by using existing web monitoring and logging tools [28].

Conclusions

The new perspective of using cognitive infocommunication to describe the learning process in a virtual laboratory helped to pinpoint new important factors that a creator of a virtual laboratory system should take into account, in order to achieve a high didactic potential. The described requirements of the new virtual laboratory system can function as a design pattern for new implementations.

The next step is to implement a new virtual laboratory system, based on this design. This new system then will be tested with the help of tutors and students in order to validate the design and to ensure that the new system successfully fulfills all the described requirements in this paper.

Acknowledgement

References

[1]   V. Potkonjak, M. Gardner, V. Callaghan, P. Mattila, C. Guetl, V. M. Petrović, K. Jovanović. Virtual laboratories for education in science, technology, and engineering: A review. Computers & Education, Vol. 95, 2016, pp. 309-327

[2]   Advances on remote laboratories and e-learning experiences. Universidad de Deusto, 2008, ISBN: 9788498306620

[3]   M. Auer, A. Pester, D. Ursutiu, C. Samoila. Distributed virtual and remote labs in engineering. IEEE International Conference on Industrial Technology, 2003

[4]   A. Peidró, O. Reinoso, A. Gil, J. M. Marín, L. Payá. A virtual laboratory to simulate the control of parallel robots, IFAC-PapersOnLine, Vol. 48 No. 29, 2015, pp. 19-24

[5]   M. Valdez,C. M. Ferreira, F. P. M. Barbosa. 3D Virtual Laboratory for Teaching Circuit Theory - A Virtual Learning Environment (VLE) 51st International Universities' Power Engineering Conference, 2016 DOI:10.1109/UPEC.2016.8114126

[6]   C. Booth, R. Cheluvappa, Z. Bellinson, D. Maguire, C. Zimitat, J. Abraham, R. Eri. Empirical evaluation of a virtual laboratory approach to teach lactate dehydrogenase enzyme kinetics, Annals of Medicine and Surgery, Vol. 8, 2016, pp. 6-13, ISSN 2049-0801

[7]   M. de Massimilian. A MATLAB-based virtual laboratory for teaching introductory quasi-stationary electromagnetics. IEEE Transactions on Education Vol. 48, No. 1, 2005, pp. 81-88

[8]   A. Ahmad, M. K. Nordin, M. F. Saaid, J. Johari, R. A. Kassim and Y. Zakaria, Remote control temperature chamber for virtual laboratory, 2017 IEEE 9th International Conference on Engineering Education (ICEED) Kanazawa, 2017, pp. 206-211

[9]   M. B. Erdem, A. Kiraz, H. Eski, Ö. Çiftçi, C. Kubat. A conceptual framework for cloud-based integration of Virtual laboratories as a multi-agent system approach. Computers & Industrial Engineering, Vol. 102, 2016, pp. 452-457

[10]   H. Majid, H. F. Manesh, M. Bal. A modular virtual reality system for engineering laboratory education. Computer Applications in Engineering Education Vol. 19, No. 2, 2011, pp. 305-314

[11]   T. Mohamed, et al. Virtual instrument systems in reality (VISIR) for remote wiring and measurement of electronic circuits on breadboard, IEEE Transactions on Learning Technologies Vol. 6, No. 1, 2013, pp. 60-72

[12]   F. Esquembre. Facilitating the Creation of Virtual and Remote Laboratories for Science and Engineering Education. IFAC-PapersOnLine, Vol 48, No 29, 2015, pp. 49-58, ISSN 2405-8963

[13]   P. Baranyi, A. Csapo. Definition and Synergies of Cognitive Infocommunications, Acta Polytechnica Hungarica, Vol. 9, No. 1, 2012, pp. 67-83

[14]   P. Baranyi., A. Csapo, G. Sallai. Cognitive Infocommunications (CogInfoCom). Springer International Publishing, 208 pages, 2015, ISBN: 978-3-319-19607-7

[15]   J. Garcia-Zubia, P. Orduna, D. Lopez-de-Ipina, G. R. Alves. Addressing software impact in the design of remote laboratories. IEEE Transactions on Industrial Electronics, Vol. 56, No. 12, 2009, pp. 4757-4767

[16]   P. Trnka, S. Vrána, B. Šulc, Comparison of Various Technologies Used in a Virtual Laboratory, IFAC-PapersOnLine, Vol. 49, No. 6, 2016, pp. 144-149

[17]   HTML5 specification, https://www.w3.org/TR/html5/ [online, last visited on: 2018.01.04]

[18]   I. Horváth: Digital Life Gap between students and lecturers. In: Proceedings of 7th IEEE Conference on Cognitive Infocommunications. Wrocław, Poland, 16-18.10.2016. Budapest: IEEE Hungary Section, 2016, pp. 353-358

[19]   MaxWhere website, http://www.maxwhere.com/ [online, last visited on: 2018.01.04]

[20]   Z. Kvasznicza: Teaching electrical machines in a 3D virtual space, 8th IEEE International Conference on Cognitive Infocommunications, Debrecen, 2017

[21]   G. Csapó, Sprego Virtual Collaboration Space, 8th IEEE International Conference on Cognitive Infocommunications, 2017

[22]   I. Horváth: Disruptive technologies in higher education, In: Proceedings of 7th IEEE Conference on Cognitive Infocommunications, Wrocław, Poland, 16-18.10.2016. Budapest: IEEE Hungary Section, 2016, pp. 347-352 (ISBN 978-1-5090-2644-9; 978-150902645-6)

[23]   I. Horváth: Innovative engineering education in the cooperative VR environment, In: Proceedings of 7th IEEE Conference on Cognitive Infocommunications. 496 p. Wrocław, Poland, 16-18.10.2016. Budapest: IEEE Hungary Section, 2016, pp. 359-364 (ISBN 978-1-5090-2644-9; 978-150902645-6)

[24]   M. Villamizar et al., Evaluating the monolithic and the microservice architecture pattern to deploy web applications in the cloud, 2015 10th Computing Colombian Conference (10CCC) Bogota, 2015, pp. 583-590

[25]   I. Horváth: The IT device demand of edu-coaching in the higher education of engineering, In: IEEE 8th International Conference on Cognitive InfoCommunications: CogInfoCom. Debrecen, Hungary, 11-14.09.2017. (IEEE) Piscataway: IEEE Computer Society, 2017, pp. 379-384

[26]   S. D. Burd, X. Luo, A. F. Seazzu. Cloud-based virtual computing laboratories. 46th Hawaii International Conference on System Sciences, 2013, pp. 5079-5088, IEEE

[27]   M. Dougiamas, P. Taylor, Moodle: Using Learning Communities to Create an Open Source Course Management System. In: World Conference on Educational Multimedia, Hypermedia and Telecommunications (EDMEDIA) 2003, Chesapeake, VA, USA

[28]   R. Atterer, M. Wnuk, A. Schmidt. Knowing the user's every move: user activity tracking for website usability evaluation and implicit interaction. In Proceedings of the 15th international conference on World Wide Web (WWW '06) ACM, New York, NY, USA, 2006 pp. 203-212

Cooperative Learning in VR Environment

Viktória Kövecses-Gősi

Apáczai Csere János Faculty, Széchenyi István University, Liszt Ferenc utca 42,
H-9022 Győr, Hungary, gosi.viktoria@sze.hu

Abstract: Nowadays it is increasingly visible that a change in the approach is needed in the field of education, thus we should move from "traditional" educational methods towards experience-oriented and cooperative teamwork-based education which considers the characteristics of the digital generation. After the brief demonstration of the methodological characteristics and the principles of digital culture, the present study aims to introduce how a lesson built on the improvement of different intelligence levels through cooperative techniques can be implemented with the help of virtual space, what opportunities are provided by the MaxWhere program for planning and organising teamwork and for supporting learning.

Keywords: cooperative learning; VR learning environment; MaxWhere; teaching methodology; digital culture; the improvement of intelligence areas; formative assessment; interactive learning-teaching

"Kids naturally know how to be in the state of flow. They learn fast because they find learning exciting. No money has to be paid for an infant for learning how to talk or walk, as he has a natural urge to improve his knowledge. However, when we close them into the school, where they have to sit and listen, it is not natural to them. This is a misunderstanding of the adult-world about how we learn."

(Mihály Csíkszentmihályi)

1 Introduction

Whatever level of the school system we look at, we can see that professionals working in education report the same problems everywhere. The lack of interest and motivation, the lack of perspectives and aims, inattentiveness, attention disorders, a fall in the quality of communication and human relations, the low level of emotional intelligence, or the seemingly higher rate of learning- and conduct disorders make pedagogues think in every area. Many do not find the way to the students, and instead of working together for the common good by cooperation, they run away in opposite directions and criticise negatively the youth whose future is dependent on us as well.

All these symptoms show that a change in approach is needed in the field of education, thus we should move from "traditional" educational methods towards experience-oriented and cooperative teamwork-based education which considers the characteristics of the digital generation. After the brief demonstration of the methodological characteristics and the principles of a digital culture, the present study aims to introduce how a lesson built on the improvement of different intelligence levels through cooperative techniques can be implemented with the help of virtual space. Also, we present, what opportunities are provided by the MaxWhere program for planning and organising teamwork and for supporting learning.

2   Cultures, Differences between Generations, Problem Areas

There have always been generational differences and conflicts; however, today it has intensified and besides the generational differences, cultural differences have evolved as well. Those parents who raise children nowadays as well as the older adults grew up in the culture of literacy; however, the children they raise and teach are the natives of the digital culture. "Today a baby boomer-aged teacher or parent (who is either close to retirement or already retired) has to bridge much more distance than a younger person of Generation Y (in their thirties) has to. It is not only about the usual generational differences, but also about how to handle the changes caused by information age and technological developments and merging them harmonically in both home training and education." (Tari A. 2011: 17)

In recent years we have seen the spread of those summaries and the related psychological descriptions that reveal the typical characteristics of the different generations. Table 1 provides a brief and schematic overview of these generations and their essential characteristics.

Table 1
The different generations and their typical characteristics

Generations (W. Strauss, N. Howe 1991)	Their typical characteristics (Tari A. 2010, 2011, 2013, 2015)
Baby boom generation: 1946-1964	"A descent fellow has one workplace." They were eager to be an adult. They did not use infocommunication tools.
Generation X: 1965-1979	They were compelled to express their feelings verbally. They have old attitude while they nurture/teach/look after the new digital generation. They try to pass value in a world where values have been transformed. Lack of parental control over the child's internet activity.

	The family communication system does not sufficiently include the educational attitudes needed in information age.
	They were raised in an authoritarian system.
Generation Y: 1980-1994	They are special; at least they may feel that, because they were cared for a lot in their childhood, much more than any other generation.
	Helicopter parents are circling over the heads of many, even in their twenties. They cannot detach.
	They like working in teams.
	They are ambitious, highly-motivated and rational.
	A high pressure is put on them as they start their adult life in a more insecure economic environment than their parents did.
	For them computer world and Internet are as natural as breathing.
Generation Z: 1995-2009 (Digital native)	They are born into the smallest family.
	They are growing faster and faster.
	They are raised by the oldest mothers so far.
	They are the most educated.
	They show mosaic maturity.
	They do not have an easy childhood. They understand a lot, but are able to process a few.
	More and more aggressive effects affect them.
	They are small consumers in the consumer society.
	They face informational surfeit.
	They are constantly in touch.(online)
Alpha generation: 2010-	They are typically raised by parents of Generation Y.
	Due to the advances in technology, it is more and more difficult for these parents to decide what is good for the child and what is early for them.
	Digitalisation has become an integral part of everyday life; touch screens are constantly present at family lunches, at bedtime, and on road trips.
	There is no established practice or norms of using the devices; it varies from family to family what is permissible and acceptable.

By reading the writings of Annamária Tari, many questions may arise. How can we help the school and out-of-school learning activities of the different generations, what effective methods and tool system can we use in education, and what is the most important, which methods support the putting forth of the personality of the youth who are isolated from each other and only keep in touch virtually with each other, as well as the enhancement of their emotional intelligence, and the improvement of their personal, live communication culture?

In an age when we gradually move from the culture of literacy towards a digital culture, several other sources of tension appear. (Gyarmathy, 2012) In case of digital natives, mainly visual experiences dominate instead of experiences through motion and perception. Instead of active activity, the operation of machines is in the centre. They very often have ready-made pictures instead of utilizing their imagination, which impedes the improvement of their creativity. Instead of linguistic expression, visual expression moves to the front. The extent of attention does not function as it did before. The nervous system does not learn the delicate comparisons, so the harmonic cooperation between the two cerebral hemispheres is in danger too. (Gyarmathy 2012) "The school traditionally favours and thus develops left-brained function. School processes lack the understanding of relationships, creative thinking, intuition, and art, although the teaching of logical, analytic, and scientific thinking is at a high-level." (Gyarmathy 2012: 53) According to Gyarmathy, the school prepares students for linear, scientific thinking, and not for life. which is diverse, full of various opportunities, and cannot be restricted to categorical thinking. The right cerebral hemisphere adds everything that is needed for problem-solving thinking of left-brained function.

The Digital culture is built upon one-sided right-brained function; however, education is unequivocally built on a left-brained one. (Gyarmathy 2012: 54) It is a question how these two so different systems can make contact with each other. They can, but only if we organise and support the learning process by giving role to methods, procedures, and forms of activities which aim at the joint activating of the two cerebral hemispheres. A basic requirement of effective learning is to harmonise the two different cultures as well as the function of the two cerebral hemispheres.

2.1   In the Digital Age the Main Pillars of Education Consist of the Following Factors

- Adaptive, differentiated instruction
- Education designed based on the theory of multiple intelligences
- The improvement of emotional intelligence
- Formative assessment
- Learning to learn
- Cooperative learning
- Project planning
- Strategic games
- Motion, music, rhythm, beat, balance exercises
- Art

I do not plan to introduce all these fields in detail in the present paper: however, briefly summarise the essential definitions and the methodological principles from the viewpoint of the topic. Then, through a practical example demonstrate the implementation options of a lesson designed based on cooperative learning and the theory of multiple intelligences with the help of VR learning environment.

The necessity of adaptive, differentiated instruction

The pupil is an active participant of the education process and not a sufferer of it, regardless of their age. The (adaptive) education environment which adapts to the pupil's personality assumes the diverse ways to success, the wide range of eligible aims, and not one of those ways to success is more valuable than the other. (R. Glaser) Differentiation that considers individual characteristics and unified teaching directed at the knowledge of individual characteristics together compose adaptive instruction. (Nádasi M. 2001: 28-40)

In adaptive learning management, which adapts to the pupils' personality in a differentiated way, a major role is given to: activating methods, the diversely used learning management ways, and to the tool system it requires. In case of adaptive learning management it is important to take into consideration that pupils engage in diverse learning and experience-gaining ways along various fields of interest with different motivations.

Education designed based on the theory of multiple intelligences

Howard Gardner, who elaborated the theory of multiple intelligences, suggests that we should know as much as we can about kids instead of trying to fit them into the eye of the same needle. Having analysed the cognitive abilities of different groups of people, Gardner found that intelligence focuses on the different areas of the brain, and these areas are connected to each other, one area builds on the other, but in case of necessity they can function independently as well, and among appropriate circumstances these areas can be improved. As a result of his research he defined eight intelligence areas, the improvement of which is indispensable in the process of education. (Kristen Nicholson – Nelson 2007: 11-12) Table 2 illustrates the intelligence areas and their typical characteristics which may serve as bases for planning.

Table 2

The characteristics of the areas of multiple intelligences

(Diane Heacox 2006), (Kristen – Nelson - Nicholson: 2007)

Intelligence area	Strengths, typical characteristics	Pupils learn the most through these
Verbal – linguistic *Tell it!*	A facility with words and linguistic delicacies, sensitivity to word order and the rhythm of words. ***Keywords:*** Reading, writing, storytelling, memorizing data, verbal thinking	Reading, listening and seeing words, talking, writing, discussion and debate
Mathematical – logical *Count it!*	The ability to understand abstract systems and relationships, ability to inductive and deductive reasoning.	Working with schemes and relations systems, systematisation, categorisation, working with abstractions

	Keywords: Mathematics, reasoning, logic, problem-solving, schemes	
Visual - spatial *Illustrate it!*	The ability to create visual – spatial forms about the world to transform them in thought or in reality. *Keywords:* Reading, maps, figures, mazes, puzzles, imagination of things, visualisation	Working with pictures and colours, visualisation, the use of internal vision, drawing
Bodily – kinesthetic *Move!*	Pupils having developed bodily – kinesthetic intelligence prefer expressing themselves in motion. *Keywords*: Athletics, dance, acting, handicraft, the use of tools	Taction, motion, the knowledge is processed through physical sensations
Musical *Hum it!*	Sensitivity to pitch, tone and the rhythms of notes, and sensitivity to the emotional load of these elements of music. *Keywords:* Singing, noting notes, recalling melodies, rhythms	Rhythm, melody, singing, listening to music
Interpersonal *Lead!*	Effective cooperation, the ability to strive for understanding the others' aims, motivations, and orientations. *Keywords*: Understanding people, leadership, organisation, communication, conflict management	Discussion with others, comparison, linking, interview, cooperation
Intrapersonal *Reflect!*	The ability to understand their own emotions, aims, and intentions. Pupils having developed intrapersonal intelligence have strong self-consciousness, are self-confident, and like working alone. They instinctively measure well their strengths and abilities. *Keywords:* Self-knowledge, the knowledge of their own strengths and weaknesses, defining aims, reflection	Working alone, performing individual-rate projects, enough space, reflection
Naturalistic *Explore!*	The ability with which natural world can be seen from a wider perspective which includes the understanding of the interrelatedness between nature	Work in nature, the exploration of wildlife, learning about plants and natural phenomena.

	and civilisation, of the symbiotic relationships in nature, and of the cycle of life.	
	Keywords: Understanding nature, distinguishing things, the recognition of flora and fauna.	

If we design the lessons, activities by considering intelligence areas, inter alia differentiation can be more effective as well. Every pupil/student has the characteristics which enable the putting forth of each area, and by this, other areas can be improved more effectively. Lessons designed based on this approach exceedingly help the harmonization of the two cerebral hemispheres' functions. This theory is applicable to any age group; either we deal with pupils from lower school in the forest school or with those adult teacher candidates who will teach children in public institutions.

Formative assessment

> *"If you treat an individual as he is, he will remain how he is. But if you treat him as if he were what he ought to be and could be, he will become what he ought to be and could be."*

> *(Goethe)*

"It means the frequent and interactive assessment of the pupils' improvement and knowledge, and its aim is to determine learning objectives and to accommodate teaching to these." (OECD CERI, 2005.) (Lénárd S. – Rapos N. 2009:20) In the course of this, assessment constantly follows and supports the learning process, which makes it possible to design the processes and possibilities of progress, the forms of differentiation as well as its tool system adapted to the pupils. In this assessment process the pupil is also an active participant as a result of which self-assessment can be improved efficiently and the development of reflective approach is supported. Assessment in this case does not only mean the reproductive testing of knowledge, but it also enables to get acquainted with changes in competences to be developed.

"Formative assessment is a system-level process during which the emotional development of pupils is of importance as well besides the diversity of assessment tools; and besides consciousness, self-assessment, empathy, cooperation, and flexibility are also important factors regarding compliance in life. When designing the lesson, not only the necessary sectioning of the curriculum must be made, but the activities necessary for the development of the given skills must be determined too besides the applicable development assessment tools and methods. It may help learning if teachers let the pupils in on the processes designed by them, thus pupils may see the purpose of the lessons in a clearer way."(Cseh Á. G.)

Formative assessment is more than diagnostic assessment because it mainly follows a preventive approach. It states the pupils' development and interprets

their learning needs. Its quintessence is actually the support of: development, the enhancement and the support of self-image, metacognition, and of self-assessment. However, in order that assessment can fulfil its developmental function, we have to know how the pupils can be motivated well, which learning strategy characterises them, which learning-methodological recommendations are useful for them, how their interest can be broadened, whether they can learn in groups by cooperating, and which thinking functions are worth strengthening. (Lénárd, Rapos, 2009) During formative assessment we can use various assessment tools like key cards, learning diaries, individual learning plans, T-cards, self-assessment, peer-assessment or team- assessment sheets or learning portfolios of different types. Portfolio is "the collection of such documents which shed light on someone's knowledge, skills, and attitude gained in a given field". (Bird 1990, cited by Falus-Kimmel 2008:196) "Is a targeted collection of the pupil's work, which introduces the pupil's efforts, development and results in one or more fields. The pupil must take part in compiling the content as the collection must include the criteria used for choosing among the documents as well as the self-reflections of the pupil." (Northwest Evaluation Association, 1990, cited by Falus-Kimmel 2008:196) Basically there are two main reasons for making a portfolio: it may serve the assessment, as well as, the facilitation of learning. With the help of the portfolio we can document the whole learning process. Its use enables constant assessment, feedback, and self-evaluation. It helps the development of reflective thinking, the cognition and the understanding of metacognitive knowledge and the knowledge we have about our own process of thinking and learning. When compiling the portfolio it is very important that pupils should get appropriate information about it as a form of assessment as well as about its compilation and the evaluation criteria. The literature distinguishes different portfolios based on what they focus on, i.e. what is the aim of collecting pupils' work. Among the many subtle types, the most common in education are as follows. **Development portfolio,** illustrates the progress of the pupil's learning by collecting documents from as many fields and as wide activities as possible. **Process portfolio,** is similar to the previous one, but here the progress process of only one determined field is in the centre, and the small steps, elements related to this are also included. **Best works portfolio,** only includes the most important works chosen by the pupil. Pupils collect these works from those which are considered to best represent themselves and theirs results. **Learning aims portfolio,** contains those aims which the pupil wants to reach during a given learning process as well as those exact examples by which it can be verified that the pupil reached these aims. Of course, there are several other forms of portfolio in practice. Various methods are known for collecting, systematising and storing pupils' work. Using a portfolio enables the pupil to be an active participant of their own learning process. The assessment process is including digital tools in more and more places. (Rapos-Lénárd 2006: 26.)

Cooperative learning

Openness towards cooperativity, the knowledge, the routines, the skills, the competences, the abilities needed for teamwork, and last but not least, the attitudes needed for these are basic criteria in the workplace of the 21st Century. However, in many cases we experience that we lack these competence elements and selfishness, self-reliance which does not take into account the interests of others, self-fulfilment, and rivalry are in the centre. Although young people behind their computers and smart phones virtually form a community and "cooperate", it is more difficult that real cooperation with shared responsibilities and the pursuit of common success should become useful and successful practice within the frames of the classroom. Slavin, Kagan, Johnson and their research groups proved that cooperative learning management has a positive effect on the acceptance and tolerance of ethnic differences.

"As a result of cooperative learning, the relationship between pupils belonging to different ethnic groups got better compared to the control group, moreover cooperative learning resulted in enhanced social development and mending social relationships." (S. Kagan 2001. 3:2) It is also a significant result that the two grades difference between the learning outcomes of American and Afro-American pupils disappeared by cooperative learning management. Afro-American pupils overtook their arrears of work. Unfortunately, today's school prioritises competitive methods in which rivalry is in the centre. The question may arise how we should prepare the growing generation for cooperation if it is not emphasised enough in the school. How can pupils work on the realisation of common problems and innovations as adults; how can they be tolerant and acceptable with others if during learning in the school they do not meet such methods and strategies which improve those basic skills, abilities and competences that are needed for that cooperation?

According to Green, cooperative learning is not only a teaching method, but an attitude of life which prioritises cooperation based on mutual respect and the individual performance of each community member. A precondition of it is the consensus, which is a result of the cooperation among the community members. Based on previous experience it can be said that those pupils who are able to use cooperative learning are also able to adapt this cooperative approach to other areas of life. (Óhidy 2011)

According to the definition of Beáta Kotschy Beáta, cooperative learning is "a small group activity based on the cooperation of participants, which may be organised to reach various aims, may help the pupils' improvement in learning, and may contribute to the evolvement of abilities and skills that are needed for cooperation as well as to the development of real self-evaluation and problem-solving thinking. It provides opportunity for practicing social behaviour forms, expressing own thoughts and emotions precisely and in a differentiated way, and for imbibing debate skills that take into account logical reasoning, concluding, and

the emotions of others. Common goals, responsibility and sharing the results facilitate the evolvement of respect for others, helpfulness and a real self-image." (Kotschy Beáta, 1997: 277-278)

During cooperative learning pupils perform their learning activity in groups of 4 to 6, where the formation of social competence also has an important role besides the improvement of intellectual abilities and knowledge transfer. Intra-group dependence, individual responsibility, and joint learning management within the group are the characteristics of cooperative teamwork. During the activities solving the task and the relationship among the group members are equally important. The teacher follows the work of the group with attention and in case of necessity interferes in a helping way. It is the task of the group to evaluate and reflect on the learning process. (Johnson – Johnson 1994) During cooperative learning it is of high importance that besides parallel simultaneous interactions we should divide the tasks among pupils so that positive dependency relationship could evolve among them in order that they could feel that their knowledge is built on each other as well. They all may contribute to successful task performance by their knowledge, motivation and skills. We can support it by appropriately distributing the roles and the responsibilities.

During the teaching of the digital generation we may successfully combine cooperative techniques and the development of different intelligence areas with digital technology, and thus we may make the teaching – learning process more interesting and more effective.

The lesson above took place among students of teacher-training who can study the so-called Cooperative learning subject in two hours of practice a week at the university. During the work built on cooperative learning with own experience, students imbibe the more theoretical parts of the curriculum with cooperative techniques.

This subject, which has been in practice for many years, is supported by VR learning environment in the 2nd semester of the 2017/2018 academic year. When designing the teaching lesson I worked with the AMR model (ATTUNEMENT – MEANING AWARENESS – REFLECTION), which "is a possible learning – learning-supporting model in favour of critical thinking and interactive learning. Students have to get personal experience of what it means to meet the information, how they should elaborate it, and how they should make the information usable for themselves as well. They have to follow the systematic path of critical thinking and the rethinking of the analytical process. So that it could happen in the community of the students, the teacher has to provide the systematic- approached, but not evident framework of thinking and learning. Being systematic is important because in this way students are able to understand and apply this process consistently. On the other hand, this framework has to be evident so that students themselves could realise where they are in the process, and in this way they can control and manage it even if they study individually". (Bárdossy – Dudás – Pethőné – Priskinné, 2002, 172-174)

To organise the lesson and to synthesise the curriculum and the tasks, from the MaxWhere spaces I chose the X-Podium which is apt for group work because it provides the placement of group-tailored tasks and teaching aids for four separate groups.
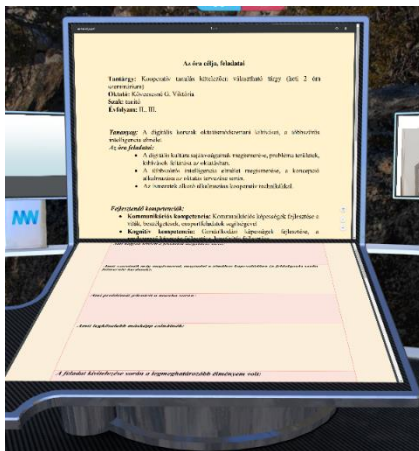

Figure 1
X-Podium

I equipped the space in a way that the middle part contains the tutorial presentations related to the lesson, the literature suggested and used for researching the topic, the objectives of the lesson, the evaluation criteria of the group work and of the individual work, and some videos related to the topic.

Figure 2
Self- and peer-assessment sheet, the objective of the lesson, the competences to be developed

The outline of the teaching lesson:

Subject: Cooperative learning (2 hours of seminar a week)

Class: II, III

Curriculum: The education methodological challenges of digital era, the theory of multiple intelligences

The tasks of the lesson:

- Getting to know the characteristics of the digital era, revealing the problematic fields and the challenges in education.

- Getting to know the theory of multiple intelligences and the application of the conception during the design of the education.

- The creative application of knowledge by cooperative techniques.

Competences to be developed:

- **Communication competence:** Developing communication competences with the help of debates, discussions, and group tasks

- **Cognitive competence:** Developing reflective competences, systematising abilities and creativity

- **Social competence**: Developing cooperative cooperation, joint problem-solving, tolerance, and adaptive ability

- **Personal competence:** Developing self-knowledge, self-assessment, self-regulatory learning, and metacognition

Applied methods: discussion, demonstration, explanation, role play, techniques developing cooperative and critical thinking (tablecloth technique, literary groups, insert technique, exit cards)

Learning management:

frontal work, cooperative group work, individual work

Tools:

text parts, tools needed for group formation, templates, photocopied materials, VR

The course of the lesson:

I   Attunement

Group formation: (4 groups, each containing 4-6 students) it took place randomly with mosaic technique. Students took the pieces of four pictures out of an envelope. Those students whose pieces matched formed a group in the given lesson (the pictures were related to cooperative learning). As the aim of the subject is to get to know various techniques of group formation, group formation has taken place in more times at the beginning of the lesson during the semester, so that the same students have not worked together throughout the whole semester.

Exploring preliminary knowledge: With structured settlement (or tablecloth) technique: each group member wrote their own end of the sentence after a brief consideration, and then after individual work, group members agreed on their

common opinion and wrote the group opinion into the middle of the figure. Groups then reported their common point of view.

I think the greatest challenge
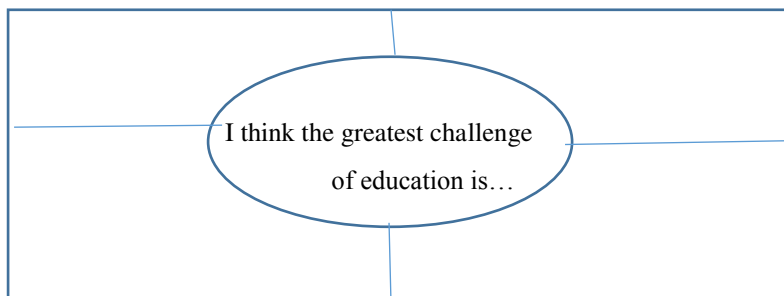
of education is…

II   Meaning creation

Group members received two types of studies in the 3D space. One of them deals generally with the education methodological challenges of the digital era, while the other study introduces the theory of multiple intelligences.

In the first part of the tasks, students read through the text with the help of INSERT technique which helps the development of intrapersonal intelligence. "INSERT means Interactive Noting System for Effective Reading and Thinking. Thus INSERT is an interactive noting procedure supporting metacognitive processes, during which procedure students, when reading the texts, use symbols on the margin according to their own understanding and knowledge. The symbols used are as follows:

✓   what I read corresponds with my preliminary knowledge and assumptions

−   what I read contradicts with my preliminary knowledge and assumptions, and differs from those

+   what I read contains new information for me

?   what I read encourages me to do further research or ask questions

✳   additional information came to mind about what I read

INSERT is an effective method which enables students to follow their own understanding process during reading, to take into account other learning motivations, while their reading becomes an active, cognitive, and metacognitive process. If students follow their own understanding process, they actively contextualise information. With the help of this procedure the intense attention may be sustained all the while."(Bárdossy, Dudás 2009:212)
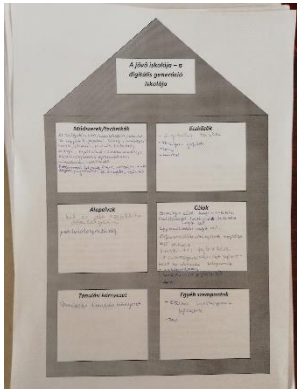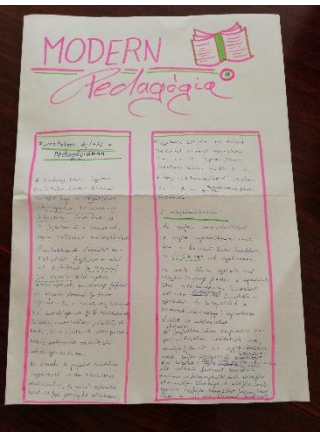
I linked the areas of multiple intelligences to the cooperative technique of literary groups with a little modification. Although the technique better fits to Hungarian

language and literature lesson, its basic concept can be used effectively in case of teaching other subjects as well. It is easy to link different types of tasks to each role, and these tasks strengthen one or the other areas of intelligence. When designing the lesson it is an essential aspect that students of teacher-training should get such knowledge which can be applied well in practice and which they can use immediately and transfer to pupils from lower school during their teaching practice.

Table 3

The development of intelligence areas with cooperative techniques

Intelligence area	Literary groups (role)	Task
Verbal – linguistic, *Interpersonal*	Report makers	Based on the text you have read, make an imaginary interview with a school's headmaster who carries out the teaching–learning practice in the school in the spirit of as described.
Mathematical – logical *Interpersonal*	Project generators	Based on the given template, make such a complex plan for a topic chosen by the group, which involves every intelligence area in the process of the activity.

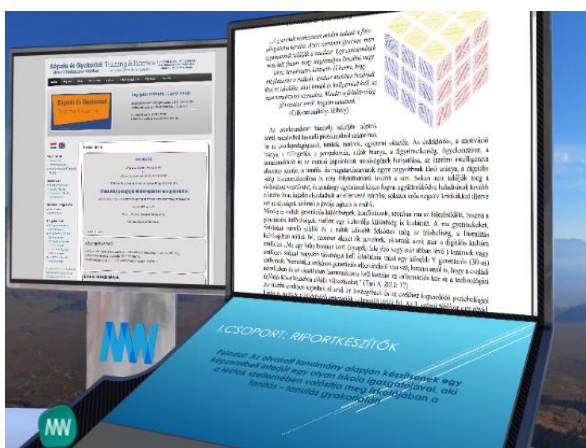| *Visual – spatial* *Interpersonal* | Poster makers | Dream the school of the future and design it with the help of the template. |
| *Verbal – linguistic* *Interpersonal* | Journalists | Make an imaginary report for the newspaper "Modern pedagogy" about a school which carries out its activity based on the theory of multiple intelligences. |

During the activity the students did not work only in the space, it was rather a help for them in the lesson. The templates, the teaching materials and the studies used in the lesson were displayed both in the classroom and in the space. (The program is not available for every student in the experimental process of curriculum

Figure 3
The "desk" of Group 1 with task description, study, and helping Internet source

development.) I placed the group tasks in the four separate parts of the space. It is easily manageable for students, the work of the other groups is not disturbing in this way. However, having done the tasks there is an opportunity for reviewing each other's tasks and for bearing in the displayed sources and educational materials.
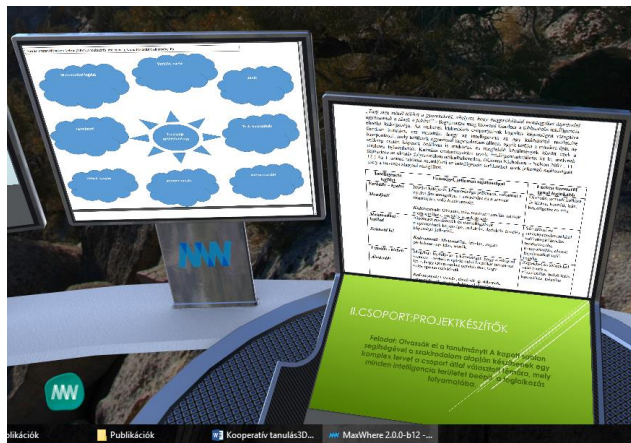

Figure 4
The "desk" of Group 2 with task description, helping template, and study
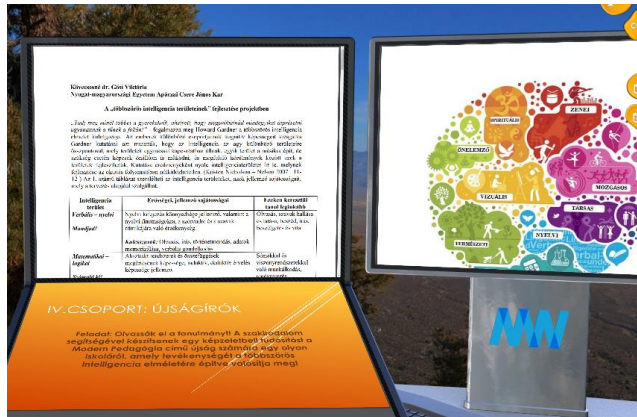

Figure 5
The "desk" of Group 3 with task description, helping template, and study

Figure 6
The "desk" of Group 4 with task description, helping template, and study

III   Reflection

"Literary groups" introduced the group tasks. After the demonstration of the groups I briefly summarised the experiences with the help of PowerPoint slides. After that we evaluated the classroom activity with the help of self-assessment and team-assessment sheets:

Table 4
Self-assessment sheet

Self-assessment sheet:
What I really liked when solving tasks:
What I would like to know more about related to the topic (questions arisen during processing):
What was a problem during the work:
What I would do differently next time:
My most decisive experience during my assignment was:
What I bring with me to my teaching practices:

Table 5

Team-assessment sheet

(Lénárd-Rapos 2009:84)

Name: …………………………………….. Date: ……Group:…………………				
	Excellent	**Very good**	**Acceptable**	**Amateur solution**
The participation of group members	every group member worked committedly	at least three fourth of the group was active	at least half of the group represent and accept the thoughts of the group	only one or two members of the group are active
Sharing responsibility	responsibility is equally shared	responsibility sharing affects most of the group members	responsibility sharing affects only half of the group	trust is related to only one or two group members
The quality of interactions	paying attention to each other and constructivism is typical, members reflect to each other's ideas, they discuss their thoughts	members communicate adeptly, and talk about the tasks in a friendly way	they have some real interactions, they pay attention to each other, some talk about something else	a few interactions, brief dialogues, there are inattentive or careless members
Intragroup roles	every member has well-circumscribed and accepted role, group members execute the tasks assigned to the roles	every member has well-circumscribed role, but roles are unclear	there are designated roles, but the system is incoherent and unclear	there are no thoughtful and designated roles in the group
Recommendations, pieces of advice for individual and group work:				

Conclusions

During my work I wanted to extend and expand my knowledge and experience gained through teaching cooperative learning, and to link them to a technology which fits to the world of the digital culture as well as to the habits and learning methods of primary and secondary school pupils, university students and young adults. Learning activity supported with VR space grabbed the attention of the students, and this new type of learning environment motivated them.

I definitely found it important that besides digital sources, some copies of studies and other teaching materials should be available for students for the group work in printed form in the lesson. The reason for this is that everybody has different learning styles with different habits, and besides some are visual type people. It is also important that motoric type young people who are used to noting and flipping through a book could also find the learning methods which are appropriate for them. However, it is a great help for the lecturer if the amount of photocopies decreases and the templates, forms, and task sheets used for cooperative learning techniques could be stored in a single place and in a form in which students can work and make the tasks, result available for others.

A definite advantage is that the space enables the storage of curriculum, teaching materials and illustrative videos related to the topic in a single place, and for students it also facilitates obtaining credible information. It is not necessary to search for information for hours because the most important information and applications are constantly available. It may result in a more organised knowledge base and a result in a collection for the lecturer as well. I think that VR digital technology, which is built on classical teaching methods, highly develops the creativity and the digital competences of both the lecturer and the student.

References

[1]   A tanulás tervezése és értékelése (Bárdossi Ildikó, Dudás Margit) Educatio Társadalmi Szolgáltató Nonprofit Kft., Bp. 2009

[2]   A tanítás – tanulás hatékony szervezése (Alkotószerk.: Réthy Endréné) Educatio, Bp. 2008

[3]   Bárdossy Ildikó – Dudás Margit – Pethőné Nagy Csilla – Priskinné Rizner Erika: A kritikai gondolkodás fejlesztése. Az interaktív és reflektív tanulás lehetőségei. Pécsi Tudományegyetem, Pécs – Budapest, 202, pp. 172-174

[4]   Didaktika (szerk.: Falus Iván) Nemzeti Tankönyvkiadó, Bp. 2003

[5]   Cseh Ágnes Gabriella: A tanulói értékelés széles körű értelmezése a gyakorlat számára, Taní-tani online folyóirat (http://www.tani-tani.info/082_cseh)

[6]   Dr. Gyarmathy Éva: Diszlexia a digitális korban, Műszaki Kiadó, Bp. 2012

[7]   Hortobágyi Katalin: Projekt kézikönyv, Altern füzetek, Iskolafejlesztési Alapítvány OKI Iskolafejlesztési Központ Bp., 1991

[8]   Kádár Annamária: Az érzelmi intelligencia fejlődése óvodás-és kisiskolás korban, Ábel Kiadó, Kolozsvár, 2012

[9]   Kimmel Magdolna-Falu Iván: A portfólió fogalma, készítésének céljai és típusai In.: A tanítás-tanulás hatékony szervezése (szerk.: Réthy Endréné) Educatio, Bp. 2008

[10]   Kotschy Beáta: Kooperatív tanulás, In.: Pedagógiai lexikon II (szerk.: Báthory Z. - Falus Iván) Keraban Kiadó, Bp. 1997

[10]   Kovátsné Németh Mária: Fenntartható oktatás és projektpedagógia, In.: Új Pedagógiai Szemle, OKI, Bp. 2006

[11]   Kováts-Németh Mária: Erdőpedagógiától a környezetpedagógiáig, Comenius Kft. Pécs, 2010

[13]   Kristen Nicholson –Nelson: A többszörös intelligencia Scholastic, SZIA Bp., 2007

[14]   Kövecsesné G. Viktória: A kooperatív tanulás szerepe, jelentősége az oktatási folyamatban, Katedra a szlovákiai magyar pedagógusok és szülők lapja, Katedra Alapítvány, Dunaszerdahely, 2016, 21-24

[15]   Kövecsesné dr. Gősi Viktória: A digitális korszak oktatásmódszertani kihívásai I., Katedra a szlovákiai magyar pedagógusok és szülők lapja, Katedra Alapítvány, Dunaszerdahely, Szlovákia XXV/7, ISSN 1335-6445, 2018, pp. 21-22

[16]   Lénárd Sándor – Rapos Nóra: Fejlesztő értékelés. Gondolat, Budapest, 2009

[17]   Lénárd Sándor – Rapos Nóra: MAGtár – Ötletek tanítóknak a fejlesztő értékeléshez és az adaptív tanulásszervezéshez OKI, BP. 2006

[18]   M. Nádasi Mária: Adaptivitás az oktatásban, Comenius Bt. Pécs, 2001

[19] Németh András – Ehrenhard Skiera: Reformpedagógia és az iskola reformja, Nemzeti Tankönyvkiadó, Bp. 1999

[20]   Óhidy Andrea: Az eredményes tanítási óra jellemzői – kooperatív tanulási formák a gyakorlatban In.: Új Pedagógiai Szemle, OKI Bp. 2011, www.upsz.hu (2011-03-13)

[21]   Spencer Kagan: Kooperatív tanulás, Önkonet, Bp. 2001

[22]   Tari Annamária: Y Generáció, Jaffa Kiadó, Bp. 2010

[23]   Tari Annamária: Z Generáció, Tericum Kiadó, Bp. 2011

The Evaluation of BCI and PEBL-based Attention Tests

J. Katona[1], A. Kovari[2]

[1]Institute of Information Technology, University of Dunaújváros, Táncsics M 1/A, 2400 Dunaújváros, Hungary, e-mail: katonaj@uniduna.hu

[2]Institute of Engineering, University of Dunaújváros, Táncsics M 1/A, 2400 Dunaújváros, Hungary, e-mail: kovari@uniduna.hu

New technological advances of the 20th and 21st Centuries provide several new opportunities for engineers in the future. Modern engineering methods feasible by these new technical solutions, however, cannot meet expectations in all fields and situations without adequate knowledge and competence. Spreading new and modern engineering methods as well as acquiring new applications is a crucial issue in education. In brain research, which is one of the most significant research areas of the past decades, many new results and meters have appeared that could be used in engineering methods, too. Based on brain activity observation, new meters open up new horizons in engineering applications. Electroencephalogram-based brain activity observation processes are very promising and have been used in several engineering research primarily for implementation of control tasks. In this paper, an EEG-based engineering research work is demonstrated, which supports the acquirement of practical knowledge and can measure cognitive ability with a device capable of brain activity observation. In the engineering research task, a brain-computer interface (BCI) had to be developed for the measurement of the average level of attention. The results of the BCI have been compared and contrasted to the results of two tests applied in cognitive psychology, the PEBL Continuous Performance Test (pCPT) and the PEBL Test of Attentional Vigilance (pTOAV). It can be stated that the results of the procession developed in this research and the results of the pCPT and the pTOAV tests are in correlation.

Keywords: brain-computer interface; Continuous Performance Test; Test of Attentional Vigilance; electroencephalogram; PEBL

1 Introduction

With the continuous development of IT systems, new opportunities have also become available in human-computer interaction. These human-machine interface systems have appeared in many applications and research areas, basically called the field of cognitive infocommunications (CogInfoCom). CogInfoCom, involves

the speechability, communication, linguistic and behavioural interaction analysis, face and gesture recognition, brain-computer interface (BCI), human cognitive interface – virtual and real avatars dealing with the complex mixture of human and artificial cognitive capabilities in human computer interaction processes [48-63]. The socio-cognitive ICT field includes collective knowledge, cognitive networks and their intelligent capabilities. Education and learning are closely related to this area, the CogInfoCom based learning abilities investigating capabilities for learning through modern informatics-based education, the educoaching including education through online collaborative systems and virtual reality solutions for example [64-80]. The human computer interaction processes including CogInfoCom aided engineering also cover this area, the industrial applications of CogInfoCom including production engineering, production management, the cognitive control contains theoretical solutions based on or targeting cognitive and other human body related processes, cognitive robotics and autonomous mental development [81-90].

Owing to research in cognitive neuroscience, several specific functions of brain activity are known, but to deeply understand the basic physiology of the brain and nervous system several revolutionary developments are now affecting this research [1]. Understanding the operation of the brain is of great importance in measuring and interpreting brain waves. The electrical and magnetic phenomena of the neural functions can be observed during brain operation by electrophysiology [2]. The most common device for the electrophysiological observation of the neural functioning of the brain is electroencephalography, which is used for observation and registration of brain electrical signals generated by brain activity [3]. EEG signals are mostly processed by the quantitative EEG (QEEG) method, where the frequency spectrum of the EEG signals is observed [4].

The EEG-based observation methods are used in several clinical and psychological examinations [3]. Brain Laboratories at New York University Medical Center have already published a computer-assisted differential diagnosis of brain dysfunctions in 1988 [5]. In this research, a computer analysis-based QEEG signal processing was used, which is a highly sensitive way to give specific interpretation of measurement results and can evaluate human electroencephalography, [6]. In the nineties, the primary use of QEEG in clinical practice included organicity detection, diagnoses of discriminant functions and epileptic source localization. [7] The earliest psychiatric use of EEG was imaging human cortical brain activity, but other application possibilities of the EEG have diagnosed the Attention Deficit Disorder [8], Learning Disability [9], sleep disorders, Alzheimer's disease [10] and stroke [11], for example. Attention-deficit/hyperactivity disorder (ADHD) has been researched to characterize and quantify the main characteristics of this disease for decades. [8]

Measuring electroencephalogram (EEG) activity requires complex, expensive, intimidating and immovable equipment. As a result of continuous development in

recent years, new, mobile EEG biosensor-based embedded devices are available for new entertainment applications, cognitive infocommunications [25] or educational purpose [36-46]. In these applications, the connection between brain activity observed by the EEG and the induced function is effectuated by a brain-computer interface (BCI) [12]. The latest brain-computer interfaces applied with biosensors, and modern signal processing units have become cheaper and mobile because of their simple structure, while their accuracy is similar to that of the clinical EEG devices [12, 13]. This technology is mainly used for solving control tasks in engineering research, for example robot [14], helicopter [15], car [16] or prostheses [30] control.

The paper is organised into five sections. Section II describes the primary objectives of the EEG-based engineering research, the theoretical background of the EEG-based measurement method and the connection between brainwaves and attention. Section III presents the main steps of designing a computer-based EEG system, in this case, an attention level measurement system. The detailed implementation is described in Section III as well. In Section IV, the evaluation of the BCI-based attention level test is compared to the results of two neuropsychological attention tests, the PEBL Continuous Performance Test (pCPT) and the PEBL Test of Attentional Vigilance (pTOAV). In Section V, the main conclusions are drawn.

2   The EEG-based Engineering Research

2.1   The EEG Measurement and Brain Waves

Electrical activity in the brain and the electrical signals resulting from ionic current flows within neurons can be measured by the EEG method placing a sensor on the scalp [17], [18]. There are millions of neurons in the brain and each of these neurons generate a minimal electric voltage field. The aggregated amplitude of these electrical signals typically ranges from about 1 uV to 100 uV in case of a healthy adult, and these messages can be detected and recorded on the scalp [17], [18].

Patterns and frequencies of these emitted analogue electrical signals are typical in different brain activities. The brain signals are commonly referred to as brain waves and their frequency spectrum are typical in different mental states [19] and can be readily determined by digital signal processors. Several new EEG-based headsets can detect these signals, for example, NeuroSky [20] or Emotive [21].

The strength of different brain wave types can be calculated by FFT (Fast Fourier Transform) algorithm, which is a mathematical method used in EEG analysis to

investigate the composition of an EEG signal. In this way, the frequency distributions (as a spectrum of brain waves) can be observed by using FFT algorithm after filtering, for example Kalman filters [47]. The spectrum of brain waves is very sensitive to the mental and emotional states of the brain, so this attribute is used to monitor mental activity [19]. Table 1 below contains the commonly-recognized brain wave frequencies, which are generated by different types of brain activity [22].

Table 1

Properties of Brain Waves [20]

Brainwave Type	Frequency range	Mental states and conditions
Delta	0.1Hz to 4Hz	Deep, non-REM sleep, unconscious
Theta	4Hz to 8Hz	Intuitive, creative, recall, fantasy, imaginary, dream
Alpha	8Hz to 13Hz	Relaxed, but not drowsy, tranquil, conscious
Low Beta	13Hz to 16Hz	Formerly SMR, relaxed yet focused, integrated
Midrange Beta	16Hz to 20Hz	Thinking, aware of self and surroundings
High Beta	20Hz to 30Hz	Alertness, agitation
Gamma	30Hz to 80Hz	Motor functions, higher mental activity

2.2   A NeuroSky EEG-based MindWave Headset

NeuroSky has been developing EEG-based measuring devices for years with the co-operation of some universities, for example, Stanford University, Carnegie Mellon University, University of Washington, University of Wollongong and Trinity College [23]. Measured and processed data provided by a NeuroSky's device has been compared and evaluated with the Biopac system, in which traditional, wet electrodes are used widely in medical examinations and research [24]. The power spectra in the 1-50 Hz range were observed based on the measurement data provided by the NeuroSky's and Biopac device, which is the frequency spectrum of specific brain waves. According to the validating results, the correlation factor between the power spectra provided by the two devices is larger than 0.7, and this means that results produced by the two devices are nearly identical [13]. The MindWave EEG headset (Figure 1) is a lightweight, portable device with wireless communication supporting Windows and Mac Operating Systems [24]. It uses only one AAA battery, and the device can run 6-8 hours. The main parameters of this device are [24]:

- Weighs 90 g;
- 30 mW rated power;
- 50 mW max power;
- 2420 – 2471 GHz RF frequency with 10 m range;
- 57600 Baud;
- 1 mV pk-pk EEG maximum signal input range;
- 12 bits ADC resolution with a 512 Hz sampling rate;
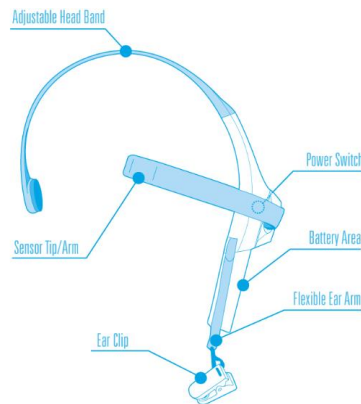- 1 Hz calculation rate.

Figure 1
MindWave EEG headset structure [24]

2.3 The Attention Level and Brain Waves

The connection between attention and brain waves was observed in the 1970s, and an EEG-based attention analyser was patented [26]. The method of attention measurement is based on the FFT spectrum intensity examination of brain waves [20]. From the observations, it could be claimed that the components of brain waves, the amplitude of alpha brain waves is rather low, while in the inattentive state it is high [26]. For examination of attention, the Frontopolar1 (Fp1) measuring position is the most suitable [27] which is located on the frontal lobe such as MindWave EEG headset uses. The difference in alteration of brain waves is the base of the patented attention analyser. Several parameters of brain signals can be determined with digital signal processing algorithms. Power spectra could be calculated using discrete Fourier-transformation (DFT) algorithm and based on the resulting brain wave intensity, results can be evaluated [28]. Using the FFT on EEG signals, the intensity of brain waves and the level of attention can be determined, which is higher when the spectrum of Beta activity is stronger and Alfa is weaker, according to Table 1.

3 The BCI Software

Brain signals are measured by EEG technology – measuring, digitalization, screening of voltage variation resulted from electrical activity of the brain – and during partial evaluation, BCI systems supply processed information. [33], [34]. With the consumption of new information, we can operate other applications and instruments. The BCI system accomplishes a sort of connection between the

individual and the working system. When carrying out BCI-based directions, the following viewpoints need to be taken into consideration [29]:

- the special features and different types of BCI instrument users.
- the way of signal processing and evaluation of the BCI instrument.
- the way of feedback and proper directions.
- the application directed by the BCI.

The whole of the effectiveness of the usage and the user's contentment determines the ISO 9241-210 (2010) with the use of the product. The efficiency determined in international standard shows how precisely individuals can fulfill the appointed purpose with their usage. The effort and time invested by users determine effectiveness. The contentment of an individual depends on convenience, efficiency and satisfaction according to user's expectations. [31]

The purposes of interface integration in brain computers are summarized in the following points [32]:

- functions required from user must be practicable, and its basis is to recognize and to forward the intention of the individual.
- representation of available functional opportunities for the user.
- control of action and connected actions execution.
- service of appropriate responses and representation for user to carry out appointed function with assistance of application's graphic user interface.

Different structural alternatives and possible limits of the forming system have to be taken into consideration during brain computer interface design. During the planning process, various solutions were needed to search and analyze for the emerging problems and validation was applied. For the end of the planning process, only those valid tests were needed to work out which refer to the implementation.

3.1   The Design of BCI the Software

As a first step, a valid and logical design had to be worked out that represents well the operation of the system and writes down its main process readily transparent. Figure 2 illustrates well one possible solution to the problem. The flowchart represents how the whole system communicates interactively with the user. To read files supplied by the EEG headset, a serial communication was needed, where the control of the appropriate work of the port is prominently essential. After setting the port successfully, the program starts a different thread to process file packages, which arrive from the headset: validating values in packages, appropriate processing of file packages and representing proper and processed items in file packages. The creation of the class diagram from UML's static diagram is based on logical diagram, as a well-planned and specified class diagram makes the implementation task easier. The execution of the software

implementation of two classes is necessary; its object samples process the data arriving from the headset and represents it on the computer screen in the form of a column graph. Furthermore, the implementation of two partial classes is needed; its objects are responsible for visual appearance and case variation of different graphical items. With the use of the logical and the permanent models, one of the most significant design tasks is the planning of the transition and co-operation of the status of the variable object. As several dynamic models are used in UML language, we used the so-called sequence diagram. Besides the static and the dynamic point of system view, it was essential to design the application from the aspect of user case of the system because with this we can easily measure the system function and behaviour with appointing characters and tasks from the user aspects.
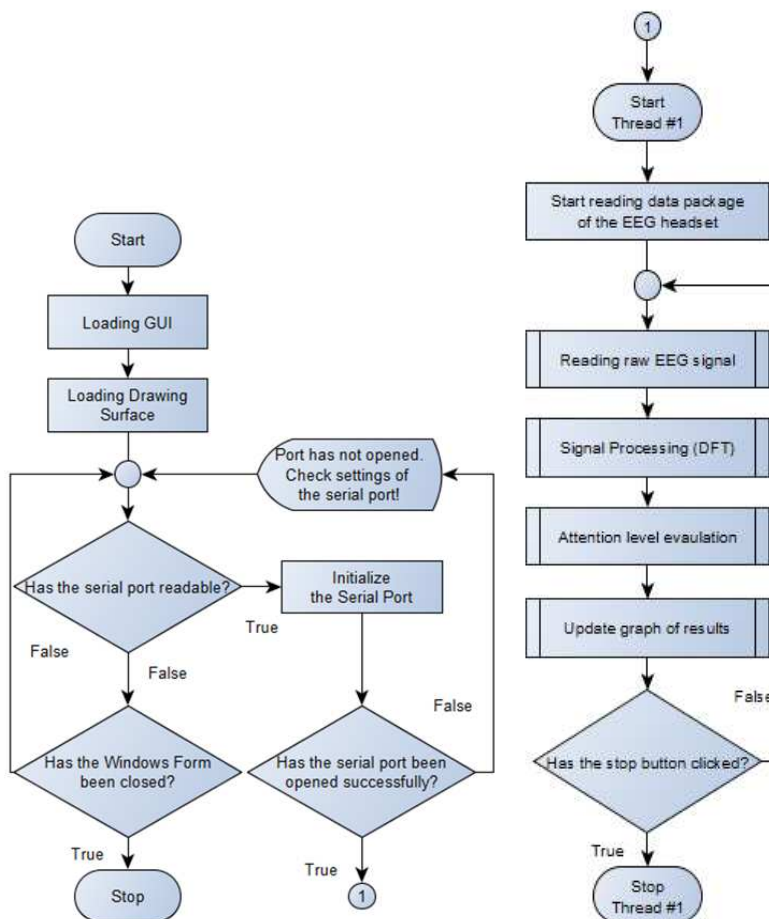
Figure 2
Logical functioning of the brain-computer system

3.2   The Implementation of the BCI Software

The software has been implemented in Microsoft Visual Studio. The development environment supports object-oriented high-level C# programming language, which is the most widely used language in Windows operating system programming. The program was divided into two main sections: data-processing and view. The data-processing component performs reading, conversion and processing of the data which arrive from the headset through serial connection, and the view part fulfills the representation of the appointed signs with the help of column and timing diagram (Figure 3). The serial port parametrization menu is visible in the window bottom left corner. After the setup of the serial port, a popup window appears to open the selected port. After successfully establishing the communication channel, we can start the measurement of brain activity by clicking "Reading Waves" button. The calculated and average values of the recorded data are visible in column graph form. The time functions of a given measurement can be examined in the top right part.
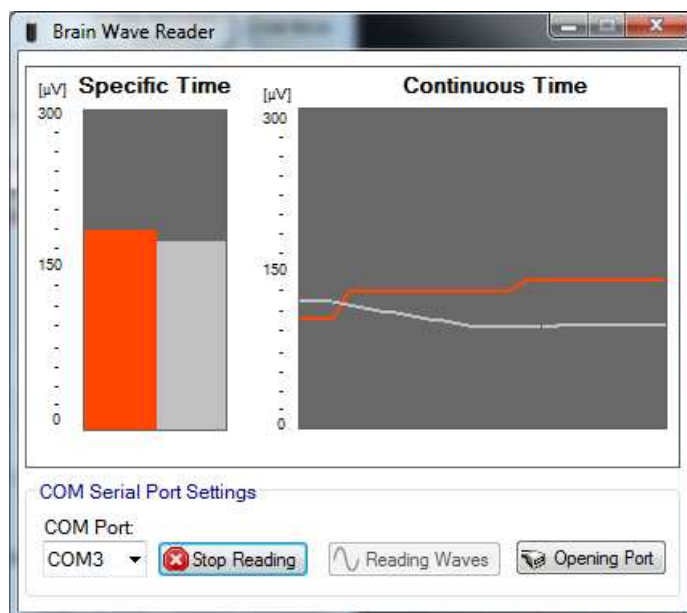

Figure 3
User Interface of the Brain-Computer Interface software

4   The Tests and Examination Results of Attention Level Meter Compared to pCPT and pTOAV

4.1   The pCPT and pTOAV Neuroscience Tests

The pCPT and pTOAV neuroscience tests are used to evaluate the attention level meter [35]. The pCPT test (Figure 4) examines concentration during a test that runs for a relatively long time, for approximately 14 minutes. During this examination, 360 letters are shown to the test subjects who should press the space key if the shown letters are not X. Having finished the pCPT, the software evaluates the results immediately, and it is available in report format.
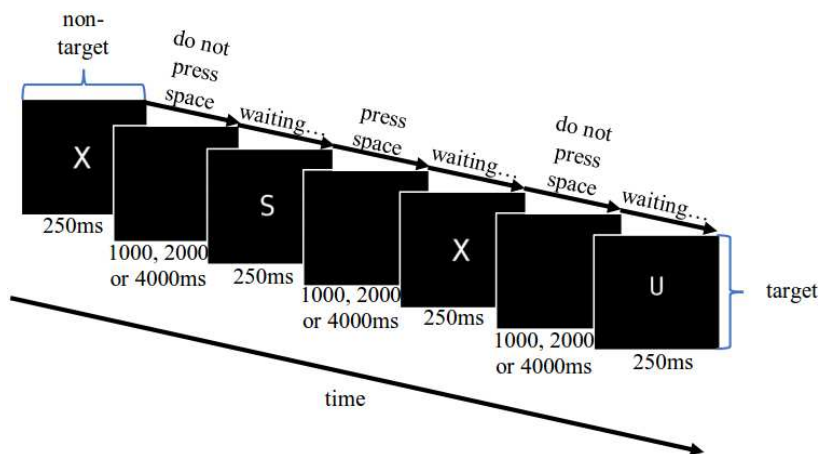
Figure 4

Test subjects must respond by pressing the space bar to all stimuli except the X.

T.O.V.A. was first used by psychologists and neurologists to examine attention deficit disorder, but it is also used in non-medical areas, such as schools or rehabilitation programs. The pTOAV test is a simple implementation of T.O.V.A.; it is a concentration/alertness test, which only examines the reaction to visual stimuli. As with Conner's continuous performance test, target gems are distinguished for this type of test as well as anti-target stimuli. In the test, a black square is located in a white square on the computer screen, randomly on either the bottom or top parts (Figure 5). Test participants should press the space key if the black square is located on the top.
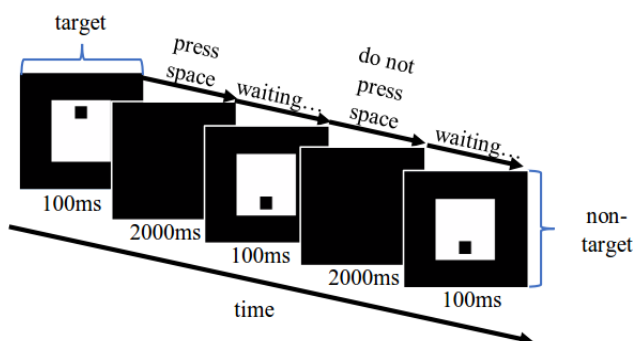
Figure 5

A black square appears randomly on the screen in a white square. Test subjects must respond only to targets when the black square is on the top. For the first half of the test, targets are rare; for the second half, they are frequent.

4.2 The Test Subjects

34 high school students participated in this experiment. All test subjects were healthy, with no history of psychiatric or neurological disorders. The age range was 14-18, the average age was 16.2, range ±1.4; 47% of girls.

4.3 The Statistical Analysis

The statistical evaluation of data in the case of the PEBL tests was made by an interval scale, while the SPCI 23 (SPSS, Inc., Chicago, IL) program pack was used on an ordinal scale for the BCI, therefore, non-parametric tests were applied for BCI results, and parametric tests were carried out with PEBL test results if parametric test conditions were fulfilled. Regarding the differences between the morning and afternoon results of PEBL tests, where test subjects are independent of each other, the pattern of results followed a normal distribution. Therefore, a related-pattern t-test was applied where the effect size was determined by Cohen d-value. As during the PEBL tests, the average attention registered by the BCI system was measured on an ordinal scale, Wilcoxon-signed rank test was carried out. In the case of the used statistical tests, the $p < 0.05$ value was found to be significant.

4.4 The Results and Discussion

During the first quantitative experiment, dependency relationship and collected metric data were examined and correlation was analysed. The next step was to find connections with the help of an independent and a dependent variable between pCPT/BCI and pTOAV/BCI attention level results.

4.4.1   Comparing the pCPT and BCI Results

The correlations and relationships between the obtained test results and BCI system results can be estimated and evaluated on the whole sample, i.e., on all test participants. To observe the correlation between individual measurements, Spearman's correlation was used, because the BCI variable was determined on an ordinal scale type, and our data was monotonic. It can be concluded that the pCPT and BCI results obtained in the morning show a significant positive correlation (Figure 6a), where r_s=0.693 p<0.01 (2-tailed). Moreover, the pCPT and BCI results obtained in the afternoon also show a significant positive correlation (Figure 6b), where r_s=0.710 p<0.01 (2-tailed).

Furthermore, a significant difference was found between morning ($M \pm SD$=315.34±5.19; D(32)=0.133 p=0.158) and afternoon ($M \pm SD$=308.81±5.92; D(32)=0.105 p=0.200) t(31)=16.16 p<0.01 (2-tailed), d=1.17 pCPT test results.

According to the Wilcoxon signed-rank test results, a significant difference (T=0 Z=-4.94 p<0.01 (2-tailed) r = 0.87 was observed in pCPT and BCI results, in the morning (Mdn=52.05) and afternoon (Mdn=45.05) hours.
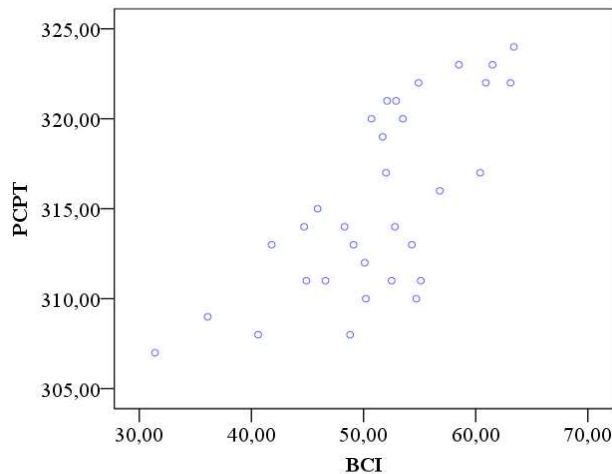

Figure 6a

Based on the results, it can be concluded that the pCPT and BCI results, obtained in the morning, show a significant positive correlation
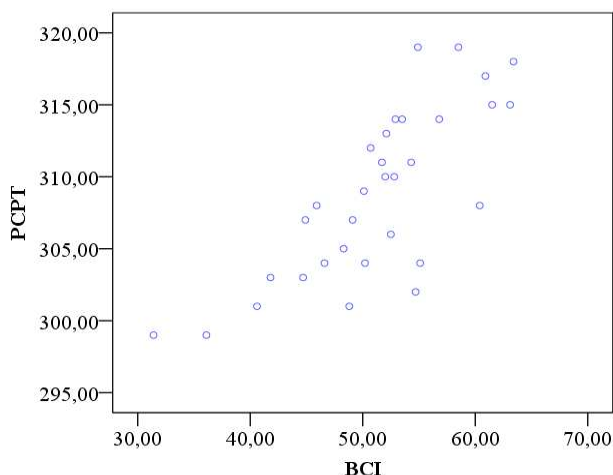
Figure 6b

The pCPT and BCI results, obtained in the afternoon, also show a significant positive correlation

A more detailed overview of correlation evaluation is given in Table 2.

Table 2

Spearman-correlation analysis for the whole sample (N = 32) on the results of the pCPT test and the difference of the mean value characteristic of the level of attention determined by the BCI

Period	Test	$M \pm SD$[1]	Correlation	p-value
morning	pCPT	315.344±5.191	0.69	<0.01 (2-tailed)
	BCI	51.259±7.401		
afternoon	pCPT	308.813±5.916	0.71	<0.01 (2-tailed)
	BCI	44.975±6.635		

[1]The arithmetic mean of the difference of the correct responses of test subjects for target stimulus

As seen in Figure 7a, medians differ in comparison to the bottom and top quartiles, so it generally appears that test subjects achieved better results in the morning hours, in addition, data grouping is rather above the median, while the results were weaker in the afternoon hours from all aspects and data disposition from the median was even smoother. Figure 7b shows that medians differ in comparison to the bottom and top quartiles and it generally appears that test subjects achieved higher level of attention in the morning hours. In the afternoon hours, the tests show decreased level of attention and data grouping from the median was smoother, too.
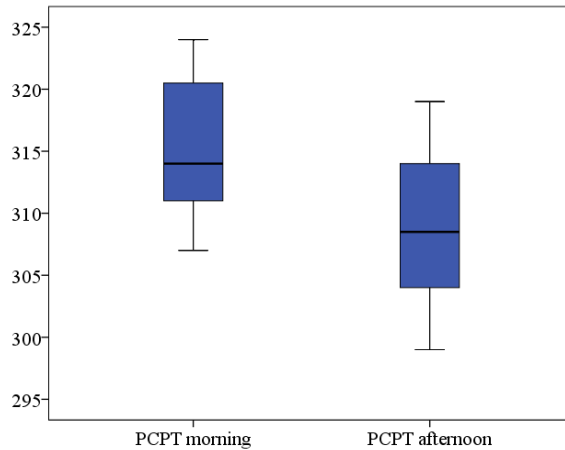
Figure 7a

a) There is a significant difference between the results measured by the pCPT in the morning and afternoon hours.
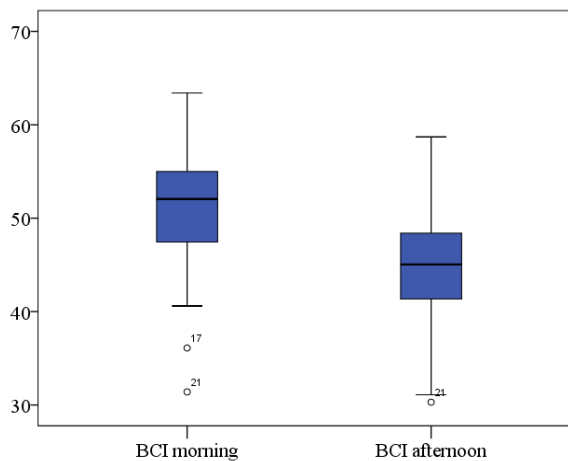

Figure 7b

b) There is a significant difference between the results of average attention level measured by the BCI system in the morning and afternoon hours.

4.4.2   Comparing the ₚTOAV and BCI Results

Another aim of this study was to examine the relationship between the pTOAV test and the average level of attention provided by the BCI system. The obtained correlations and relationships between the test results and the measurement provided by the BCI system can be estimated and evaluated on all samples, on all

test subjects. Spearman's correlation was used with two-sided tests to specify the correlation because in case of the BCI variable, ordinal scale type was determined, and our data were monotonic.

The results show that pTOAV and BCI results obtained in the morning have a significant positive correlation (Figure 8a), where r_s=0.73 p<0.01 (2-tailed). The pTOAV and BCI results in the afternoon also show a significant positive correlation (Figure 8b), where r_s=0.72 p<0.01 (2-tailed).
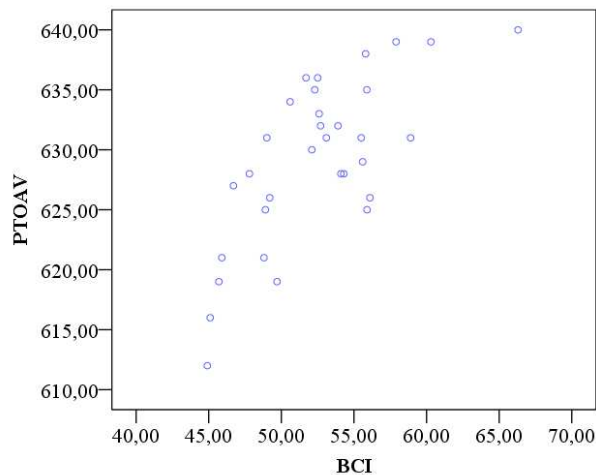

Figure 8a
The results show that the pTOAV and BCI results obtained in the morning show a significant positive correlation
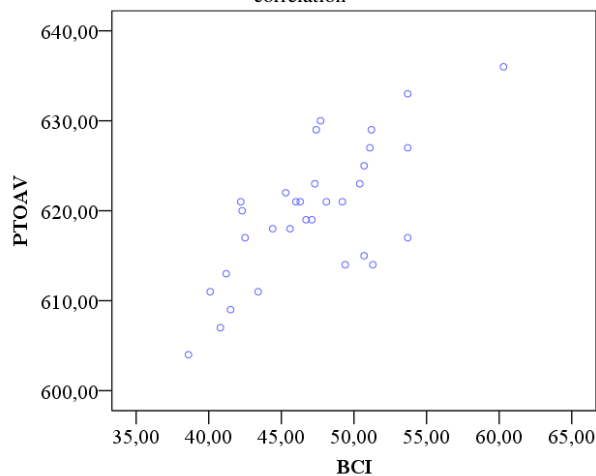

Figure 8b
pTOAV and BCI results in the afternoon also show a significant positive correlation

More details of the evaluation of correlation can be seen in Table 3.

Table 3

Spearman-correlation analysis for the whole sample (N = 32) on the results of the pTOAV test and the difference of the mean value characteristic of the level of attention determined by the BCI

Period	Test	M±SD[1]	Correlation	p-value
morning	PTOAV	629.156±6.933	0.73	<0.01 (2-tailed)
	BCI	52.493±4.803		
afternoon	PTOAV	619.843±7.445	0.72	<0.01 (2-tailed)
	BCI	47.184±4.842		

[1]The arithmetic mean of the difference between the correct response of test subjects for the target stimulus

Moreover, pTOAV tests in the morning ($M\pm SD$=629.16±6.93; $D(32)$=0.105 p=0.200) and afternoon ($M\pm SD$=619.84±5.92; $D(32)$=0.095 p=0.200) have a significant difference $t(31)$=13.29 p<0.01 (2-tailed), d=1.29

The results of the Wilcoxon-signed rank tests show that the difference between the average level of attention measured by the BCI system was significant (T=0 Z=-4.94 p<0.01 (2-tailed) r=0.87) in the morning (Mdn=52.55) and afternoon (Mdn=47.20) hours.

According to Figure 9a medians differ in comparison to the bottom and top quartiles and it can be seen that in the morning, the test subjects achieved a higher level of attention and data disposition of the afternoon results is more noticeable below the median.

Figure 9b shows that the medians differ in comparison to the bottom and top quartiles and it can be seen that in the morning, the BCI system recorded higher level of attention, while the data disposition is smoothly distributed around the median. In the afternoon hours, the results of the BCI system and the pTOAV test have decreased, and distribution from the median was even smoother.
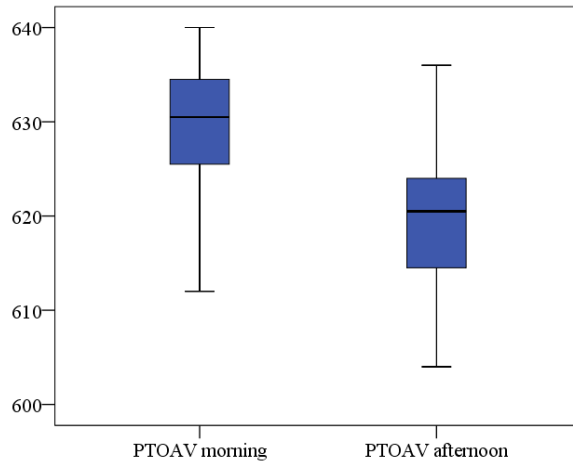
Figure 9a
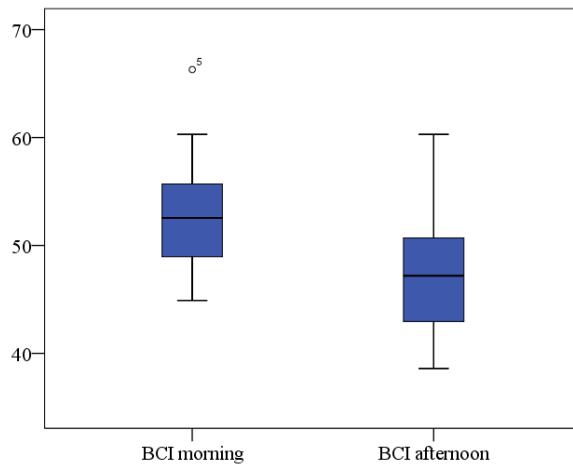There is a significant difference between the pTOAV test results in the morning and afternoon

Figure 9b
There is a significant difference between the results of average attention level measured by the BCI
system in the morning and afternoon hours

Conclusions

With regard to the advantages of the processed BCI system, it is visible based on the test results that relatively high, above 0.6 correlation is shown between the test results of both the morning and the afternoon hours, and it shows a strong relationship between the observed characteristics. This means that comparing to the applied test-based measuring methods of the examination of attention; the implemented BCI system could be an alternative method to investigate attention level.

The paper presented a new application area of the BCI system with psychological measurement tests. The research implementation includes the BCI system, the evaluation of test results and calculation of the relationship between the BCI and the related PEBL tests.

Acknowledgement

References

[1]   F. E. Bloom, A. Lazerson, Brain, Mind, and Behavior. New York, NY: W. H. Freeman and Company, 2nd ed., 1985

[2]   M. Scanziani, M. Häusser, "Electrophysiology in the age of light," Nature, Vol. 461, pp. 930-939, 2009

[3]   E. Niedermeyer, F. L. da Silva, Electroencephalography: Basic Principles, Clinical Applications, and Related Fields. New York, Lippincot Williams & Wilkins, 5th ed., 2012

[4]   R. J. Davidson, D. C. Jackson, C. L. Larson, Human Electroencephalography in Handbook of Psychophysiology. Cambridge, UK: Cambridge University Press, 2nd ed., pp. 27-52, 2000

[5]   E. R. John, L. S. Prichep, J. Firdman, P. Easton, "Neurometrics: Computer-assisted differential diagnosis of brain dysfuncitons," Science, Vol. 239, pp. 162-169, 1988

[6]   F. H. Duffy, J. R. Hughes, F. Miranda, P. Bernad, P. Cook, "Status of Quantified EEG (QEEG) in Clinical Practice," Clinical Electroencephalography, Vol. 25, No. 4, pp. 6-22, 1994

[7]   Z. Z. Major, A. D. Buzoianu, L. Perju-Dumbravă, I. Mărginean, I. C. Bocşan, K. A. Major, "QEEG: Relative power findings in epilepsy," Therapeutics, Pharmacology and Clinical Toxicology, Vol. 14, No. 4, pp. 269-273, 2010

[8]   S. K. Loo, S. Makeig, "Clinical utility of EEG in attention-deficit/hyperactivity disorder: a research update," Neurotherapeutics, Vol. 9, No. 3, pp. 569-587, 2012

[9]   J. F. Lubar, K. J. Bianchini, W. H. Calhoun, E. W. Lambert, Z. H. Brody, H. S. Shabsin, "Spectral analysis of EEG differences between children with and without learning disabilities," Journal of Learning Disabilities, Vol. 18, No. 7, pp. 403-408, 1985

[10]   J. Dauwels, F. Vialatte, A. Cichocki, "Diagnosis of Alzheimer's disease from EEG signals: where are we standing?," Current Alzheimer Research, Vol. 7, No. 6, pp. 487-505, 2010

[11] K. Herron, D.-J. Dijk, P. Dean, E. Seiss, A. Sterr, "Quantitative Electroencephalography and Behavioural Correlates of Daytime Sleepiness in Chronic Stroke," BioMed Research International, Vol. 2014, p. 11, 2014

[12] M. A. Lebedev, M. A.L. Nicolelis, "Brain-machine interfaces: past, present and future," Trends in Neurosciences, Vol. 29, No. 9, pp. 536-546, 2006

[13] NeuroSky, Brain Wave Signal (EEG) of NeuroSky. NeuroSky Inc., 2009

[14] K. Bouyarmane, J. Vaillant, N. Sugimoto, F. Keith, J. Furukawa, J. Morimoto, "Brain-machine interfacing control of whole-body humanoid motion," Frontiers in Systems Neuroscience, Vol. 8, No. 138, pp. 1-10, 2014

[15] K. LaFleur, K. Cassady, A. Doud, K. Shades, E. Rogin, B. He, "Quadcopter control in three-dimensional space using a noninvasive motor imagery-based brain-computer interface," Journal of Neural Engineering, Vol. 10, No. 4, p. 046003, 2013

[16] S. Haufe, M. S. Treder, M. F. Gugler, M. Sagebaum, G. Curio, B. Blankertz, "EEG potentials predict upcoming emergency brakings during simulated driving," Journal of Neural Engineering, Vol. 8, No. 5, p. 056001, 2011

[17] F. S. Tyner, J. R. Knott, W. B. Mayer Jr., Fundamentals of EEG Technology: Vol. 1: Basic Concepts and Methods. USA, Lippincott Williams & Wilkins, 1st ed., 1983

[18] F. S. Tyner, J. R. Knott, W. B. Mayer Jr., Fundamentals of EEG Technology: Vol. 2: Clinical Correlates. USA, Raven Press, 1st ed., 1989

[19] G. Buzsaki, Rhythms of the brain. Oxford University Press., 2011

[20] W. Sałabun, "Processing and spectral analysis of the raw EEG signal from the MindWave," Przeglad Elektrotechniczny, Vol. 90, No. 2, pp. 169-174, 2014

[21] N. A. Badcock, P. Mousikou, Y. Mahajan, P. de Lissa, J. Thie, G. McArthur, "Validation of the Emotiv EPOC® EEG gaming system for measuring research quality auditory ERPs," PeerJ, Vol. 38, p 17, 2013

[22] E. Thompson, The neuroscience of meditation: An introduction to the scientific study of meditation impacts the brain, iAwake Technologies, p. 10, 2014

[23] Scientifics Direct, Inc. (2014, Dec. 10). NeuroSky MindWave - EEG Brain Wave Activities [Online] Available: http://www.scientificsonline.com/product/neurosky-mindwave

[24] NeuroSky, MindWave User Guide. NeuroSky Inc., 2011

[25] P. Baranyi, A. Csapo, and Gy. Sallai: Cognitive Infocommunications (CogInfoCom) Springer, 2015

[26]   K. Montor, "Attention-level analyzer," U.S. Patent 3 877 466, April 15, 1975

[27]   Cardinal RN, Parkinson JA, Hall J, Everitt: Emotion and motivation: the role of the amygdala, ventral striatum, and prefrontal cortex, Neuroscience & Biobehavioral Reviews, 26:321352

[28]   A. V. Oppenheim, R. W. Schafer, J. R. Buck, "Discrete-time signal processing", Upper Saddle River, N.J.: Prentice Hall, 1999

[29]   A. Kübler, B. Blankertz, K. R. Müller, C. Neuper, "A model of BCI-control", 5th International Brain-Computer Interface Conference, pp. 100-103, 2011

[30]   Ungureanu G. M. and R. Strungaru, "Considerations on EEG-based BCIs Applied in the Control of Intelligent Prostheses," Nonlinear Optics and Quantum Optics, October 2009, Vol. 39, issue 2-3, pp. 257-269

[31]   C. Zickler, et al., "A brain-computer interface as input channel for a standard assistive technology software," Clinical EEG and Neuroscience, Vol. 42, pp. 236-244, 2011

[32]   J. R. Wolpaw, N. Birbaumer, D. J. McFarland, G. Pfurtscheller, T. M. Vaughan, „Brain-computer interfaces for communication and control," Clinical Neurophysiology, Vol. 113, pp. 767-791, 2002

[33]   T. O. Zander and C. Kothe, "Towards passive brain-computer interfaces: applying brain-computer interface technology to human-machine systems in general," Journal of Neural Engineering, Vol. 8, No. 2, p. 025005, 2011

[34]   T. O. Zander, C. Kothe, S. Jatzev and M. Gaertner, "Enhancing Human-Computer Interaction with Input from Active and Passive Brain-Computer Interfaces," Brain-Computer Interfaces Human-Computer Interaction Series, Springer, pp. 181-199, 2010

[35]   S. T. Muller, B. J. Piper, "The Psychology Experiment Building Language (PEBL) and PEBL Test Battery", Journal of Neuroscience Methods, Vol. 222, pp. 250-259, 2014

[36]   K. Biró, Gy. Molnár, D. Pap, Z. Szűts: The Effects of Virtual and Augmented Learning Environments on the Learning Process in Secondary School, Proceedings of 8th IEEE International Conference on Cognitive Infocommunications (CogInfoCom 2017) Debrecen, Hungary, 2017, pp. 371-375

[37]   I. Horváth: Innovative engineering education in the cooperative VR environment, Proceedings of 7th IEEE International Conference on Cognitive Infocommunications (CogInfoCom 2016) Wroclaw, Poland, 2016, pp. 359-364

[38]   I. Horváth: Disruptive technologies in higher education, Proceedings of 7th IEEE International Conference on Cognitive Infocommunications (CogInfoCom 2016) Wroclaw, Poland, 2016, pp. 347-352

[39]   E. Gogh, A. Kovacs, G. Sziladi: Application of E-diary to analyze the effectiveness of learning, Proceedings of 8th IEEE International Conference on Cognitive Infocommunications (CogInfoCom 2017) Debrecen, Hungary, 2017, pp. 419-422

[40]   I. Horváth: The IT device demand of the edu-coaching method in the higher education of engineering, Proceedings of 8th IEEE International Conference on Cognitive Infocommunications (CogInfoCom 2017) Debrecen, Hungary, 2017, pp. 379-384

[41]   Z. Kvasznicza: Teaching electrical machines in a 3D virtual space, Proceedings of 8th IEEE International Conference on Cognitive Infocommunications (CogInfoCom 2017) Debrecen, Hungary, 2017, pp. 385-388

[42]   A. D. Kovács: The application opportunities of green roof, as an interactive educational space, Proceedings of 8th IEEE International Conference on Cognitive Infocommunications (CogInfoCom 2017) Debrecen, Hungary, 2017, pp. 389-393

[43]   A. Kutikova, J. Balata, Z. Mikovec: Explorations into ICT Usage and Behavior in Travel Related Activities of Wheelchair Users, Proceedings of 8th IEEE International Conference on Cognitive Infocommunications (CogInfoCom 2017) Debrecen, Hungary, 2017, pp. 231-236

[44]   M. Tariq, L. Uhlenberg, P. Trivailo, K. S Munir, and M. Simic: Mu-Beta Rhythm ERD/ERS Quantification for Foot Motor Execution and Imagery Tasks in BCI Applications, Proceedings of 8th IEEE International Conference on Cognitive Infocommunications (CogInfoCom 2017) Debrecen, Hungary, 2017, pp. 91-96

[45]   A. Kovács, I. Winkler, K. Vicsi: EEG correlates of speech: examination of event related potentials elicited by phoneme classes, Proceedings of 8th IEEE International Conference on Cognitive Infocommunications (CogInfoCom 2017) Debrecen, Hungary, 2017, pp. 115-120

[46]   D. Geszten, B. P. Hámornik, K. Hercegfi: Measurement of team mental model as a part of a new team usability testing method, Proceedings of 8th IEEE International Conference on Cognitive Infocommunications (CogInfoCom 2017) Debrecen, Hungary, 2017, pp. 291-294

[47]   A. Odry, J. Fodor and P. Odry, "Stabilization of a Two-Wheeled Mobile Pendulum System using LQG and Fuzzy Control Techniques", International Journal On Advances In Intelligent Systems, Vol. 9, No. 1, 2, pp. 223-232

[48]   G. Kiss, et al.: Connection between body condition and speech parameters-especially in the case of hypoxia, Proceedings of 5th IEEE International Conference on Cognitive Infocommunications (CogInfoCom 2014) Vietri sul Mare, Italy, 2014, pp. 333-336

[49]   Lambrechts, et al.: Temporal dynamics of speech and gesture in Autism Spectrum Disorder, Proceedings of 5th IEEE International Conference on Cognitive Infocommunications (CogInfoCom 2014) Vietri sul Mare, Italy, 2014, pp. 349-353

[50]   A. K. Varga, and L. Czap.: Development of an online subjective evaluation system for recorded speech of deaf and hard of hearing children, Proceedings of 5th IEEE International Conference on Cognitive Infocommunications (CogInfoCom 2015) Győr, Hungary, 2015, pp. 455-458

[51]   O. Matarazzo, B. Pizzini, C. Greco, M. Carpentieri: Effect of a Chance Task Outcome on the Offers in the Ultimatum Game: The Mediation Role of Emotions, Proceedings of the 7th IEEE International Conference on Cognitive Infocommunications (CogInfoCom 2016) Wroclaw, Poland, 2016, pp. 295-300

[52]   D. Sztahó, M. Gábriel Tulics, K. Vicsi, I. Valálik: Automatic Estimation of Severity of Parkinson's Disease Based on Speech Rhythm Related Features, Proceedings of 8th IEEE International Conference on Cognitive Infocommunications (CogInfoCom 2017) Debrecen, Hungary, 2017, pp. 11-16

[53]   L. Izsó: The significance of cognitive infocommunications in developing assistive technologies for people with non-standard cognitive characteristics: CogInfoCom for people with nonstandard cognitive characteristics, Proceedings of 5th IEEE International Conference on Cognitive Infocommunications (CogInfoCom 2015) Győr, Hungary, 2015, pp. 77-82

[54]   D. Balla, T.Mester, Á. Botos, T. J. Novák, M. Zichar, J. Rásó, A. Karika: Possibilities of spatial data visualization with web technologies for cognitive interpretation, Proceedings of 8th IEEE International Conference on Cognitive Infocommunications (CogInfoCom 2017) Debrecen, Hungary, 2017, pp. 17-20

[55]   A. Csapo, A. Kristjansson, H. Nagy, Gy.Wersenyi: Evaluation of Human-Myo Gesture Control Capabilities in Continuous Search and Select Operations, Proceedings of the 7th IEEE International Conference on Cognitive Infocommunications (CogInfoCom 2016) Wroclaw, Poland, 2016, pp. 415-420

[56]   M. G. Tulics, K. Vicsi: Phonetic-class based correlation analysis for severity of dysphonia, Proceedings of 8th IEEE International Conference on

Cognitive Infocommunications (CogInfoCom 2017) Debrecen, Hungary, 2017, pp. 21-26

[57]   R. Vassiliki, D. Arfani, K. Fragkopoulou, E. Danasi, S. Varlokosta, G. Paliouras: Automatic detection of linguistic indicators as a means of early detection of Alzheimer's disease and of related dementias: A computational linguistics analysis, Proceedings of 8th IEEE International Conference on Cognitive Infocommunications (CogInfoCom 2017) Debrecen, Hungary, 2017, pp. 33-38

[58]   R. Sperandeo, E. Moretto, G. Baldo, S. Dell'Orco, N. M. Maldonato: Executive Functions and Personality Features: a Circular Interpretative Paradigm, Proceedings of 8th IEEE International Conference on Cognitive Infocommunications (CogInfoCom 2017) Debrecen, Hungary, 2017, pp. 63-66

[59]   I. Schmitt, G. Wirsching, R. Römer, M. Wolff: Denormalized Quantum Density Operators for Encoding Semantic Uncertainty in Cognitive Agents, Proceedings of 8th IEEE International Conference on Cognitive Infocommunications (CogInfoCom 2017) Debrecen, Hungary, 2017, pp. 165-170

[60]   A. Esposito, A. M. Esposito, M. Maldonato, C. Vogel: Differences between hearing and deaf subjects in decoding foreign emotional faces, Proceedings of 8th IEEE International Conference on Cognitive Infocommunications (CogInfoCom 2017) Debrecen, Hungary, 2017, pp. 175-180

[61]   A. Hayakawa, C. Vogel, N. Campbell, S. Luz: Perception changes with and without a video channel: A study from a speech-to-speech, machine translation mediated map task, Proceedings of 8th IEEE International Conference on Cognitive Infocommunications (CogInfoCom 2017) Debrecen, Hungary, 2017, pp. 401-406

[62]   Michael Beetz; Matthias Scheutz; Fereshta Yazdani: Guidelines for improving task-based natural language understanding in human-robot rescue teams, Proceedings of 8th IEEE International Conference on Cognitive Infocommunications (CogInfoCom 2017) Debrecen, Hungary, 2017, pp. 203-208

[63]   J. Henshaw, W. Liu, D. Romano: Improving SSVEP-BCI Performance Using Pre-Trial Normalization Methods, Proceedings of 8th IEEE International Conference on Cognitive Infocommunications (CogInfoCom 2017) Debrecen, Hungary, 2017, pp. 247-252

[64]   V. Sarathy, M. Scheutz, B. Malle: Learning behavioral norms in uncertain and changing contexts, Proceedings of 8th IEEE International Conference on Cognitive Infocommunications (CogInfoCom 2017) Debrecen, Hungary, 2017, pp. 301-306

[65]　G. Wilcock, K. Jokinen: Bringing Cognitive Infocommunications to small language communities, Proceedings of 8th IEEE International Conference on Cognitive Infocommunications (CogInfoCom 2017) Debrecen, Hungary, 2017, pp. 259-264

[66]　A. Ghosh, E. Stepanov, M. Danieli, G. Riccardi: Are You Stressed? Detecting High Stress from User Diaries, Proceedings of 8th IEEE International Conference on Cognitive Infocommunications (CogInfoCom 2017) Debrecen, Hungary, 2017, pp. 265-270

[67]　C. Rigóczki, D. Andrei, and K. Györgyi-Ambró: Gamification on the edge of educational sciences and pedagogical methodologies, Journal of Applied Technical and Educational Sciences, Vol. 7, No. 4, pp. 79-88, Nov. 2017

[68]　F. Alam, M. Danieli, G. Riccardi: Can We Detect Speakers' Empathy? A Real-Life Case Study, Proceedings of the 7th IEEE International Conference on Cognitive Infocommunications (CogInfoCom 2016) Wroclaw, Poland, 2016, pp. 59-64

[69]　M. Koutsombogera, C. Vogel: Ethical Responsibilities of Researchers and Participants in the Development of Multimodal Interaction Corpora, Proceedings of 8th IEEE International Conference on Cognitive Infocommunications (CogInfoCom 2017) Debrecen, Hungary, 2017, pp. 277-282

[70]　A, Moró, Gy. Szaszák: A prosody inspired RNN approach for punctuation of machine produced speech transcripts to improve human readability, Proceedings of 8th IEEE International Conference on Cognitive Infocommunications (CogInfoCom 2017) Debrecen, Hungary, 2017, pp. 219-224

[71]　S. Ondas, L.Mackova, D. Hladek: Emotion Analysis in DiaCoSk Dialog Corpus, Proceedings of the 7th IEEE International Conference on Cognitive Infocommunications (CogInfoCom 2016) Wroclaw, Poland, 2016, pp. 151-156

[72]　F. Mónus and C. Lechner: An innovative way in education for sustainable development: e-School4s – e-school for sustainability in the Danube region, Journal of Applied Technical and Educational Sciences, Vol. 7, No. 4, pp. 89-96, Nov. 2017

[73]　S. Savić, M. Gnjatovic, D. Mišković, J. Tasevski, N. Maček: Cognitively-Inspired Symbolic Framework for Knowledge Representation, Proceedings of the 7th IEEE International Conference on Cognitive Infocommunications (CogInfoCom 2016) Wroclaw, Poland, 2016, pp. 315-320

[74]　C. Vogel, M. R. Lopes, A. Esposito: Gender differences in the language of the Map Task dialogues, Proceedings of 8th IEEE International Conference on Cognitive Infocommunications (CogInfoCom 2017) Debrecen, Hungary, 2017, pp. 151-156

[75]   L. Gazdi, K. D. Pomazi, B. Radostyan, B. Forstner, L. Szegletes: Experimenting with classifiers in biofeedback-based mental effort measurement, Proceedings of the 7th IEEE International Conference on Cognitive Infocommunications (CogInfoCom 2016) Wroclaw, Poland, 2016, pp. 331-336

[76]   M. Meier, M. Borsky, E. H. Magnusdottir, K. R. Johannsdottir, J. Gudnason: Vocal tract and voice source features for monitoring cognitive workload, Proceedings of the 7th IEEE International Conference on Cognitive Infocommunications (CogInfoCom 2016) Wroclaw, Poland, 2016, pp. 97-102

[77]   G. Szabó et al: Investigation of public attitude towards renewable energy sources by word association method in Hungarian settlements, Journal of Applied Technical and Educational Sciences, Vol. 8, No. 1, pp. 6-24, Apr. 2018

[78]   K. D. Pomazi, L. Gazdi, B. Radostyan, B. Forstner, L. Szegletes: Self-Standardizing Cognitive Profile Based on Gardner's Multiple Intelligence Theory, Proceedings of the 7th IEEE International Conference on Cognitive Infocommunications (CogInfoCom 2016) Wroclaw, Poland, 2016, pp. 317-322

[79]   B. Radostyan, K. D.Pomazi, L. Gazdi, B. Forstner, L. Szegletes: Adaptive Figural Abstraction Test with Generated Exercises, Proceedings of the 7th IEEE International Conference on Cognitive Infocommunications (CogInfoCom 2016) Wroclaw, Poland, 2016, pp. 327-330

[80]   M. Szabo, K. D. Pomazi, B. Radostyan, L. Szegletes, B. Forstner: Estimating Task Difficulty in Educational Games, Proceedings of the 7th IEEE International Conference on Cognitive Infocommunications (CogInfoCom 2016) Wroclaw, Poland, 2016, pp. 397-402

[81]   F. R. Izullah, M. Koivisto, A. Aho, T. Laine, H. Hämäläinen, P. Qvist, A. Peltola, P. Pitkäkangas, M. Luimula: NeuroCar Virtual Driving Environment - Simultaneous Evaluation of Driving Skills and Spatial Perceptual-attentional Capacity, Proceedings of the 7th IEEE International Conference on Cognitive Infocommunications (CogInfoCom 2016) Wroclaw, Poland, 2016, pp. 31-36

[82]   P. Qvist, N.B.Trygg, M. Luimula, A. Peltola, T. Suominen, V. Heikkinen, P. Tuominen, O. Tuusvuor: Demo: Medieval Gastro Box – Utilizing VR Technologies in Immersive Tourism Experience, Proceedings of the 7th IEEE International Conference on Cognitive Infocommunications (CogInfoCom 2016) Wroclaw, Poland, 2016, pp. 77-78

[83]   S. Pieskä, M. Luimula, H. Kaartinen, P. Qvist, T. Suominen, O. Tuusvuor: Multidisciplinary Wow Experiences Boosting SMEi, Proceedings of the 7th IEEE International Conference on Cognitive Infocommunications (CogInfoCom 2016) Wroclaw, Poland, 2016, pp. 309-316

[84]   M. Gnjatović, J. Tasevski, D. Mišković, S. Savić, B. Borovac, A. Mikov,R. Krasnik: Pilot Corpus of Child-Robot Interaction in Therapeutic Settings, Proceedings of 8th IEEE International Conference on Cognitive Infocommunications (CogInfoCom 2017) Debrecen, Hungary, 2017, pp. 253-258

[85]   A. Mecocci, F. Micheli, C. Zoppetti, A. Baghini: Automatic Falls Detection in Hospital-Room Context, Proceedings of the 7th IEEE International Conference on Cognitive Infocommunications (CogInfoCom 2016) Wroclaw, Poland, 2016, pp. 127-132

[86]   B. Lewandowska-Tomaszczyk, P. Wilson: Compassion, Empathy and Sympathy Expression Features in Affective Robotics, Proceedings of the 7th IEEE International Conference on Cognitive Infocommunications (CogInfoCom 2016) Wroclaw, Poland, 2016, pp. 65-70

[87]   J. Irastorza, M. I. Torres: Analyzing the expression of annoyance during phone calls to complaint services, Proceedings of the 7th IEEE International Conference on Cognitive Infocommunications (CogInfoCom 2016) Wroclaw, Poland, 2016, pp. 103-106

[88]   D. Nguyen, G. Bailly, Frederic Elisei: Conducting neuropsychological tests with a humanoid robot: design and evaluation, Proceedings of the 7th IEEE International Conference on Cognitive Infocommunications (CogInfoCom 2016) Wroclaw, Poland, 2016, pp. 337-342

[89]   Gy. Kovacs, T. Grosz, T. Varadi: Topical Unit Classification Using Deep Neural Nets and Probabilistic Sampling, Proceedings of the 7th IEEE International Conference on Cognitive Infocommunications (CogInfoCom 2016) Wroclaw, Poland, 2016, pp. 199-204

[90]   M. Rusko, M. Finke: Using Speech Analysis in Voice Communication A new approach to improve Air Traffic Management Security, Proceedings of the 7th IEEE International Conference on Cognitive Infocommunications (CogInfoCom 2016) Wroclaw, Poland, 2016, pp. 181-186

Examining the Learning Efficiency by a Brain-Computer Interface System

J. Katona[1], A. Kovari[2]

[1]Institute of Information Technology, University of Dunaújváros, Táncsics M 1/A, 2400 Dunaújváros, Hungary, e-mail: katonaj@uniduna.hu

[2]Institute of Engineering, University of Dunaújváros, Táncsics M 1/A, 2400 Dunaújváros, Hungary, e-mail: kovari@uniduna.hu

Brain research is one of the most significant research areas of the last decades, in which many developments and modern engineering technologies are applied. The electroencephalogram (EEG)-based brain activity observation processes are very promising and have been used in several engineering research fields. Objective: The main goal of this research was to develop a Brain-Computer Interface (BCI) system to observe the level of vigilance calculated by Think Gear-ASIC Module (TGAM1) technology and to evaluate the output with learning efficiency tests applied in cognitive neuroscience. Methods: The performance of the BCI system is evaluated in a comparative study. The BCI system was tested by thirty-two test subjects and the attention level output was compared by the Psychology Experiment Building Language's (PEBL's) Corsi block test ($_p$CORSI) and PEBL's Ebbinghaus procedure ($_p$EBBINGHAUS) tasks. Results: Using the BCI, we have shown statistically significant results between the BCI and the conventional cognitive neuroscience tests. The correlation between the tests and the average attention of the BCI was slightly strong for $_p$CORSI Total Score (r=.63, p<.01 (2-tailed) and slightly strong for $_p$EBBINGHAUS Total Correct (r=-.71, p<.01 (2-tailed). The average level of attention measured by the BCI system during the $_p$CORSI test was 49.00%, while in case of the $_p$EBBINGHAUS test it was 52.41% on all samples. Conclusion: The developed BCI system has a significant correlation with $_p$CORSI and $_p$EBBINGHAUS cognitive neuroscience tests. The BCI system is capable of observing attentional vigilance continuously. Significance: The developed BCI system is applicable to observe vigilance level in real-time while the level of attention depends on activities.

Keywords: brain-computer interface; Corsi block; Ebbinghaus procedure; electroencephalogram; PEBL; learning efficiency

1   Introduction

In order to understand the progress of studying, the human brain can be examined as a system, in which long-term changes occur, at least regarding fulfilling certain functions, that remain for quite a long period. During studying, this change in the

brain means the alteration of the brain cells system and due to the modification of the connections between the cells, human functions could be better fulfilled. [1-3]

Efficient and successful learning, apart from understanding, interpretative [42-45] and problem-solving skills [46-49], is mainly determined by attention as a cognitive skill that also depends on emotional and motivational requirements and can be defined as a way of concertation on important information. [4-5, 53] Recently, relatively cheap and portable Electroencephalogram (EEG)-based signal processing devices have become available to observe the bioelectrical activities of the brain, with which the electrical signals generated by the activities of the brain can be measured and processed [51]. These EEG biosensors are able to digitally register and process the electrical activity of brain neurons in real time. The strength of the brainwaves could be determined by The Fast Fourier Transform (FFT)-based evaluation of information, from which the level of attention could be concluded.

If the attention of students can be examined by a device that measures brain and bioelectrical activity, the features of determining the efficiency of learning can be inferred. By observing the attention level, the most important factor in studying becomes continuously measurable, from which the efficiency of learning through the lesson can permanently be observed and that means continuous feedback could be received about the efficiency of teaching and learning processes. For instance, after recognising the decrease of the efficiency value, the method of knowledge transfer can be changed by using more effective teaching methods or even by keeping a relaxing break.

1.1 Human-Computer Interfaces and Cognitive Infocommunication

The fields of infocommunications, media informatics and media communications has developed a lot in the last ten years. The evolution of these disciplines has resulted in newer fields within this topic. Baranyi and Csapo summarize the scopes and goals of cognitive infocommunications (CogInfoCom) in [53], [54].

The human-machine interaction is described as the performance of the communication and feedback between humans and technical systems. This cognitive based communication is generally solved by IT systems. The human-machine interface helps the human being operate the machine, control actuators and handle the machine's use. On the other hand the human has to sense and exchange information; communicate with the machine which informs the user about the operation conditions of the machine. But from another perspective everything that communicates with humans by cognitive level using IT system can be expressed as CogInfoCom. CogInfoCom covers several disciplines appearing in applications and research areas also. CogInfoCom is available technology from socio-cognitive ICT [55-65] to cognitive aided engineering [66-77] and its related

aspects in terms of online collaborative systems and virtual reality solutions [78-80], teaching-learning [81-86] and human cognitive interfaces such as brain-computer interfaces (BCIs) [87-92] and medicals [93-96].

1.2   The Brain-Computer Interface

Nowadays BCI is the most developing multidisciplinary research area, which only goes back two decades. The design, development, implementation, and application of these devices are in the spotlight. The aim of the first BCI researchers was to create a direct communicational channel for those in need to help their quality of life, particularly of those suffering from devastating conditions, such as amyotrophic lateral sclerosis (ALS), spinal cord injury, stroke and cerebral palsy. [6-13]

BCI is a direct functional interface between the brain and the computer or another device that can observe and decode the electromagnetic signals of brain activities and transfers the received information towards an external device [6, 7, 50]. Non-invasive BCIs have been an active research area; they include EEG, Near-infrared Spectroscopy (NIRS), functional-MRI (fMRI), among others [22-24]. The most popular BCI systems are based on scalp EEG signals due to their low cost, and to the fact that they are non-invasive and easy to use.

Certain functions of brain activity are known due to the results of brain research and cognitive neuroscience [25]. Understanding the operation of the brain is of great importance in measuring and interpreting brain waves [26]. The electrical and magnetic phenomena of neural function can be observed during brain operation using a routinely applied method called electrophysiology [27]. The most common method of electrophysiological observation is electroencephalography, whereby the brain electrical signals generated by brain activities are measured and registered by biosensors [28].

Brain cells communicate by sending electric signals to each other; the more signals are sent, the more electricity the brain will produce, and an EEG can measure the pattern of this electrical activity. The EEG signals are mostly processed by the quantitative EEG (QEEG) method, in which the frequency spectrum of the EEG signals is observed [29]. Conducting an EEG has previously required complex, expensive, large and immobile equipment.

As a result of ongoing technological developments in recent years, mobile EEG biosensor-based embedded devices are now available for use in new applications, for instance in entertainment, controlling or for educational purposes. In these applications, the connection between the brain activity observed by the EEG and the induced function is effectuated by a BCI [30].

The latest BCIs applied with biosensors and modern signal processing units have become cheaper and more portable because of their simple structure, while their

accuracy is similar to that of the clinical EEG devices [10, 31, 32]. The research trends that deal with BCI systems include many other application areas of use, for instance, using BCI for observing the brain's procession of information [13-16] or implementing navigation tasks [17-20]. Beside these, the implementation of such a complex system and the observation of its efficiency can greatly be used in the field of education either among interested students or in teacher-managed projects. [21].

The research in this article deals with forecasting the efficiency of attention-based learning with the established BCI system, of which applicability is compared to the cognitive tests for the efficiency of learning applied in cognitive psychological examinations, i.e., the PEBL's Corsi block test ($_p$CORSI) and PEBL's Ebbinghaus test ($_p$EBBINGHAUS).

2   An Overview of the BCI System

A BCI system acquires EEG signals from the human brain by an EEG headset, which is filtered, pre-processed and the features of the signals are extracted, classified and transferred to an output signal and visualized by a computer application interface (Fig. 1). This output signal relates to the brain activity of the user and contains the information detected by brain activities. The user receives feedback from the output or the application interface, so the BCI system realizes a closed-loop system.

During the EEG, the electrodes are placed on different symmetrical points of the skull, where the conducts could be evolved as unipolar or bipolar. In unipolar evolving, an active and a null-reference electrode are used, while in case of bipolar measurement, the potential alteration between two different electrodes is conducted. A correlating system known as the internationally accepted 10/20 electrode arrangement system (Fig. 2) was made in connection with the suiting of the electrodes, in which anatomical correlating points are defined. For the unequivocal identification of conduct fields, every point on the human cranium has been given a letter (Fp, F, T, C, P, O) and a numerical feature, where the letters identify the lobe position (Frontal polar, Frontal, Temporal, Central, Practical, Occipital), and even numbers identify the right, while odd numbers the left hemisphere. [29, 31, 32] The electrical activities of the brain, the electrical signals resulting from ionic current flows within the neurons, can be measured by the EEG by placing a sensor on the scalp [29, 31, 32]. The frequency spectra of brain signals are typical in different mental states [26, 52] and can easily be determined by digital signal processors using Fourier-transform, for example, NeuroSky [31]. This spectrum of the brain waves is very sensitive to the mental and emotional states of the brain, so this attribute is used to monitor mental activity [26].
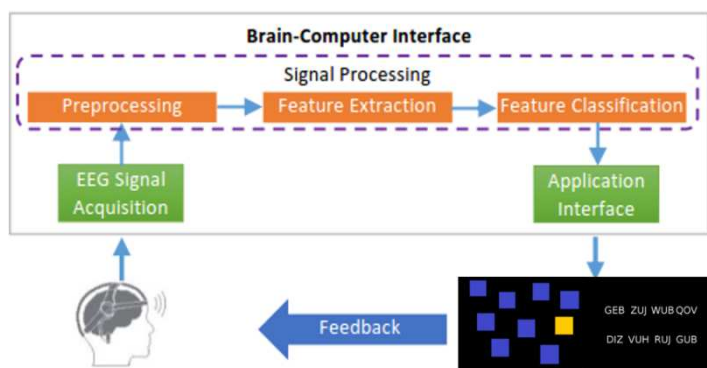
Figure 1
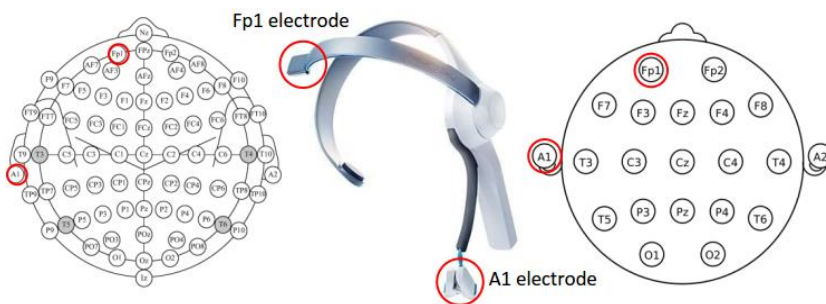BCI model applying pCORSI and pEBBINGHAUS

Figure 2
The international 10/10 and 10/20 system for EEG electrodes with the electrodes of the NeuroSky
MindWave EEG headset highlighted in red circles

2.1 The NeuroSky EEG-based MindWave Headset

NeuroSky has been developing EEG-based measuring devices for years with the co-operation of some universities, for example, Stanford University, Carnegie Mellon University, University of Washington and University of Wollongong [33]. The MindWave EEG headset is a lightweight, portable device with wireless communication [34] and unipolar conduction. Fig. 2, illustrates the locations of the electrodes of the MindWave EEG headset in the 10/20 system and in a later 10/10 system. The active electrode both in the 10/10 and 10/20 systems measures the activity of the frontal lobe that can be executed in the position of Fp1, slightly left from the midline, while A1 position, the left earlobe, was chosen for the reference point.

2.2 The Evaluation of Vigilance Level Based on Brain Waves

The connection between attention and brain waves was observed in the 1970s and an EEG-based attention analyser was patented [35]. The method applied for determining the intensity of attention is based on the examination of the Power Spectrum Density (PSD) determined by the Discrete Fourier Transform (DFT) algorithm of brain waves. The spectrum can be calculated using samples of the brain signals. The sequence of N complex numbers $x_0, x_1, ..., x_{N-1}$ can be transformed into a sequence of complex numbers with periodic N [39,40]:

$$X_k = \sum_{n=0}^{N-1} x_n e^{-i2\pi\frac{n}{N}} k = 0,...,N-1 \tag{1}$$

where X_k encodes the amplitude and phase of a sinusoidal component of function x_n, which is a complex number. The intensity of brain waves and the aim of this research, the magnitude of attention, can be determined.

The inverse of it:

$$x_n = \frac{1}{N}\sum_{n=0}^{N-1} x_k e^{i2k\pi\frac{n}{N}} \tag{2}$$

The continuous Fourier transform could be evaluated over a finite interval rather than from $-\infty$ to $+\infty$ if the waveform is periodic. Similarly, if there are only a finite number of sampled data, the DFT handles the data as if it is periodic. (samples 0 to $N-1$ is the same as N to $2N-1$). Therefore, DFT is evaluated for the fundamental frequency $\frac{1}{NT}$ Hz, $\frac{2\pi}{NT}$ rad/s.

Performing DFT needs a lot of calculation, but this can be decreased by optimizing the algorithm. In case of DFT, calculation demand is $O(N^2)$, while performing the FFT process, it could be decreased to the $O(N \cdot logN)$ value (where N is the data size). By FFT algorithm, brain bioelectric spectrum can be calculated, where the strength of certain brain waves specific to the encephalic operation could be defined.

NeuroSky developed a ThinkGear measurement technology to calculate the PSD using 512 samples per second sampling frequency and eSense Attention meter algorithm to indicate the intensity of attention, which occurs during intense concentration. The device amplifies and digitalizes the voltage difference (to achieve better common mode rejection) between a single dry sensor on the forehead and a reference on the ear. The brain signal is filtered by analog and digital, low and high pass filters in the 1-50 Hz range. Each second, the signal is analysed in the time domain to detect and correct noise, a standard FFT is performed, and finally, the signal is rechecked for noise and artifacts in the frequency domain to get brainwave strengths and eSense Attention and Mediation values. eSense algorithm is dynamically learning, so ThinkGear sensors are able

to operate on a wide range of individuals, and on a wide range of personal and environmental conditions.

ThinkGear has been compared with Biopac system as a reference, which is a well-known wet electrode EEG system widely used in medical and research applications. Data were fixed simultaneously and during the study, the sensors were fixed to identical places near to each other. The determined performance-spectrum, which was determined by the measuring data supplied by the two instruments, was compared in a 1-50 Hz frequency range, which is the frequency range of certain typical brain wave types. The result they showed was that the correlation factor supplied by the two devices among the performance-spectrum is bigger than 0.7, and it is determinable that the information supplied by the two instruments are nearly identical [32].

eSense Attention meter output value ranges from 0 to 100. Values between 40 to 60 are considered "neutral", 60 to 80 "slightly elevated", 80 to 100 are considered "elevated", meaning they are strongly indicative of heightened levels of attention. Values between 20 and 40 indicate "reduced" levels of the eSense and 1-20 indicates "strongly lowered" level. An intense meter value of 0 is a special value indicating the ThinkGear is unable to calculate the eSense level.

2.3   The Implementation of the BCI System

A Windows Forms Application Interface has been developed to evaluate and visualize the brain wave data of the MindWave EEG headset. This BCI program can run on MS Windows and has been written in C#. Microsoft Visual Studio was used to implement the program, which is a developing environment that supports modern object-oriented programming. During the software implementation of the BCI, the system development life cycle (SDLC) terminology was applied, where certain software development cycles could be separated and defined well, making the development process easier to follow. During performing the software, we created the clear code, in order to make an easy-to-overview and easy-to-maintain application.

2.3.1   The Structure of the Implemented BCI System

The application consists of seven classes and their connections (Fig. 3). The base class of the application is the PacketHeader, which features contain all data values sent by the EEG headset that are not brain wave values in feature type method (Fig. 3). SYNC1, SYNC2: these byte values indicate the beginning of fresh data packs, and their value is 0xAA (decimal 170). pLENGTH: A Packet's Data Payload (PAYLOAD) indicates the section length in a byte. The complete length of a pack sent by the EEG headset is always pLENGTH + 4. POOR_SIGNAL_Quality is an unsigned one-byte integer value, which indicates the quality of the signal measured by the headset. The value range could be 0-255,

the bigger the number, the louder the noise. vLENGTH ("Value Length") only appears if the pack differs from the expected value. ASIC_EEG_POWER_INT is a value that specifies the representation of brain wave values in the sent pack. Storing brain wave values is implemented in an extension of the PacketHeader class, in the BrainWave class, where data could only be reached with the help of feature data (Fig. 3). The perceived data are processed in the SignalAcquisition class. The Visualize class implements functions responsible for objects specifying visualization, attribute values and changing events. The EEGSignalPower class shows the display of the on-screen information. Data storage and their statistic procession are determined in the Storage Class.
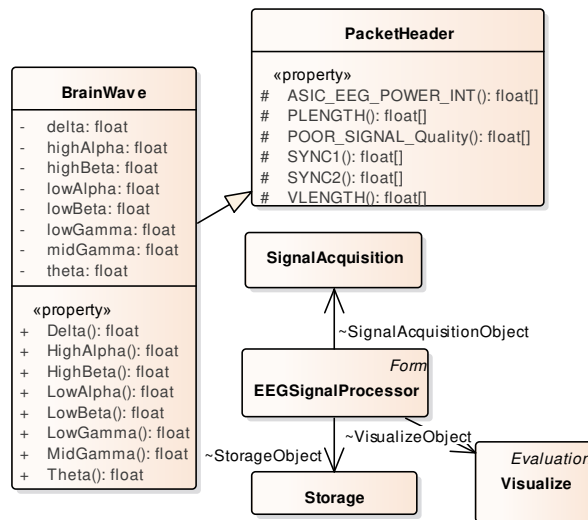

Figure 3

The structure of the implemented BCI software-based UML (Unified Modeling Language) class diagram

2.3.2   The Functions of the Implemented BCI System

The application is responsible for supplying different functions. These functions contain handling appropriate serial communication, receiving data packs from the EEG headset at appropriate intervals as well as processing them according to the protocol, visualizing brain wave values of the data pack in a particular time and continually, storing of the brain wave values in a pre-determined data structure, or providing pre-determined statistics from the brain wave values for further use.

The pseudocode of one of the main functions of the implemented software could be seen in Figure 4. This method is responsible for the appropriate procession of the incoming data packs and their refreshing according to the sampling time (1 s).

Algorithm 1 Update ThinkGear Packet algorithm

1: **procedure** UPDATEPACKET
2:　　**if** $objectOfSerialPort.IsOpen$ **then**
3:　　　　Initialize $bytes \leftarrow objectOfSerialPort.BytesToRead$
4:　　　　Initialize $buffer[bytes]$ as new arrays
5:　　　　**return** OBJECTOFSERIALPORT.READ($buffer$,0,$bytes$)
6:　　　　**for** each $item \in buffer$ **do**
7:　　　　　　$LatestByte \leftarrow item$
8:　　　　　　**if** $IsInPacket$ **then**
9:　　　　　　　　**if** $PacketIndex = 0$ **then**
10:　　　　　　　　　　$PL \leftarrow LatestByte$
11:　　　　　　　　　　**if** $PL \neq MAX\_PACKET\_LENGTH$ **then**
12:　　　　　　　　　　　　$IsInPacket \leftarrow false$
13:　　　　　　　　　　**else**
14:　　　　　　　　　　　　$IsPLCorrect \leftarrow true$
15:　　　　　　　　　　**end if**
16:　　　　　　　　**else if** $PacketIndex \leq PL$ and $IsPLCorrect$ **then**
17:　　　　　　　　　　$PacketData[PacketIndex - 1] \leftarrow LatestByte$
18:　　　　　　　　　　$CA \mathrel{+}= LatestByte$
19:　　　　　　　　**else if** $PacketIndex \geq PL$ and $IsPLCorrect$ **then**
20:　　　　　　　　　　$Checksum \leftarrow LatestByte$
21:　　　　　　　　　　$CA \leftarrow CA \wedge 0xFF$
22:　　　　　　　　　　$CA = \neg CA \wedge 0xFF$
23:　　　　　　　　　　**if** $Checksum = CA$ **then**
24:　　　　　　　　　　　　$ParseSuccess \leftarrow$ **return**PARSEPACKET()
25:　　　　　　　　　　　　**if** $ParseSuccess$ **then**
26:　　　　　　　　　　　　　　$FreshPacket \leftarrow true$
27:　　　　　　　　　　　　**end if**
28:　　　　　　　　　　**end if**
29:　　　　　　　　　　$IsInPacket \leftarrow false$
30:　　　　　　　　　　$IsPLCorrect \leftarrow false$
31:　　　　　　　　**end if**
32:　　　　　　　　$PacketIndex \leftarrow PacketIndex + 1$
33:　　　　　　**else**
34:　　　　　　　　$IsPLCorrect \leftarrow true$
35:　　　　　　**end if**
36:　　　　　　**if** $LatestByte = LastByte = 170$ and $\neg IsInPacket$ **then**
37:　　　　　　　　$IsInPacket \leftarrow true$
38:　　　　　　　　$PacketIndex \leftarrow 0$
39:　　　　　　　　$PL \leftarrow 0$
40:　　　　　　　　$Checksum \leftarrow 0$
41:　　　　　　　　$CA \leftarrow 0$
42:　　　　　　**end if**
43:　　　　　　$LastByte \leftarrow LatestByte$
44:　　　　**end for**
45:　　**end if**
46:　　**if** $FreshPacket = true$ **then**
47:　　　　$FreshPacket \leftarrow false$
48:　　　　**return** $true$
49:　　**else**
50:　　　　**return** $false$
51:　　**end if**
52: **end procedure**

Figure 4

One of the main functions of the procession of the data pack from the MindWave EEG headset.
Require: $IsInPacket$ = false, $HasPower$ = false, $IsPLCorrect$ = false, $PacketIndex$ = 0, PL = 0, CA = 0, $Checksum$ = 0, MAX_PACKET_LENGTH = 32; Comment {PL = PacketLength; IsPLCorrect = IsPacketLengthCorrect; CA = CheksumAccumulator}

3   Materials and Methods

According to the objectives of the research, to analyse the experiment on the efficiency of studying, we have to be able to measure effectiveness itself. The aim of the measurement is examining memorizing, which means storing certain information in the long-term memory.

The items of information that are emphasized during attention do not faint but are moved to the short-term memory [41], which refers to the fact that attention decides which information is important and which one is not. The least important ones are evaluated at a lower level of information procession and after a while they faint and become forgotten. As coded information can get into the long-term memory only through the short-term memory, all data stored in the short-term memory has a key role in the learning process and knowledge acquisition. The information put into the short-term memory is mainly determined by the level of attention, therefore, there is a direct connection between learning and paying attention. Based on these facts, short-term memory tests could be used for examining knowledge acquisition and learning process by the mediation of attention. In the following, $_p$CORSI and $_p$EBBINGHAUS tests implemented in PEBL environment will shortly be demonstrated for the examination of work memory, viz., short-term memory and learning skills.

The BCI system was tested by test subjects, and the vigilance level output of the BCI system was compared to $_p$CORSI and $_p$EBBINGHAUS tasks. The aim of this research is to define the strength and direction of the connection between the results of PEBL's memorizing efficiency tests and the attention level determined by the EEG-based BCI equipment.

3.1   The $_p$CORSI and the $_p$EBBINGHAUS Tests

In neurobehavioral studies, the Psychology Experiment Building Language (PEBL) environment is widely used for implementing algorithms of test procedures. Most experiments are carried out with the use of shapes, texts, letters that appear on the computer screen while using computer peripherals (mouse, keyboard) for fixing the reactions given to the experimental target stimulus of the test subject. [38]

$_p$Corsi is a measuring test where the test subject is sitting in front of the computer with a black background screen; on which nine identical squares appear in different positions keeping one second breaks (Fig. 5). After the test is started, some squares in a pre-determined order are chosen by the program and the task of the subject is to click on the same squares in the same order. If the test subject can repeat two out of two series, the number of the blocks increases with another one until the number of successfully repeated series falls below two. With this test, we could get information about how precisely the test subject can recall the right

order by using the information stored in the short-term memory with the help of attention.
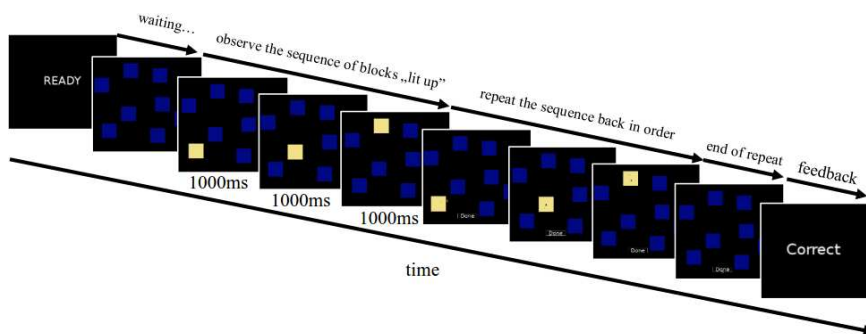

Figure 5

The block sequence was presented in the encoding phase, and the test subject recalled the sequence immediately afterward

pEBBINGHAUS is a short (5-10 minutes) examination based on Hermann Ebbinghaus' self-experiments. During the test, the test subjects have to study eight different three-letter words (Fig. 6). The software generates words that are non-similar to words of any mother tongues or any words that may appear in the languages spoken by the subject. The words are built up of three letters, in which the first and the third characters are consonants and the middle one is a vowel. The list of the eight words is repeated by the program until the test subjects are able to recall them correctly twice. After that, the software generates a new list and repeats that again until it is recalled flawlessly twice by the test subjects. At the end of the successful recall of the two lists, the software goes back to the first list and the process starts again. The test ends when the test subjects can correctly recall both lists twice.
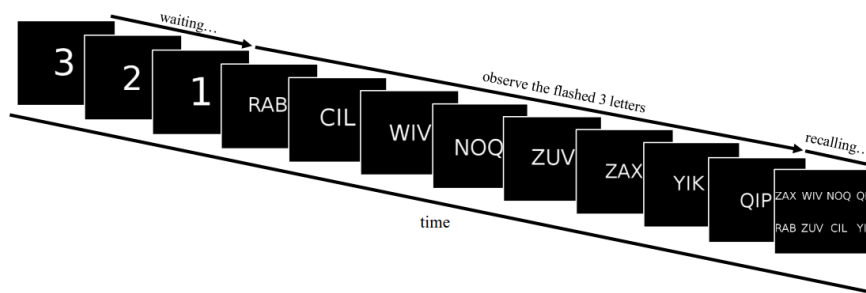

Figure 6

After flashing eight 'words' of three letters, the test subjects have to recall them in the correct order. The 'words' are repeated until the participants are able to recall them correctly twice.

3.2   The Participants

In this experiment thirty-two high school students participated. All subjects were healthy, with no past history of psychiatric or neurological disorders. The age distribution was 14-18, the average age was 16.2, range ±1.4; 47% girls.

3.3   The Procedures

During the procedure, first the $_p$CORSI, then the $_p$EBBINGHAUS test was accomplished. The testing was carried out in one separated room, in which five or fewer participants could be tested at the same time. Before the experiment, the test subjects had to put the EEG headset on, and then the details of the procedures were described to them. After the introduction and the calibration of the device, the test subjects could start the tests. (Fig. 7a, b) Testing was performed using a desktop computer running Windows 10, using 22.0" computer screen at a resolution of 1920x1080 with 90% contrast (responses were using keyboard and mouse).

Figure 7a
A test subject doing the $_p$CORSI. The data measured by the EEG headset are continually being monitored.
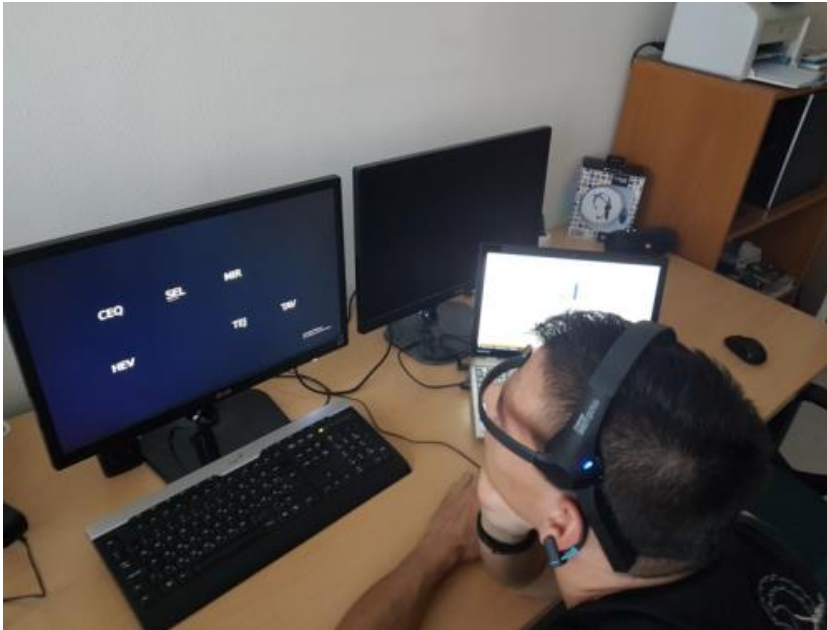
Figure 7b
A test subject doing the pEBBINGHAUS tests. The data measured by the EEG headset are continually being monitored.

3.4 Statistical Analysis

The statistical analysis of PEBL tests was made by an interval scale, while in case of the BCI, it was done on an ordinal scale with SPSS 23 (SPSS, Inc., Chicago, IL) program pack. As an ordinal scale was defined for the BCI, in the use of the BCI results, non-parametric tests were applied, while in connection with PEBL test results, if parametric test conditions were fulfilled, parametric tests were done. To define the difference between the morning and afternoon test results of the psychological tests, since test subjects in PEBL tests are independent of each other, with the exception pCORSI, the samples showed normal distribution and at least were scale typed, furthermore, as the standard deviation homogeneity is not needed to be done in case of related patterns, we used related-pattern t-test, where the effect size was determined by Cohen d-value. As during the psychological tests, in case of defining the differences between the morning and afternoon results of the average attention level measured by the BCI system, the variables were measured on an ordinal scale and the test subjects were independent of each other, Wilcoxon signed-rank test were applied, where the effect size was determined by the z-value of the test statistics and the ratio of the root of the total sample element number. In case of the applied statistical tests, $p < 0,05$ value was determined as significant.

4   The Results and Discussion

During our primer type quantitative experiment, we examined dependency relationship and collected metric data, from which we analysed correlation. The aim of our next research was to find connections with the help of an independent and a dependent variable between $_p$CORSI and the BCI and $_p$EBBINGHAUS and the BCI system-specified attention level results.

4.1   Comparing the Results of $_p$CORSI and BCI

The aim of the examination and evaluation is to investigate the correlation between two variables, an outstanding result of the $_p$CORSI test and the average attention level provided by the BCI system. The correlations and relationships between the results of the obtained test and the measurement provided by the BCI system can be estimated and evaluated on the whole sample, i.e., on all test subjects.

The strength of the connections was determined by one of the results of the $_p$CORSI test, which is an outstanding value, the most typical parameter of the test result. To examine the correlation between the measurement results, Spearman's correlation was used with two-sided tests, since in case of the BCI variable, an ordinal scale type was determined, and our data changed monotonically. During the test, the difference between the morning and afternoon results were evaluated in case of each subject so that the differences in individual ability did not play a role in the learning test results, but the level of attention of the morning and afternoon tests did.

In the $_p$CORSI test examining the efficiency of memorization, comparing the change in the results of the more alert and more tired state tests to the change of difference of the mean value characteristic of attention determined by the data processed by the BCI system, a significant positive correlation (Fig. 8) where r_s=0.630 p<0.01 (2-tailed) can be shown.
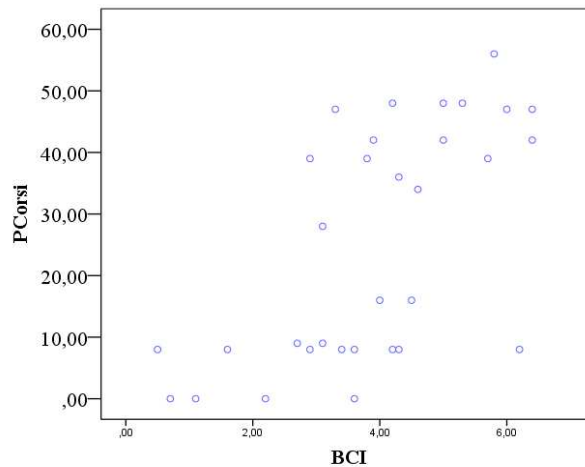
Figure 8

The pCORSI test showed a significant positive correlation with the value of differences of average level of attention determined by the BCI system

A more detailed overview of correlation evaluation is given in Table 1.

Table 1

Spearman-correlation analysis for the whole sample (N = 32) on the results of the pCORSI test and the difference of the mean value characteristic of the level of attention determined by the BCI

Period	Test	$M \pm SD^1$	Correlation	p-value
morning-afternoon	pCORSI	24.875±3.353	0.63	<0.01 (2-tailed)
	BCI	3.884±1.587		

[1] The arithmetic mean of the difference of the correct response of test test subjects for target stimulus.

Moreover, regarding the pCORSI tests for examining short-term memory, between the morning (Mdn=96, $D(32)$=0.406 p<0.01 (2-tailed)) and the afternoon (Mdn=88, $D(32)$=0.241 p<0.01 (2-tailed)) results, a significant difference can be seen (T=0 Z=-4.64 p<0.01 (2-tailed) r=0.83).

According to the Wilcoxon signed-rank test results, during the short–term memory examination via the pCORSI test, there is a significant difference in the results of the average level of attention measured by the BCI system (T=0 Z=-4.94 p<0.01 (2-tailed) r=0.87) in the morning (Mdn=54.35) and in the afternoon (Mdn=50.10) hours.

Figure 9a shows that the medians differ in comparing the two conditions; it can be seen that in the morning, the test subjects achieved better results. Data disposition is more likely to be seen above the median, while weaker results appeared in the afternoon from all aspects, moreover, data disposition from the median can be

seen below the median. Figure 9b shows that the medians differ in comparing the two conditions, it is generally apparent that the BCI system recorded higher level of attention on average in the morning and data disposition was slightly below the median. In the afternoon, the BCI system, regarding the average attention level, similarly to the results of the pCORSI test, shows a downturn, and data disposition is below the median.
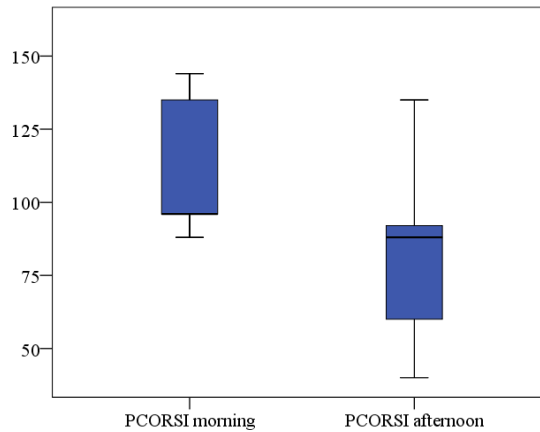

Figure 9a
There is a significant difference between the results of average attention level measured by the pCORSI in the morning and afternoon hours
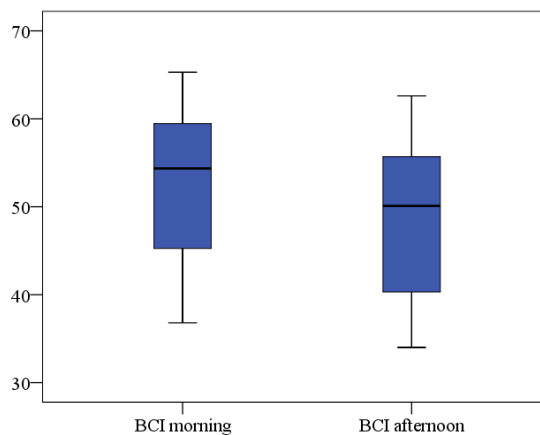

Figure 9b
There is a significant difference between the results of average attention level measured by the BCI system in the morning and afternoon hours

4.2   Comparing the Results of ₚEBBINGHAUS and BCI

The further aim of the examination and evaluation is to evaluate the correlation between two variables, a chosen outstanding result of the ₚEBBINGHAUS test and the average level of attention provided by the BCI system. The obtained correlations and relationships between the results of the test and the measurement provided by the BCI system can be estimated and evaluated on all samples, on all test subjects. The strength of the relationships was determined by an outstanding result of the ₚEBBINGHAUS test, i.e., by one of the most typical parameters of the final test results. Spearman's correlation was used with two-sided tests to examine the correlation between individual measurements, since in case of the BCI variable, ordinal scale type was determined, and our data were monotonic. During the test, the difference between morning and afternoon results of the test subjects was evaluated to ensure that the differences in individual skills did not play role in the results of the learning test, only the different magnitude of attention in the morning and afternoon hours did.

In the ₚEBBINGHAUS test on the efficiency of short-term memory, comparing the changes of the test results of alert and tired states to the change of the difference of the mean value, a characteristic of the level of attention determined by the data processed by the BCI system, it can be stated that a significant negative correlation can be shown (Fig. 10), where r_s=-0.71 p<0.01 (2-tailed).
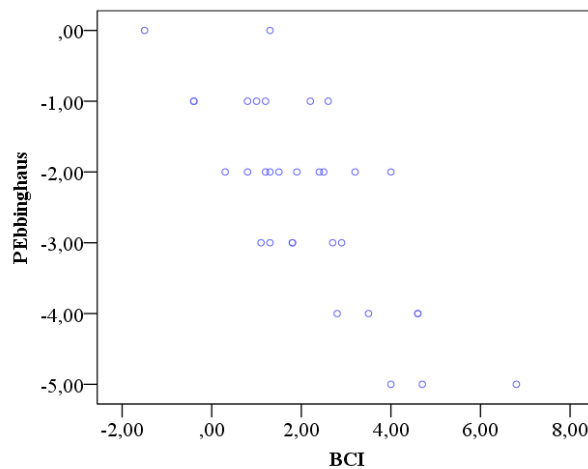

Figure 10

The ₚEBBINGHAUS test results show a significant negative correlation with the value of difference of the level of average attention determined by the BCI

More details of the evaluation of correlation can be seen in Table 2.

Table 2

Spearman-correlation analysis for the whole sample (N = 32) on the results of the $_p$EBBINGHAUS test and the difference of the mean value characteristic of the level of attention determined by the BCI

Period	Test	$M \pm SD^I$	Correlation	p-value
morning-afternoon	PE.^{2}	-2.375±1.385	-0.71	<0,01 (2-tailed)
	BCI	2.141±1.724		

^{1}The arithmetic mean of the difference of the correct response of test test subjects for target stimulus.
^{2}$_p$EBBINGHAUS

In addition, in case of the $_p$EBBINGHAUS test, a significant difference $t(31)=-9.70$ $p<0.01$ (2-tailed), $d=0.40$ could be found in the results of the morning ($M \pm SD=6.47 \pm 2.76$, and $D(32)=0.108$ $p=0.200$) and the afternoon ($M \pm SD=8.84 \pm 3.16$, and $D(32)=0.097$ $p=0.200$) tests. According to the results of the Wilcoxon-signed rank test, regarding the $_p$EBBINGHAUS test, there is a significant difference ($T=6.17$ $Z=-4.59$ $p<0.01$ (2-tailed) $r=0.81$) as well between the results of the average level of attention measured by the BCI system in the morning ($Mdn=55.10$) and afternoon hours ($Mdn=52.55$).

As it can be seen in Fig. 11a, the medians differ comparing the two conditions. Overall, it is evident that in the morning the test subjects made fewer mistakes, data disposition rather appears below the median, while weaker results were achieved in the afternoon, and data disposition is below the median, too. Fig. 11b shows that the medians are different in comparison the two conditions. It can be seen that in the morning the BCI system recorded an average higher level of attention and data are distributed evenly around the median. In the afternoon, regarding the average level of attention, the BCI system, similarly to the results of the $_p$EBBINGHAUS test, shows a downturn, and data disposition is below the median.
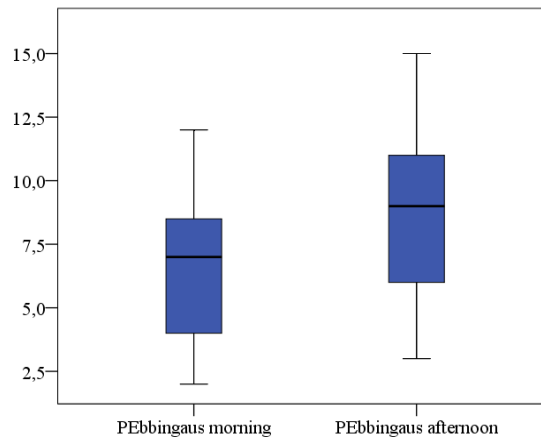
Figure 11a
There is a significant difference between pEbbinghaus test results for short-term memory in the
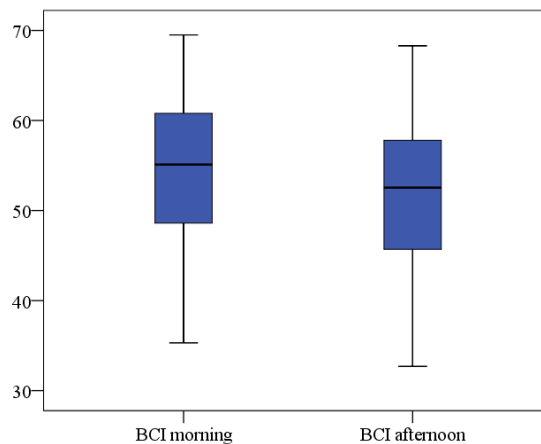morning and afternoon results

Figure 11b
There is a significant difference between the results of the BCI system for short-term memory in the
morning and afternoon results

Similarly to the $_P$CORSI test, it can be shown that the changes of the results of the $_P$EBBINGHAUS learning test done in the more alert and tired states and the changes of the mean level of attention determined on the basis of the data processed by the BCI system are related to each other. In case of the $_P$EBBINGHAUS test, the magnitude of correlation is negative because the number of mistakes inversely proportional to the level of average attention were compared.

Since there is a cause-effect relationship according to the multiple spatial theory between attention and learning as a memorization, at a certain time the expectable

success of learning can be concluded based on the level of attention. Relying on the statistical analysis of Table 1 and Table 2, the expectable efficiency of the $_p$CORSI block and $_p$EBBINGHAUS memorization and learning tests can be concluded from the magnitude of the mean value characteristic of the level of attention provided by the BCI system. Consequently, the momentary learning ability of the test subject can be concluded.

From the given correlation values, we could see that there is a relatively high, over 0.6, correlation between the test results of the learning efficiency tests and the average attention level measured by the EEG-based brain computer interface. This means that the implemented BCI system measuring method could be used as an alternative procedure besides the $_p$CORSI and $_p$EBBINGHAUS tests for measuring attention-based memorizing efficiency.

In general, at the lower level of concentration the measured values are lower and more unequable than at the higher concentration level measured ones, which are higher and harmonized.

Conclusions

It could be stated from the research data that the brain-computer interface attention values and the results of the memorizing tests have a significant relationship. According to this, in a given time interval we could indirectly conclude the expectable learning efficiency by the measured attention level. On the basis of the experiment topic, the research results and the given conclusions, it clearly seems that experiments based on the bioelectrical processes of the brain could open new areas of research and application in the future. With the help of a brain-computer interface test, attention level could be measured continuously in real time, which is one of the important influential factors in the learning process. With this information, the pedagogue could get continuous feedback about the level of attention of students. If it becomes lower, the information processing ability is lower as well and it makes a negative effect on memorizing. If these changes are recognised, the method of teaching could be changed or even a short relaxing break could be kept during the lesson, so instead of the traditionally structured lessons that start at a given time, last for a given time and finish in a given time, we could organize so-called students' attention level-synchronized lessons, in which the teaching of important curriculum and extra knowledge elements could be organized and reorganized according to the attention level of students even during a lesson. As the attention level changes, the hierarchy of learning, the organisation of the lessons could be changed. All in all, with this method the efficiency of teaching and studying could be increased and optimized besides opening new pedagogical approach and methodology in learning organization.

References

[1]   E. Vaadia: Cognitive neuroscience: Learning how the brain learns, Nature, 2000, 405, pp. 523-525

[2]   V. Calhoun, M. Amin, D. Hjelm, E. Damaraju and S. Plis: A deep-learning approach to translate between brain structure and functional connectivity, In Proceedings of the 2017 IEEE International Conference on Acoustics, Speech and Signal Processing (ICASSP 2017) New Orleans, United States, 2017, pp. 6155-6159

[3]   A. Darden: Understanding How the Brain Learns Should Inform Our Teaching Practices, Journal of Microbiology & Biology Education, 2012, 13(2) pp. 202-203

[4]   J. Gottlieb: Attention, Learning, and the Value of Information, Neuron, 2012, 76(2) pp. 281-295

[5]   E. Eldar, J. Cohen, and Y. Niv: The effects of neural gain on attention and learning, Nature Neuroscience, 2013, 16(8) pp. 1146-1153

[6]   T. O. Zander and C. Kothe: Towards passive brain-computer interfaces: applying brain-computer interface technology to human-machine systems in general, Journal of Neural Engineering, 2011, 8(2) p. 025005

[7]   M. A. Lebedev and M. A. L. Nicolelis: Brain-machine interfaces: past, present, and future, Trends in Neurosciences, 2006, 29(9) pp. 536-546

[8]   Y. Li and C. Nam: Collaborative Brain-Computer Interface for People with Motor Disabilities [Research Frontier] IEEE Computational Intelligence Magazine, 2016, 11(3) pp. 56-66

[9]   H. Hsu, I. Lee, H. Tsai, H. Chang, K. Shyu, C. Hsu, H. Chang, T. Yeh, C. Chang and P. Lee: Evaluate the Feasibility of Using Frontal SSVEP to Implement an SSVEP-Based BCI in Young, Elderly and ALS Groups, IEEE Transactions on Neural Systems and Rehabilitation Engineering, 2016, 24(5) pp. 603-615

[10]   K. Ullah, M. Ali, M. Rizwan and M. Imran: Low-cost single-channel EEG based communication system for people with lock-in syndrome, In Proceedings of the 2011 IEEE 14th International Multitopic Conference (INMIC 2011) Karachi, Pakistan, 2011, pp. 120-125

[11]   G. Pfurtscheller, G. Muller-Putz, R. Scherer, and C. Neuper: Rehabilitation with Brain-Computer Interface Systems, Computer, 2008, 41(10) pp. 58-65

[12]   W. Kaysa, Suprijanto and A. Widyotriatmo: Design of Brain-computer interface platform for semi-real-time commanding electrical wheelchair

simulator movement, In Proceedings of the 2013 3rd International Conference on Instrumentation Control and Automation (ICA 2013) Ungasan, Indonesia, 2013, pp. 39-44

[13]   M. Choubisa and P. Trivedi: Analysing EEG signals for detection of mind awake stage and sleep deprivation stage, In Proceedings of the 2015 International Conference on Green Computing and Internet of Things (ICGCIoT 2015) Noida, India, 2015, pp. 1209-1211

[14]   J. Katona: Examination and comparison of the EEG based attention test with CPT and TOVA, In Proceedings of the 15th IEEE International Symposium on Computational Intelligence and Informatics (CINTI 2014) Budapest, Hungary, 2014, pp. 117-120

[15]   M. Murugappan, R. Nagarajan and S. Yaacob: Appraising human emotions using Time-Frequency Analysis based EEG alpha band features, In Proceedings of the 2009 Innovative Technologies in Intelligent Systems and Industrial Applications (CITISIA 2009) Monash, Malaysia, 2009, pp. 70-75

[16]   C. Dongwei, W. Fang, W. Zhen, L. Haifang and C. Junjie: EEG-based emotion recognition with brain network using independent components analysis and granger causality, In Proceedings of the 2013 International Conference on Computer Medical Applications (ICCMA 2013) Sousse, Tunisia, 2013, pp. 1-6

[17]   A. Vourvopoulos and F. Liarokapis: Robot Navigation Using Brain-Computer Interfaces, In Proceedings of the 2012 IEEE 11th International Conference on Trust, Security and Privacy in Computing and Communications (TrustCom 2012) Liverpool, UK, 2012, pp. 1785-1792

[18] J. Katona, T. Ujbanyi, G. Sziladi, and A. Kovari: Speed control of Festo Robotino mobile robot using NeuroSky MindWave EEG headset based Brain-Computer Interface, In Proceedings of the 7th IEEE International Conference on Cognitive Infocommunications (CogInfoCom 2016) Wroclaw, Poland, 2016, pp. 251-256

[19]   J. Katona, A. Kovari: EEG-based Computer Control Interface for Brain-Machine Interaction, International Journal of Online Engineering, 2015, 11(6) pp. 43-38

[20]   K. LaFleur, K. Cassady, A. Doud, K. Shades, E. Rogin and B. He: Quadcopter control in three-dimensional space using a noninvasive motor imagery-based brain-computer interface, Journal of Neural Engineering, 2013, 10(4) p. 046003

[21]   J. Katona, A. Kovari: A Brain-Computer Interface Project Applied in Computer Engineering, IEEE Transaction on Education, 2016, 59(4) pp. 319-324

[22] K. Watanabe, H. Tanaka, K. Takahashi, Y. Niimura, K. Watanabe, and Y. Kurihara: NIRS-Based Language Learning BCI System, IEEE Sensors Journal, 2016, 16(8) pp. 2726-2734

[23] Y. Tomita, F. Vialatte, G. Dreyfus, Y. Mitsukura, H. Bakardjian and A. Cichocki: Bimodal BCI Using Simultaneously NIRS and EEG, IEEE Transactions on Biomedical Engineering, 2014, 61(4) pp. 1274-1284

[24] N. Weiskopf, K. Mathiak, S. Bock, F. Scharnowski, R. Veit, W. Grodd, R. Goebel and N. Birbaumer: Principles of a Brain-Computer Interface (BCI) Based on Real-Time Functional Magnetic Resonance Imaging (fMRI), IEEE Transactions on Biomedical Engineering, 2014, 51(6) pp. 966-970

[25] F. E. Bloom, A. Lazerson: Brain, Mind, and Behavior, New York, NY: W. H. Freeman and Company, 3rd edition, 2005, pp. 1-457

[26] G. Buzsaki: Rhythms of the brain, Oxford University Press, 2011, pp. 1-448

[27] M. Scanziani, M. Häusser: Electrophysiology in the age of light, Nature, 2009, 461, pp. 930-939

[28] D. L. Schomer and F. L. da Silva: Niedermeyer's Electroencephalography: Basic Principles, Clinical Applications, and Related Fields, New York, Lippincot Williams & Wilkins, 6th ed., 2010, pp. 1-1296

[29] F. S. Tyner, J. R. Knott, and W. B. Mayer Jr.: Fundamentals of EEG Technology: Vol. 1: Basic Concepts and Methods, USA, Lippincott Williams & Wilkins, 1st ed., 1983, pp. 1-332

[30] F. H. Duffy, J. R. Hughes, F. Miranda, P. Bernad, P. Cook: Status of Quantified EEG (QEEG) in Clinical Practice, Clinical Electroencephalography, 1994, 25(4) pp. 6-22

[31] W. Sałabun: Processing and spectral analysis of the raw EEG signal from the MindWave, Przeglad Elektrotechniczny, 2014, 90(2) pp. 169-174

[32] NeuroSky: Brain Wave Signal (EEG) of NeuroSky, NeuroSky Inc., 2009

[33] Scientifics Direct, Inc. (2014, Dec. 10): NeuroSky MindWave - EEG Brain Wave Activities [Online] Available: http://www.scientificsonline.com/product/neurosky-mindwave

[34] NeuroSky: MindWave User Guide, NeuroSky Inc., 2011

[35] K. Montor: Attention-level analyzer, U.S. Patent 3 877 466, April 15, 1975

[36] M. Murugappan, S. Murugappan, Balaganapathy, C. Gerard: Wireless EEG signals based Neuromarketing system using Fast Fourier Transform (FFT), In Proceedings of 2014 IEEE 10th International Colloquium on Signal Processing & its Applications (CSPA 2014) Kuala Lumpur, Malaysia, 2014, pp. 25-30

[37] M. Murugappan, S. Murugappan: Human emotion recognition through short time Electroencephalogram (EEG) signals using Fast Fourier Transform (FFT), In Proceedings of 2013 IEEE 9th International Colloquium on Signal Processing & its Applications (CSPA 2013) Kuala Lumpur, Malaysia, 2013, pp. 289-294

[38] S. T. Muller, B. J. Piper: The Psychology Experiment Building Language (PEBL) and PEBL Test Battery, Journal of Neuroscience Methods, 2014, 222, pp. 250-259

[39] J. Cooley, P. Lewis and P. Welch: The finite Fourier transform, IEEE Trans. Audio Electroacoustics, 1969, 17(2) pp. 77-85

[40] A. V. Oppenheim, R. W. Schafer and J. R. Buck: Discrete-time signal processing, Upper Saddle River, N.J.: Prentice Hall, 1999, pp. 1-897

[41] A. D. Baddeley: Working Memory, Clarendon Press, 1986. pp. 1-289

[42] K. Biró, Gy. Molnár, D. Pap, Z. Szűts: The Effects of Virtual and Augmented Learning Environments on the Learning Process in Secondary School, Proceedings of 8th IEEE International Conference on Cognitive Infocommunications (CogInfoCom 2017) Debrecen, Hungary, 2017, pp. 371-375

[43] I. Horváth: Innovative engineering education in the cooperative VR environment, Proceedings of 7th IEEE International Conference on Cognitive Infocommunications (CogInfoCom 2016) Wroclaw, Poland, 2016, pp. 359-364

[44] I. Horváth: Disruptive technologies in higher education, Proceedings of 7th IEEE International Conference on Cognitive Infocommunications (CogInfoCom 2016) Wroclaw, Poland, 2016, pp. 347-352

[45] E. Gogh, A. Kovacs, G. Sziladi: Application of E-diary to analyze the effectiveness of learning, Proceedings of 8th IEEE International Conference on Cognitive Infocommunications (CogInfoCom 2017) Debrecen, Hungary, 2017, pp. 419-422

[46] I. Horváth: The IT device demand of the edu-coaching method in the higher education of engineering, Proceedings of 8th IEEE International Conference on Cognitive Infocommunications (CogInfoCom 2017) Debrecen, Hungary, 2017, pp. 379-384

[47] Z. Kvasznicza: Teaching electrical machines in a 3D virtual space, Proceedings of 8th IEEE International Conference on Cognitive Infocommunications (CogInfoCom 2017) Debrecen, Hungary, 2017, pp. 385-388

[48] A. D. Kovács: The application opportunities of green roof, as an interactive educational space, Proceedings of 8th IEEE International Conference on

Cognitive Infocommunications (CogInfoCom 2017) Debrecen, Hungary, 2017, pp. 389-393

[49]   A. Kutikova, J. Balata, Z. Mikovec: Explorations into ICT Usage and Behavior in Travel Related Activities of Wheelchair Users, Proceedings of 8th IEEE International Conference on Cognitive Infocommunications (CogInfoCom 2017) Debrecen, Hungary, 2017, pp. 231-236

[50]   M. Tariq, L. Uhlenberg, P. Trivailo, K. S Munir, and M. Simic: Mu-Beta Rhythm ERD/ERS Quantification for Foot Motor Execution and Imagery Tasks in BCI Applications, Proceedings of 8th IEEE International Conference on Cognitive Infocommunications (CogInfoCom 2017) Debrecen, Hungary, 2017, pp. 91-96

[51]   A. Kovács, I. Winkler, K. Vicsi: EEG correlates of speech: examination of event-related potentials elicited by phoneme classes, Proceedings of 8th IEEE International Conference on Cognitive Infocommunications (CogInfoCom 2017) Debrecen, Hungary, 2017, pp. 115-120

[52]   D. Geszten, B. P. Hámornik, K. Hercegfi: Measurement of team mental model as a part of a new team usability testing method, Proceedings of 8th IEEE International Conference on Cognitive Infocommunications (CogInfoCom 2017) Debrecen, Hungary, 2017, pp. 291-294

[53]   P. Baranyi, A. Csapo and Gy. Sallai: Cognitive Infocommunications (CogInfoCom) Springer, 2015

[54]   P. Baranyi, A. Csapo: Definition and Synergies of Cognitive Infocommunications, Acta Polytechnica Hungarica, Vol. 9, No. 1, 2012, pp. 67-83

[55]   G. Kiss, et al.: Connection between body condition and speech parameters-especially in the case of hypoxia, Proceedings of 5th IEEE International Conference on Cognitive Infocommunications (CogInfoCom 2014) Vietri sul Mare, Italy, 2014, pp 333-336

[56]   Lambrechts, et al.: Temporal dynamics of speech and gesture in Autism Spectrum Disorder, Proceedings of 5th IEEE International Conference on Cognitive Infocommunications (CogInfoCom 2014) Vietri sul Mare, Italy, 2014, pp. 349-353

[57]   A. K. Varga, and L. Czap.: Development of an online subjective evaluation system for recorded speech of deaf and hard of hearing children, Proceedings of 5th IEEE International Conference on Cognitive Infocommunications (CogInfoCom 2015) Győr, Hungary, 2015, pp. 455-458

[58]   D. Sztahó, M. Gábriel Tulics, K. Vicsi, I. Valálik: Automatic Estimation of Severity of Parkinson's Disease Based on Speech Rhythm Related Features, Proceedings of 8th IEEE International Conference on Cognitive

Infocommunications (CogInfoCom 2017) Debrecen, Hungary, 2017, pp. 11-16

[59]   L. Izsó: The significance of cognitive infocommunications in developing assistive technologies for people with non-standard cognitive characteristics: CogInfoCom for people with nonstandard cognitive characteristics, Proceedings of 5th IEEE International Conference on Cognitive Infocommunications (CogInfoCom 2015) Győr, Hungary, 2015, pp. 77-82

[60]   R. Sperandeo, E. Moretto, G. Baldo, S. Dell'Orco, N. M. Maldonato: Executive Functions and Personality Features: a Circular Interpretative Paradigm, Proceedings of 8th IEEE International Conference on Cognitive Infocommunications (CogInfoCom 2017) Debrecen, Hungary, 2017, pp. 63-66

[61]   G. Wilcock, K. Jokinen: Bringing Cognitive Infocommunications to small language communities, Proceedings of 8th IEEE International Conference on Cognitive Infocommunications (CogInfoCom 2017) Debrecen, Hungary, 2017, pp. 259-264

[62]   F. Alam, M. Danieli, G. Riccardi: Can We Detect Speakers' Empathy? A Real-Life Case Study, Proceedings of the 7th IEEE International Conference on Cognitive Infocommunications (CogInfoCom 2016) Wroclaw, Poland, 2016, pp. 59-64

[63]   C. Vogel, M. R. Lopes, A. Esposito: Gender differences in the language of the Map Task dialogues, Proceedings of 8th IEEE International Conference on Cognitive Infocommunications (CogInfoCom 2017) Debrecen, Hungary, 2017, pp. 151-156

[64]   S. Pieskä, M. Luimula, H. Kaartinen, P. Qvist, T. Suominen, O. Tuusvuor: Multidisciplinary Wow Experiences Boosting SMEi, Proceedings of the 7th IEEE International Conference on Cognitive Infocommunications (CogInfoCom 2016) Wroclaw, Poland, 2016, pp. 309-316

[65]   O. Matarazzo, B. Pizzini, C. Greco, M. Carpentieri: Effect of a Chance Task Outcome on the Offers in the Ultimatum Game: The Mediation Role of Emotions, Proceedings of the 7th IEEE International Conference on Cognitive Infocommunications (CogInfoCom 2016) Wroclaw, Poland, 2016, pp. 295-300

[66]   M. G. Tulics, K. Vicsi: Phonetic-class based correlation analysis for severity of dysphonia, Proceedings of 8th IEEE International Conference on Cognitive Infocommunications (CogInfoCom 2017) Debrecen, Hungary, 2017, pp. 21-26

[67]   I. Schmitt, G. Wirsching, R. Römer, M. Wolff: Denormalized Quantum Density Operators for Encoding Semantic Uncertainty in Cognitive Agents, Proceedings of 8th IEEE International Conference on Cognitive

Infocommunications (CogInfoCom 2017) Debrecen, Hungary, 2017, pp. 165-170

[68] A. Hayakawa, C. Vogel, N. Campbell, S. Luz: Perception changes with and without a video channel: A study from a speech-to-speech, machine translation mediated map task, Proceedings of 8th IEEE International Conference on Cognitive Infocommunications (CogInfoCom 2017) Debrecen, Hungary, 2017, pp. 401-406

[69] Michael Beetz; Matthias Scheutz; Fereshta Yazdani: Guidelines for improving task-based natural language understanding in human-robot rescue teams, Proceedings of 8th IEEE International Conference on Cognitive Infocommunications (CogInfoCom 2017) Debrecen, Hungary, 2017, pp. 203-208

[70] M. Koutsombogera, C. Vogel: Ethical Responsibilities of Researchers and Participants in the Development of Multimodal Interaction Corpora, Proceedings of 8th IEEE International Conference on Cognitive Infocommunications (CogInfoCom 2017) Debrecen, Hungary, 2017, pp. 277-282

[71] A, Moró, Gy. Szaszák: A prosody inspired RNN approach for punctuation of machine produced speech transcripts to improve human readability, Proceedings of 8th IEEE International Conference on Cognitive Infocommunications (CogInfoCom 2017) Debrecen, Hungary, 2017, pp. 219-224

[72] B. Radostyan, K. D.Pomazi, L. Gazdi, B. Forstner, L. Szegletes: Adaptive Figural Abstraction Test with Generated Exercises, Proceedings of the 7th IEEE International Conference on Cognitive Infocommunications (CogInfoCom 2016) Wroclaw, Poland, 2016, pp. 327-330

[73] F. R. Izullah, M. Koivisto, A. Aho, T. Laine, H. Hämäläinen, P. Qvist, A. Peltola, P. Pitkäkangas, M. Luimula: NeuroCar Virtual Driving Environment - Simultaneous Evaluation of Driving Skills and Spatial Perceptual-attentional Capacity, Proceedings of the 7th IEEE International Conference on Cognitive Infocommunications (CogInfoCom 2016) Wroclaw, Poland, 2016, pp. 31-36

[74] B. Lewandowska-Tomaszczyk, P. Wilson: Compassion, Empathy and Sympathy Expression Features in Affective Robotics, Proceedings of the 7th IEEE International Conference on Cognitive Infocommunications (CogInfoCom 2016) Wroclaw, Poland, 2016, pp. 65-70

[75] J. Irastorza, M. I. Torres: Analyzing the expression of annoyance during phone calls to complaint services, Proceedings of the 7th IEEE International Conference on Cognitive Infocommunications (CogInfoCom 2016) Wroclaw, Poland, 2016, pp. 103-106

[76] Gy. Kovacs, T. Grosz, T. Varadi: Topical Unit Classification Using Deep Neural Nets and Probabilistic Sampling, Proceedings of the 7th IEEE International Conference on Cognitive Infocommunications (CogInfoCom 2016) Wroclaw, Poland, 2016, pp. 199-204

[77] M. Rusko, M. Finke: Using Speech Analysis in Voice Communication A new approach to improve Air Traffic Management Security, Proceedings of the 7th IEEE International Conference on Cognitive Infocommunications (CogInfoCom 2016) Wroclaw, Poland, 2016, pp. 181-186

[78] D. Balla, T. Mester, Á. Botos, T. J. Novák, M. Zichar, J. Rásó, A. Karika: Possibilities of spatial data visualization with web technologies for cognitive interpretation, Proceedings of 8th IEEE International Conference on Cognitive Infocommunications (CogInfoCom 2017) Debrecen, Hungary, 2017, pp 17-20

[79] P. Qvist, N. B. Trygg, M. Luimula, A. Peltola, T. Suominen, V. Heikkinen, P. Tuominen, O. Tuusvuor: Demo: Medieval Gastro Box − Utilizing VR Technologies in Immersive Tourism Experience, Proceedings of the 7th IEEE International Conference on Cognitive Infocommunications (CogInfoCom 2016) Wroclaw, Poland, 2016, pp. 77-78

[80] D. Nguyen, G. Bailly, Frederic Elisei: Conducting neuropsychological tests with a humanoid robot: design and evaluation, Proceedings of the 7th IEEE International Conference on Cognitive Infocommunications (CogInfoCom 2016) Wroclaw, Poland, 2016, pp. 337-342

[81] V. Sarathy, M. Scheutz, B. Malle: Learning behavioral norms in uncertain and changing contexts, Proceedings of 8th IEEE International Conference on Cognitive Infocommunications (CogInfoCom 2017) Debrecen, Hungary, 2017, pp. 301-306

[82] S. Savić, M. Gnjatovic, D. Mišković, J. Tasevski, N. Maček: Cognitively-Inspired Symbolic Framework for Knowledge Representation, Proceedings of the 7th IEEE International Conference on Cognitive Infocommunications (CogInfoCom 2016) Wroclaw, Poland, 2016, pp. 315-320

[83] C. Rigóczki, D. Andrei, and K. Györgyi-Ambró: Gamification on the edge of educational sciences and pedagogical methodologies, Journal of Applied Technical and Educational Sciences, Vol. 7, No. 4, pp. 79-88, Nov. 2017

[84] K.D. Pomazi, L. Gazdi, B. Radostyan, B. Forstner, L. Szegletes: Self-Standardizing Cognitive Profile Based on Gardner's Multiple Intelligence Theory, Proceedings of the 7th IEEE International Conference on Cognitive Infocommunications (CogInfoCom 2016) Wroclaw, Poland, 2016, pp. 317-322

[85] L. Major: The model of the environmental attitude of teacher candidates, Journal of Applied Technical and Educational Sciences, Vol. 8, No. 1, pp. 25-35, Apr. 2018

[86] M. Szabo, K. D. Pomazi, B. Radostyan, L. Szegletes, B. Forstner: Estimating Task Difficulty in Educational Games, Proceedings of the 7th IEEE International Conference on Cognitive Infocommunications (CogInfoCom 2016) Wroclaw, Poland, 2016, pp. 397-402

[87] A. Csapo, A. Kristjansson, H. Nagy, Gy. Wersenyi: Evaluation of Human-Myo Gesture Control Capabilities in Continuous Search and Select Operations, Proceedings of the 7th IEEE International Conference on Cognitive Infocommunications (CogInfoCom 2016) Wroclaw, Poland, 2016, pp. 415-420

[88] A. Esposito, A. M. Esposito, M. Maldonato, C. Vogel: Differences between hearing and deaf subjects in decoding foreign emotional faces, Proceedings of 8th IEEE International Conference on Cognitive Infocommunications (CogInfoCom 2017) Debrecen, Hungary, 2017, pp. 175-180

[89] J. Henshaw, W. Liu, D. Romano: Improving SSVEP-BCI Performance Using Pre-Trial Normalization Methods, Proceedings of 8th IEEE International Conference on Cognitive Infocommunications (CogInfoCom 2017) Debrecen, Hungary, 2017, pp. 247-252

[90] S. Ondas, L.Mackova, D. Hladek: Emotion Analysis in DiaCoSk Dialog Corpus, Proceedings of the 7th IEEE International Conference on Cognitive Infocommunications (CogInfoCom 2016) Wroclaw, Poland, 2016, pp. 151-156

[91] L. Gazdi, K. D. Pomazi, B. Radostyan, B. Forstner, L. Szegletes: Experimenting with classifiers in biofeedback-based mental effort measurement, Proceedings of the 7th IEEE International Conference on Cognitive Infocommunications (CogInfoCom 2016) Wroclaw, Poland, 2016, pp. 331-336

[92] M. Meier, M. Borsky, E. H. Magnusdottir, K. R. Johannsdottir, J. Gudnason: Vocal tract and voice source features for monitoring cognitive workload, Proceedings of the 7th IEEE International Conference on Cognitive Infocommunications (CogInfoCom 2016) Wroclaw, Poland, 2016, pp. 97-102

[93] R. Vassiliki, D. Arfani, K. Fragkopoulou, E. Danasi, S. Varlokosta, G. Paliouras: Automatic detection of linguistic indicators as a means of early detection of Alzheimer's disease and of related dementias: A computational linguistics analysis, Proceedings of 8th IEEE International Conference on Cognitive Infocommunications (CogInfoCom 2017) Debrecen, Hungary, 2017, pp. 33-38

[94] A. Ghosh, E. Stepanov, M. Danieli, G. Riccardi: Are You Stressed? Detecting High Stress from User Diaries, Proceedings of 8th IEEE International Conference on Cognitive Infocommunications (CogInfoCom 2017) Debrecen, Hungary, 2017, pp. 265-270

[95] M. Gnjatović, J. Tasevski, D. Mišković, S. Savić, B. Borovac, A. Mikov,R. Krasnik: Pilot Corpus of Child-Robot Interaction in Therapeutic Settings, Proceedings of 8th IEEE International Conference on Cognitive Infocommunications (CogInfoCom 2017) Debrecen, Hungary, 2017, pp. 253-258

[96] A. Mecocci, F. Micheli, C. Zoppetti, A. Baghini: Automatic Falls Detection in Hospital-Room Context, Proceedings of the 7th IEEE International Conference on Cognitive Infocommunications (CogInfoCom 2016) Wroclaw, Poland, 2016, pp. 127-132